



IAEA

International Atomic Energy Agency

IAEA TECDOC SERIES

No. 2095

Distribution Coefficients for Soil, Freshwater and Marine Systems for Exposure Assessments

Report of Working Group 4

Modelling and Data for Radiological Impact Assessments
(MODARIA I and MODARIA II) Programmes

IAEA SAFETY STANDARDS AND RELATED PUBLICATIONS

IAEA SAFETY STANDARDS

Under the terms of Article III of its Statute, the IAEA is authorized to establish or adopt standards of safety for protection of health and minimization of danger to life and property, and to provide for the application of these standards.

The publications by means of which the IAEA establishes standards are issued in the **IAEA Safety Standards Series**. This series covers nuclear safety, radiation safety, transport safety and waste safety. The publication categories in the series are **Safety Fundamentals**, **Safety Requirements** and **Safety Guides**.

Information on the IAEA's safety standards programme is available at the IAEA Internet site

www.iaea.org/resources/safety-standards

The site provides the texts in English of published and draft safety standards. The texts of safety standards issued in Arabic, Chinese, French, Russian and Spanish, the IAEA Safety Glossary and a status report for safety standards under development are also available. For further information, please contact the IAEA at: Vienna International Centre, PO Box 100, 1400 Vienna, Austria.

All users of IAEA safety standards are invited to inform the IAEA of experience in their use (e.g. as a basis for national regulations, for safety reviews and for training courses) for the purpose of ensuring that they continue to meet users' needs. Information may be provided via the IAEA Internet site or by post, as above, or by email to Official.Mail@iaea.org.

RELATED PUBLICATIONS

The IAEA provides for the application of the standards and, under the terms of Articles III and VIII.C of its Statute, makes available and fosters the exchange of information relating to peaceful nuclear activities and serves as an intermediary among its Member States for this purpose.

Reports on safety in nuclear activities are issued as **Safety Reports**, which provide practical examples and detailed methods that can be used in support of the safety standards.

Other safety related IAEA publications are issued as **Emergency Preparedness and Response** publications, **Radiological Assessment Reports**, the International Nuclear Safety Group's **INSAG Reports**, **Technical Reports** and **TECDOCs**. The IAEA also issues reports on radiological accidents, training manuals and practical manuals, and other special safety related publications.

Security related publications are issued in the **IAEA Nuclear Security Series**.

The **IAEA Nuclear Energy Series** comprises informational publications to encourage and assist research on, and the development and practical application of, nuclear energy for peaceful purposes. It includes reports and guides on the status of and advances in technology, and on experience, good practices and practical examples in the areas of nuclear power, the nuclear fuel cycle, radioactive waste management and decommissioning.

DISTRIBUTION COEFFICIENTS
FOR SOIL, FRESHWATER
AND MARINE SYSTEMS
FOR EXPOSURE ASSESSMENTS

The following States are Members of the International Atomic Energy Agency:

| | | |
|------------------------|---------------------------|-----------------------------|
| AFGHANISTAN | GEORGIA | PAKISTAN |
| ALBANIA | GERMANY | PALAU |
| ALGERIA | GHANA | PANAMA |
| ANGOLA | GREECE | PAPUA NEW GUINEA |
| ANTIGUA AND BARBUDA | GRENADA | PARAGUAY |
| ARGENTINA | GUATEMALA | PERU |
| ARMENIA | GUINEA | PHILIPPINES |
| AUSTRALIA | GUYANA | POLAND |
| AUSTRIA | HAITI | PORTUGAL |
| AZERBAIJAN | HOLY SEE | QATAR |
| BAHAMAS, THE | HONDURAS | REPUBLIC OF MOLDOVA |
| BAHRAIN | HUNGARY | ROMANIA |
| BANGLADESH | ICELAND | RUSSIAN FEDERATION |
| BARBADOS | INDIA | RWANDA |
| BELARUS | INDONESIA | SAINT KITTS AND NEVIS |
| BELGIUM | IRAN, ISLAMIC REPUBLIC OF | SAINT LUCIA |
| BELIZE | IRAQ | SAINT VINCENT AND |
| BENIN | IRELAND | THE GRENADINES |
| BOLIVIA, PLURINATIONAL | ISRAEL | SAMOA |
| STATE OF | ITALY | SAN MARINO |
| BOSNIA AND HERZEGOVINA | JAMAICA | SAUDI ARABIA |
| BOTSWANA | JAPAN | SENEGAL |
| BRAZIL | JORDAN | SERBIA |
| BRUNEI DARUSSALAM | KAZAKHSTAN | SEYCHELLES |
| BULGARIA | KENYA | SIERRA LEONE |
| BURKINA FASO | KOREA, REPUBLIC OF | SINGAPORE |
| BURUNDI | KUWAIT | SLOVAKIA |
| CABO VERDE | KYRGYZSTAN | SLOVENIA |
| CAMBODIA | LAO PEOPLE'S DEMOCRATIC | SOMALIA |
| CAMEROON | REPUBLIC | SOUTH AFRICA |
| CANADA | LATVIA | SPAIN |
| CENTRAL AFRICAN | LEBANON | SRI LANKA |
| REPUBLIC | LESOTHO | SUDAN |
| CHAD | LIBERIA | SWEDEN |
| CHILE | LIBYA | SWITZERLAND |
| CHINA | LIECHTENSTEIN | SYRIAN ARAB REPUBLIC |
| COLOMBIA | LITHUANIA | TAJIKISTAN |
| COMOROS | LUXEMBOURG | THAILAND |
| CONGO | MADAGASCAR | TOGO |
| COOK ISLANDS | MALAWI | TONGA |
| COSTA RICA | MALAYSIA | TRINIDAD AND TOBAGO |
| CÔTE D'IVOIRE | MALI | TUNISIA |
| CROATIA | MALTA | TÜRKİYE |
| CUBA | MARSHALL ISLANDS | TURKMENISTAN |
| CYPRUS | MAURITANIA | UGANDA |
| CZECH REPUBLIC | MAURITIUS | UKRAINE |
| DEMOCRATIC REPUBLIC | MEXICO | UNITED ARAB EMIRATES |
| OF THE CONGO | MONACO | UNITED KINGDOM OF |
| DENMARK | MONGOLIA | GREAT BRITAIN AND |
| DJIBOUTI | MONTENEGRO | NORTHERN IRELAND |
| DOMINICA | MOROCCO | UNITED REPUBLIC OF TANZANIA |
| DOMINICAN REPUBLIC | MOZAMBIQUE | UNITED STATES OF AMERICA |
| ECUADOR | MYANMAR | URUGUAY |
| EGYPT | NAMIBIA | UZBEKISTAN |
| EL SALVADOR | NEPAL | VANUATU |
| ERITREA | NETHERLANDS, | VENEZUELA, BOLIVARIAN |
| ESTONIA | KINGDOM OF THE | REPUBLIC OF |
| ESWATINI | NEW ZEALAND | VIET NAM |
| ETHIOPIA | NICARAGUA | YEMEN |
| FIJI | NIGER | ZAMBIA |
| FINLAND | NIGERIA | ZIMBABWE |
| FRANCE | NORTH MACEDONIA | |
| GABON | NORWAY | |
| GAMBIA, THE | OMAN | |

The Agency's Statute was approved on 23 October 1956 by the Conference on the Statute of the IAEA held at United Nations Headquarters, New York; it entered into force on 29 July 1957. The Headquarters of the Agency are situated in Vienna. Its principal objective is "to accelerate and enlarge the contribution of atomic energy to peace, health and prosperity throughout the world".

IAEA-TECDOC-2095

DISTRIBUTION COEFFICIENTS
FOR SOIL, FRESHWATER
AND MARINE SYSTEMS
FOR EXPOSURE ASSESSMENTS

REPORT OF WORKING GROUP 4

MODELLING AND DATA
FOR RADIOLOGICAL IMPACT ASSESSMENTS
(MODARIA I AND MODARIA II) PROGRAMMES

INTERNATIONAL ATOMIC ENERGY AGENCY
VIENNA, 2025

COPYRIGHT NOTICE

All IAEA scientific and technical publications are protected by the terms of the Universal Copyright Convention as adopted in 1952 (Geneva) and as revised in 1971 (Paris). The copyright has since been extended by the World Intellectual Property Organization (Geneva) to include electronic and virtual intellectual property. Permission may be required to use whole or parts of texts contained in IAEA publications in printed or electronic form. Please see www.iaea.org/publications/rights-and-permissions for more details. Enquiries may be addressed to:

Publishing Section
International Atomic Energy Agency
Vienna International Centre
PO Box 100
1400 Vienna, Austria
tel.: +43 1 2600 22529 or 22530
email: sales.publications@iaea.org
www.iaea.org/publications

For further information on this publication, please contact:

Waste and Environmental Safety Section
International Atomic Energy Agency
Vienna International Centre
PO Box 100
1400 Vienna, Austria
Email: Official.Mail@iaea.org

© IAEA, 2025
Printed by the IAEA in Austria
June 2025
<https://doi.org/10.61092/iaea.jitd-59bo>

IAEA Library Cataloguing in Publication Data

Names: International Atomic Energy Agency.
Title: Distribution coefficients for soil, freshwater and marine systems for exposure assessments / International Atomic Energy Agency.
Description: Vienna : International Atomic Energy Agency, 2025. | Series: IAEA TECDOC series, ISSN 1011-4289 ; no. 2095 | Includes bibliographical references.
Identifiers: IAEAL 25-01771 | ISBN 978-92-0-113825-5 (paperback : alk. paper) | ISBN 978-92-0-113725-8 (pdf)
Subjects: LCSH: Radiation — Management. | Radiation — Environmental aspects. | Radiation — Safety measures.

FOREWORD

The IAEA has been organizing international model testing programmes for the transfer of radionuclides in the environment and the estimation of radiation exposures since the 1980s. These programmes have contributed to a general improvement in such models, both in the transfer of data and in the capabilities of modellers in Member States. IAEA publications on this subject over the past three decades demonstrate the comprehensive nature of the programmes and record the associated advances that have been made.

From 2012 to 2015, the IAEA organized a programme entitled Modelling and Data for Radiological Impact Assessments (MODARIA). The first phase of the programme focused on testing the performance of models; developing and improving models for particular environments; reaching consensus on data sets that are generally applicable in environmental transfer models; and providing an international forum for the exchange of experience, ideas and research information.

From 2016 to 2019, the IAEA organized the second phase of the programme (MODARIA II), where seven working groups continued much of the work of the first phase of the programme. This publication describes part of the work undertaken by Working Group 4 — Transfer Processes and Data for Radiological Impact Assessment — under both phases of the MODARIA programme. It specifically reports on the work to update and improve the quality of distribution coefficients (K_d) for soil, freshwater and marine systems used within models for exposure assessment.

The IAEA is grateful to all those who participated in these activities within Working Group 4 and who contributed to the development of this publication, in particular the leaders of Working Group 4, B. Howard (United Kingdom) and K. Kelleher (Ireland). The IAEA officers responsible for this publication were J. Brown of the Division of Radiation, Transport and Waste Safety and A.R. Harbottle of the Division of Physical and Chemical Sciences.

EDITORIAL NOTE

This publication has been prepared from the original material as submitted by the contributors and has not been edited by the editorial staff of the IAEA. The views expressed remain the responsibility of the contributors and do not necessarily represent the views of the IAEA or its Member States.

Guidance and recommendations provided here in relation to identified good practices represent expert opinion but are not made on the basis of a consensus of all Member States.

Neither the IAEA nor its Member States assume any responsibility for consequences which may arise from the use of this publication. This publication does not address questions of responsibility, legal or otherwise, for acts or omissions on the part of any person.

The use of particular designations of countries or territories does not imply any judgement by the publisher, the IAEA, as to the legal status of such countries or territories, of their authorities and institutions or of the delimitation of their boundaries.

The mention of names of specific companies or products (whether or not indicated as registered) does not imply any intention to infringe proprietary rights, nor should it be construed as an endorsement or recommendation on the part of the IAEA.

The authors are responsible for having obtained the necessary permission for the IAEA to reproduce, translate or use material from sources already protected by copyrights.

The IAEA has no responsibility for the persistence or accuracy of URLs for external or third party Internet web sites referred to in this publication and does not guarantee that any content on such web sites is, or will remain, accurate or appropriate.

CONTENTS

| | |
|---|----|
| SUMMARY | 1 |
| 1. INTRODUCTION | 3 |
| 1.1. BACKGROUND | 3 |
| 1.2. OBJECTIVE | 4 |
| 1.3. SCOPE..... | 4 |
| 1.4. STRUCTURE..... | 5 |
| REFERENCES TO CHAPTER 1 | 5 |
| 2. THE K_D CONCEPT | 6 |
| 2.1. INTRODUCTION TO K_D | 6 |
| 2.1.1. Assumptions and constraints of the K_d concept..... | 8 |
| 2.1.2. Methods of deriving K_d values..... | 8 |
| 2.2. GEOCHEMICAL PROCESSES CONTROLLING RADIONUCLIDE INTERACTION WITH SOLIDS | 11 |
| 2.2.1. Introduction..... | 11 |
| 2.2.2. Geochemical radionuclide processes in terrestrial and aqueous systems..... | 12 |
| 2.2.3. Adsorption and desorption processes | 15 |
| 2.2.4. Precipitation and dissolution processes | 17 |
| 2.2.5. Absorption processes | 18 |
| 2.3. SORPTION MODELS | 18 |
| 2.3.1. Parametric K_d model | 18 |
| 2.3.2. Coupling K_d and kinetic approach | 18 |
| 2.3.3. Isotherm sorption (empirical) models | 19 |
| 2.3.4. Surface complexation models..... | 20 |
| REFERENCES TO CHAPTER 2 | 21 |
| 3. K_D VARIABILITY IN SOILS..... | 26 |
| 3.1. COMPARISON BETWEEN SHORT TERM SORPTION AND LONG TERM DESORPTION K_D VALUES IN JAPANESE PADDY FIELD SOILS | 26 |
| 3.1.1. Element concentrations in soil and river sediment | 26 |
| 3.1.2. Differences between short term and long term K_d values for Mn, Ni, Se, Sr and Cs | 30 |
| 3.2. TREATMENT OF K_D VARIABILITY..... | 31 |
| 3.2.1. Introduction..... | 31 |
| 3.2.2. The cumulative distribution function statistical approach..... | 31 |
| 3.2.3. Construction of cumulative distribution functions from the K_d datasets..... | 33 |
| 3.3. CREATION OF A CRITICALLY REVIEWED SOIL K_D DATASET TO DERIVE PROBABILISTIC DISTRIBUTION COEFFICIENTS (K_D) IN SOILS..... | 34 |
| 3.3.1. Solid and liquid phases considered in the soil dataset..... | 34 |
| 3.3.2. Introduction to the published IAEA soil K_d dataset compilations..... | 35 |

| | | |
|--------|--|-----|
| 3.3.3. | Revision of criteria for the acceptance of data in K_d in future IAEA compilations | 36 |
| 3.3.4. | Compilation of soil K_d dataset within MODARIA..... | 37 |
| 3.3.5. | Approach for providing best estimate soil K_d values for Cs and Am based on grouping data according to selected factors..... | 38 |
| 3.3.6. | Key findings from the analysis of the soil K_d dataset..... | 54 |
| | REFERENCES TO CHAPTER 3 | 55 |
| 4. | FRESHWATER K_D DATASET | 59 |
| 4.1. | SEDIMENTS IN FRESHWATER SYSTEMS AND K_D APPROACHES | 59 |
| 4.1.1. | Suspended sediments in aquatic systems..... | 59 |
| 4.1.2. | Deposited sediment in aquatic systems (oxic and anoxic layers)..... | 60 |
| 4.2. | INTRODUCTION TO PREVIOUS COMPILATIONS OF K_D | 62 |
| 4.2.1. | The need to update K_d compilations | 63 |
| 4.2.2. | Objectives for updating and supplementing the freshwater K_d database..... | 65 |
| 4.3. | EXPANSION OF THE FRESHWATER K_D DATASET | 65 |
| 4.3.1. | Analyses of the updated freshwater K_d dataset..... | 74 |
| 4.4. | CONCLUSIONS FROM ANALYSIS OF THE FRESHWATER K_D DATASET | 83 |
| | REFERENCES TO CHAPTER 4 | 83 |
| 5. | MARINE K_D DATASET..... | 88 |
| 5.1. | PREVIOUSLY AVAILABLE INFORMATION ON MARINE K_D DATA | 88 |
| 5.1.1. | The derivation of K_d values in TRS 422..... | 89 |
| 5.1.2. | Impact of different factors on changes in water–sediment interaction of radionuclides with time | 91 |
| 5.2. | MARINE K_D DATA FROM THE COASTAL AREAS OF JAPAN..... | 92 |
| 5.2.1. | Consideration of the impact of the exchangeable phase of elements in sediment on marine K_d | 92 |
| 5.2.2. | Studies on K_d in marine areas of Japan before and after the accident at the Fukushima Daiichi Nuclear Power Plant (FDNPP) | 94 |
| 5.3. | DETERMINATION OF $K_{D(A)}$ USING THE IAEA’S MARIS DATABASE – A BALTIC SEA CASE STUDY | 101 |
| 5.3.1. | The MARIS Database..... | 102 |
| 5.3.2. | Conclusions from the MARIS case study for the Baltic Sea..... | 106 |
| 5.4. | PRELIMINARY CONCLUSIONS FROM MARINE STUDIES ON K_D | 107 |
| | REFERENCES TO CHAPTER 5 | 108 |
| 6. | CONCEPT FOR A K_D DATABASE AND SOFTWARE TOOL FOR DERIVING K_D DATA | 113 |
| 6.1. | DEVELOPMENT OF A PROPOSED DATABASE STRUCTURE.... | 113 |

| | | |
|--|---|-----|
| 6.1.1. | End user needs | 114 |
| 6.1.2. | The proposed K_d database structure | 114 |
| 6.2. | CURRENT STATUS OF THE PROTOTYPE K_D DATABASE..... | 115 |
| 6.3. | EXTRACTION AND REFINEMENT OF K_D DATA FROM THE PROTOTYPE DATABASE..... | 115 |
| 6.3.1. | Example of refinement of soil Cs K_d and estimation of the radiocaesium interception potential using the Tableau application..... | 116 |
| 6.3.2. | Example of refinement of marine K_d values using the prototype database | 117 |
| 6.3.3. | Preliminary outcomes of using the Tableau application with the prototype K_d database | 118 |
| 6.4. | THE WAY FORWARD..... | 118 |
| REFERENCES TO CHAPTER 6 | | 119 |
| 7. | SUMMARY AND CONCLUSIONS | 120 |
| REFERENCES TO CHAPTER 7 | | 122 |
| APPENDIX I. | PROTOTYPE K_D DATABASE TABLES AND FIELDS..... | 123 |
| ANNEX I. | EXAMPLES OF THE USE OF K_D VALUES IN MODELS AND CODES | 129 |
| REFERENCES..... | | 136 |
| ANNEX II. | EFFECT OF MICROBIAL ACTIVITY ON THE K_D OF RADIOCARBON AND RADIOIODINE | 138 |
| REFERENCES..... | | 142 |
| ANNEX III. | EXAMPLE OF COUPLING BETWEEN K_D AND KINETIC APPROACHES | 143 |
| REFERENCES..... | | 145 |
| ANNEX IV. | RELATIONSHIP BETWEEN K_D AND ADSORPTION AND DESORPTION KINETICS..... | 146 |
| ANNEX V. | IMPACT OF THE ACCIDENT AT THE FUKUSHIMA DAIICHI NUCLEAR POWER STATION ON THE DISTRIBUTION OF RADIOCAESIUM IN COASTAL WATERS..... | 147 |
| REFERENCES..... | | 150 |
| LIST OF ABBREVIATIONS | | 153 |
| CONTRIBUTORS TO DRAFTING AND REVIEW | | 155 |
| LIST OF PARTICIPANTS OF WORKING GROUP 4, SUBGROUP 1..... | | 157 |

SUMMARY

The IAEA has a long history in supporting the development of models for radiological impact assessments for members of the public through the coordinated collation of radiological parameter datasets to quantify the transfer of radionuclides in the terrestrial and aquatic environment. Through the Environmental Modelling for Radiation Safety (EMRAS and EMRAS II) and Modelling and Data for Radiological Impact Assessments (MODARIA I and MODARIA II) programmes, the IAEA has continued the updating and improvement of the quality of data used to quantify the transfer processes leading to exposures to humans and non-human biota. This publication describes the work undertaken by Working Group 4, Transfer Processes and data for Radiological Impact Assessment, subgroup 1 on distribution coefficients (K_d) within IAEA's Modelling and Data for Radiological Impact Assessments (MODARIA I) programme (2012–2015) and its continuation in the MODARIA II programme (2016–2019).

Previous reporting of K_d value datasets in earlier IAEA Technical Report Series (TRS) publications has provided best estimate K_d values (such as a geometric mean). Improved K_d datasets for soils and freshwater sediments have now been developed which include chemical, physical, mineralogical, and other ancillary properties associated with the K_d values, as well as information on the methodology followed to determine the K_d values, to assist the end user to select appropriate K_d values. The variability in K_d can be greatly reduced by grouping K_d data on the basis of identified key factors for both solid and liquid phases that influence radionuclide sorption. These key factors were identified for a number of radionuclides through statistical analysis of the datasets and knowledge of the mechanisms governing interaction. For some radionuclides with sufficiently large datasets, it has been possible to generate distribution functions of K_d for some radionuclide solid matrix combinations, thereby permitting sensitivity analyses, as well as quantitative estimation of their variability.

A significant number of K_d data for marine sediments have been compiled based on information from Japan, the Baltic Sea, and the IAEA MARIS database¹. These values have been compared with those in the IAEA publication TRS 422 entitled “Sediment Distribution Coefficients and Concentration Factors for Biota in the Marine Environment”, where a fixed single exchangeable fraction was applied to all elements. The proportion of the exchangeable phase in the new MODARIA dataset differed between radioactive and stable isotopes, although the difference was small for marine sediments. This observation, together with other data on soils and fresh water, indicated that it is preferable to quantify exchangeable fractions for elements.

The structure and content for a database of K_d values for soil, freshwater and marine systems is proposed and is illustrated for soil K_d values for Cs and U. It is envisaged that a user would be able to generate a cumulative distribution function of soil K_d , based on key soil properties that influence K_d variability for Cs and U. A graphic of the potential output from such a database demonstrates the potential usefulness of an enhanced global K_d database that can be used in conjunction with models to improve REIA and to gain a better understanding of the behaviour of radionuclides in all environmental compartments.

¹ <https://www.iaea.org/resources/databases/marine-radioactivity-information-system-maris>

1. INTRODUCTION

BRENDA HOWARD

UK Centre for Ecology and Hydrology, UNITED KINGDOM
University of Nottingham, Nottingham, UNITED KINGDOM

KEVIN KELLEHER

Environmental Protection Agency, IRELAND

ANDRA-RADA HARBOTTLE

International Atomic Energy Agency

1.1. BACKGROUND

Following the release of radionuclides to the environment, radiation exposure of members of the public is assessed using models describing transfer of radionuclides through different ecosystems and compartments of the environment [1.1]. The output of such models is a key element of the regulatory control of nuclear facilities and activities in planned, existing and emergency exposure situations. The reliability of the models depends on the quality of data parameters underpinning them and the accurate description of the environmental conditions for a specific exposure assessment.

The IAEA has a long history in supporting the development of models for radiological impact assessments for members of the public, has provided guidance on model applications and has coordinated the collation of radiological parameter datasets to quantify the transfer of radionuclides in the terrestrial and aquatic environment [1.2–1.5]. This has been carried out in the framework of the international model test and comparison programmes comprising: Biosphere Modelling and Assessment (BIOMASS) in 1996–2002, Environmental Models for Radiation Safety (EMRAS) in 2003–2007 (Phase I) and 2009–2011 (Phase II), and Modelling and Data for Radiological Impact Assessment (MODARIA) in 2012–2015 (Phase I) and 2016–2019 (Phase II).

Within ten working groups (WGs), the MODARIA I programme focused on the following areas: (a) remediation of contaminated areas, including urban environments and naturally occurring radioactive material (NORM), WGs 1, 2 and 3; (b) uncertainties in exposure assessments due to gaps in model parameter data and uncertainties and variability of radiological impact assessments in planned exposure situations and for radioactive waste disposal facilities, harmonization of models for accidental tritium releases (WGs 4 and 5); (c) exposures and effects on biota (WGs 8 and 9); and (d) marine modelling (WG10).

The follow-up MODARIA II programme, implemented in the period 2016–2019, addressed the following topics: (a) assessment and decision making of existing exposure situations for NORM and nuclear legacy sites (WG1); (b) assessment of exposures and countermeasures in urban environments (WG2); (c) assessments and control of exposures to the public and biota for planned releases to the environment (WG3); (d) transfer processes and data for radiological impact assessment (WG4); (e) exposure and effects to biota (WG5); (f) biosphere modelling for long term safety assessments of high level waste disposal facilities (WG6); and (g) assessment of fate and transport of radionuclides released in the marine environment (WG7) [1.6].

Under the EMRAS programmes, data compilations of distribution coefficients (K_d) parameter values were made available in the form of the Technical Reports Series (TRS) publication TRS 472 [1.3] for soils and freshwater systems, along with an earlier one on marine systems (TRS 422 [1.4]). These are currently widely used in assessments to estimate doses to humans and internal and external dose rates for wildlife, especially when site specific data are missing. Increased knowledge and available data on K_d parameter values has led to the need to update and improve the quality of K_d values for soil, freshwater and marine systems used within models for exposure assessment.

1.2. OBJECTIVE

The general aim of the MODARIA programmes was to improve capabilities in the field of radiological environmental impact assessment (REIA) by the acquisition of improved data for model testing and comparison, reaching consensus on modelling philosophies, approaches and parameter values, and development of improved methods and exchange of information. This publication aims:

- (1) To improve the quality and amount of information provided for K_d values for soil, freshwater and marine systems;
- (2) To present the preliminary developments of the structure and content for a global database of K_d values for soil, freshwater and marine systems, using an example of soil K_d values (for Cs, U), with a proposed end user functionality that would allow the refinement of K_d values based on factors influencing radionuclide sorption in the environment.

This TECDOC describes the activities of WG4 under the MODARIA programmes on the analysis and improvement of the quality and quantity of K_d data for human and wildlife for REIA, and on identifying factors that can explain the large range of variation in values.

1.3. SCOPE

This publication focuses on K_d parameter values that are relevant for estimating the transfer of radionuclides through environmental compartments and for assessing radiation doses to people and the environment. The publication is potentially useful for radioecological researchers, professionals from national regulatory bodies, operating organizations and decision makers that are responsible for planning and implementing source and environmental radiation monitoring and exposure assessments. The publication covers the following topics:

- (1) Updating the current data compilations of freshwater sediment K_d values in TRS 472 [1.3] through a critical review of the literature;
- (2) Illustrating (for Am and Cs) the improvement of the selection and derivation of soil K_d values for given situations using a new approach based on secondary soil properties and an improved statistical treatment of the data;
- (3) Defining suitable review processes and criteria necessary for inclusion of data in the datasets;
- (4) Identifying statistical approaches and tools that can be used to describe variability in K_d ;
- (5) Identifying ancillary data that can be used to reduce the variability associated with the K_d best estimate values and to provide end users with information to make better informed decisions about the use and selection of K_d values for different sets of conditions;
- (6) Consideration of available data and approaches used for K_d values for marine systems and further data for potential future inclusion;
- (7) Preliminary developments of the content and structure of a global database of K_d values for soil, freshwater and marine systems;

- (8) Providing an example of a soil K_d database (for Cs and U), with end user functionality that would allow the refinement of K_d values based on factors influencing radionuclide sorption in the environment.

1.4. STRUCTURE

This publication consists of seven chapters, one Appendix and six Annexes. An overview on the theoretical background on K_d concept is given in Chapter 2, including the methods for deriving K_d values, geochemical processes controlling radionuclide interactions with solids, sorption models. Chapter 3 focuses on reducing the variability associated with best estimates of K_d values for soils and the development and analysis of improved datasets for K_d values in soils, using Am and Cs as examples. Methods to provide improved information on K_d values that are categorized according to the main factors that influence K_d values are also reported. A substantial improvement of K_d datasets for the freshwater environment is reported in Chapter 4, by including three conditions of measurement, namely sorption, desorption and *in situ*, and of two environmental components, namely suspended sediments, and deposited sediments. Chapter 5 considers relevant information on improved K_d values in marine systems. Preliminary developments of the structure and content for a K_d database for soil, freshwater and marine environments, and an example of the use of such a database for deriving soil K_d data for Cs is presented in Chapter 6. Chapter 7 summarizes the conclusions of this publication. The Appendix provides information on the key features of the proposed K_d database. A series of five Annexes gives associated information supporting the main chapters, which cover: examples of the use of K_d values in models and codes; the effect of microbial activity on the K_d of radiocarbon and radioiodine; an example of coupling between K_d and kinetic approaches; the relationship between K_d and adsorption and desorption kinetics; and the impact of the accident at the Fukushima Daiichi Nuclear Power Plant on the distribution of radiocaesium in coastal waters.

REFERENCES TO CHAPTER 1

- [1.1] INTERNATIONAL ATOMIC ENERGY AGENCY, Generic Models for Use in Assessing the Impact of Discharges of Radioactive Substances to the Environment, Safety Reports Series No. 19, IAEA, Vienna (2001).
- [1.2] INTERNATIONAL ATOMIC ENERGY AGENCY, Handbook of Parameter Values for the Prediction of Radionuclide Transfer in Temperate Environments, Technical Reports Series No. 364, IAEA, Vienna (1994).
- [1.3] INTERNATIONAL ATOMIC ENERGY AGENCY, Handbook of Parameter Values for the Prediction of Radionuclide Transfer in Terrestrial and Freshwater Environment, Technical Reports Series No. 472, IAEA, Vienna (2010).
- [1.4] INTERNATIONAL ATOMIC ENERGY AGENCY, Sediment Distribution Coefficients and Concentration Factors for Biota in the Marine Environment, Technical Reports Series No. 422, IAEA, Vienna (2004).
- [1.5] INTERNATIONAL ATOMIC ENERGY AGENCY, Quantification of Radionuclide Transfer in Terrestrial and Freshwater Environments for Radiological Assessments, IAEA-TECDOC-1616, IAEA, Vienna (2009).
- [1.6] INTERNATIONAL ATOMIC ENERGY AGENCY, Environmental Transfer of Radionuclides in Japan following the Accident at the Fukushima Daiichi Nuclear Power Plant, IAEA-TECDOC-1927, IAEA, Vienna (2020).

2. THE K_d CONCEPT

DANIEL KAPLAN

Savannah River Ecology Laboratory, University of Georgia, USA

MIQUEL VIDAL, ANNA RIGOL, ORIOL RAMÍREZ-GUINART

Universitat de Barcelona, SPAIN

PATRICK BOYER

Institut de Radioprotection et de Sûreté Nucléaire (IRSN), FRANCE

ANNE-MAJ LAHDENPERA

Saanio & Riekkola Oy, FINLAND

KEVIN KELLEHER

Environmental Protection Agency, IRELAND

BRENDA HOWARD

UK Centre for Ecology and Hydrology, UNITED KINGDOM

University of Nottingham, Nottingham, UNITED KINGDOM

The parameter, K_d is often used to describe how radionuclides partition between solids and water in terrestrial soils, freshwater sediments, and marine sediments. It is most commonly used to predict how radionuclides distribute in porous and fractured media and surface water and, specifically, how they are partitioned between water, suspended and bottom sediments in freshwater and marine systems. K_d values are also used to predict the desorption of radionuclides from various materials. As K_d values affect estimates of radionuclide content in soil pore water, they may also affect estimates of radionuclide uptake via plant roots. A few models (such as Symbiose [2.1, 2.2]) use K_d values to predict soil–plant transfer for a number of radionuclides. As described in Annex I, the radionuclide activity concentration in the aqueous phase of soils (i.e. soil pore waters) can be calculated from K_d values and soil activity concentrations, which can then be used to predict activity concentrations in plants.

One challenging aim of the MODARIA WG4 activities was to enhance the statistical description of K_d distributions for several radionuclides in different ecosystems to improve the K_d information that was currently available in IAEA TRS 472 [2.3] for soil and freshwater systems.

2.1. INTRODUCTION TO K_d

Soil and sediments are major sinks for both natural and artificial radionuclides. The extent of transfer of radionuclides from these important environmental compartments to both humans and other organisms is a key determinant of their impact and has to be quantified in radiological impact assessments. As elements in solution may be environmentally mobile, they are more likely to be transported to other environmental compartments than if they were bound to soil or sediment. Therefore, if radionuclides are not immobilized because they have a low affinity to bind onto soil and/or sediments, then they will be potentially available to transfer along food chains to both humans and other organisms. Conversely, high radionuclide affinity for binding and retention in the upper layers of soils and surface sediment can lead not only to lower environmental mobility, but also to enhanced external doses. Therefore, it is important to adequately quantify the mechanisms controlling how a radionuclide is bound to solid phases in soils in terrestrial environments and to sediments in aquatic systems, to enable reliable estimation of both internal and external doses to humans and other organisms.

Under the broad term of sorption, there are different processes characterizing the binding of dissolved radionuclide ions to solid surfaces. Models for the description of radionuclide sorption are often based on empirical K_d values (also known as partition coefficients). The use of K_d values constitutes the simplest sorption model available. It is commonly defined as the ratio between the activity concentration of a radionuclide sorbed on a specified solid phase C_{solid} (mass activity density referred to dry mass (DM)) and the radionuclide activity concentration in a specified liquid phase C_{liquid} (volumetric activity density) (K_d , L/kg DM) [2.4]:

$$K_d = C_{solid} / C_{liquid} \quad (2.1)$$

Assumptions regarding K_d are discussed in following sections.

Whereas K_d is the simplest approach to assess the fraction of radionuclides associated with the aqueous and solid phases, there are alternatives, such as the non-linear isotherm approach (including Langmuir or Freundlich equations) [2.5], dynamic modelling (including the E-K sorption model [2.6]), or mass-action based thermodynamic models (including the ion exchange and surface complexation models [2.7]). These empirical and semimechanistic approaches typically involve numerous measurements of relevant environmental variables used in the models. However, the lack of relevant, site specific data to apply them may, in some cases, limit their usefulness. Although the K_d approach amalgamates many processes, it needs less data to use than a more mechanistic approach. Consequently, the application of K_d values remains widely used in models and codes because of its simplicity and straightforward implementation into radiological impact assessment models (see also Annex I).

The variability of K_d values for a given radionuclide can extend over a few orders of magnitude, depending upon the characteristics of the solid and liquid phases. Sensitivity analysis has demonstrated that K_d values are one of the most important sources of uncertainty in radiological impact assessments [2.8–2.10]. Therefore, K_d variability has to be suitably addressed to reduce uncertainty by considering any key properties that may govern radionuclide sorption onto solid phases.

Several K_d compilations have been reported in the literature. Some of them propose K_d best estimates for a given radionuclide, with a partially reduced variability by grouping K_d values based on a given environmental factor [2.3, 2.11, 2.12–2.17]. The current compilations usually report separate K_d values for soils (and for soils of different textures or physicochemical characteristics), freshwater and marine systems. K_d values for many elements have previously been reported, or derived, in IAEA publications. The most recent relevant publications are TRS 422 [2.11] for marine systems and TRS 472 [2.3] for soils and freshwater systems.

The reporting and application of K_d described above has clear disadvantages, as it:

- (1) Only provides information on sorption for a small number of radionuclides;
- (2) Does not adequately describe the variability in K_d values;
- (3) Does not adequately account for the differences in reported K_d values derived from various experimental methods used to measure K_d values.

Terrestrial, freshwater, and marine scientists tend only to report metadata associated with their discipline. For example, marine scientists commonly report salinity, but rarely report sediment properties associated with the K_d values. Conversely, terrestrial scientists provide several properties of the sediment, while often omitting aqueous salinity values.

In the long term, it would be preferable to unify these data sets. Even though the relative importance of certain environmental factors differs between terrestrial, freshwater and marine systems, there are also many factors that justify the consideration of a common approach to compiling data for the three types of environments. In MODARIA WG4, a process was initiated to develop a coordinated approach towards the compilation and reporting of K_d values from the three environmental systems in a manner which considers the complexity and variability of these natural ecosystems. Such organization of the data will make it easier to search the metadata associated with the K_d values.

2.1.1. Assumptions and constraints of the K_d concept

While the basic concept of K_d is simple, the process of the partitioning of radionuclides between solids and water is complex and many factors influence it. K_d , as defined in Eq. 2.1, represents the radionuclide activity concentration ratio of the solid to liquid fractions. The K_d term assumes the following [2.18, 2.19]:

- (1) The system is totally reversible due to fast reaction kinetics (Reversible Sorption Law);
- (2) Sorption is independent of the radionuclide activity concentration in the aqueous phase (Linear Sorption Law);
- (3) The system is at equilibrium (Equilibrium Law);
- (4) The concentration of free or unoccupied surface sorption sites is much greater than the concentration of bound radionuclide. Such an assumption is necessary because the model assumes that the presence of a bound species does not influence the tendency for a dissolved species to sorb.

Several of these assumptions, especially assumptions (2) and (4), are compromised in the most common protocols used to measure K_d values. In relation to the first assumption, the elapsed time since the incorporation of the radionuclide onto soils or sediments affects the quantification of desorption K_d through an ageing effect (the processes by which radionuclides become more strongly retained by sediments) related to sorption dynamics. Furthermore, changes with time in radionuclide speciation in the solid phase may occur. Therefore, there may be a significant impact of time on the sorption K_d measured, especially after long contact times, or on the desorption K_d estimated for previously contaminated samples. The difference is a source of variability for the K_d values of a radionuclide, and its significance, compared with other sources of variability such as solid phase properties, needs to be examined where possible. As will be discussed in more detail below, experimental methods used to measure K_d values are an additional source of variability.

2.1.2. Methods of deriving K_d values

Various methodological approaches can be used to quantify K_d in the field or the laboratory. The method used may be one of the main sources of K_d variability, as it may quantify different ‘types’ of K_d values. Therefore, the impact of the method to determine the K_d values needs to be considered, where possible, when trying to derive a best estimate K_d value.

2.1.2.1. K_d derived from short term laboratory studies

The quantification of K_d from short term studies (typically of less than a few weeks), in which the radionuclide has been recently added, can be used to derive values from conditions which are closer to reversibility than K_d determinations using other methods (described below).

Batch sorption tests are the most widely used approach to estimate K_d values for radionuclides in soils, and they are also used for sediments, especially bottom sediments [2.20–2.23]. In batch tests, a known amount of unconsolidated or disaggregated, clean solid sample, is put into contact with a volume of solution containing a radionuclide of interest. ‘Clean’ refers to an initial radionuclide activity concentration in the solid sample, which is negligible compared with the sorbed activity concentration after contact with the solution. Batch tests often use high liquid-to-mass (L/M) ratios, and the resulting suspensions are shaken for short contact times.

Batch sorption tests are particularly useful for carrying out inexpensive, relatively simple K_d measurements in which a single parameter can be varied while other parameters potentially impacting K_d values are kept reasonably constant. Batch sorption tests are particularly applicable in providing relative rankings of sorption affinity for a given radionuclide for specified solid environmental materials [2.24]. They are also used to develop an understanding of radionuclide binding processes to soil or sediment. Through their use, K_d values can be derived from simple studies with a well mixed uniform soil or sediment, various control samples, and additions of known quantities of radionuclides. They also have the added benefit that the assumptions of ‘reversibility’ and ‘steady state’ of the K_d measurements can be demonstrated.

However, batch sorption tests may not precisely simulate sorption characteristics that would naturally occur in geological media under undisturbed environmental conditions. The outcome will depend on many factors, including the activity concentration and chemical form of the radionuclide and the geochemical conditions (solid properties; pH and redox potential of the contact solution; composition and ionic strength of the contact solution; biological conditions) [2.24]. Therefore, short term sorption experiments are often conducted for different hydrochemical and mineralogical combinations at various radionuclide activity concentrations or various mass concentrations.

Quantification of K_d values may be affected by experimental conditions, such as temperature, filtration of the resulting solution, contact time, and L/M ratios [2.23, 2.24]. Variability due to changing experimental conditions is normally much lower than that arising from radionuclide and solid phase characteristics. Experimental conditions are often defined by international guidelines to facilitate and encourage good comparability of the results [2.21–2.23]. L/M ratios applied in batch sorption tests are typically between 10:1 and 50:1 L/kg; these values are not fully representative for soils *in situ*, although they can be more valid for freshwater and marine sediments. Although equilibrium is reached rapidly for certain systems, such as through processes of interlayer ion exchange reactions of clays, some sorption processes (i.e. those not simply based on simple, ion exchange mechanisms) may need longer contact times to allow equilibrium to be established.

Undertaking experiments at higher activity concentrations than those that could be expected in the environment after a radioactive release is commonly avoided, as the K_d values may decrease over a given threshold activity concentration. Relatively high mass concentrations may occur in experiments when radionuclide sorption is simulated using stable isotopes of a radionuclide (or of analogue elements). Therefore, it is better to predict sorption behaviour in environmental compartments using values obtained within the lowest concentration range of a sorption isotherm, approximating the radionuclide activity concentration in the study site.

A desorption K_d can be quantified to predict processes related to the remobilization of a radionuclide from recently contaminated solid phases, [2.24]. The desorption K_d value may be higher under similar experimental conditions to those applied in a previous sorption test, due to (i) the fraction of the radionuclide irreversibly sorbed, which no longer contributes to the solid–

solution equilibrium, or (ii) a slow desorption process so the solution concentration takes a long time to equilibrate with the solid. Differences between sorption and desorption K_d values are radionuclide dependent and are often lower than the inherent variability associated with the K_d values for a given combination of radionuclide and solid phase [2.24].

2.1.2.2. *Desorption K_d values derived from tests with 'long term incorporated' radionuclides*

K_d values may be quantified for samples in which the target radionuclide has been incorporated into the solid phase for a long time by applying desorption experiments, such as leaching tests [2.24]. The 'long term incorporated' concept is an ambiguous term that refers to a situation in which the time elapsed since the incorporation of the radionuclide is adequately long to ensure maximum irreversibility in the sorption process, thereby leading to a higher K_d than that of short term experiments with a recently added radionuclide. Depending on the radionuclide, the period defining long term situations may vary from several months to several years.

A relevant, frequently used example is when a stable isotope originally present in the solid phase (hereinafter termed as 'indigenous element') is taken as a surrogate for the behaviour of a target radionuclide and used to derive K_d values [2.24]. In studies dealing with indigenous elements, various experimental conditions are applied to quantify the element in the solid (e.g. total digestion with hydrofluoric acid; acid extraction in milder conditions; radionuclide extractable content) and in the liquid phases (e.g. soil solution, with a L/M ratio <1; water soluble, with L/M ratios >5), leading to K_d values with high variability that are dependent on the procedure being applied [2.25]. The K_d values derived from the total concentration in the solid phase will be much higher than that derived from the extractable concentration, as it would represent conditions of maximum irreversibility. Therefore, K_d values derived from indigenous data will be classified in this publication as either 'short term desorption' or 'long term incorporated', depending on the procedure followed to estimate the radionuclide activity concentration in the solid phase (extractable or total activity concentration, respectively).

2.1.2.3. *In situ apparent $K_{d(a)}$*

A few publications distinguish between distribution ratio and distribution coefficient [2.20]. The distribution ratio (R_d) or apparent distribution coefficient (here termed $K_{d(a)}$) are terms used to identify distribution coefficients that may not adhere to all the assumptions inherent in the theoretical K_d definition (such as the assumption of equilibrium and/or wholly reversible and instantaneous exchanges). In this publication, the term $K_{d(a)}$ is used for K_d values measured *in situ*. It is particularly relevant for freshwater or in marine systems. For example, in the coastal areas near the Fukushima Daiichi Nuclear Power Plant (FDNPP), which is an open system with considerable temporal variation in radionuclide activity concentrations in water, true equilibrium is not reached.

The apparent $K_{d(a)}$ values, derived from empirical measurements *in situ*, are estimated from the ratio of measured concentrations of an element or radionuclide in a geological material (e.g. a soil or sediment) and its corresponding contact solution (e.g. water column, groundwater) [2.24].

The use of *in situ* $K_{d(a)}$ is widespread, particularly for freshwater and marine systems [2.24]. *In situ* $K_{d(a)}$ values are most appropriate when the level of contamination in the solid phase is high enough to disregard the variability in obtaining and measuring a representative sample of the liquid phase, thereby easing analytical detection limitations. However, this approach may lead to $K_{d(a)}$ values that include sorbed radionuclide that is not reversibly bound due to the time elapsed since the radionuclide was incorporated into the solid phase, and thus not available for

exchange with the liquid phase. Therefore, *in situ* values may be higher than those derived from methods aiming at estimating reversible K_d .

Different approaches can be used to determine *in situ* $K_{d(a)}$, and each significantly affects the representativeness of the derived values [2.24]. In aquatic systems, *in situ* $K_{d(a)}$ values are usually determined for either bottom or for suspended sediments (SS) using different methods to separate the solid and liquid phases. For suspended sediments, separation may be achieved using sediment traps located in the waterflow, or by various gravitational, centrifugal, or filtration/ultrafiltration methods. Recent data from Japan showed the impact of the methodology used, as $K_{d(a)}$ values determined for caesium at Fukushima with sediment traps are generally lower than those obtained by filtration because these two methods do not generate the same particle size sorting [2.26]. Thus, the quantification of *in situ* $K_{d(a)}$ depends on whether dissolved or particulate forms of radionuclides in suspended or bottom sediments are being considered.

2.1.2.4. K_d derived from (laboratory) mass transport experiments

K_d values can be derived from the diffusion based mass transport pattern of a radionuclide in compacted solids, mainly in columns or in diffusion cells [2.24]. The approach considers the retardation of the radionuclide due to interactions with porous materials. The migration of radionuclides through solids under saturated and/or unsaturated conditions is simulated through mass transport experiments. They allow evaluation of radionuclide migration rates, while preserving the structure and compaction degree of soils. As a result, there is less solid particle alteration than that which occurs in batch experiments, and mass transport experiments can often produce more representative site specific results than the methods described above.

Mass transport experiments are usually carried out inside columns of sediment. A high pressure apparatus is used for experimentation on intact and fissured solid with low permeability. The associated equipment costs, time constraints, experimental complications, and variability of the resultant data limit the applicability of this approach [2.27].

Comparisons of K_d values from batch and mass transport experiments are currently based on scarce data and suggest contradictory information on whether the batch sorption methods over or underestimates K_d values [2.28, 2.29]. To date, more lower K_d values have been reported that have been derived from mass transport experiments in comparison to those derived from batch experiments, mostly due to the experimental conditions adopted in the batch studies, such as shaking and a higher L/M ratio [2.30].

Many fewer K_d data have been derived from mass transport experiments than from batch tests. For this reason, mass transport derived K_d values for soils and sediments are currently not included in the MODARIA K_d datasets. The inclusion of such data in the K_d datasets is a remaining challenge for the future.

2.2. GEOCHEMICAL PROCESSES CONTROLLING RADIONUCLIDE INTERACTION WITH SOLIDS

2.2.1. Introduction

An understanding of the assumptions and limitations of using K_d values in transport and radiological impact models is important for interpreting the derived results, adequately representing the modelled system, and identifying possible shortcomings of the model outcomes.

For example, one of the assumptions in K_d measurement and use in transport modelling is that of linearity (discussed in Chapter 3, Section 3.1.1), which states that the K_d remains constant, irrespective of the activity concentration of the radionuclide in the system. This is typically not an issue for radiological impact modellers because radionuclide activity concentrations are normally low in the environment. However, this becomes a compromising assumption for trivalent and tetravalent actinides near sources, such as facilities for disposal of highly radioactive waste, where elevated activity concentrations commonly exceed the solubility of the radionuclide, resulting in radionuclide partitioning in a non-linear manner.

K_d values are also used indirectly to estimate a wide range of different transport processes, including:

- (1) How rapidly the dissolved radionuclides move through porous or fractured media (i.e. retardation factor, R_f);
- (2) How rapidly radionuclides diffuse through porous media (i.e. effective diffusion coefficient, D_e);
- (3) The transport of radionuclides that move up and down the soil column (i.e. rate constant, λ , which is related to R_f);
- (4) Radionuclide partitioning in marine and stream systems between the aqueous/dissolved and the suspended solid fractions;
- (5) Uptake of available radionuclides by plants from the soil solution.

K_d values will vary for different environments as well as between radionuclides. Thus, the modeler has to understand not only the mathematics associated with the K_d construct, but also the biogeochemistry it is attempting to describe. To aid the end user in achieving this, the following sections describe the different geochemical processes that control radionuclide–soil interactions.

2.2.2. Geochemical radionuclide processes in terrestrial and aqueous systems

2.2.2.1. Processes in the aqueous phase

Typically, data indicating the extent of contamination (the total concentration of several dissolved substances) in an aqueous plume are provided to transport modellers, with little information on radionuclides mobility and bioavailability or the forms in which these are present in the plume. Contaminants can occur as soluble free, soluble complexed, adsorbed, organically complexed, precipitated, or coprecipitated species [2.5]. Insights into the geochemical processes involved in the formation of these species and their potential effects on the transport of contaminants are briefly discussed below.

Groundwater samples may contain over 100 different soluble species [2.31]. These soluble species commonly involve metal cations and organic or inorganic ligands. For example, the aqueous species $\text{Pu}(\text{Cl})_4$ (*aq*) is composed of the central atom of Pu and the ligand Cl (chloride). Similarly, the HCO_3^- complexes is composed of the central molecule CO_3^{2-} (carbonate) and the H^+ ligand. An inner-sphere complex is a compound in which the central group and ligand are in direct contact. An outer-sphere complex is a compound in which one or more water molecules exist between the central group and a ligand. Outer-sphere complexes are much less stable than inner-sphere complexes because the former has much weaker bonds formed between the central group and ligand.

Common groundwater anionic ligands include $\text{HCO}_3^-/\text{CO}_3^{2-}$, Cl^- , SO_4^{2-} and humic substances (i.e. natural organic materials) [2.5]. Dissolved PO_4^{3-} is typically present at much lower

concentrations but its presence, even at low concentrations, may have a profound effect on the speciation of radionuclides, especially multivalent cations, such as U and Pu. A general ranking of the propensity of these anionic ligands to form complexes with many metals is as follows: $\text{CO}_3^{2-} > \text{SO}_4^{2-} > \text{PO}_4^{3-} > \text{Cl}^-$ [2.19]. However, this ranking assumes equal ligand concentrations, which rarely happens in nature. Furthermore, some specific combination of radionuclides and ligands form especially strong complexes due to their electron orbital configurations, such as BaSO_4 (aq), SrSO_4 (aq), and various uranium phosphate species [2.32, 2.33]. There can be many dissolved, small chain humic substances present in groundwater and their complexation properties with cationic radionuclides are not well understood but are probably important when present in substantial amounts (>1 mg/L). For example, humic materials present in significant concentrations in shallow aquifers can dominate the metal chemistry [2.34]. Some organometallic ligand complexes can be quite stable and need either low or high pH conditions to dissociate.

Most of the time, the solution concentration of the central molecule is lowered through complexation (i.e. uncomplexed free species). Consequently, complexation may lower the potential for sorption and increase its solubility, both of which can enhance mobility. Conversely, some complexants, such as large molecular weight organic matter (OM) (e.g. humic acids) readily bond to soils and will reduce mobility of the complexed metals [2.35].

2.2.2.2. Oxidation–reduction (redox) processes

According to Ref. [2.5], the chemical reaction which involves a complete transfer of electrons from one species (the reductant) to another (the oxidant) is named an oxidation–reduction (redox) reaction. The consequence of this process is that the oxidation state of the radionuclide changes, which typically has considerable effects on K_d values. For example, Tc in the oxidized form, Tc(VII), has K_d values of about 1 mL/g, whereas in the reduced form, Tc(IV) has a K_d of about 1000 mL/g [2.36]. Similarly, Pu in the oxidized form Pu(V) may have a K_d of about 15 mL/g, whereas in the same soil, the reduced form Pu(IV) has a K_d value of about 6000 mL/g [2.36]. Other radionuclides that show significant changes in K_d values, depending on their oxidation state, include Np, Se and U. In general, radionuclide sorption increases as the oxidation state of the radionuclide decreases (i.e. under reducing conditions). However, a notable exception is radioiodine, as IO_3^- reduces to I^- [2.36, 2.37]. For both elements, the K_d values decrease by about an order of magnitude, as they are reduced to their lower oxidation state. Table 2.1 lists several redox sensitive metals and the valence states in which they may exist in the soil/groundwater system.

The sequence in which inorganic elements become reduced is well established (Table 2.2). When an oxidized system undergoes reduction, the order in which oxidized species become reduced (at pH 7) is O_2 , NO_3^- , Mn^{4+} , Fe^{3+} , SO_4^{2-} , and organic matter. As the redox potential E_h of the system drops below 0.6 V, enough electrons become available to reduce O_2 to H_2O [2.19].

TABLE 2.1 REDOX-SENSITIVE METALS AND THEIR MOST COMMON VALENCE STATES IN SOIL/GROUNDWATER SYSTEMS [2.19]

| Element | Common Valence States | Element | Common Valence States |
|-----------|-----------------------|------------|-----------------------|
| Americium | +3 | Neptunium | +4 and +5 |
| Antimony | +3 and +5 | Plutonium | +3, +4, +5 and +6 |
| Chromium | +3 and +6 | Selenium | -2, +4, and +6 |
| Iron | +2 and +3 | Technetium | +4 and +7 |
| Iodine | -1 and +5 | Uranium | +4 and +6 |
| Manganese | +2 and +3 | | |

TABLE 2.2. SEQUENCE OF PRINCIPLE ELECTRON ACCEPTORS IN NEUTRAL pH AQUATIC SYSTEMS [2.19]

| Reduction Half-Reactions | Range of Initial Eh Values (V) |
|--|----------------------------------|
| $0.5O_2(g) + 2e^- + 2H^+ = H_2O$ | 0.6 to 0.4 |
| $NO_3^- + 2e^- + 2H^+ = NO_2^- + H_2O$ | 0.5 to 0.2 |
| $MnO_2(s) + 2e^- + 4H^+ = Mn^{2+} + 2H_2O$ | 0.4 to 0.2 |
| $FeOOH(s) + e^- + 3H^+ = Fe^{2+} + 2H_2O$ | 0.3 to 0.1 |
| $SO_4^{2-} + 8e^- + 9H^+ = HS^- + 4H_2O$ | 0 to -0.15 |
| $H^+ + e^- = 0.5H_2(g)$ | -0.15 to -0.22 |
| $(CH_2O)_n = (n/2)CO_2(g) + (n/2)CH_4^a$ | -0.15 to -0.22 |

^a $(CH_2O)_n$ is representative of natural OM.

In other words, below an Eh of 0.6 V, $O_2(aq)$ is not stable in pH neutral systems. Below Eh 0.6 V, $O_2(g)$ is used in respiration by aerobic microorganisms. As the Eh decreases below 0.5 V, electrons become available to reduce NO_3^- to NO_2^- and below about 0.4 V, electron activity becomes sufficient to support the reduction of iron and manganese in solid phases. Only when O_2 and NO_3^- are depleted will iron reduction occur. In the case of iron and manganese, decreasing Eh results in the dissolution of Mn(IV) and Fe(III) solid phases. The increase in the dissolved concentrations of Fe(II) and Mn(II/III) is expected from the effect of lowered Eh , however a marked increase is usually detected in the concentrations of associated metals, such as cadmium, chromium and lead, in the aqueous phase, and of ligands, such as $H_2PO_4^-$ [2.19]. Typically, the metals released, including iron and manganese, are soon re-adsorbed by solids that are stable at lower Eh values (e.g. clay minerals or OM), and become exchangeable species. As Eh becomes negative, sulphate reduction can take place. Metals and radionuclides can react with bisulphide (HS^-) to form metal sulphides that are quite insoluble.

The oxidation state of non-radioactive soil constituents has a considerable impact on K_d values. The various redox couples have different tendencies to complex radionuclides. For example, $FeOOH(s)$ (iron oxide minerals) can immobilize many radionuclides, and once it undergoes reduction to form Fe^{2+} , the bound radionuclides are released into the mobile aqueous phase (Table 2.2). Similarly, as $MnO_2(s)$ solid mineral phases become reduced to a dissolved form of Mn^{2+} , the radionuclides bound to $MnO_2(s)$ are released into the aqueous phase. Therefore, the effective K_d values decrease under reducing conditions, as opposed to oxidizing conditions, as the Fe and Mn solid phases dissolve. Conversely, under reducing conditions, sulphides tend to accumulate in the solid phase, and they promote the precipitation of many transition metals, including Cr, Cd, Am, Cm, and Eu [2.24].

2.2.2.3. Consideration of the gaseous phase and soil microorganism processes in deriving K_d values for some radionuclides

Some elements, such as carbon, selenium and iodine, are re-emitted from soil to the atmosphere in gaseous forms [2.38–2.42]. For example, iodine can be emitted, mainly as methyl iodide (CH_3I), through the action of soil bacteria [2.38]. The volatilization process affects K_d values, as the gaseous phase of a radionuclide is not usually considered. If a proportion of a given radionuclide in the soil solution is emitted into the air, the resulting K_d value will be overestimated.

The presence of microorganisms is a major factor influencing the volatilization of some radionuclides and has been studied for radioisotopes such as ^{14}C and I. Microorganisms have been shown to contribute to the partitioning of ^{14}C in soils [2.40]. When the action of soil

microorganisms was inhibited, only a low fraction of the added ^{14}C was released into the air, whereas up to about 70% of the added ^{14}C was released from untreated (uninhibited) samples. An effect of microbial activity on iodide (I^-) partitioning in solid, liquid, and gaseous phases has been shown in Japanese agricultural soils under varying temperatures in batch sorption experiments [2.43, 2.44]. The limited amount of iodide partitioning to the gas and solid phases at 4°C was attributed to diminished microbial activity at low temperature, resulting in reduced iodide fixation by soil microorganisms and increased volatilization. This process had a significant effect on the iodide K_d values, with GM values increasing between temperatures of 4°C and 23°C in both paddy (from 22 to 67 L/kg) and upland soils (from 9 to 21 L/kg). The mechanisms are probably related to soil organisms that are involved in the fixation of iodine from soil solution onto soil particles [2.45]. Further details of these two cases are described in Annex II.

2.2.2.4. *Processes leading to the sorption of radionuclides in the solid/solution system*

Sorption is a generic term, unrelated to mechanisms governing the partitioning of aqueous phase constituents to a solid phase. Without extensive testing or the use of spectroscopic or microscopic techniques, it is not possible to determine whether a radionuclide is adsorbed onto the surface of a solid, absorbed into the solid structure, precipitated on the solid surface of the solid, or partitioned into OM [2.24, 2.46].

In many natural systems, the extent of sorption is controlled by the electrostatic surface charge of the mineral phase. For some minerals, such as aluminium, iron, and manganese oxyhydroxides and OM, the surface charge varies with the pH. Variably charged surfaces are especially important for sorbing radionuclides in semitropical and tropical regions, and in young soils that originate from volcanic activity. In variably charged soils, the magnitude and polarity of the net surface charge changes with several factors, including pH [2.19]. The negative charge of the surface increases with increasing pH as an increasing number of hydroxides, OH^- , bind to the surface. As the pH decreases, there is a general increase in positive charge as an increasing number of protons, H^+ , bind to the surface. The positive charge provides an electrostatic attraction to anions, a trait that is very weak or non-existent in permanently charged minerals (which tend to be negatively charged [2.47]).

2.2.3. **Adsorption and desorption processes**

Adsorption is defined as the accumulation of matter at the interface between two phases, solid and aqueous solution, respectively [2.48]. Adsorption is the uptake of dissolved radionuclides onto the surface of the structure layers of the mineral. Adsorption and precipitation differ, as the latter includes the development of a three dimensional molecular structure. The adsorbate is matter that accumulates at the interface, in two dimensional molecular arrangements, and the adsorbent is the solid surface on which the matter accumulates.

Adsorption onto clay particle surfaces can take place via two mechanisms [2.48]. The first mechanism involves formation of an inner-sphere surface complex that is in direct contact with the adsorbent surface and lies within the Stern Layer (Fig. 2.1) [2.47]. The second mechanism creates an outer-sphere surface complex that has at least one water molecule between the cation and the adsorbent surface. These ions reside in the Gouy Diffuse Layer extending from the outer limit of the Stern Layer surface into the surrounding liquid ('bulk water').

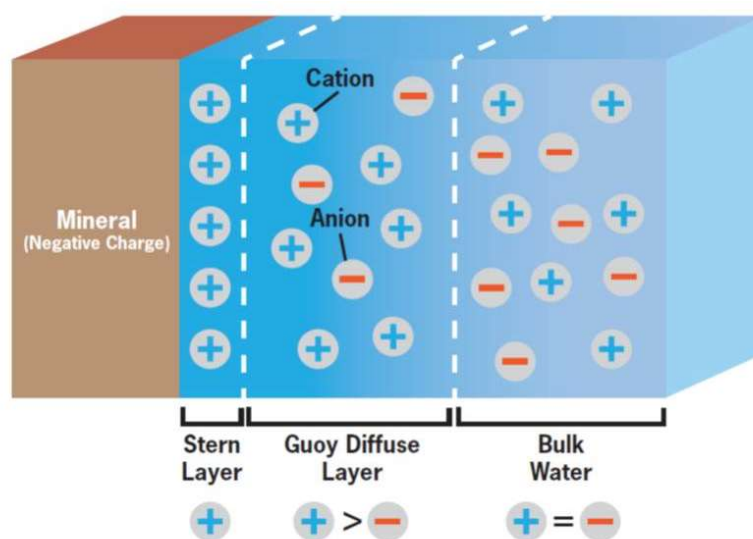


FIG. 2.1. Stern layer and Gouy diffuse layer in the water in contact with a negatively charged surface.

Anions also adsorb by inner- and outer-sphere surface complexation [2.18]. Anionic radionuclides that are likely to form a greater proportion of outer-sphere bonds to mineral surfaces include TcO_4^{2-} , I^- , HCO_3^- , Cl^- , and SeO_3^{2-} , whereas IO_3^- and SeO_4^{2-} are more likely to form inner-sphere bonds [2.18, 2.37].

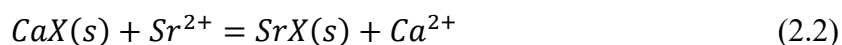
Generally, an increased tendency of a free metal cation to form inner-sphere surface complexes (correlated to a higher ionic potential of the cation) relates to an increased relative affinity of a sorbent for that cation. Based on these considerations and laboratory observations, the relative adsorption affinity of metals has been described, as follows [2.18]:

- (a) Group IA elements: $\text{Cs}^+ > \text{Rb}^+ > \text{K}^+ > \text{Na}^+ > \text{Li}^+$
- (b) Group IIA elements: $\text{Ba}^{2+} > \text{Sr}^{2+} > \text{Ca}^{2+} > \text{Mg}^{2+}$
- (c) Transition elements: $\text{Hg}^{2+} > \text{Cd}^{2+} > \text{Zn}^{2+}$
- (d) Influence of element valence: $\text{Fe}^{3+} > \text{Fe}^{2+}$

These rankings follow trends related to the periodic table. The relative adsorption affinity of Group IA (a) and IIA (b) elements increases with atomic weight. There is a general trend amongst the transition elements (c) that higher atomic weight elements within a periodic group tend to have greater relative adsorption affinity to charged surfaces. Finally, the greater the valence of an element (d), the greater its relative adsorption affinity.

Ionic potential alone cannot explain the adsorption affinity for transition metal cations since electron configuration also plays an important role in the complexation of these cations. Their relative affinities tend to follow the Irving-Williams order: $\text{Cu}^{2+} > \text{Ni}^{2+} > \text{Co}^{2+} > \text{Fe}^{2+} > \text{Mn}^{2+}$. The molecular basis for this trend is discussed in Ref. [2.49].

Ion exchange is a common adsorption reaction in soils, involving an exchange of an ionic species between a solid phase and an aqueous solution in contact with the solid. Thus, a previously sorbed ion of weaker affinity is exchanged on the soil and replaced with another ion with a stronger affinity ion from the surrounding aqueous solution. Most metals in aqueous solution adsorb primarily in response to electrostatic attraction due to their occurrence as charged ions, for example, in the cation exchange reaction shown in Eq. (2.2):



The amount of Ca or Sr bound to exchange sites is termed CaX(s) and SrX(s). Sr²⁺ replaces Ca²⁺ at the exchange site, X. The equilibrium constant (K_{ex}) for the exchange reaction is defined by Eq. (2.3):

$$K_{ex} = \frac{\{SrX(s)\}\{Ca^{2+}\}}{\{CaX(s)\}\{Sr^{2+}\}} \quad (2.3)$$

There are numerous ion exchange models from which K_d can be derived (such as those described by [2.31] and [2.19]). For example, in Eq. (2.2), because the concentration of calcium is commonly much greater than the concentration of strontium in a system, the concentration of Ca²⁺ and CaX can be assumed to remain constant. This assumption permits setting K_{ex} equal to K_d :

$$K_d = K_{ex} = \frac{\{SrX(s)\}}{\{Sr^{2+}\}} \quad (2.4)$$

2.2.4. Precipitation and dissolution processes

The precipitation reaction of dissolved species is a special case in which a solid is formed by two or more aqueous species. Precipitation may be particularly important for multivalent radionuclides (e.g. Pu(IV), U(IV), and Am(III)) in soil/groundwater systems [2.18]. Precipitation occurs when the dissolved radionuclide concentration exceeds a solubility limit, that varies with radionuclide and the aqueous chemistry. For instance, the pH can greatly influence the solubility limit of most radionuclides (an example is presented below). Precipitation is an especially important process controlling radionuclide aqueous concentrations near point sources, such as disposed radionuclide waste.

In solubility controlled models, it is assumed that a known solid is present, or rapidly forms, and controls the concentration of the constituents (i.e. radionuclides) in the aqueous phase. These are thermodynamic equilibrium models in which the time (i.e. kinetics) needed to dissolve or completely precipitate the constituents is not considered. An empirical solubility release model² can be generated from data resulted from empirical solubility experiments. A solubility limit is not a constant value when the system is chemically dynamic but is determined by the product of the thermodynamic concentrations (more specifically, ionic strength corrected activities) of species that constitute the solid. If the chemistry of the system changes, especially in terms of pH and/or redox state, then the concentrations of individual species often change. For example, if the controlling solid for plutonium is the hydrous oxide Pu(OH)₄, the solubility product, K_{sp} , is the plutonium concentration multiplied by the hydroxide activity taken to the fourth power, i.e. $[Pu][OH]^4 = K_{sp}$. If the pH decreases by one unit (i.e. the OH concentration decreases by a factor of 10), then for K_{sp} to remain constant, the concentration of Pu has to increase by 10⁴. Therefore, the solubility product is highly dependent on the chemistry of the aqueous phase and needs to be calculated for each set of environmental conditions.

² An empirical solubility release model is mathematically similar to the solubility construct but has no well-identified thermodynamically controlling solid.

2.2.5. Absorption processes

By definition, the process of radionuclide absorption results in extremely strong bonds being formed with the solid phase, typically forming structural bonds with the solid phase. There are three classical examples of radionuclide absorption. The first example is Cs^+ uptake into the edge sites of illitic minerals (vermiculite/mica-type clays) [2.50]. This is the most extensively studied reaction between radionuclides and mineral surfaces in the literature, primarily because of its unique nature, its potential application in treating waste streams and in environmental remediation, and its ease of measurement [2.51]. The second example of absorption is the long term migration of divalent cations into zeolites [2.52]. The third example involves initial coprecipitation of the radionuclide, followed by ageing in the subsurface, resulting in the coprecipitate phase being buried beneath subsequent precipitation [2.53–2.56]. A few examples include U being absorbed into iron oxyhydroxide phases [2.56], and Sr and Ba being absorbed into carbonate phases [2.53, 2.54].

2.3. SORPTION MODELS

This section provides a brief description of some of the more common sorption models, of which several are directly based on the K_d concept. It also describes the underlying assumptions of the various models and provides references to more detailed information.

2.3.1. Parametric K_d model

A parametric K_d model is derived from aqueous and solid phase independent variables as a function of empirically derived multivariate relationships, often obtained from a series of measurements made over a range of conditions. Parametric K_d models have the distinct advantage of being more robust, as it becomes unnecessary to determine new K_d values for each set of environmental conditions. Standard linear or non-linear regression, stepwise regression, and adaptive learning networks (see Refs [2.17, 2.57]) are used through statistical methods to derive quantitative predictor equations. Parametric K_d equations are only appropriate for use to calculate K_d values for systems within the range of the independent variables that have been included to create the equation. For example, the following parametric K_d model has been developed for Ce based on the characteristics of a given radioactive waste disposal site [2.57]:

$$\lg K_d(\text{Ce}) = 3.51 + 0.5440 (\text{pH}) - 0.0220 (\text{sand}) - 0.0220 (\text{silt}) - 0.0047 (\text{clay} \times \text{pH}) \quad (2.5)$$

where the units for K_d is L/kg, sand and silt are wt% (weight percentage), and the interaction term of ‘clay × pH’ is unitless. This multiple regression equation indicates that $\lg K_d(\text{Ce})$ values increase with pH and decrease with sand and silt concentrations. Equation (2.5) can be used to estimate $K_d(\text{Ce})$ values at this potential disposal site as a function of pH, sand, silt, and clay contents. As is true for all correlation type statistics, these types of parametric relationships do not address causality and, therefore, provide no information on the mechanism by which the radionuclide is partitioned between the solution and the solid phase.

2.3.2. Coupling K_d and kinetic approach

The K_d model describes equilibrium conditions, even though it is well known that sorption may change with time. Models have been developed that include both equilibrium and kinetic situations that take into consideration that the K_d may gradually approach steady state. Such

models, though important, are outside the scope of this publication because no effort is made here to parameterize such models.

The processes of sorption are not instantaneous, and the time taken for equilibrated conditions to be reached depends on the radionuclide and the environmental conditions. Consequently, the modelling of complex conditions characterized by a succession of different conditions of sorption needs at least some consideration of K_d values specific to each set of conditions, as well as the kinetics of each process. Under such conditions, an alternative and operational approach is to combine partition equilibrium and kinetic sorption approaches [2.4, 2.58–2.61]. Examples of such coupled models can be found in Annexes III and IV.

2.3.3. Isotherm sorption (empirical) models

A mathematical description of the experimental data that is not based on a particular theory or mechanistic understanding defines an empirical model. For example, the K_d , Freundlich isotherm and Langmuir isotherm are considered empirical models by this definition [2.31].

A ‘sorption isotherm’ can be derived from experiments that include a suite of different tests to evaluate the effect of various parameters, such as pH, concentrations of competing ions, or initial radionuclide activity concentrations, on the radionuclide activity concentration in solution or sorbed, while other parameters are held constant (Fig. 2.2). For soils, radionuclide sorption can deviate from a linear relationship between aqueous and soil bound radionuclide activity concentration, especially when activity concentrations are elevated. At low radionuclide activity concentrations, the ratio of sorption sites to radionuclide molecules is high and, therefore, ideal for rapid sorption during which the presence of a sorbed solute will not interfere with the subsequent sorption of other radionuclides. Once this ratio decreases below a critical point, the surface bound radionuclides interfere with additional sorption and the sorption isotherm becomes non-linear, often referred to as the Freundlich portion of the isotherm (Fig. 2.2).

$$C_{solid} = K_F \times C_{liquid}^N \quad (2.6)$$

where:

- C_{solid} is the activity concentration of radionuclide sorbed per unit mass;
- C_{liquid} is the equilibrium radionuclide activity concentration in solution;
- K_F is the Freundlich adsorption constant;
- N is a constant approximating site heterogeneity (unitless).

As the aqueous radionuclide activity concentration in an adsorption isotherm continues to increase, all the sorption sites may become saturated, resulting in a plateau of the isotherm referred to as the sorption site saturation point. Such an isotherm behaviour is commonly referred to as a Langmuir model, as described by the following equation:

$$C_{solid} = \frac{K_L \times A_m \times C_{liquid}}{1 + K_L \times C_{liquid}} \quad (2.7)$$

where:

- K_L is the Langmuir adsorption constant related to the energy of adsorption;
- A_m is the maximum adsorption capacity of the solid.

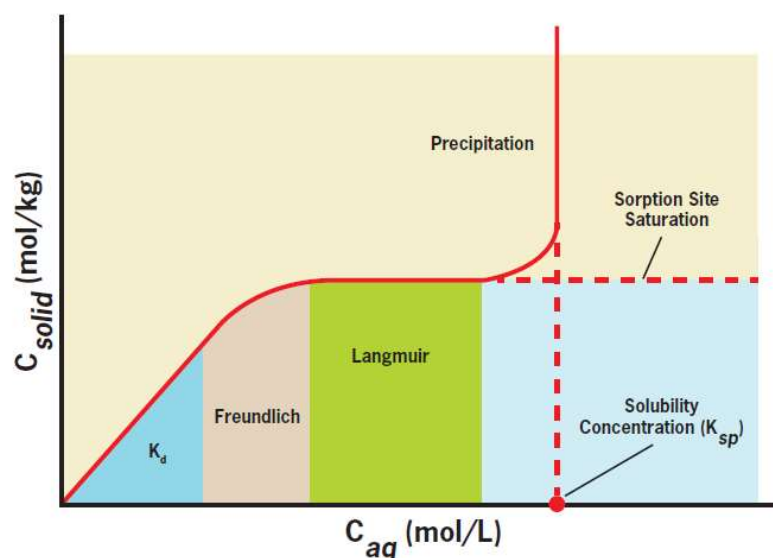


FIG. 2.2. Sorption isotherm (aqueous radionuclide activity concentration, C_{liquid} (C_i), versus surface bound radionuclide, C_{solid} (A_i)) identifying the linear range (K_d), non-linear range (Freundlich sorption), the plateau region (Langmuir sorption), and the solubility concentration (K_{sp}).

Alternatively, at high radionuclide activity concentrations, precipitation may occur, at which point the aqueous radionuclide activity concentration does not increase as additional radionuclides are added to the system and the sorption is no longer a linear process. This is referred to as a solubility controlled system. Therefore, for the compilation of K_d values in the MODARIA dataset, attempts were made to select only those data that were in the linear range of the adsorption isotherm.

2.3.4. Surface complexation models

Surface complexation models (SCMs) are semimechanistic models that determine the chemical and electrostatic forces involved in ion retention by minerals. Properties, such as radionuclide activity concentration, competing ion concentration, variable surface charge on the adsorbent and/or solute species solution distribution, are accounted for in SCMs. SCMs are more robust than the K_d model for predicting how radionuclide sorption varies as a function of changing aqueous chemistry; however, they need a great deal of additional site specific information. Equally important, they necessitate a much greater knowledge of geochemistry to implement. SCMs have been in use since the 1950s and have been reviewed in the literature [2.31, 2.62–2.65].

Thermodynamic concepts, such as reactions described by mass action laws, material balance equations, and surface charge are the basis of SCMs. They do not explicitly address kinetic considerations. The three most used surface charge models are: the constant capacitance model, the diffuse layer model, and the triple layer model (reviewed in Ref. [2.31]). Each of these models assume that: (1) protons are the dominant potential determining ion, meaning that protons control surface charge; (2) all surfaces have a single type of binding site; (3) each site can undergo two protonation reactions; and (4) there is a strict distinction between inner- and outer-sphere complexes (see Fig. 2.1). A key application of SCMs is their contribution to increased understanding of the chemistry at the aqueous and solid phase interface and their use in describing data from complex multicomponent systems, for which the mathematical formulation for an empirical model might not be obvious.

REFERENCES TO CHAPTER 2

- [2.1] GONZE, M.A., et al., SYMBIOSE: a simulation platform for conducting radiological risk assessments. International Conference on Radioecology and Environmental Radioactivity (ICRER). 19–24 June 2011, Hamilton, Ontario, Canada (2011).
- [2.2] SIMON-CORNU, M., et al., Evaluating variability and uncertainty in radiological impact assessment using SYMBIOSE, *J. Environ. Radioact.* **139** (2015) 91.
<https://doi.org/10.1016/j.jenvrad.2014.09.014>
- [2.3] INTERNATIONAL ATOMIC ENERGY AGENCY, Handbook of Parameter Values for the Prediction of Radionuclide Transfer in Terrestrial and Freshwater Environment, Technical Reports Series No. 472, IAEA, Vienna (2010).
- [2.4] INTERNATIONAL COMMISSION ON RADIATION UNITS AND MEASUREMENTS, Quantities, Units and Terms in radioecology, ICRU Report 65, Nuclear Technology Publishing (2001).
<https://www.icru.org/report/quantities-units-and-terms-in-radioecology-report-65/#:~:text=This%20Report%20provides%20the%20first,highly%20interdisciplinary%20field%20of%20radioecology.>
- [2.5] SPARKS, D.L., Environmental Soil Chemistry – 2nd Edition, Academic Press, New York (2003). <https://doi.org/10.1016/C2009-0-02455-6>
- [2.6] GARCIA-SANCHEZ, L., LOFFREDO, N., MOUNIER, S., MARTIN-GARIN, A., COPPIN, F. Kinetics of selenate sorption in soil as influenced by biotic and abiotic conditions: a stirred flow-through reactor study. *J. Environ. Radioact.* **138** (2014) 38. <https://doi.org/10.1016/j.jenvrad.2014.07.009>
- [2.7] GOLDBERG, S., et al., Adsorption – desorption processes in subsurface reactive transport modeling, *Vadose Zone J.* **6** (2007) 407.
<https://doi.org/10.2136/vzj2006.0085>
- [2.8] TEBES-STEVENSON, C.L., ESPINOZA, F., VALOCCHI, A.J., Evaluating the sensitivity of a subsurface multicomponent reactive transport model with respect to transport and reaction parameters. *Journal of Contaminant Hydrology* **52** (2001) 3.
[https://doi.org/10.1016/S0169-7722\(01\)00151-6](https://doi.org/10.1016/S0169-7722(01)00151-6)
- [2.9] PIEPHO, M.G., SERNE, R.J., KAPLAN, D.I., LANGFORD, D.W., Importance Ranking of Near- and Far-Field Transport Parameters for a LLW Glass Performance Assessment, Rep. No. WHC-8H210-MGP-18. Westinghouse Hanford Company, Richland, W.A. (1994).
- [2.10] ZHENG, C., BENNETT, G.D., Applied contaminant transport modeling, Wiley-Interscience, New York (2002) 656p.
- [2.11] INTERNATIONAL ATOMIC ENERGY AGENCY, Sediment Distribution Coefficients and Concentration Factors for Biota in the Marine Environment, Technical Reports Series No. 422, IAEA, Vienna (2004).
- [2.12] THIBAUT, D.H., SHEPPARD, M.I., SMITH, P.A., A critical compilation and review of default soil solid/liquid partition coefficients, K_d , for use in environmental assessments, AECL 10125, Atomic Energy of Canada Limited, Pinawa, Manitoba, Canada (1990).
<https://www.nrc.gov/docs/ML0403/ML040370028.pdf>

- [2.13] INTERNATIONAL ATOMIC ENERGY AGENCY, Handbook of Parameter Values for the Prediction of Radionuclide Transfer in Temperate Environments, Technical Reports Series No. 364, IAEA, Vienna (1994).
- [2.14] ALLISON, J.D., ALLISON, T.L., Partition coefficient for metals in surface water, soil, and waste, EPA/600/R-05/074 Washington, DC, United States (2005).
https://cfpub.epa.gov/si/si_public_record_report.cfm?dirEntryId=135783&Lab=NERL
- [2.15] DURRIEU, G., CIFFROY, P., GARNIER, J.M., A weighted bootstrap method for the determination of probability density functions of freshwater distribution coefficients (K_{ds}) of Co, Cs, Sr and I radioisotopes, Chemosphere. **65** (2006) 1308.
<https://doi.org/10.1016/j.chemosphere.2006.04.028>
- [2.16] CIFFROY, P., DURRIEU, G., GARNIER, J.-M., Probabilistic distribution coefficients (K_{ds}) in freshwater for radioisotopes of Ag, Am, Ba, Be, Ce, Co, Cs, I, Mn, Pu, Ra, Ru, Sb, Sr and Th. – Implications for uncertainty analysis of models simulating the transport of radionuclides in rivers, J. Environ. Radioact. **100** (2009) 785. <https://doi.org/10.1016/j.jenvrad.2008.10.019>
- [2.17] SHEPPARD, S.C., Robust Prediction of K_d from Soil Properties for Environmental Assessment, Human and Ecological Risk Assessment: An International Journal **17** (2011) 263. <https://doi.org/10.1080/10807039.2011.538641>
- [2.18] SPOSITO, G., The Chemistry of Soils – 3rd Edition, Oxford University Press, New York (2016). <https://doi.org/10.1093/oso/9780190630881.001.0001>
- [2.19] STUMM, W., MORGAN, J.J., Aquatic Chemistry, Chemical Equilibria and Rates in Natural Waters, John Wiley & Sons, Inc., New York (2012).
- [2.20] AMERICAN SOCIETY FOR TESTING AND MATERIALS, Standard American Society for Testing and Materials D4319-93. Standard test method for distribution ratios by the short-term batch method. ASTM Publications, West Conshohocken, PA, US (2001). https://standards.iteh.ai/catalog/standards/astm/3b73c0be-e839-4efa-889c-3b73ed0610b9/astm-d4319-93?srsId=AfmBOorJE1Lz9qJGSOdMXuoAsVbvS72xuhno-mBJ-7JanvrElpQyx_8B
- [2.21] ORGANISATION FOR ECONOMIC COOPERATION AND DEVELOPMENT, Guideline for the testing of chemicals: Adsorption-desorption using a batch equilibrium method, Guideline 106 (2000).
<https://doi.org/10.1787/9789264069602-en>
- [2.22] AMERICAN SOCIETY FOR TESTING AND MATERIALS, Standard American Society for Testing and Materials D4646-03. Standard Test Method for 24-h Batch-type Measurement of Contaminant Sorption by Soils and Sediments. ASTM Publications, West Conshohocken, PA (2003).
<https://www.astmonline.com/standards/ASTM-D4646-03/>
- [2.23] AMERICAN SOCIETY FOR TESTING AND MATERIALS, Standard American Society for Testing and Materials C1733–10. Standard Test Method for Distribution Coefficients of Inorganic Species by the Batch Method. ASTM Publications, West Conshohocken, PA (2010).
<https://cdn.standards.iteh.ai/samples/75092/ef6c41120d824aeb8b57361d4d80af25/ASTM-C1733-10.pdf>

- [2.24] KRUPKA, K.M., KAPLAN, D.I., WHELAN, G., SERNE, R.J., MATTIGOD, S.V., Understanding Variation in Partition Coefficient, K_d , Values. Volume II: Review of Geochemistry and Available K_d Values for Cadmium, Cesium, Chromium, Lead, Plutonium, Radon, Strontium, Thorium, Tritium (3H), and Uranium, EPA 402-R-99-004, US-EPA, Washington DC (1999).
<https://ouci.dntb.gov.ua/en/works/lxGAaaL4/>
- [2.25] HAAPANEN, R., ARO, L., HELIN, J., IKONEN, A., LAHDENPERÄ, A.M., POSIVA Report WR-2012-102. Studies on reference mires: 1. Lastensuo and Pesänsuo in 2010-2011, Posiva, Eurajoki (2013).
https://www.researchgate.net/publication/305475855_Studies_on_reference_mires_1_Lastensuo_and_Pesansuo_in_2010-2011
- [2.26] EYROLLE-BOYER, F., et al., Behaviour of radiocaesium in coastal rivers of the Fukushima Prefecture (Japan) during conditions of low flow and low turbidity – Insight on the possible role of small particles and detrital organic compounds, *J. Environ. Radioact.* **151** (2016) 328. <https://doi.org/10.1016/j.jenvrad.2015.10.028>
- [2.27] YU, C., KAMBOJ, S., WANG, C., CHENG, J.J., Data collection handbook to support modeling impacts of radioactive material in soil and building structures, ANL/EVS/TM-14/4. Environmental Science Division, Argonne National Laboratory, Lemont (2015).
- [2.28] OCHS, M., LOTHENBACH, B., WANNER, H., SATO, H., YUI, M., An integrated sorption-diffusion model for the calculation of consistent distribution and diffusion coefficients in compacted bentonite, *J. Contam. Hydrol.* **47** (2001) 283.
[https://doi.org/10.1016/S0169-7722\(00\)00157-1](https://doi.org/10.1016/S0169-7722(00)00157-1)
- [2.29] WANG, T.-H., LI, M.-H., TENG, S.P., Bridging the Gap between Batch and Column Experiments: A Case Study of Cesium Adsorption on Granite, *J. Hazard. Mater.* **161** (2009) 409. <https://doi.org/10.1016/j.jhazmat.2008.03.112>
- [2.30] ALDABA, D., RIGOL, A., VIDAL, M., Diffusion experiments for estimating radiocesium and radiostrontium sorption in unsaturated soils from Spain: Comparison with batch sorption data, *J. Hazard. Mater.* **181** (2010) 1072.
<https://doi.org/10.1016/j.jhazmat.2010.05.124>
- [2.31] SPOSITO, G., *The Surface Chemistry of Soils*, Oxford University Press, New York (1984).
- [2.32] KIM, J.I., Chemical behavior of transuranic elements in aquatic systems, *Handbook on the Physics and Chemistry of the Actinides* (FREEMAN, A.J., KELLER, C., Eds), Elsevier Science Publishers, Amsterdam (1986) 413.
- [2.33] RAI, D., et al., Uranium (IV) hydrolysis constants and solubility product of $UO_2 \times H_2O(am)$, *Inorg. Chem.* **29** (1990) 260. <https://doi.org/10.1021/ic00327a022>
- [2.34] KALBITZ, K., et al., Controls on the dynamics of dissolved organic matter in soils: a review, *Soil Sci.* **165** (2000) 277.
https://journals.lww.com/soilsci/abstract/2000/04000/controls_on_the_dynamics_of_dissolved_organic.1.aspx
- [2.35] XU, C., et al., Plutonium immobilization and re-mobilization by soil mineral and organic matter in the far-field of the Savannah River Site, USA, *Environ. Sci. Technol.* **48** (2014) 3186. <https://doi.org/10.1021/es404951y>

- [2.36] KAPLAN, D.I., Geochemical Data Package for Performance Assessment and Composite Analysis at the Savannah River Site, SRNL-STI-2009-00473. Rev. 1, Savannah River National Laboratory, Aiken, SC (2016). DOI: [10.13140/RG.2.1.2288.4085](https://doi.org/10.13140/RG.2.1.2288.4085)
- [2.37] KAPLAN, D.I., et al., Radioiodine biogeochemistry and prevalence in groundwater, *Critical Rev. Environ. Sci. Technol.* **44** (2014) 2287. <https://doi.org/10.1080/10643389.2013.828273>
- [2.38] AMACHI, S., et al., Microbial participation in iodine volatilization from soils, *Environ. Sci. Technol.* **37** (2003) 3885. DOI: [10.1021/es0210751](https://doi.org/10.1021/es0210751)
- [2.39] DORAN, J.W., ALEXANDER, M., Microbial Formation of Volatile Selenium Compounds in Soil, *Soil Sci. Soc. Am. J.* **41** (1977) 70. <https://doi.org/10.2136/sssaj1977.03615995004100010022x>
- [2.40] ISHII, N., KOISO, H., TAKEDA, H., UCHIDA, S., Partitioning of ^{14}C into solid, liquid, and gas phases in various paddy soils in Japan, *J. Nucl. Sci. Technol.* **47** (2010) 238. DOI: [10.1080/18811248.2010.9711950](https://doi.org/10.1080/18811248.2010.9711950)
- [2.41] REDEKER, K.R., et al., Emissions of methyl halides and methane from rice paddies, *Science* **290** (2000) 966. DOI: [10.1126/science.290.5493.966](https://doi.org/10.1126/science.290.5493.966)
- [2.42] WHITEHEAD, D., The volatilisation from soils and mixtures of soil components of iodine added as potassium iodide, *J. Soil Sci.* **32** (1981) 97. <https://doi.org/10.1111/j.1365-2389.1981.tb01689.x>
- [2.43] ISHIKAWA, N., UCHIDA, S., TAGAMI, K., Iodide sorption and partitioning in solid, liquid and gas phases in soil samples collected from Japanese paddy fields, *Radiat. Prot. Dosim.* **146** (2011) 155. <https://doi.org/10.1093/rpd/ncr126>
- [2.44] ISHIKAWA, N.K., TAGAMI, K., UCHIDA, S., Effect of biological activity due to different temperatures on iodide partitioning in solid, liquid, and gas phases in Japanese agricultural soils, *J. Radioanal. Nucl. Chem.* **295** (2013) 1763. <https://doi.org/10.1007/s10967-012-2096-0>
- [2.45] JOHANSON, K.J., Iodine in Soil. Technical Report TR-00-21, Svensk Kärnbränslehantering AB, Stockholm (2000). <https://www.skb.se/publikation/18295/TR-00-21.pdf>
- [2.46] SELIM, H.M., SPARKS, D.L., Heavy Metals Release in Soils, CRC Press, Boca Raton, FL (2001) 249. <https://doi.org/10.1201/9780367801366>
- [2.47] HIEMENZ, P.C., RAJAGOPALAN, R., Principles of Colloid and Surface Chemistry, Marcel Dekker, Inc., New York (1997) 491p. <https://doi.org/10.1201/9781315274287>
- [2.48] KABATA-PENDIAS, A., Trace Elements in Soils and Plants, CRC Press, Boca Raton, FL (2010) 377. <https://doi.org/10.1201/b10158>
- [2.49] COTTON, F.A., WILKINSON, G., MURILLO, C.A., BOCKMAN, M., Advanced Inorganic Chemistry, 6th Edition. John Wiley (2000).
- [2.50] FRANCIS, C.W., BRINKLEY, F.S., Preferential adsorption of ^{137}Cs to micaceous minerals in contaminated freshwater sediment, *Nature* **260** (1976) 511. <https://doi.org/10.1038/260511a0>
- [2.51] CORNELL, R., Adsorption of cesium on minerals: A review, *J. Radioanal. Nucl. Chem.* **171** (1993) 771. <https://doi.org/10.1007/BF02219872>

- [2.52] RIVERA, N., et al., Cesium and strontium incorporation into zeolite-type phases during homogeneous nucleation from caustic solutions, *Am. Mineralogist* **96** (2011) 1809. DOI: [10.2138/am.2011.3789](https://doi.org/10.2138/am.2011.3789)
- [2.53] TESORIERO, A., PANKOW, J.F., Solid solution partitioning of Sr²⁺, Ba²⁺, and Cd²⁺ to calcite, *Geochim. Cosmochim. Acta* **60** (1996) 1053. [https://doi.org/10.1016/0016-7037\(95\)00449-1](https://doi.org/10.1016/0016-7037(95)00449-1)
- [2.54] MORSE, J.W., ARAKAKI, T., Adsorption and coprecipitation of divalent metals with mackinawite (FES), *Geochim. Cosmochim. Acta* **57** (1993) 3635. [https://doi.org/10.1016/0016-7037\(93\)90145-M](https://doi.org/10.1016/0016-7037(93)90145-M)
- [2.55] XU, Y.-F., MARCANTONIO, F., Speciation of strontium in particulates and sediments from the Mississippi River mixing zone, *Geochim. Cosmochim. Acta* **68** (2004) 2649. DOI: [10.1016/j.gca.2003.12.016](https://doi.org/10.1016/j.gca.2003.12.016)
- [2.56] DUFF, M.C., COUGHLIN, J.U., HUNTER, D.B., Uranium co-precipitation with iron oxide minerals, *Geochim. Cosmochim. Acta* **66** (2002) 3533. [https://doi.org/10.1016/S0016-7037\(02\)00953-5](https://doi.org/10.1016/S0016-7037(02)00953-5)
- [2.57] SHEPPARD, S., et al., Solid/liquid Partition Coefficients (K_d) for Selected Soils and Sediments at Forsmark and Laxemar-Simpevarp, R-09-27, Swedish Nuclear Fuel and Waste Management Co., Stockholm (2009). <https://www.skb.com/publication/1951648>
- [2.58] CAMERON, D.A., KLUTE, A., Convective-diffusive transport with a combined kinetic and equilibrium model, *Water Resour. Res.* **13** (1977) 183. <https://doi.org/10.1029/WR013i001p00183>
- [2.59] VAN GENUCHTEN, M.Th., WAGENET R.J., Two-site/two region models for pesticide transport and degradation: theoretical development and analytical solutions, *Soil Sci. Soc. Am. J.* **53** (1989) 1303. <https://doi.org/10.2136/sssaj1989.03615995005300050001x>
- [2.60] KONOPEV, A.V., et al., Influence of agricultural countermeasures on the ratio of different chemical forms of radionuclides in soil and soil solution, *Sci. Total Environ.* **137** (1993) 147. [https://doi.org/10.1016/0048-9697\(93\)90383-H](https://doi.org/10.1016/0048-9697(93)90383-H)
- [2.61] ABSALOM, J.P., CROUT, N.M.J., YOUNG, S.D., Modelling radiocaesium fixation in upland organic soils of Northwest England, *Environ. Sci. Technol.* **30** (1996) 2735. <https://doi.org/10.1021/es950899y>
- [2.62] SCHINDLER, P.W., SPOSITO, G., Surface complexation at (hydro)oxide surfaces, *Interactions at the Soil Colloid-Soil Solution Interface*, (BOLT, G.H., et al., Eds), Kluwer Academic Press, Boston (1991) 115.
- [2.63] WESTALL, J., HOHL, H., A comparison of electrostatic models for the oxide/solution interface, *Adv. Colloid Interf. Sci.* **12** (1980) 265. [https://doi.org/10.1016/0001-8686\(80\)80012-1](https://doi.org/10.1016/0001-8686(80)80012-1)
- [2.64] WESTALL, J., Reactions at the Oxide-Solution Interface: Chemical and Electrostatic Models, American Chemical Society, In: *Geochemical Processes at Mineral Surfaces*, Chapter 4, 54-78, Washington, DC (1987).
- [2.65] WESTALL, J., Modeling of the association of metal ions with heterogeneous environmental sorbents. Proceedings of the XVIII International Symposium on the Scientific Basis for Nuclear Waste Management, Materials Research Society, Warrendale, PA (1994) 1.

3. K_d VARIABILITY IN SOILS

MIQUEL VIDAL, ANNA RIGOL, ORIOL RAMÍREZ-GUINART
Universitat de Barcelona, SPAIN

DANIEL KAPLAN
Savannah River Ecology Laboratory, University of Georgia, USA

KEIKO TAGAMI, SHIGEO UCHIDA
National Institute for Quantum Science and Technology, JAPAN

SANAE SHIBUTANI, KEISUKE ISHIDA
Nuclear Waste Management Organization, JAPAN

Soil K_d values in soils commonly range over about five orders of magnitude. It is therefore beneficial to narrow their range using ancillary information for factors that affect the K_d value for each radionuclide. Reducing the range in K_d value can be achieved, for example, by considering the properties of the solid and liquid phases and the experimental approach applied for the quantification of K_d values. Deriving probabilistic K_d from partial datasets grouped according to key soil factors allows the derivation of best estimates K_d with a lower associated variability.

This chapter provides approaches to quantify and understand variability of K_d values in soils by using examples that illustrate how various ancillary factors that influence K_d values can be grouped to provide input data with lower variability. Such an approach is useful for radiological impact assessments, particularly for complex conditions when more realistic assessments are needed. A detailed examination of the effect of the experimental approach applied for the quantification of K_d values on the variability of K_d values is presented in the context of Japanese paddy field soils.

3.1. COMPARISON BETWEEN SHORT TERM SORPTION AND LONG TERM DESORPTION K_d VALUES IN JAPANESE PADDY FIELD SOILS

Soil K_d data derived from indigenous elements can be included in the main datasets because they can be considered as surrogates for the long term behaviour of the target radionuclides [3.1]. However, for caesium, sorption K_d values derived from radiotracer experiments tend to be lower than K_d derived from the solid total concentration of the indigenous element. Such differences in K_d values for elements other than caesium have rarely been studied or compared, especially for the same soil samples [3.2]. Recent studies that partially address this deficiency are briefly discussed below.

3.1.1. Element concentrations in soil and river sediment

Soil is formed from the weathering of rocks by water, microorganisms, and wind and the incorporation of natural organic matter from the decomposition of plants and animals. Figure 3.1 shows the GM of element concentrations (95% confidence range) in Japanese river sediments ($N = 3024$), which have been shown to partially reflect the properties of contributing weathered rock [3.3], and paddy field soils ($N = 93$) [3.4] collected throughout Japan. The ratios of GM concentrations of paddy field soil to river sediment of each element ($R_{\text{soil_sed}}$) are shown in Fig. 3.2.

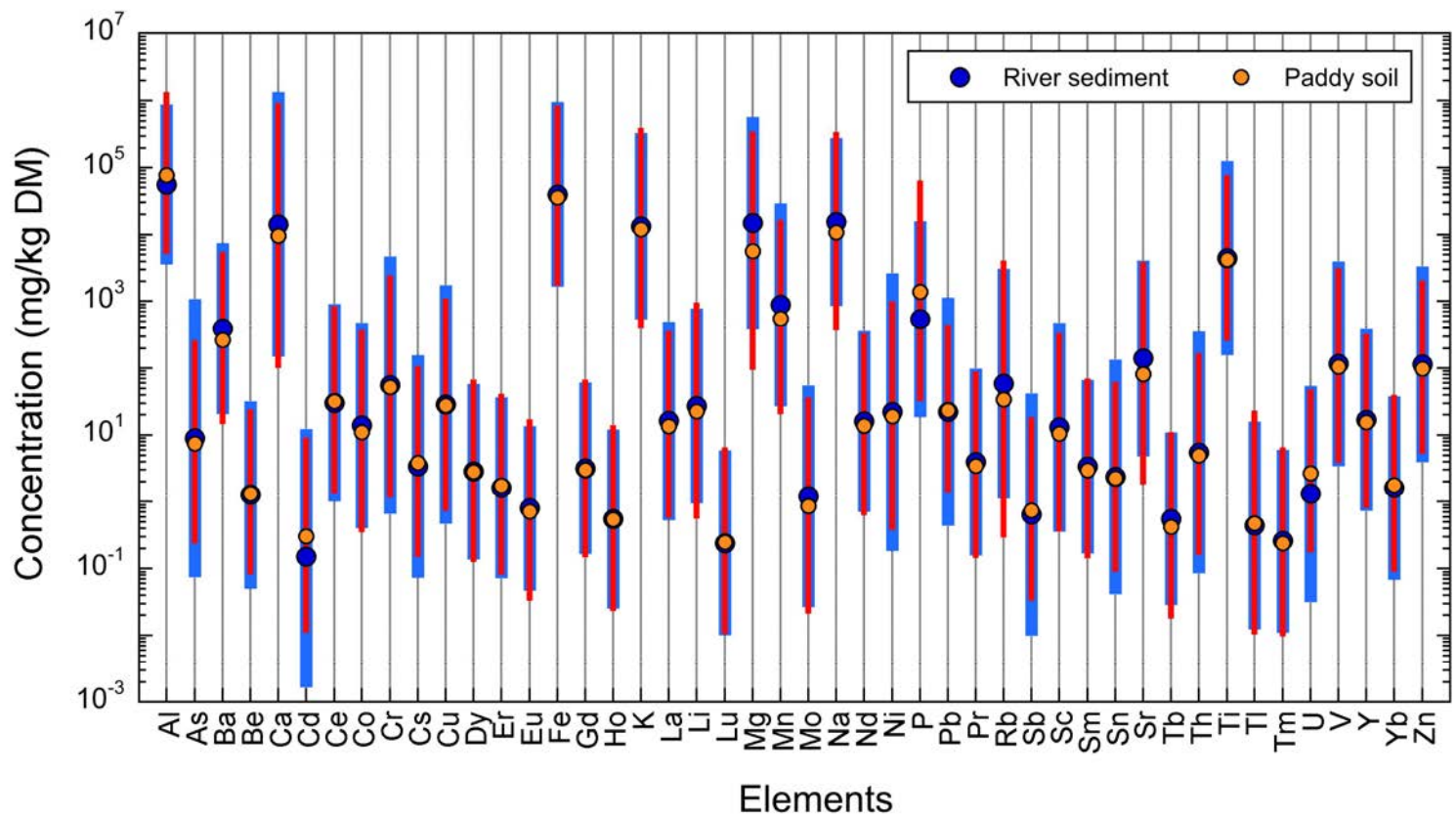


FIG. 3.1. Geometric means of concentrations (mg/kg DM) of elements in paddy field soils and river sediments collected throughout Japan. Bars show 95% confidence range.

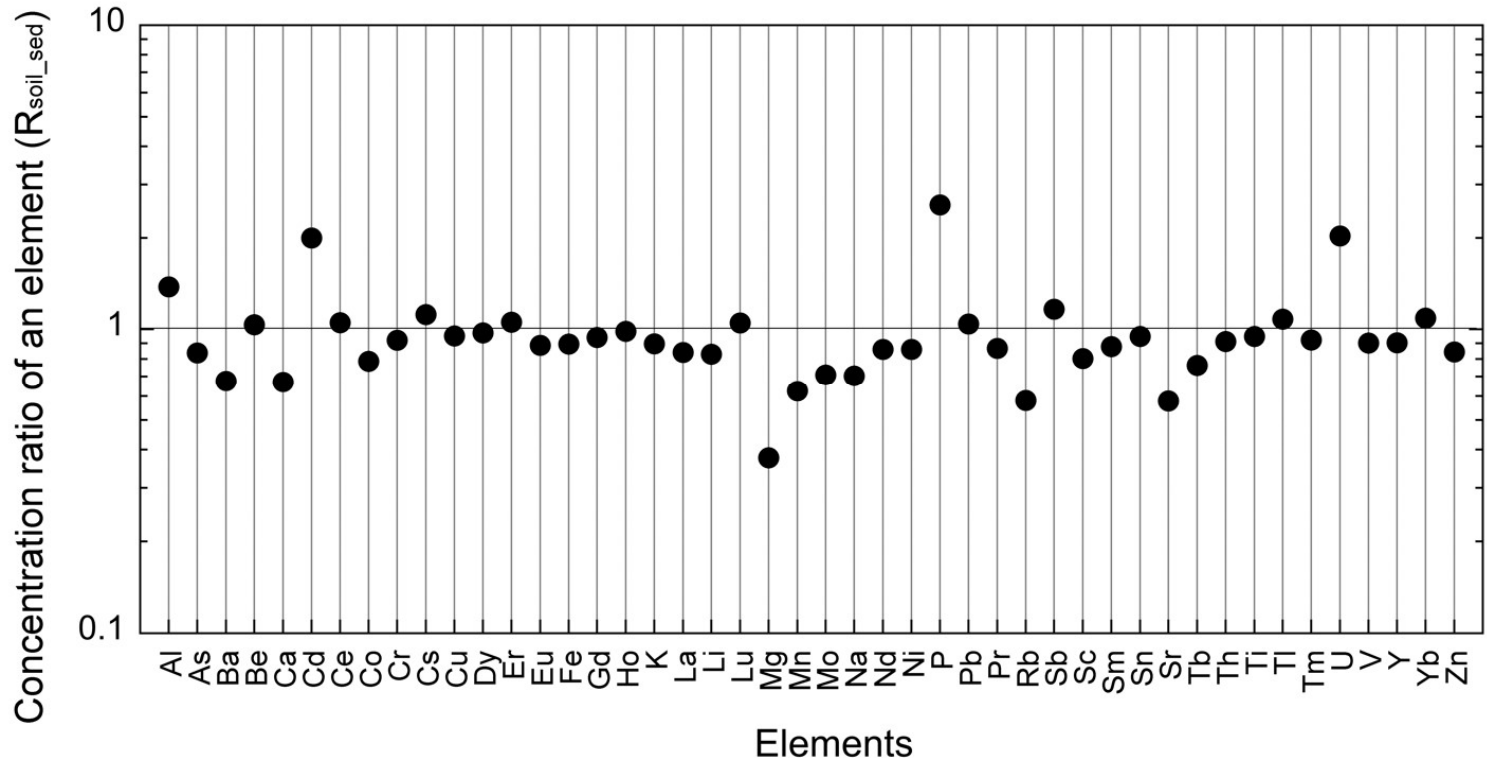


FIG. 3.2. Ratios of element GM concentration in paddy field soils versus river sediments.

Almost all elements, except Al, Cd, P and U, had a lower or similar concentration in soils to that in river sediments. P and U concentrations in paddy soils were higher due to the addition of phosphorus fertilizer to Japanese paddy fields [3.5]. Uranium naturally coexists in phosphate fertilizers. For Al, paddy soils absorb dissolved Al from irrigation water [3.6] and Japanese soils tended not to release Al [3.7]; which can lead to accumulation of Al in paddy soils. The same mechanism applies because of a high K_d for Cd in suspended sediments (see Chapter 4).

Depleted elements ($GM R_{soil_sed} < 0.8$; which are below the dilution effect by soil organic matter) include alkaline and alkaline earth elements such as Ba, Ca, Mg, Na, Rb and Sr as well as Co, Mn and Mo. For other elements, the $GM R_{soil_sed}$ were close to 1, as the river water in contact to sediments does not solubilize them. These elements are relatively immobile in the environment, so K_d values derived from the total concentration of indigenous elements are higher for these elements than those obtained by other methods.

Batch sorption tests in 32 paddy field soils have been carried out to obtain short term sorption K_d using radiotracers, namely ^{54}Mn , ^{63}Ni , ^{75}Se , ^{85}Sr , and ^{137}Cs [3.8, 3.9]. Another experiment measuring indigenous elements in the same soils used total digestion with hydrofluoric acid of the solid phase to measure water soluble amounts of elements from the soil solid phase providing long term desorption K_d values. Geometric mean K_d values for the elements, summarized in Table 3.1, indicate that the difference between the long term and short term K_d values varies by 3–12 times. Long term K_d values are consistently higher than the short term values for all five elements examined. Except for Sr and Se, short term and long term $lg K_d$ values were well correlated ($R > 0.5$; $p < 0.01$). The results indicate that, by applying a correction factor, short term K_d values could be estimated from indigenous based, long term K_d values for Mn, Ni and Cs. The correction factors are 0.86 ± 0.15 for Mn, 0.72 ± 0.06 for Ni, and 0.76 ± 0.06 for Cs. For Sr and Se, the factors are 0.76 ± 0.08 and 0.83 ± 0.16 , respectively, but there is no significant correlation between indigenous elements and radiotracers for these two elements.

TABLE 3.1. CORRELATION FACTOR VALUES FOR SHORT TERM (ST) AND LONG TERM (LT) K_d VALUES (L/kg) OF Mn, Ni, Se, Sr AND Cs FOR JAPANESE PADDY FIELDS

| Type of K_d | R | P-value | GM | GSD | Min | Max |
|---------------|------|---------|-------------------|-----|-------------------|-------------------|
| ST ^{54}Mn | | | 9.4×10^2 | 5.1 | 1.7×10^2 | 1.4×10^5 |
| LT Mn | 0.62 | < 0.001 | 2.8×10^3 | 3.2 | 5.2×10^2 | 8.4×10^4 |
| ST ^{63}Ni | | | 7.0×10^2 | 1.8 | 2.0×10^2 | 3.1×10^3 |
| LT Ni | 0.54 | 0.0015 | 8.7×10^3 | 2.1 | 1.9×10^3 | 5.0×10^4 |
| ST ^{75}Se | | | 2.5×10^2 | 3.1 | 3.3×10^1 | 1.6×10^3 |
| LT Se | 0.43 | 0.014 | 7.6×10^2 | 2.0 | 2.1×10^2 | 2.7×10^3 |
| ST ^{85}Sr | | | 4.0×10^2 | 1.7 | 1.7×10^2 | 1.8×10^3 |
| LT Sr | 0.25 | 0.17 | 2.9×10^3 | 2.0 | 8.1×10^2 | 1.1×10^4 |
| ST ^{137}Cs | | | 2.6×10^3 | 2.4 | 5.5×10^2 | 1.7×10^4 |
| LT Cs | 0.73 | < 0.001 | 3.0×10^4 | 2.4 | 7.4×10^3 | 4.4×10^5 |

GM: geometric mean; GSD: geometric standard deviation.

R: Pearson correlation factor; P-value: statistical significance of the correlation.

3.1.2. Differences between short term and long term K_d values for Mn, Ni, Se, Sr and Cs

It may be difficult to estimate short term K_d values from long term K_d values without a previously established relationship or correction factor. Such an approach has been suggested for marine sediments [3.10], using a correction factor based on the exchangeable fraction which gives ratios of exchangeable K/total K, exchangeable Ca/total Ca, 0.1M oxalic acid extractable Al/total Al or 0.1M oxalic acid extractable Fe/total Fe. Of the four elements considered above (Fig. 3.2), only Ca was depleted in paddy field soils compared with river sediments which may be due to Ca in soil being relatively mobile compared with the other measured elements. The mobile fraction can be part of the exchangeable fraction of the soil.

To explore this approach, a hypothesis was tested that exchangeable Ca can be used as an indicator of the exchangeable fraction for other indigenous elements in soils. For each soil sample, the ratio between exchangeable Ca and total Ca in each soil sample was used to estimate the exchangeable fraction for other indigenous elements. The corresponding K_d value was recalculated (as the corrected long term K_d), allowing conversion of the long term indigenous K_d data into a value for short term K_d data.

The resulting data in Table 3.2 show that the exchangeable Ca/total Ca ranged from 0.05 to 1.0 (GM = 0.20). For all studied elements, by adopting the exchangeable Ca ratio, the differences between short term and long term corrected K_d were 0.62–2.6 times lower than those before correction (3–12 times). Long term corrected K_d was correlated to short term K_d values for Mn, Se and Cs ($p < 0.05$) but with a low Pearson correlation factor ($R = 0.37$ – 0.62). For Ni and Sr, long term corrected K_d were not correlated to the short term K_d ($p > 0.05$).

The results suggest that using exchangeable Ca as an indicator of the exchangeable fraction may be useful for some elements but is not a reliable approach to apply for all elements. Further studies are needed to identify suitable correction factors to convert indigenous long term data for various radionuclide to estimated short term K_d values.

TABLE 3.2. CORRECTED LONG TERM (LT) K_d VALUES USING EXCHANGEABLE Ca/TOTAL RATIOS IN SOIL AND SHORT TERM (ST) K_d VALUES (L/kg) OF Mn, Ni, Se, Sr AND Cs

| Element | R | P-value | Corrected long term K_d | | | | GM ratio ST K_d /corrected LT K_d |
|---------|------|---------|---------------------------|-----|-------------------|-------------------|--|
| | | | GM | GSD | Min. | Max. | |
| Mn | 0.62 | < 0.001 | 5.8×10^2 | 3.5 | 8.9×10^1 | 1.5×10^4 | 1.09 ± 0.20 |
| Ni | 0.24 | 0.18 | 1.8×10^3 | 3.0 | 3.0×10^2 | 1.1×10^4 | 0.89 ± 0.13 |
| Se | 0.37 | 0.035 | 1.6×10^2 | 2.7 | 1.5×10^1 | 9.2×10^2 | 1.13 ± 0.27 |
| Sr | 0.18 | 0.33 | 6.0×10^2 | 2.1 | 1.9×10^2 | 4.2×10^3 | 0.95 ± 0.12 |
| Cs | 0.54 | 0.001 | 6.1×10^3 | 3.6 | 6.7×10^2 | 1.1×10^5 | 0.92 ± 0.12 |

ST: short term; LT: long term.

GM: geometric mean; GSD: geometric standard deviation.

R: Pearson correlation factor; P-value: statistical significance of the correlation.

3.2. TREATMENT OF K_d VARIABILITY

3.2.1. Introduction

As noted above, there is no single K_d value for a given radionuclide as K_d values may vary over as much as 5–6 orders of magnitude. Variability in K_d for a given radionuclide in an environmental sample arises from the effect of the methodology applied for its determination (e.g. sorption and desorption batch tests or *in situ* experiments) and the characteristics of the solid and liquid phases that affect sorption mechanisms (e.g. pH, Eh , particle size, organic matter content, water column/soil solution composition), which in turn may modify radionuclide speciation. The relative importance of each factor contributing to the variability is radionuclide dependent. Sources of variability are difficult to reduce because they are not univariate or independent.

Cumulative distribution functions (CDFs) of a dataset can be used to give a description of the distribution and variability of K_d values. CDF equations describe the values of a random variable (i.e. a function mapping the probability of a variable – in this case of K_d , over a range of real values) and their associated cumulative frequency. This means that the probability of a K_d value that is less than, or equal to, a given value can be continuously described by means of this function. CDFs indicate the most probable K_d value, corresponding to the 50th percentile of the CDF, and provide a range of potential values and their probability of occurrence [3.11]. Confidence intervals of K_d values can also be derived from the CDF of a K_d dataset by calculating the associated percentile ranges (e.g. the 90% and 95% confidence intervals corresponding to the ranges based on the 5th–95th and 2.5th–97.5th percentiles, respectively).

3.2.2. The cumulative distribution function statistical approach

CDFs are built using the statistical parameters of the underlying frequency distribution or probability density function (PDF) that adequately represent the distribution of the individual values of a certain dataset for the target variable. The K_d parameter is calculated as a ratio and constrained to positive values. Its values are expected to follow a log-normal distribution [3.12]; this implies that the log-transformed K_d values, or $\lg K_d$, follows a Normal or Gaussian distribution. Therefore, the corresponding PDF can be expressed as follows:

$$p(\lg K_d) = \frac{1}{\sigma\sqrt{2\pi}} 10^{-\left[\frac{(\lg(K_d)-\mu)^2}{2\sigma^2}\right]} ; \quad K_d > 0 \quad (3.1)$$

where:

- p is the probability of a given $\lg K_d$ value;
- μ is the location parameter corresponding to the arithmetic mean of the $\lg K_d$ distribution;
- σ is the scale parameter corresponding to the standard deviation of the $\lg K_d$ distribution.

For symmetrical $\lg K_d$ distributions, the location parameter (μ) can be considered as a best estimate of the most probable $\lg K_d$ value, whereas the scale parameter (σ) estimates the dispersion amongst $\lg K_d$ values. Statistical parameters (μ and σ) can be quantified: (i) from the arithmetic mean (and its standard deviation) of the experimental $\lg K_d$ values of a dataset; or (ii) adjusting the cumulative distribution of a $\lg K_d$ dataset to the theoretical CDF equation for the normal distribution, as follows:

$$P(\lg K_{d,i} \leq \lg K_{d,j}) = \sum_{\lg K_{d,i} \leq \lg K_{d,j}} p(\lg K_{d,i}) = \frac{1}{2} + \frac{1}{2} \operatorname{erf} \left[\frac{\lg(K_{d,i}) - \mu}{\sigma\sqrt{2}} \right]; \quad K_{d,i} > 0 \quad (3.2)$$

where:

P is the cumulative probability;
 erf is an error function.

Figure 3.3 shows a graphical representation of the PDF and CDF of an ideal log-normally distributed dataset.

The statistical parameters calculated, or derived, from a log-normally distributed dataset (μ , σ and percentiles) are presented on a logarithmic scale, so that derived values are not directly comparable with experimental data. Therefore, the corresponding antilog parameters are preferred, and the GM and geometric standard deviation (GSD) are given instead of the μ and σ parameters, as well as confidence intervals (percentile ranges) of K_d values instead of those of $\lg K_d$:

$$\text{GM}(K_d) = \left(\prod_{i=1}^N K_{d_i} \right)^{\frac{1}{N}} = 10^{\left(\frac{1}{N} \sum_{i=1}^N \lg(K_{d_i}) \right)} = 10^\mu = \text{antilog}(\mu) \quad (3.3)$$

$$\text{GSD}(K_d) = 10^{\left(\sqrt{\frac{\sum_{i=1}^N \left(\lg \frac{K_{d_i}}{\text{GM}} \right)^2}{n}} \right)} = 10^\sigma = \text{antilog}(\sigma) \quad (3.4)$$

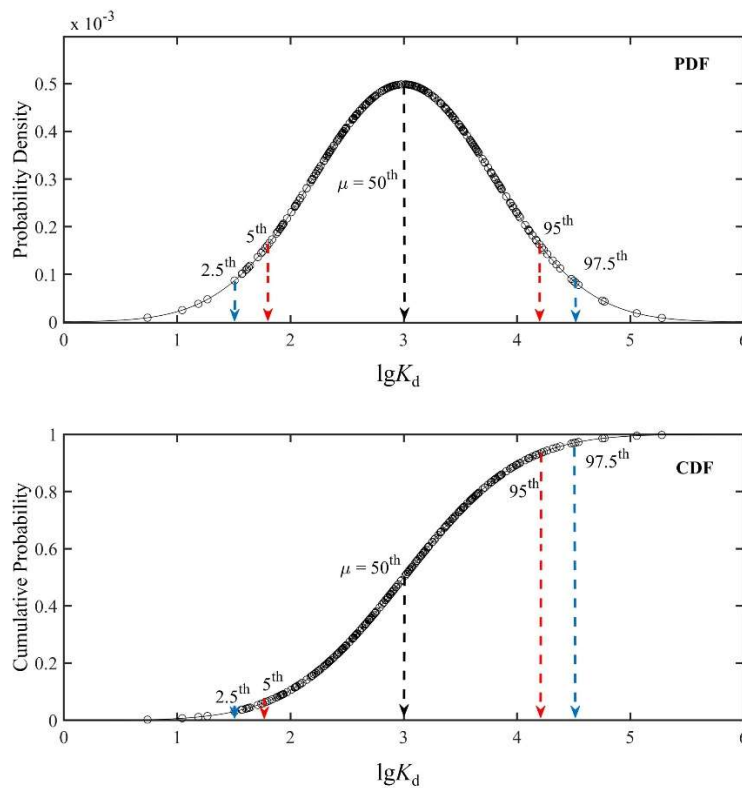


FIG. 3.3. Probability Density Function (PDF) and Cumulative Distribution Function (CDF) of a $\lg K_d$ dataset.

TABLE 3.3. ALTERNATIVE STATISTICAL DISTRIBUTIONS FOR PDF/CDF CONSTRUCTION OF K_d DATASET

| Distribution | PDF | CDF | Statistical parameters |
|----------------|--|--|--|
| Log-uniform | $\begin{cases} \frac{1}{(b-a)}; \lg K_d \in [a, b] \\ 0; \lg K_d \notin [a, b] \end{cases}$ | $\begin{cases} 0; \lg K_d < a \\ \frac{(\lg K_d - a)}{(b-a)}; \lg K_d \in [a, b] \\ 1; b \leq \lg K_d \end{cases}$ | $\begin{aligned} a &= \text{minimum } \lg K_d \\ b &= \text{maximum } \lg K_d \\ \text{Best estimate} &= \frac{a+b}{2} \end{aligned}$ |
| Log-triangular | $\begin{cases} 0; \lg K_d < a \\ \frac{2(x-a)}{(b-a)(c-a)}; a \leq \lg K_d < c \\ \frac{2}{(b-a)}; \lg K_d = c \\ \frac{2(b-\lg K_d)}{(b-a)(b-c)}; c < \lg K_d \leq b \\ 0; b < \lg K_d \end{cases}$ | $\begin{cases} 0; \lg K_d < a \\ \frac{(x-a)^2}{(b-a)(c-a)}; a < \lg K_d \leq c \\ 1 - \frac{(b-\lg K_d)^2}{(b-a)(b-c)}; c < x < b \\ 1; b \leq \lg K_d \end{cases}$ | $\begin{aligned} a &= \text{minimum } \lg K_d \\ b &= \text{maximum } \lg K_d \\ c &= \text{mode } \lg K_d \\ \text{Best estimate} &= \frac{a+b+c}{3} \end{aligned}$ |
| Exponential | $\lambda e^{-\lambda x}; K_d > 0$ | $1 - e^{-\lambda x}; K_d > 0$ | $\lambda = \text{arithmetical mean } K_d$ |

The CDF approach has limitations, as large datasets are needed to adequately derive the statistical parameters necessary to construct reliable CDFs. For small K_d datasets with few data, the best statistical distribution to describe the dataset may not be log-normal, but an alternative distribution, such as log-uniform, log-triangular, or exponential. Table 3.3 summarizes the PDFs, CDFs and statistical parameters related to these alternative statistical distributions.

However, the log-normal distribution is generally the most appropriate for describing the variability in K_d data, but initially this assumption has to be tested. Unequivocal attribution to a log-normal distribution and subsequent construction of a PDF or a CDF will be only possible when datasets with an adequate number of values (usually $N \geq 10$) are available [3.11, 3.13].

3.2.3. Construction of cumulative distribution functions from the K_d datasets

CDFs can be built for an entire K_d dataset, or for a part of it, after filtering data based on a specific factor. Initially, an evaluation was carried out to determine whether the dataset followed a log-normal distribution. The presence of possible outlier $\lg K_d$ values in the datasets, which may distort their distribution, was investigated by an exploratory box-and-whisker analysis. The occurrence frequency is $1/N$ for each datum in a dataset of N different values. However, the K_d datasets may have included several repetitions of the same value. To account for this potential redundancy, the occurrence frequency was assumed to be equal to n/N , where n is the number of K_d entries with the same value and N is the total number of K_d entries in the dataset. For each log-transformed dataset, the experimental cumulative frequency distribution was then constructed by sorting the $\lg K_d$ data by increasing value. The Kolmogorov-Smirnov statistical test was then applied to confirm whether K_d datasets were log-normally distributed. This was confirmed for all cases where $N \geq 10$. No CDFs were calculated for datasets where $N < 10$.

After testing the K_d frequency distribution, the μ and σ parameters were derived by means of a Robust Least Squares fitting of the cumulative frequency distributions to the Normal CDF equation using the Least Absolute Residuals method. Subsequently, the GM, GSD and 5th and 95th percentiles were calculated. Figure 3.4 summarizes the process followed.

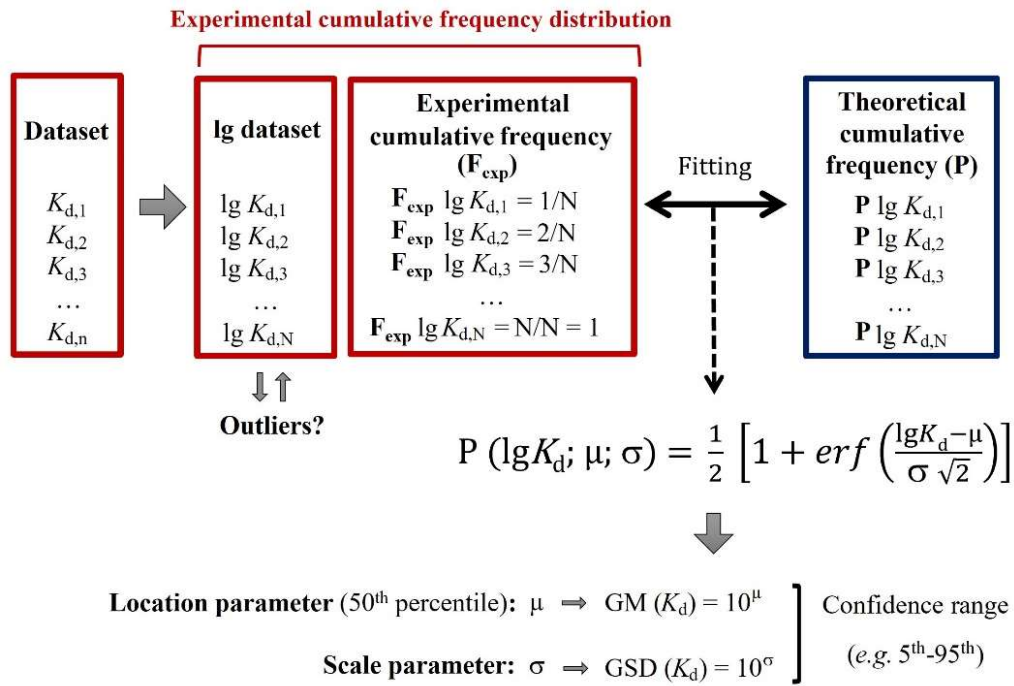


FIG. 3.4. Schematic process to construct CDFs and to derive statistical parameters from K_d datasets.

As stated earlier, the construction of CDFs also facilitates the quantification of 90% or 95% confidence intervals. Comparison between the values within the confidence interval values and the minimum–maximum ranges help to evaluate K_d variability. Confidence interval ranges that are narrower than the minimum–maximum ranges indicate that: (i) there is a good fit of the experimental data to the CDFs; (ii) the experimental data are well distributed over the full interval of values; and (iii) extremely low or high values can be excluded without jeopardizing the representativeness of the best estimate values, based on the 50th percentile. In some cases, the confidence interval ranges may be wider than minimum–maximum ranges. In such cases, it is possible that there is a poor fit between the experimental data and the CDF due to the low number of values included in the distribution.

3.3. CREATION OF A CRITICALLY REVIEWED SOIL K_d DATASET TO DERIVE PROBABILISTIC DISTRIBUTION COEFFICIENTS (K_d) IN SOILS

3.3.1. Solid and liquid phases considered in the soil dataset

3.3.1.1. Solid phases

The different types of solid phases considered are briefly described as follows:

- *Soils and subsoils:* Soil samples refer mostly to the soil profile within the unsaturated zone, which typically have pore spaces that are not completely filled with water. The soil zone supports plant growth and it is generally one to two metres thick, with living roots. The porosity and permeability of the zone under the topsoil (subsoil) varies in thickness in different areas; this zone is often referred to as the intermediate zone, as it is generally higher than that in the underlying material.

- *Gyttja*: Gyttja is a rapidly accumulating, organic, muddy deposit, characteristic of eutrophic lakes, and formed from the partial decay of peat [3.14]. The precise nature of Gyttja varies depending on the specific decomposing organisms (e.g. small algae and/or macrophytes), which contribute to the Gyttja.
- *Till*: Till is an “unstratified or crudely stratified glacial deposit, consisting of a stiff matrix or fine rock fragments and old soil” [3.15] containing subangular stones of various sizes and compositions. It forms a mantle with a thickness that is between ≤ 1 m and ≥ 100 m, covering areas that carried an ice sheet or glaciers during the Pleistocene and Holocene periods.

3.3.1.2. *Liquid phases*

The liquid phase (L) within the dataset is defined as the aqueous phase, which is in contact with the environmental sample (M), and the organic and inorganic substances dissolved in it. Depending on the methodological approach, a distinction is made between the soil solution (*in situ* and laboratory) and the contact solution at higher L/M ratios (laboratory).

3.3.2. Introduction to the published IAEA soil K_d dataset compilations

TRS 472 [3.16] and the related TECDOC-1616 [3.17] summarize the main descriptors of a soil K_d dataset compilation that was a major update of the previous compilation in TRS 364 [3.18]. Data are compiled from *in situ* and laboratory experiments and largely comprise soils contaminated by radionuclides from various contamination sources and are mostly based on references from 1990 onwards. Data from the former TRS 364 [3.18] and related reports [3.19], reviewed papers and grey literature are included. In most cases, data from experiments using materials other than soils (e.g. sediments, mined clays or Fe–Mn–Al oxides, rock materials) or from stable isotopes are not considered. Data from isotopes of the same element are pooled.

The TRS 472 [3.16] compilation contains around 2900 records for 67 elements. The caesium and strontium datasets have the greatest number of observations. Other datasets that have more than 100 entries were for I, U, Co, K, Sb and Se.

The K_d values in TRS 472 [3.16] are grouped according to the OM content and sand and clay fractions of the mineral matter (referred to as the ‘Texture–OM criterion’) as follows:

- For the mineral soils, three groups were created according to the percentage sand and clay content:
 - (1) ‘Sand group’, containing a sand fraction of $\geq 65\%$ and a clay fraction $< 18\%$;
 - (2) ‘Clay group’, containing a clay fraction of $\geq 35\%$;
 - (3) ‘Loam group’, comprising the remaining fraction.
- An ‘Organic group’ was defined for soils with OM content of $\geq 20\%$.

For a limited number of radionuclides, for which there were adequate data, the K_d values are also grouped, according to specific factors based on soil properties that are responsible for the interaction of the target radionuclide in soils (soil factors). The groupings therefore differ for the different radionuclides as follows for:

- (a) Radiocaesium – radiocaesium interception potential (RIP) [3.20] and concentration of K (an analogue of radiocaesium) in the soil solution;

- (b) Radiostrontium – cationic exchange capacity and concentration of Ca and Mg (analogues of radiostrontium) in the soil solution;
- (c) Radioiodine – speciation data and water regime (which affect partitioning of radioiodine);
- (d) Uranium and heavy metal radionuclides – pH (only for those heavy metals for which the number of observations was large enough).

Geometric mean (GM) and geometric standard deviation (GSD) parameters, as well as minimum and maximum values, were preferred to describe K_d data. Box-and-whisker plots were constructed to identify and exclude potential outliers and decrease data variability.

In TRS 472, a few conclusions are drawn from the soil K_d dataset [3.16] that suggest further work is needed. Although a significant amount of new data was included in the TRS 472 dataset [3.16], compared with the former TRS 364 dataset [3.18], there are still evident gaps in K_d values for a substantial number of radionuclides and soil types. In some cases, the K_d values originated from a single reference. These deficiencies, in many cases, restrict the possibility of proposing reliable best estimates. The derived GM and single values ought to be considered as approximate estimates that are mostly suitable for screening purposes. For filling these gaps, it is suggested that the data could be supplemented using analogue data, either from other elements or from geological materials other than soils, a strategy that needs to be quantitatively validated.

The large number of methodological approaches and experimental conditions used to quantify K_d values (see Chapter 2, Section 2.1.2) are identified in TRS 472 as being partly responsible for the observed variability in K_d for various radionuclide–soil type combinations, suggesting that the measurement method could be considered as an additional factor when grouping K_d data. The dataset was extended by including data from stable isotopes, but only using those K_d values derived using concentrations that were low enough to ensure linear sorption and the absence of precipitation.

Multiple factors, associated with the type of radionuclide and various soil properties, determine soil–radionuclide interactions. Thus, the quantification of K_d values for soil groups in TRS 472 is a satisfactory approach for establishing the K_d estimated values for a number of radionuclides that exhibit low variability. However, moving forward, in addition to texture and OM content, additional relevant soil and radionuclide properties could now be compiled for an increased number of radionuclides, compared with those included in TRS 472 [3.16], to facilitate a better estimation of K_d values and to decrease their variability. This will lead to a more representative set of K_d values being generated for use in screening level REIA alongside a list of factors for consideration in more complex, site specific REIA.

3.3.3. Revision of criteria for the acceptance of data in K_d in future IAEA compilations

The criteria applied in the K_d compilation in TRS 472 [3.16] to accept the K_d data and ancillary information have been critically reviewed and revised by the Working Group. To improve the quality of K_d entries compiled in future datasets, the criteria applied to accept or reject K_d data and ancillary information in TRS 472 [3.16] have been critically reviewed and revised by the Working Group. The revised criteria to accept or reject K_d data, both from the former dataset or from newly available publications, are as follows:

- (1) Data not derived from experimental approaches (e.g. K_d values calculated from parametric equations or from empirical regressions correlating soil properties and K_d values) are not included in the dataset (or are removed from the TRS 472 dataset);

- (2) Data corresponding to best estimate values from former compilations or to pooled values (e.g. arithmetic mean or geometric mean values) are removed from the TRS 472 dataset and substituted, where possible, by the individual data from which they were calculated;
- (3) Data previously gathered from solid materials considered as potential soil analogues (e.g. surface sediments, till, gyttja and subsoil samples) are accepted, but are flagged so that they can be considered separately from the soil data. Data from pure mineral phases or rock materials are not accepted;
- (4) Data for stable isotopes (e.g. from desorption tests of indigenous elements or derived from the lowest concentration range of sorption isotherms) are accepted. In the latter case, only those K_d values derived using concentrations that are low enough to ensure linear sorption or the absence of precipitation are accepted, as they represent scenarios that are similar to most radionuclide release scenarios;
- (5) Only K_d data determined for samples in which the contamination of the target element originates from soluble sources are accepted;
- (6) Data gathered from soils or other accepted solid materials by applying experimental conditions that are not representative of terrestrial ecosystems or contamination scenarios (e.g. extremely high or low pH values) are rejected.

In addition to the revision of the data acceptance/rejection criteria, all entries from the former dataset in TRS 472 or from newly available publications have now been flagged based on the K_d measurement method, making it possible to distinguish between the following categories: (I) sorption tests for short term incorporated radionuclides, (II) desorption tests for short term incorporated radionuclides, (III) desorption for long term incorporated radionuclides, and (IV) *in situ* data. Finally, no *in situ* data are available for the soil dataset. K_d values for the same sample obtained under varying experimental conditions that were not considered as a grouping factor (e.g. K_d data obtained at different solid–liquid ratios or contact times) will be pooled into a single value corresponding to the GM of the individual values in the future.

3.3.4. Compilation of soil K_d dataset within MODARIA

Under the MODARIA programme, soil K_d data were collected. Besides data published in peer reviewed journals or accessible in reports, a large number of data were incorporated from studies that were made available by scientists and/or research groups from the Swedish Nuclear Fuel and Waste Management Company, (Sweden), Research Center for Radiation Protection (Japan), University of Barcelona (Spain), Savannah River National Laboratory (US), Saanio and Riekkola-Posiva (Finland) and Nuclear and Radiation Safety Center (China). These data were reviewed to ensure that they met the acceptance criteria detailed in Section 3.3.3 above. More than 5000 soil K_d values were compiled for 82 elements for soils, which is significantly more than in TRS 472, as shown in Table 3.4 [3.16]. Approximately 2000 entries of K_d data were also gathered from environmental solid materials other than soils, such as subsoils, gyttja and till, for 75 elements. An increase in the number of soil K_d values for elements such as Am, Sm, Eu, Ni, Cs, Sr, U, Ru and Co is now available. Table 3.4 compares the K_d data compiled during MODARIA for each element, alongside the information on the data entries available in the TRS 472 dataset [3.16]. Table 3.4 shows that there are now soil K_d values for more elements than were compiled in TRS 472 (55 vs 36 elements).

TABLE 3.4. SUMMARY OF SOIL K_d DATA

| Element | TRS 472 [3.16] | MODARIA (this study) ^a | Element | TRS 472 [3.16] | MODARIA (this study) ^a |
|---------|-------------------|--------------------------------------|---------|-------------------|--------------------------------------|
| Ac | 4 | 4 (2) | Na | 30 | 45 (26) |
| Ag | 9 | 22 (30) | Nb | 11 | 23 (42) |
| Al | — ^b | 7 (23) | Nd | — | 8 (9) |
| Am | 62 | 109 (33) | Ni | 64 | 308 (48) |
| As | 7 | 22 (28) | Np | 26 | 40 (31) |
| B | — | 7(17) | Os | — | 6 (3) |
| Ba | 1 | 20 (29) | P | 6 | 19 (21) |
| Be | 5 | 24 (17) | Pa | 4 | 4 |
| Bi | 6 | 18 (5) | Pb | 23 | 44 (38) |
| Br | 4 | 17 (21) | Pd | 6 | 7 (2) |
| C | — | — | Pm | 2 | 2 |
| Ca | 34 | 56 (26) | Po | — | 49 (1) |
| Cd | 61 | 75 (32) | Pr | — | 8 (9) |
| Ce | 11 | 19 (19) | Pt | 1 | 16 (1) |
| Cf | — | — | Pu | 62 | 59 (5) |
| Cl | 22 | 30 (35) | Ra | 51 | 103 (37) |
| Cm | 18 | 18 | Rb | 4 | 12 (9) |
| Co | 118 | 119 (153) | Re | — | 7 (6) |
| Cr | 31 | 38 (38) | Rh | 1 | 12 |
| Cs | 469 | 769 (123) | Ru | 15 | 21 (4) |
| Cu | 11 | 26 (31) | S | — | 7 (17) |
| Dy | 2 | 10 (9) | Sb | 152 | 165 (13) |
| Er | — | 7 (9) | Sc | 2 | 8 (6) |
| Eu | — | 32 (12) | Se | 172 | 269 (59) |
| Fe | 23 | 35 (36) | Si | 4 | 11 (17) |
| Ga | 2 | 10 (9) | Sm | 4 | 50 (9) |
| Gd | — | 8 (9) | Sn | 12 | 95 (13) |
| Ge | — | 7 (9) | Sr | 255 | 645 (56) |
| H | 1 | 1 | Ta | 5 | 11 (4) |
| Hf | 6 | 13 (9) | Tb | 2 | 9 (8) |
| Hg | 1 | 7 (10) | Tc | 33 | 48 (55) |
| Ho | 4 | 11 (9) | Te | 2 | 8 (4) |
| I | 250 | 571 (71) | Th | 46 | 54 (22) |
| In | 2 | 2 | Ti | — ^d | 6 (4) |
| Ir | 1 | 18 | Tl | — | 8 (7) |
| K | 237 | 231 (27) | Tm | 1 | 8 (7) |
| La | 1 | 9 (9) | U | 178 | 196 (63) |
| Li | — | 7 (16) | V | 2 | 17 (25) |
| Lu | 1 | 8 (8) | Y | 7 | 18 (14) |
| Mg | 30 | 53 (26) | Yb | — | 8 (9) |
| Mn | 83 | 94 (32) | Zn | 92 | 123 (26) |
| Mo | 9 | 26 (31) | Zr | 11 | 26 (26) |

Notes:

^a Values in parentheses correspond to additional K_d data gathered from solid environmental materials other than soils.^b —: data not available.

3.3.5. Approach for providing best estimate soil K_d values for Cs and Am based on grouping data according to selected factors

Preliminary evaluation of the data compiled within MODARIA showed that K_d values in soils for most radionuclides are highly variable, which may compromise the reliability of the derived best estimate value or CDF derived from the overall dataset for a given radionuclide. The aim of enhancing the available data was to efficiently decrease and explain the K_d variability and, consequently, be able to derive K_d data with a lower associated variability for the purposes of radiological impact assessment. Therefore, an approach has been developed, based on: (i) a stepwise grouping of the K_d data according to various key factors governing the interaction of the target element with soils; and (ii) the subsequent construction of CDFs, where possible.

Examples of the derivation of best estimates for two elements (i.e. radiocaesium and americium) are presented with the aim of better describing and reducing the variability of K_d values. The analyses illustrate the potential benefits of the data treatment and the improved soil dataset. The derivation of CDFs and the potential decrease in the variability of K_d for other radionuclides, based on their interaction mechanisms, have not yet been undertaken.

The first case considered was radiocaesium, an element for which interactions in soils have been extensively studied, thereby providing an extensive dataset. The compiled information in the dataset includes K_d (Cs) values with associated soil properties potentially affecting Cs sorption (and for which specific soil factors were already identified to be suitable for K_d (Cs) data grouping in TRS 472 [3.16]).

Conversely, the second case considered was americium, for which the main soil properties governing its interaction in soils have only recently been elucidated, and for which limited K_d data were previously available. No specific soil factors were applied to group K_d (Am) data in TRS 472 [3.16]. In all cases, statistical differences among derived partial datasets were tested (Fisher's least significant differences (FLSD) test for multiple means; 95% confidence level).

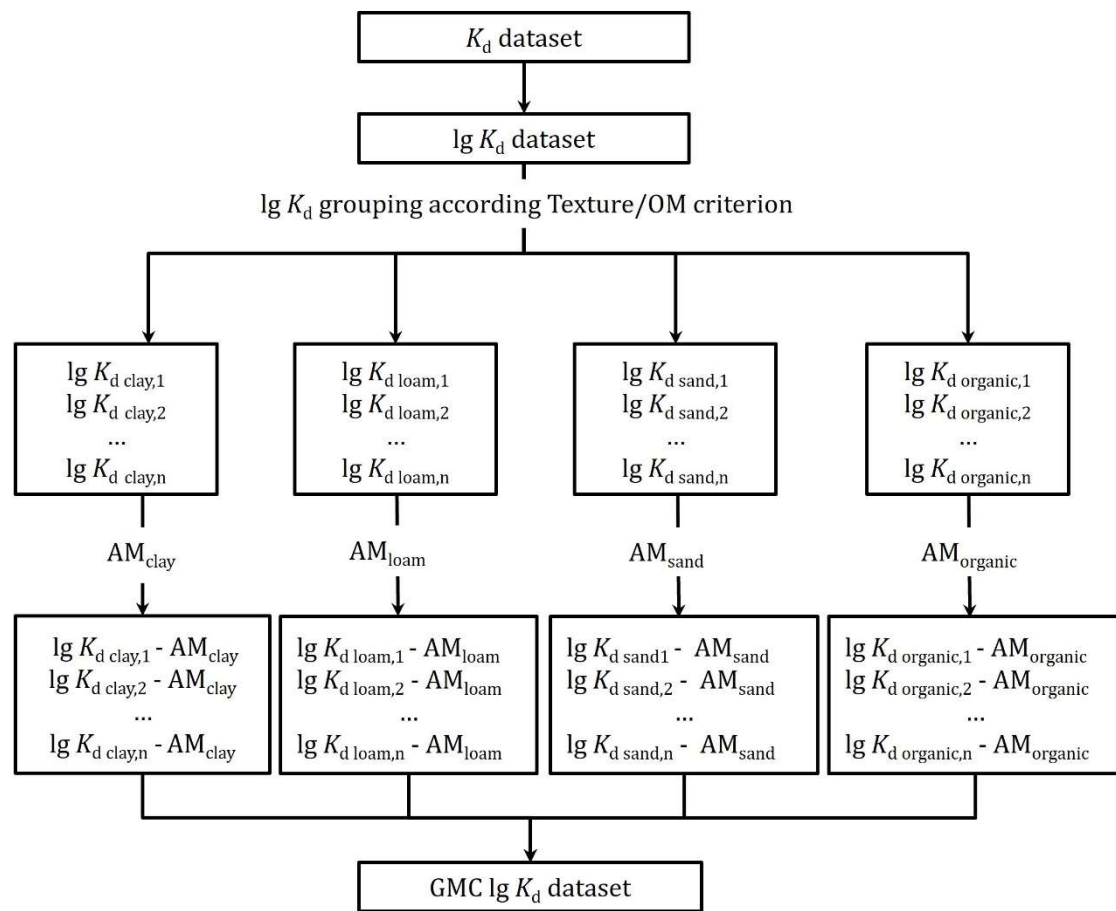
For partial datasets containing few entries (generally, $N < 10$), GM values were calculated directly from experimental data to provide K_d best estimate values. For larger partial datasets, the 50th percentile value along with the 5th–95th percentile range were derived from the CDF, which were used to quantify the best estimate (GM) values and the variability of the K_d datasets, respectively.

In addition to examining and identifying the main soil factors relevant to Cs and Am sorption in soils, the influence of methodological approaches applied in the quantification of Cs and Am K_d data has been evaluated for the first time. The analysis of the influence of methodology made it possible to evaluate whether partial datasets can be created based on methodology before analysing other soil factors to reduce variability.

To reach this goal, a hierarchical analysis of two factors was carried out to create partial datasets according to the experimental approach used to derive K_d data. The first factor applied was the time elapsed since the target elements were sorbed to soils, thus distinguishing between short term and long term situations. The second factor applied was the subdivision of each category previously created (short term and long term) according to the type of experimental method applied. In the case of Cs and Am, the analysis distinguished between K_d values compiled from sorption and desorption tests for the short term category, and data from desorption tests for the long term partial datasets. The appropriate subdivision may differ for other elements.

The influence of the type of experimental method applied on the variability of K_d values in a given dataset was evaluated using a multivariate process. Group mean centering (GMC) data treatment was applied to reduce the effect of other factors (such as soil properties) on the variability of K_d . To do this:

- (1) K_d values were logarithmically transformed;
- (2) $\lg K_d$ values were grouped according to a given soil factor previously identified as probably being relevant to the sorption of the target element (e.g. RIP, pH, K concentration in soil solution, soil texture and OM content);
- (3) Each entry was normalized with respect to the location parameter (μ) (see Eq. (3.1) in Section 3.2.2 above) of the partial dataset created based on a given soil factor.



GMC $\lg K_d$ grouping according to methodology factors

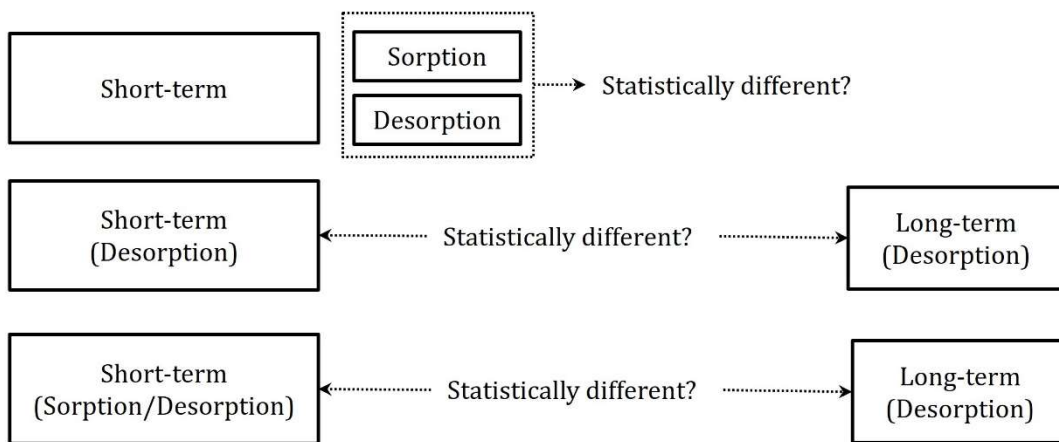


FIG. 3.5. Schematic representation of the strategy applied to evaluate the influence of the experimental approaches on K_d data. In this example, group mean centering (GMC) was performed for consideration of organic matter (OM) content and soil texture factors.

Statistical tests were then applied to the normalized partial datasets to determine whether differences existed between them (FLSD test for multiple samples; 95% confidence level). Figure 3.5 summarizes an example of how the methodology was applied to a K_d dataset, taking account of relevant factors, by performing a GMC for partial datasets based on the soil texture and OM content.

A further comparison between K_d data for the target elements in soils and K_d data for a selected group of other environmental materials (subsoils, tills, gyttjas) was also conducted to evaluate whether these other materials can be considered as soil analogues to: (i) extend the conclusions drawn for K_d data in soils to other environmental materials; and (ii) explore the possibility of complementing soil K_d datasets that have insufficient entries with K_d data for other types of environmental materials (to construct a reliable CDF). In addition, the use of chemical analogues was also tested for Am.

3.3.5.1. K_d best estimate values and cumulative distribution functions for radiocaesium

The updated MODARIA Cs dataset contains 769 entries of K_d (Cs) values, along with related soil characteristic data and information on the experimental approach applied for their quantification. The K_d (Cs) data varies by up to five orders of magnitude, with a minimum–maximum range of 4.0×10^0 – 4.5×10^5 L/kg. Data for other environmental materials, such as subsoils, surface sediments, till and gyttja, were also collected, allowing the development of a dataset ($N = 123$) with the same structure as that of the soil dataset.

The large variability in K_d (Cs) within the MODARIA dataset denotes the strong influence of the contrasting soil properties and/or the different experimental approaches applied to quantify K_d (Cs) values. Therefore, a unique CDF and derived best estimate constructed using the overall dataset is considered unsuitable for the purposes of radiological impact assessment, even for screening scenarios, since it will be associated with a high uncertainty.

The soils were first grouped according to the same criteria that were previously adopted in TRS 472 to create partial K_d (Cs) datasets with an ‘*a priori*’ lower associated variability than the overall MODARIA dataset [3.16]. The grouping criteria were: (i) the ratio between the RIP (discussed below in relation to Eq. (3.5)) of the soil and the potassium concentration in soil solution (K_{ss}) (the RIP/ K_{ss} ratio is related to the mechanisms governing Cs interactions and is a good predictor of the reversible K_d (Cs) [3.21, 3.22]); and (ii) Texture-OM. For this latter criterion, the effect of the experimental approach on the quantification and variability of the K_d (Cs) values was examined.

K_d (Cs) grouped according to the RIP/ K_{ss} criterion

The MODARIA dataset, after being filtered according to the RIP/ K_{ss} criterion, had a larger number of K_d values ($N = 328$) than the dataset reported in TRS 472 ($N = 257$), with K_d (Cs) values varying by five orders of magnitude (Range: 9.6×10^0 – 4.5×10^5 L/kg). Table 3.5 summarizes the K_d (Cs) data obtained by applying the RIP/ K_{ss} criterion. Figure 3.6 represents the CDFs constructed for the four partial datasets derived using the RIP/ K_{ss} criterion.

The resulting MODARIA GM values are similar to those in TRS 472 [3.16]. They consistently show that K_d values increase with increases in RIP/ K_{ss} ratios. The derived partial datasets often have a relatively low variability in K_d (Cs) of less than two orders of magnitude, as opposed to the five orders of magnitude range for the overall dataset (see K_d values comprised in the 5th – 95th percentile ranges).

TABLE 3.5. K_d (Cs) (L/kg DM) FOR SOILS GROUPED ACCORDING TO RIP/ K_{ss} CRITERION

| Partial dataset | N | GM | GSD | Min | Max | 5 th | 95 th |
|-------------------------------|-----|-------------------|-----|-------------------|-------------------|-------------------|-------------------|
| $RIP/K_{ss} < 10^2$ | 74 | 6.9×10^1 | 2.7 | 9.6×10^0 | 1.7×10^3 | 2.6×10^1 | 5.7×10^2 |
| $10^2 \leq RIP/K_{ss} < 10^3$ | 116 | 3.8×10^2 | 4.5 | 2.9×10^1 | 2.9×10^3 | 4.2×10^1 | 4.4×10^3 |
| $10^3 \leq RIP/K_{ss} < 10^4$ | 83 | 1.6×10^3 | 3.4 | 5.9×10^1 | 9.2×10^3 | 2.9×10^2 | 1.9×10^4 |
| $RIP/K_{ss} \geq 10^4$ | 55 | 1.0×10^4 | 4.1 | 7.3×10^2 | 3.8×10^5 | 1.2×10^3 | 9.5×10^4 |

N: Sample size; GM: Geometric Mean; GSD: Geometric Standard Deviation; Min: Minimum; Max: Maximum; 5th: 5th percentile; 95th: 95th percentile.

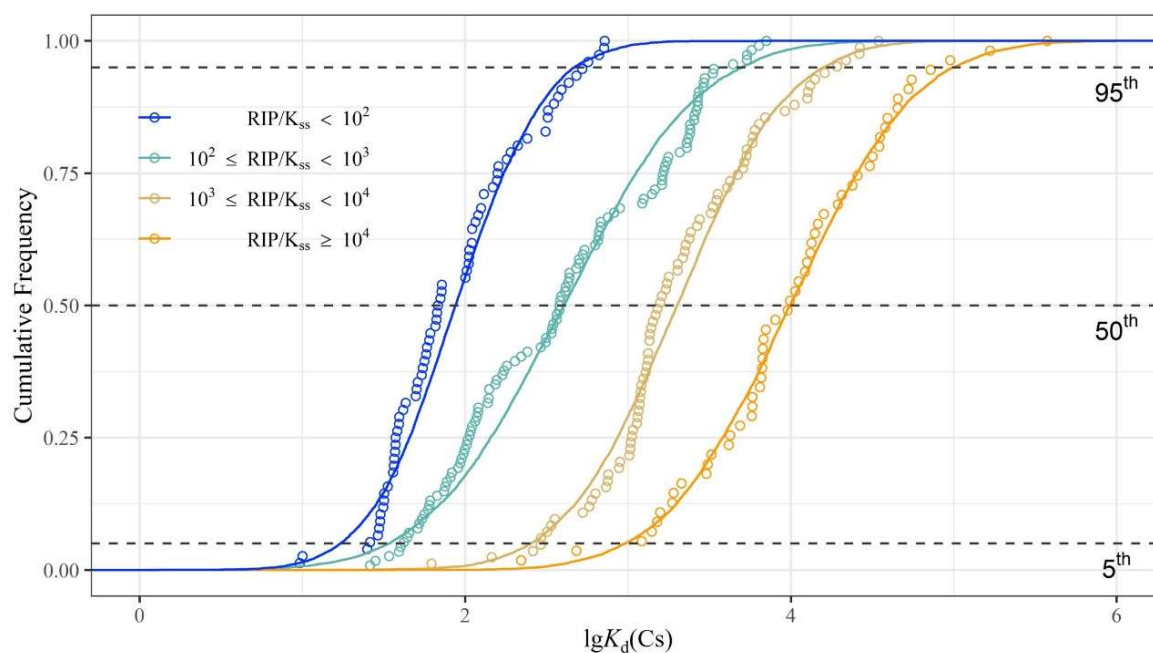


FIG. 3.6. CDFs of K_d d/kg DM (Cs) for soils grouped according to RIP/ K_{ss} criterion.

In addition, the application of the RIP/ K_{ss} criterion generated partial datasets with contrasting K_d (Cs) distributions with little overlap (see the 5th–95th region of the CDFs depicted in Fig. 3.6). However, in this case, investigation of the GM K_d (Cs) is of a lesser importance, as an end user who has relevant RIP and K_{ss} data does not need to use the K_d (Cs) best estimates because the RIP/ K_{ss} ratio can be calculated instead.

Therefore, the CDFs and derived data from the RIP/ K_{ss} criterion are suitable for REIA if data on the RIP of the soil considered and the K in soil solution are available. K_d (Cs) can readily be predicted from RIP/ K_{ss} ratios, as the two variables are highly correlated [3.22]. However, as was already highlighted in TRS 472 [3.16], the major limitation of the RIP/ K_{ss} approach is that the end user cannot predict a K_d (Cs) value for a soil which does not have a reported RIP value. Instead, an equation facilitating the prediction of a RIP from soil properties can be used as soil properties are commonly available to end users, or easier to determine, compared with the RIP parameter itself. Soil clay and silt contents are sufficient for a rough prediction of RIP [3.22, 3.23]. Here, a multiple linear regression is provided, that has been created from the MODARIA dataset and additional studies ($N = 225$) [3.24–3.27], that describes around 70% of RIP variability and reliably correlates RIP values with soil clay and silt contents (referred to total soil weight), as follows:

$$\lg RIP = 1.24 (\pm 0.17) + 0.76 (\pm 0.13) \lg Clay + 0.68 (\pm 0.12) \lg Silt \quad (3.5)$$

where the units for RIP is mmol/kg and $Clay$ and $Silt$ are in wt% referred to as the soil, and ‘ \pm ’ values in parentheses provided for each term in the equation represents the confidence range (95%) of the coefficient of each correlation term. Despite the reasonably good correlation, the improvement of the previous equation to predict RIP values from clay mineralogy rather than clay content remains a future challenge.

Influence of sorption dynamics and methodology approach on K_d (Cs) data

According to the methodological factors established above and the available data, the Cs dataset can be subdivided into two partial datasets containing: (i) data from short term sorption tests; and (ii) data from desorption tests of long term incorporated Cs.

The FLSD test for multiple means (95% confidence level) performed to the GMC pretreated dataset showed that K_d (Cs) data values originating from short term and long term incorporated Cs were significantly different. This implies that different K_d data could be used to derive K_d best estimates, depending on the contamination scenario considered. Table 3.6 summarizes the K_d (Cs) data obtained from the short term and long term partial datasets, and Fig. 3.7 shows a graphical representation of the constructed CDFs.

TABLE 3.6. K_d (Cs) (L/kg DM) FOR SOILS GROUPED ACCORDING TO THE METHODOLOGY CRITERION

| Partial dataset | N | GM | GSD | Min | Max | 5 th | 95 th |
|-----------------|-----|-------------------|-----|-------------------|-------------------|-------------------|-------------------|
| Short term | 601 | 1.6×10^3 | 6.6 | 4.3 | 3.8×10^5 | 4.0×10^1 | 2.2×10^4 |
| Long term | 168 | 2.4×10^4 | 4.2 | 1.1×10^1 | 4.5×10^5 | 1.6×10^3 | 1.5×10^5 |

N: Sample size; GM: Geometric Mean; GSD: Geometric Standard Deviation; Min: Minimum; Max: Maximum; 5th: 5th percentile; 95th: 95th percentile.

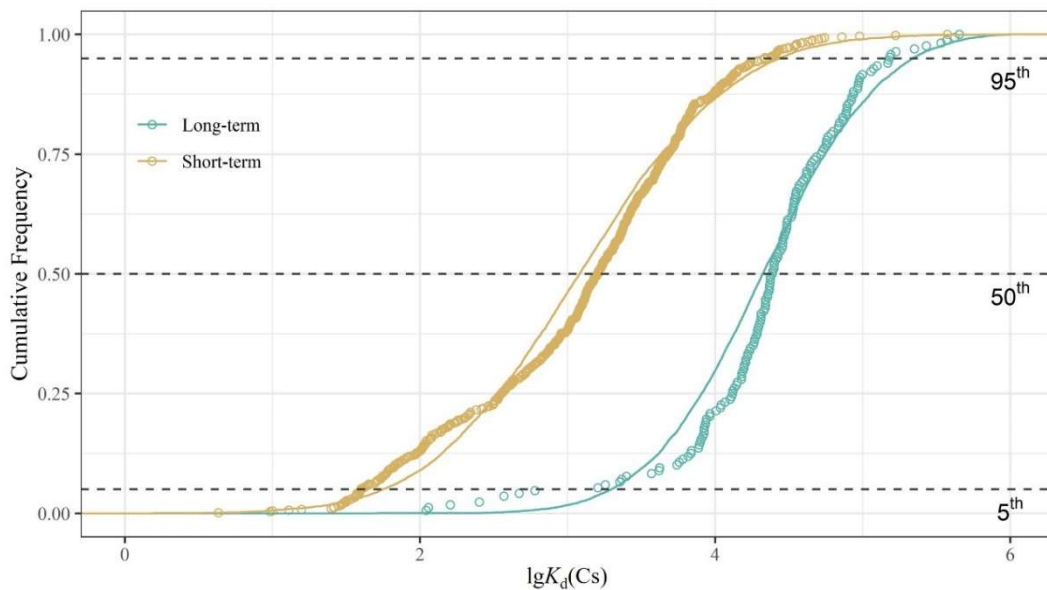


FIG. 3.7. CDFs for K_d (Cs) data in soils according to the methodology criterion.

The K_d (Cs) data for long term incorporated Cs (GM and 5th–95th percentile range values) were one or more orders of magnitude higher than those for short term incorporated Cs. Therefore, the long term CDF (depicted below) had clearly shifted to higher K_d (Cs) values, compared with the short term CDF. This difference can be attributed to changes in Cs sorption with time, as long term incorporated Cs may have undergone an ageing process, which led to an increase in Cs sorption irreversibility. From the exploratory analysis presented here, it is suggested that the user selects either short term or long term K_d (Cs) best estimates, depending on the scenario to be assessed.

K_d (Cs) grouped according to the OM+Texture criterion: redefinition of the OM% thresholds to distinguish between organic and mineral soils

When the RIP/ K_{ss} data of the target soil are not available, best estimates of K_d (Cs) can be derived for different soil types classified according to their (1) OM content, and (2) soil texture or (3) OM content (OM+Texture). Because Cs behaviour in soils is controlled by the clay fraction, unless its content is negligible, the criterion to define an ‘organic soil’ (i.e. the OM content threshold) for K_d (Cs) within the OM+Texture criterion was re-evaluated before attempting to create K_d (Cs) partial datasets using a hierarchical application of the experimental approach and the OM+Texture grouping criteria. To do this, soils were first grouped according to the experimental approach, distinguishing between K_d (Cs) data derived from short term and long term situations, and these two partial datasets were then further split into ‘Mineral’ and ‘Organic’ partial datasets, based on the OM content of the soils. Subsequently, the Mineral dataset was split into textural groups.

The K_d (Cs) GM values and related 5th–95th intervals indicated that, for short term K_d values, an OM threshold of 50% can be used because the variability in the K_d data within the Organic and Mineral partial datasets is much lower than the 20% OM threshold. For K_d data related to long term incorporated Cs, the optimal OM threshold obtained was 90%, giving the lowest variability in K_d data and the most significantly different GM values between the examined partial datasets. As an additional confirmation to revise OM thresholds, similar GM values were obtained for the short term and long term organic datasets, as the effect of interaction dynamics on K_d (Cs) for organic soils is expected to be negligible. Table 3.7 summarizes the K_d (Cs) data obtained using the optimized OM thresholds and compares these data with those derived using the 20% OM threshold previously used for the OM+Texture criterion.

TABLE 3.7. COMPARISON OF K_d (Cs) (L/kg DM) DATA GROUPED ACCORDING TO PREVIOUS AND OPTIMIZED %OM THRESHOLDS

| <i>Short term K_d (Cs)</i> | | | | | | | | |
|---|--------------|-----|-------------------|-----|-------------------|-------------------|-------------------|-------------------|
| Partial dataset | OM threshold | N | GM | GSD | Min | Max | 5 th | 95 th |
| Organic | 20% | 60 | 1.8×10^2 | 6.1 | 1.3×10^1 | 7.2×10^4 | 2.0×10^1 | 4.1×10^3 |
| | 50% | 38 | 8.9×10^1 | 4.2 | 1.3×10^1 | 1.9×10^3 | 1.3×10^1 | 1.9×10^3 |
| Mineral | 20% | 345 | 2.7×10^3 | 4.3 | 1.0×10^1 | 1.7×10^5 | 1.3×10^2 | 2.4×10^4 |
| | 50% | 367 | 2.5×10^3 | 4.5 | 1.0×10^1 | 1.7×10^5 | 1.2×10^2 | 2.4×10^4 |
| <i>Long term K_d (Cs)</i> | | | | | | | | |
| Partial dataset | OM threshold | N | GM | GSD | Min | Max | 5 th | 95 th |
| Organic | 20% | 20 | 2.0×10^3 | 7.4 | 7.3×10^1 | 1.5×10^5 | 1.1×10^2 | 9.2×10^4 |
| | 90% | 7 | 3.7×10^2 | 2.4 | 7.3×10^1 | 1.6×10^3 | 1.1×10^2 | 1.6×10^3 |
| Mineral | 20% | 148 | 2.8×10^4 | 2.6 | 2.3×10^3 | 4.5×10^5 | 6.8×10^3 | 1.5×10^5 |
| | 90% | 161 | 2.5×10^4 | 3.2 | 1.1×10^2 | 4.5×10^5 | 4.2×10^3 | 1.5×10^5 |

N: Sample size; GM: Geometric Mean; GSD: Geometric Standard Deviation; Min: Minimum; Max: Maximum; 5th: 5th percentile; 95th: 95th percentile.

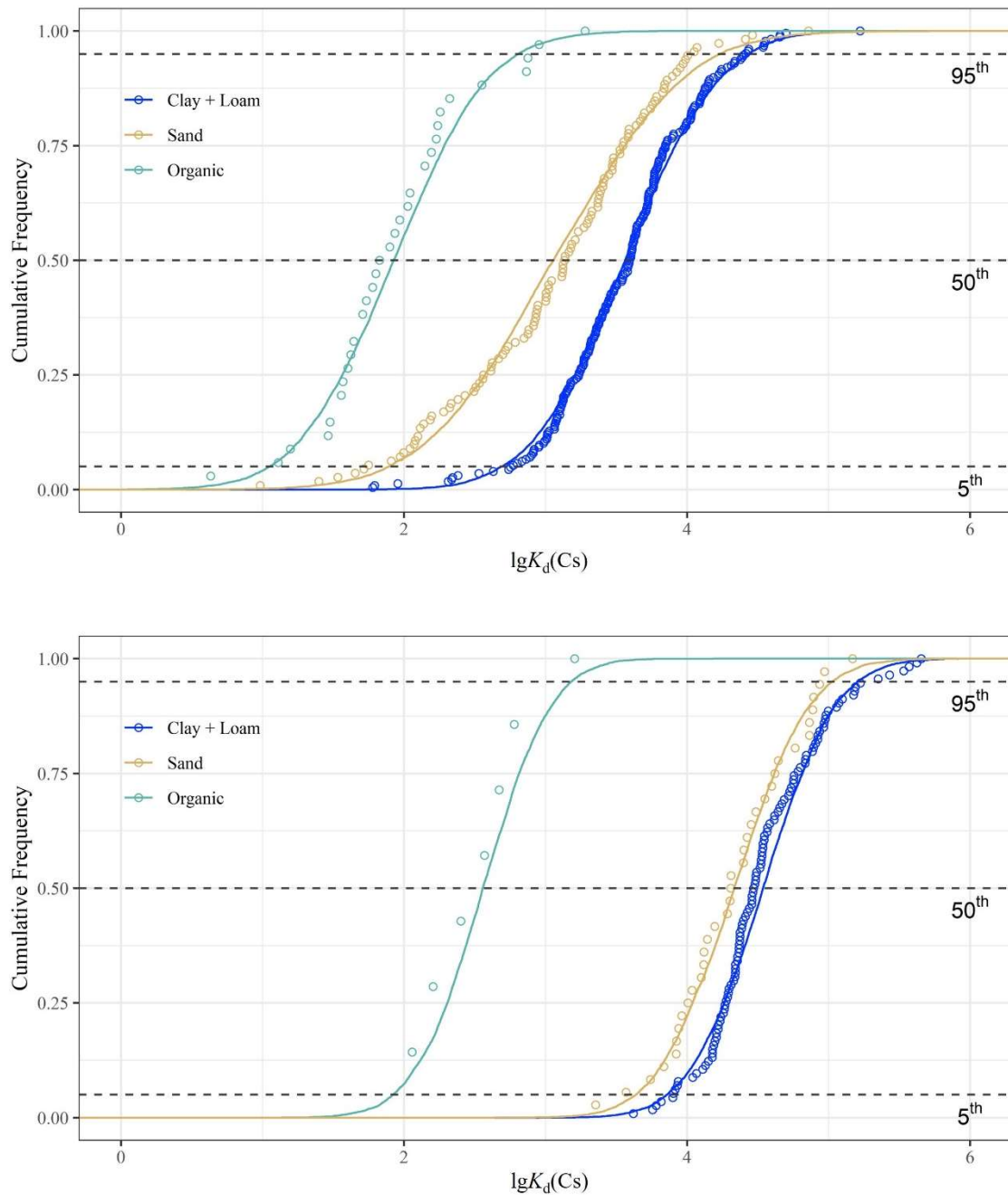


FIG. 3.8. CDFs of K_d (Cs) based on redefined OM+Texture criterion. (A). Short term. (B) Long term.

In all cases, GM for mineral soils were higher than for organic soils. The ‘Mineral’ datasets were split into ‘Sand’, ‘Loam’ and ‘Clay’ textural groups. Although no statistically significant differences existed between the K_d (Cs) data of the ‘Clay’ and ‘Loam’ partial datasets, K_d (Cs) increased with the clay content ($GM_{\text{Sand}} < GM_{\text{Loam}} < GM_{\text{Clay}}$). Figure 3.8 shows CDFs constructed from the partial organic and mineral texture datasets obtained by grouping the MODARIA dataset into a short term and a long term dataset using the revised OM+texture criterion).

This pattern is consistent with Cs sorption mechanisms, namely that Cs sorption is strongly influenced by particle surface area to volume ratio, the greater binding affinities of clay

minerals, and the relatively weak complexation of Cs to natural OM. The resulting partial datasets have a much lower variability than those that had been generated only using the classical OM+Texture criterion. They differ significantly according to the FLSD test for multiple means (95% confidence level, except for the K_d (Cs) data compiled from the ‘Loam’ and ‘Clay’ texture partial datasets). In addition, for a given textural soil group, the long term K_d (Cs) data are systematically higher (by about one order of magnitude) than the equivalent short term data (numerical details are given in Table 3.8).

The above analysis indicates that soil texture can be a relevant factor in K_d (Cs) determination, which, if accounted for, can further decrease variability in K_d (Cs), thereby providing better input data for radiological impact assessments. In doing so, it is necessary to first decide whether the conditions considered correspond to a short term radioactive release (for instance, after a recent introduction of radioisotopes into the environment) or to a long term discharge (such as in the context of safety and performance assessments of deep geological disposal facilities, long term impact assessment, or assessment of impacts under steady state conditions). Also, for each set of conditions, it is important to adequately distinguish between organic and mineral soils using the newly established OM thresholds, since GM values for organic and mineral soils may differ by up to two orders of magnitude.

K_d (Cs) data from environmental solid materials analogous to soils

The number of K_d (Cs) data for soils available in the literature was sufficiently large to successfully apply different grouping criteria, which substantially decreased the initial variability of the overall K_d (Cs) data from 4–5 orders of magnitude to 1–2 orders of magnitude. Therefore, for Cs the use of data from other environmental solid materials was not needed to derive reliable K_d (Cs) best estimates or to properly describe K_d (Cs) variability.

The interaction of Cs with other environmental solid materials, such as gyttja, tills or subsoils, is also relevant for site specific studies that potentially may be of high radioecological interest [3.28, 3.29]. Consequently, an evaluation was carried out to determine whether the K_d (Cs) data may be suitable to assess the partitioning of Cs in such samples.

The K_d (Cs) values for surface sediment, subsoil, gyttja and till samples collected in the MODARIA dataset were grouped, where possible, according to the experimental method and the redefined OM+Texture criterion and were compared with the corresponding soil data. Table 3.9 summarizes the groups that were created and the number of available data entries in each case.

The FLSD test for multiple means (95% confidence level) generally revealed no significant differences between the K_d (Cs) data for soils and those for the other environmental solid materials. The conclusions drawn from the analysis are to be treated with care, due to the limited number of observations in the partial datasets created, but they suggest that the K_d (Cs) best estimates for soils are also suitable for predicting the Cs sorption in other environmental solid materials.

TABLE 3.8. SUMMARY OF K_d (Cs) DATA (L/kg DM) FOR DIFFERENT CONTAMINATION SCENARIOS AND SOIL TYPES

| Available information | K_d (Cs) group | GM | GSD | 5 th | 95 th | |
|---|------------------|-------------------------------|-------------------|-------------------|-------------------|-------------------|
| None | Overall | 2.5×10^3 | 8.6 | 5.0×10^1 | 6.3×10^4 | |
| Elapsed time since contamination | Short term | 1.6×10^3 | 6.6 | 4.0×10^1 | 2.2×10^4 | |
| | Long term | 2.4×10^4 | 4.2 | 1.6×10^3 | 1.5×10^5 | |
| Elapsed time since contamination; %OM | Short term | Organic (OM \geq 50%) | 8.9×10^1 | 4.2 | 1.3×10^1 | 1.9×10^3 |
| | | Mineral (OM < 50%) | 2.5×10^3 | 4.5 | 1.2×10^2 | 2.4×10^4 |
| | Long term | Organic (OM \geq 90%) | 3.7×10^2 | 2.4 | 1.1×10^2 | 1.6×10^3 |
| | | Mineral (OM < 90%) | 2.5×10^4 | 3.2 | 4.2×10^3 | 1.5×10^5 |
| Elapsed time since contamination; %OM; soil texture | Short term | Clay+Loam | 3.9×10^3 | 3.3 | 5.9×10^2 | 2.6×10^4 |
| | | Sand | 1.4×10^3 | 5.2 | 5.6×10^1 | 1.1×10^4 |
| | Long term | Clay+Loam | 3.0×10^4 | 2.6 | 8.0×10^3 | 2.2×10^5 |
| | | Sand | 2.0×10^4 | 2.7 | 3.7×10^3 | 9.4×10^4 |
| Radiocaesium Interception Potential (RIP)*; potassium in soil solution (K_{ss}) | Short term | $RIP/K_{ss} < 10^2$ | 6.9×10^1 | 2.7 | 2.6×10^1 | 5.7×10^2 |
| | | $10^2 \leq RIP/K_{ss} < 10^3$ | 3.8×10^2 | 4.5 | 4.2×10^1 | 4.4×10^3 |
| | | $10^3 \leq RIP/K_{ss} < 10^4$ | 1.6×10^3 | 3.4 | 2.9×10^2 | 1.9×10^4 |
| | | $RIP/K_{ss} \geq 10^4$ | 1.0×10^4 | 4.1 | 1.2×10^3 | 9.5×10^4 |

GM: Geometric Mean; GSD: Geometric Standard Deviation; 5th: 5th percentile; 95th: 95th percentile.
 * RIP can be estimated from Eq. (3.5).

TABLE 3.9. SUMMARY OF K_d (Cs) ENTRIES AVAILABLE FOR ENVIRONMENTAL SOLID MATERIALS OTHER THAN SOILS

| Material | Partial dataset | N | |
|------------------|-----------------|--------------|----|
| Surface sediment | Short term | All textures | 22 |
| | | Sand | 8 |
| Subsoil | Short term | All textures | 12 |
| | | Sand | 7 |
| Gyttja | Long term | All textures | 16 |
| | | Clay | 4 |
| | | Sand | 1 |
| | | Organic | 1 |
| Till | Short term | All textures | 28 |
| | | Clay | 1 |
| | | Loam | 1 |
| | | Sand | 18 |
| | Long term | All textures | 17 |
| | | Loam | 9 |
| | | Sand | 8 |

Proposal of K_d (Cs) best estimates from the analysis of the MODARIA dataset

Analyses performed with the K_d (Cs) dataset have shown that sorption dynamics had a strong impact on the K_d (Cs) values, which could be taken into consideration to generate more realistic radiological impact assessments. In addition, they also show that soil properties affected the K_d (Cs) values either directly via the mechanisms ruling Cs sorption in soils, such as soil RIP and potassium concentration in soil solution, or indirectly via factors such as the soil OM and, to a lesser extent, the soil texture.

Consequently, the use of a single K_d (Cs) best estimate and/or CDF has limited practical value for modelling because of the large variability (five orders of magnitude). The approach developed in MODARIA provides a viable alternative that can be utilized by modellers and end users to select the CDF and best estimates from the values summarized in Table 3.8 to better reflect the conditions of the scenario and the characteristics of the soil to be assessed.

Initially, it is important to distinguish whether the assessment is being carried out for a recent radioactive release (short term scenario) or for a release that occurred long enough ago to assume a long term scenario. Secondly, if the OM content of the target soil is available, the CDF corresponding to the soil type (Organic or Mineral) can be used. If soil texture data are also available, the CDF can be further refined based on the textural group. Finally, if the radiological impact assessment is carried out for a short term scenario and the RIP and K_{ss} data are available, the CDF of the corresponding RIP/ K_{ss} group is preferable to any of the values previously proposed. For those soils, no RIP value and $OM \leq 20\%$, the RIP can be predicted directly from the clay and silt contents of the soil using the regression provided in Eq. (3.5) above.

3.3.5.2. K_d best estimate values and cumulative distribution functions for americium

The MODARIA Am dataset contains 109 entries of K_d (Am) values, an increase of 47 values compared to TRS 472 [3.16]. The values range over four orders of magnitude, with a minimum–maximum range of 2.7×10^1 – 2.8×10^5 L/kg. In addition, 33 entries for other samples, such as subsoils and surface sediments, are available.

New grouping criteria for K_d (Am)

Recent studies have reported that Am sorption in soils is governed by pH, OM and specific surface area (SSA)³, in addition to the strong effect of Am speciation [3.30, 3.31]. An increase in pH leads to an increase in the negative charge of the soil sorption sites. As the dominant Am species within a pH range of roughly 3–9 are cationic, a pH increase would lead to an increase in Am sorption. At $pH \geq 9$, there is a much stronger tendency for processes other than sorption to occur, including precipitation and/or coprecipitation with carbonate phases, and considerably higher K_d (Am) values would be expected. Conversely, in soil–water systems with high dissolved carbonate content, anionic carbonate complexes of Am are predominant, so significantly lower K_d (Am) would be expected.

Furthermore, in soils with a high OM content, leading to a high concentration of dissolved organic species in the soil solution, Am will form negatively charged humate complexes that remain in solution, especially at pH values exceeding 6. Therefore, under such conditions, Am is sorbed to a lesser extent compared with soils with a low OM. Complicating matters further, at $pH < 6$, the OM itself may enhance Am sorption, as the negative humate complexes may sorb at the positively charged mineral surfaces, thereby providing additional Am sorption sites. Finally, Am sorption increases in soils with a higher SSA, which is a factor indirectly related to the soil texture.

³ The specific surface area (SSA) is defined as the total surface area of a material per unit of mass (m^2/kg or m^2/g) or solid volume (m^2/m^3 or l/m).

The high number of known variables affecting Am sorption implies that it may be difficult to reduce the variability of K_d (Am) on the sole basis of pH, OM or specific surface area. Multiple linear regressions calculated from the analysis of a range of different soils has recently been developed (see Eqs (3.13) and (3.14)) to roughly estimate the K_d (Am) values in soils, based on properties related to the soil factors mentioned above [3.31], as follows:

$$\lg K_d(\text{Am}) = 2.2(\pm 0.5) + 0.5 (\pm 0.2) \lg \text{BET} + 0.25 (\pm 0.08) \text{pH}; [r = 0.79] \quad (3.6)$$

$$\lg K_d(\text{Am}) = 5.0(\pm 0.3) - 0.7(\pm 0.2) \lg \text{DOC} + 0.5(\pm 0.2) \lg \text{CaCO}_3; [r = 0.79] \quad (3.7)$$

where BET is a measure of SSA ($\text{m}^2/\text{g DM}$); DOC represents the dissolved organic carbon (mg/L), CaCO_3 represents the carbonate content in the soil solid phase ($\text{wt}\%$ referred as to the soil), and the ‘ \pm ’ values in parentheses provided for each term in Eqs (3.6) and (3.7) represent the confidence range of the coefficient of each correlation term.

To take into account the various factors discussed above that may affect K_d (Am) values in soils, grouping criteria need to be developed that combine readily available, or easy to determine, soil properties.

The SSA is often not available from routine soil characterization data, so it is not possible to apply a grouping criterion based on this parameter. Nevertheless, since the soil SSA is related to the presence of the finest soil particles ($<200 \mu\text{m}$), the effect of the SSA factor could be partially evaluated by considering a surrogate soil texture factor, as it is expected that $\text{SSA}_{\text{Clay}} > \text{SSA}_{\text{Loam}} > \text{SSA}_{\text{Sand}}$. The inadequacy of the OM+Texture alone for grouping K_d (Am) data to decrease its variability was observed in TRS 472 [3.14]. One reason that may explain this observation is that an OM threshold of 20% was used to distinguish between minerals and organic soils. Recent work has shown that, even for lower OM contents, the concentration of dissolved organic compounds is sufficient to affect the Am speciation in solution and, consequently, its interaction with the soil matrix [3.31]. Accordingly, the OM+Texture can be redefined for K_d (Am) by establishing an OM threshold of 10% for a soil to be included within the organic group.

Americium sorption in soils is highly dependent on the pH value. Therefore, a new grouping criterion based on the pH factor has also been evaluated by partitioning the Am K_d values into pH categories [3.30]. The pH ranges adopted were:

- pH 3–6: positively charged sorption sites, with expected lower K_d (Am) due to existence of cationic Am species (primarily as Am^{3+});
- pH 6–7.5: deprotonated sorption sites, which result in an increase in the sorption of cationic Am species (mainly $[\text{Am}(\text{OH})_2]^+$ and $[\text{AmCO}_3]^+$);
- pH 7.5–9: increases in negatively charged sorption sites, with expected high K_d (Am). In soil–water systems with a high content of dissolved carbonate, lower K_d values may occur due to the formation of the anionic $[\text{Am}(\text{CO}_3)_2]^-$ species;
- pH > 9: much lower K_d (Am) are anticipated since anionic and neutral Am species (primarily as $[\text{Am}(\text{CO}_3)_3]^{3-}$ and $[\text{Am}(\text{OH})_3]$) prevail, unless Am precipitation or coprecipitation occurs.

As the effect of pH on Am sorption in organic soils is much more complex and more difficult to systematize, a second grouping criterion based on the pH and OM (the pH+OM criterion) was applied. This combined criterion is aimed at creating pH partial datasets for mineral soils only.

Since specific surface area influences the Am sorption in soils, an improvement in K_d (Am) data grouping was assessed by further splitting the pH-mineral partial datasets containing K_d data at $\text{pH} < 9$ according to the soil texture (sand, loam and clay), resulting in partial datasets containing K_d (Am) data only from a given soil texture. The reason for not splitting the mineral $\text{pH} \geq 9$ partial dataset according to soil texture is that the resulting K_d variability could be mainly caused by the inclusion of K_d data compiled for soil–water systems in which Am precipitation occurs, a process that cannot be captured by soil texture.

Influence of methodology on K_d (Am) data

The K_d (Am) data available in the MODARIA dataset originated from only sorption and desorption tests in which Am was recently added and was, therefore, only representative for the short term interaction of Am in soils. The statistical tests performed to the GMC pretreated dataset indicated that no significant difference exists between K_d (Am) values obtained from sorption versus desorption tests, suggesting that the variability in K_d (Am) values is mostly due to the contrasting properties of the soils, and that potential effect of sorption dynamics on K_d (Am) would play a minor role.

K_d (Am) grouped according to the redefined Texture-OM criterion

A total of 55 entries in the MODARIA dataset were suitable to apply the redefined OM+Texture criterion, with an OM threshold of 10%. Table 3.10 summarizes the K_d (Am) data generated. The application of a lower OM threshold led to partial datasets corresponding to Organic and Mineral soils with more contrasting K_d distributions, enabling a better distinction between the K_d data of these two groups of soils. The GMs derived from the Mineral dataset were slightly higher than that of the Organic soils, and the GM values of the textural groups increased with increasing soil clay content, which is consistent with expected Am sorption mechanisms in soils and improves upon the values provided in TRS 472 [3.16].

The initial 4 orders of magnitude variability of the overall dataset decreased down to 2–3 orders of magnitude depending on the partial dataset applied. The K_d (Am) values for the redefined Organic group fell within only a 2 orders of magnitude range, thus reducing data variability for this type of soils. Data variability remained high for mineral soils, as some of the factors relevant to Am sorption, such as pH, are not included in the redefined OM+Texture criterion.

Application of the pH criterion to group K_d (Am) data

Table 3.11 summarizes the K_d (Am) data generated when the dataset ($N = 87$) was grouped solely based on the pH criterion. The four partial datasets created according to the pH criterion presented contrasting GM values showing that the K_d (Am) best estimates clearly increased within the 3–9 pH range, and decreased at higher pH values, which agrees with expected Am sorption mechanisms. The 5th–95th percentile ranges derived from partial datasets included K_d (Am) values that were within around two orders of magnitude, except for soils with $\text{pH} \geq 9$, which suggests that other interaction mechanisms need to be considered to assess the K_d (Am) data in these soils as stated above.

TABLE 3.10. K_d (Am) (L/kg DM) DATA GROUPED ACCORDING TO THE REDEFINED TEXTURE-OM CRITERION

| Partial dataset | N | GM | GSD | Min | Max | 5 th | 95 th |
|-------------------------|----|-------------------|------|-------------------|-------------------|-------------------|-------------------|
| Organic (OM \geq 10%) | 10 | 5.1×10^3 | 3.9 | 2.1×10^2 | 4.9×10^4 | 2.1×10^2 | 4.9×10^4 |
| Mineral (OM < 10%) | 45 | 8.8×10^3 | 6.2 | 6.7×10^1 | 1.1×10^5 | 2.8×10^2 | 9.1×10^4 |
| Clay | 3 | 1.1×10^4 | n.a. | 2.8×10^2 | 5.6×10^4 | n.a. | n.a. |
| Loam | 25 | 1.2×10^4 | 4.3 | 4.1×10^2 | 1.1×10^5 | 9.9×10^2 | 1.0×10^5 |
| Sand | 13 | 4.8×10^3 | 5.2 | 6.7×10^1 | 3.7×10^4 | 6.7×10^1 | 3.7×10^4 |

N: Sample size; GM: Geometric Mean; GSD: Geometric Standard Deviation; Min: Minimum; Max: Maximum; 5th: 5th percentile; 95th: 95th percentile; n.a. not available.

TABLE 3.11. K_d (Am) (L/kg DM) FOR SOILS GROUPED ACCORDING TO pH

| Partial dataset | N | GM | GSD | Min | Max | 5 th | 95 th |
|--------------------------|----|-------------------|-----|-------------------|-------------------|-------------------|-------------------|
| $3 \leq \text{pH} < 6$ | 34 | 3.2×10^3 | 4.5 | 6.7×10^1 | 5.2×10^4 | 2.0×10^2 | 4.8×10^4 |
| $6 \leq \text{pH} < 7.5$ | 23 | 7.3×10^3 | 5.3 | 6.7×10^1 | 4.7×10^4 | 1.8×10^2 | 3.6×10^4 |
| $7.5 \leq \text{pH} < 9$ | 21 | 1.1×10^4 | 5.8 | 9.1×10^1 | 1.1×10^5 | 1.3×10^3 | 1.0×10^5 |
| $\text{pH} \geq 9$ | 9 | 4.8×10^2 | 8.7 | 2.7×10^1 | 2.2×10^4 | 2.7×10^1 | 2.2×10^4 |

N: Sample size; GM: Geometric Mean; GSD: Geometric Standard Deviation; Min: Minimum; Max: Maximum; 5th: 5th percentile; 95th: 95th percentile

Hierarchical application of soil factors related to Am sorption to group K_d (Am) data

When excluding the K_d (Am) data for organic soils (OM \geq 10%) from the partial datasets based on pH (pH+OM criterion), the GM values derived for the CDFs of each Mineral-pH partial dataset were not significantly different from those previously generated using the pH criterion according to the FLSD test for multiple means ($p > 0.05$). This outcome confirms the role of the pH in Am sorption in soils. However, the 5th–95th percentile regions of the CDFs constructed from the Mineral-pH partial datasets did not overlap and the variability in K_d was lower than for the pH partial datasets. Therefore, if data on the pH and OM are available, the K_d (Am) CDFs constructed for the different pH+Mineral categories, after excluding soils with OM \geq 10% can be used.

When pH+textural partial datasets are created, only partial datasets corresponding to loamy soils had sufficient data to reliably construct a CDF. Therefore, to apply the pH+OM+Texture approach, either more data on Am sorption in soils or analogue data would need to be included to fill the gaps and/or increase the relative number of entries in each dataset. The strategy of using analogue data is considered in the following text.

Comparison between K_d (Am) data in soils and K_d data from analogue elements and/or environmental samples

All entries in the MODARIA soil K_d dataset corresponding to: (i) K_d data for Am compiled for environmental materials other than soils (subsoils and surface sediments); and (ii) K_d data for trivalent lanthanides and actinides (La, Sm, Eu, Gd, Er, Lu and Cm) compiled either for soils or other solid environmental materials (gyttjas, tills and subsoils) were pooled in the same dataset (Am+analogue K_d dataset) after testing that there were no statistical differences among element and material datasets created after grouping data based on a given soil factor. This strategy drastically increased the number of entries in each partial dataset.

Table 3.12 summarizes the information derived from the Am+analogue K_d dataset for Organic and pH+Mineral datasets. After applying the FLSD test for multiple means, there were significant differences between the GM values of the ‘Mineral’ and ‘Organic’ datasets ($p < 0.05$), especially due to the low variability of the ‘Organic’ dataset, with values ranging within one order of magnitude (see Fig. 3.9). The derived OM+texture partial datasets also led to GM that were statistically different, following the sequence $GM_{\text{Sand}} < GM_{\text{Loam}} < GM_{\text{Clay}}$ (see Table 3.13).

The GM of the pH partial datasets created with the mineral soils were also statistically different (FLSD test for multiple means; $p < 0.05$), with values systematically increasing with pH, and then decreasing from pH 9 onwards. The CDFs had minor overlaps and 5th–95th ranges of two orders of magnitude (see Fig. 3.10).

Proposed K_d (Am) data based on analysis of the Am MODARIA dataset

The K_d (Am) values in soils in the MODARIA dataset varied by up to four orders of magnitude because of the strong effect that a few soil properties have on K_d (Am). Therefore, it is not suggested to perform REIA with a single K_d (Am) best estimate and its associated CDF. K_d (Am) best estimates and CDFs were derived with much lower variability when K_d values were grouped based on soil properties relevant to the Am sorption in soils. Modellers and end users may choose the most suitable CDFs from those summarized in Table 3.13 depending on the data available for the soil and scenario under assessment.

Among those soil variables available in routine analyses, pH and OM content are the properties that most strongly affect the K_d (Am) data. A single CDF can be suggested for organic soils ($OM \geq 10\%$), whereas for mineral soils ($OM < 10\%$) it is necessary to take into consideration texture and/or pH to further decrease data variability.

CDFs constructed for the different pH+mineral categories have also been provided, although the lack of relevant data made it difficult to further subdivide the categories according to textural groups. Therefore, a future challenge is to extend the detailed information for the different textural soil groups and for all pH ranges.

The CDFs provided here to describe K_d (Am) in soils can also be applied to predict K_d (Am) values for Gytija, Till and subsoil samples, as well as K_d data for other trivalent actinides (Cm) and lanthanides (e.g. La, Eu, Sm, Gd, and Lu) in mineral and organic soils.

TABLE 3.12. K_d (L/kg DM) OF Am + ANALOGUE DATASET GROUPED ACCORDING TO OM AND pH CRITERION

| Partial dataset | N | GM | GSD | Min | Max | 5 th | 95 th |
|------------------------|-----|-------------------|------|-------------------|-------------------|-------------------|-------------------|
| Organic | 84 | 4.5×10^3 | 2.7 | 2.1×10^2 | 6.1×10^4 | 1.3×10^3 | 1.5×10^4 |
| Mineral | 156 | 1.1×10^4 | 5.7 | 6.7×10^1 | 3.9×10^5 | 3.5×10^2 | 9.6×10^4 |
| 3 ≤ pH < 6 (Mineral) | 54 | 2.1×10^3 | 5.4 | 6.7×10^1 | 8.0×10^4 | 2.5×10^2 | 5.2×10^4 |
| 6 ≤ pH < 7.5 (Mineral) | 48 | 1.0×10^4 | 5.2 | 6.7×10^1 | 6.3×10^4 | 1.9×10^2 | 4.7×10^4 |
| 7.5 ≤ pH < 9 (Mineral) | 62 | 3.7×10^4 | 4.6 | 2.2×10^2 | 2.6×10^5 | 1.3×10^3 | 1.1×10^5 |
| pH ≥ 9 (Mineral) | 12 | 3.8×10^3 | 10.4 | 2.7×10^1 | 2.2×10^4 | 2.7×10^1 | 3.6×10^4 |

N: Sample size; GM: Geometric Mean; GSD: Geometric Standard Deviation; Min: Minimum; Max: Maximum; 5th: 5th percentile; 95th: 95th percentile.

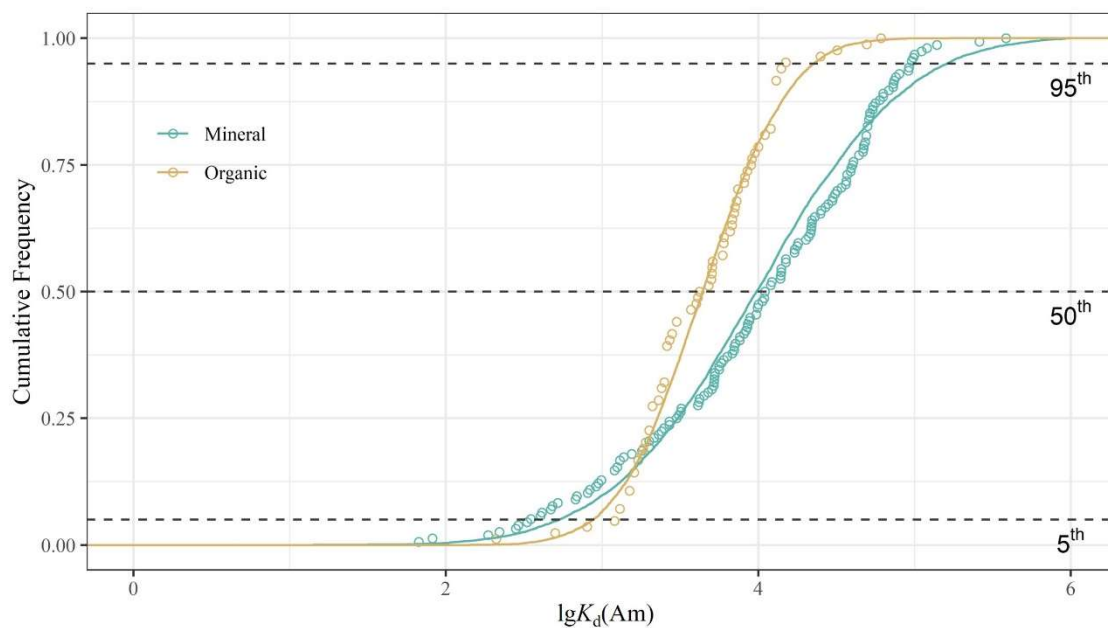


FIG. 3.9. CDFs of K_d (Am) on the basis of redefined OM criterion.

TABLE 3.13. SUMMARY OF K_d (L/kg DM) (Am) CDFs FOR DIFFERENT TYPES OF SOILS AND pH (L/kg)

| Available information | K_d (Am) group | GM | GSD | 5 th | 95 th | |
|-----------------------|--------------------------|--------------------------|-------------------|-------------------|-------------------|-------------------|
| None | Overall | 7.4×10^3 | 4.8 | 4.7×10^2 | 7.8×10^4 | |
| %OM | Organic | 4.5×10^3 | 2.7 | 1.3×10^3 | 1.5×10^4 | |
| | Mineral | 1.1×10^4 | 5.7 | 3.5×10^2 | 9.6×10^4 | |
| %OM; Texture | Clay | 5.6×10^4 | 5.7 | 2.8×10^2 | 3.9×10^5 | |
| | Loam | 1.9×10^4 | 3.4 | 2.7×10^3 | 9.1×10^4 | |
| | Sand | 4.9×10^3 | 5.1 | 2.2×10^2 | 3.7×10^4 | |
| pH | $3 \leq \text{pH} < 6$ | 3.0×10^3 | 3.6 | 4.1×10^2 | 3.9×10^4 | |
| | $6 \leq \text{pH} < 7.5$ | 9.8×10^3 | 4.3 | 2.8×10^2 | 6.1×10^4 | |
| | $7.5 \leq \text{pH} < 9$ | 3.7×10^4 | 5.1 | 6.9×10^2 | 1.4×10^5 | |
| | $\text{pH} \geq 9$ | 8.8×10^3 | 16 | 2.7×10^1 | 2.2×10^5 | |
| pH; %OM | Mineral | $3 \leq \text{pH} < 6$ | 2.1×10^3 | 5.4 | 2.5×10^2 | 5.2×10^4 |
| | Mineral | $6 \leq \text{pH} < 7.5$ | 1.0×10^4 | 5.2 | 1.9×10^2 | 4.7×10^4 |
| | Mineral | $7.5 \leq \text{pH} < 9$ | 3.7×10^4 | 4.6 | 1.3×10^3 | 1.1×10^5 |
| | Mineral | $\text{pH} \geq 9$ | 3.8×10^3 | 10 | 2.7×10^1 | 3.6×10^4 |

GM: Geometric Mean; GSD: Geometric Standard Deviation; Min: Minimum; Max: Maximum; 5th: 5th percentile; 95th: 95th percentile.

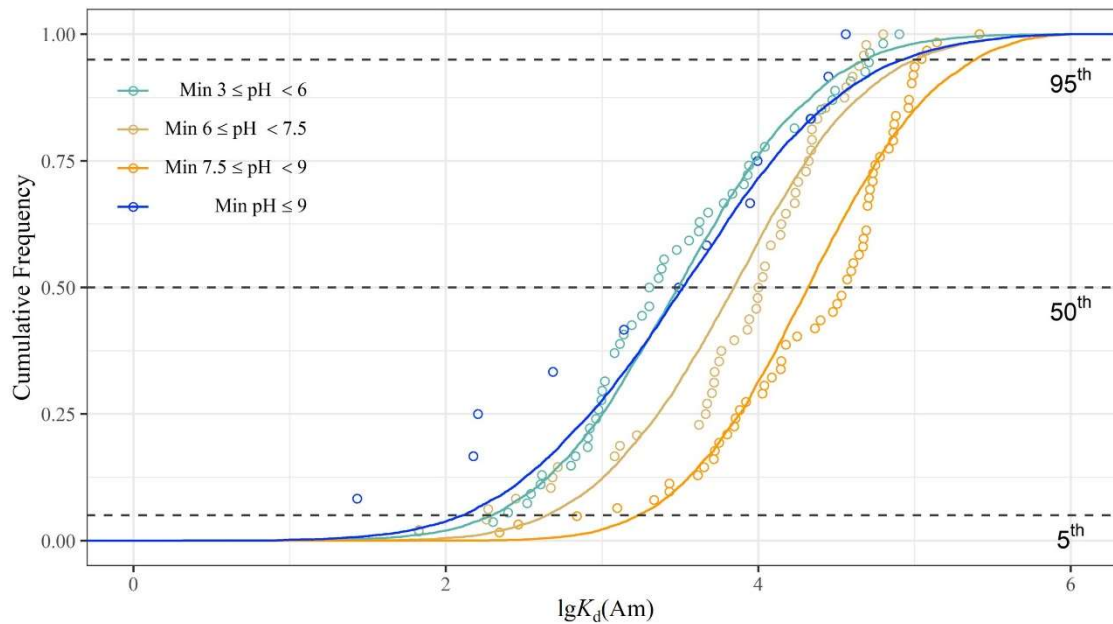


FIG. 3.10. CDFs of K_d (Am) based on pH+OM criterion.

3.3.6. Key findings from the analysis of the soil K_d dataset

The compilation of soil K_d values provided in TRS 472 [3.16] is generally summarized in large tables with overall GM values for radionuclides. The K_d values do not consider the scenario to be assessed. The variation of K_d with soil is often classified solely according to the texture, which is not the main factor affecting K_d variability for many radionuclides. Other soil factors were only taken into account for a few cases leading to decreases in the variability of the K_d resulting in more reliable GM values. Also, the influence of the methodology used for the quantification of the K_d (e.g. sorption and desorption experiments with recently or long term incorporated radionuclide) is not considered in the soil dataset analyses in TRS 472 [3.16].

The description of soil K_d distributions with CDFs derived from the MODARIA datasets for the examples of Cs and Am provided a statistical derivation of the K_d best estimates (as the GM is derived from the 50th percentile of the distribution) and a statistically based approach to disregard extremely low and high K_d values by establishing percentile thresholds, thereby excluding a percentage of the overall distribution (e.g. using 5th and 95th percentiles). The approach is a clear step forward with respect to previous analyses of the soil dataset in TRS 472 [3.16].

The large variability in K_d data could be decreased by grouping K_d values based on the applied methodology and on the parameters that account for soil mechanisms governing radionuclide–soil interaction. This is a better approach than using a single CDF and K_d best estimate without consideration of the properties of a soil (e.g. pH; OM content; texture) or the conditions to be assessed (e.g. short term vs. long term).

To do this, it is suggested that grouping criteria be established based on key factors governing the target radionuclide interaction to create more homogenous partial datasets for which CDFs and K_d best estimates with a lower variability can subsequently be derived. As knowledge of the mechanisms governing the interactions of radionuclides in soils improves and the number of entries in datasets increases, a better analysis of the relevant factors affecting the K_d variability will be possible. The K_d grouping criterion are likely to vary as mechanisms governing interactions with soil also differ from one radionuclide to another.

Although soil K_d datasets are continuously updated, there are still evident gaps in K_d values for many radionuclides and soil types. However, the use of data from environmental solid materials other than soils can be used to fill gaps in some cases, and, conversely, data from soils can be used to predict the sorption of radionuclides in environmental solid materials other than soils.

The information provided in this publication has shown the potential of what can be done to improve soil K_d compilations that can be used for assessments. In the future, the approach could be extended to other radionuclides important for REIA, once the main factors that are needed to create partial datasets have been elucidated for radionuclides with an adequately large numbers of entries.

The substantial increase in soil K_d values for some elements made it possible to: (i) confirm the sorption mechanisms governing the radionuclide interactions already identified in TRS 472 [3.16]; (ii) to validate, or otherwise, the effect of major soil factors, such as soil texture and OM content, on K_d values; (iii) to examine the correlation between K_d values and soil properties for radionuclides that were not included in TRS 472 [3.16]; and (iv) to explore the use of chemical analogues to fill the existing data gaps, as is the case of data from lanthanides and actinides, which can be used to fill gaps relating to both chemical families of radionuclides.

REFERENCES TO CHAPTER 3

- [3.1] KRUPKA, K.M., KAPLAN, D.I., WHELAN, G., SERNE, R.J., MATTIGOD, S.V., Understanding Variation in Partition Coefficient, K_d , Values. Volume I: The K_d Model Measurement and Application of Chemical Reaction Codes, Rep. No. EPA402-R-99-004A, EPA, Washington, DC. (1999).
<https://www.epa.gov/sites/default/files/2015-05/documents/402-r-99-004a.pdf>
- [3.2] SHEPPARD, S.C., LONG, J., SANIPELLI, B., SOHLENIUS, G., Solid/liquid partition coefficients (K_d) for selected soils and sediments at Forsmark and Laxemar-Simpevarp, No. SKB-R-09-27, Swedish Nuclear Fuel and Waste Management Co., Sweden (2009). <https://www.skb.com/publication/1951648>
- [3.3] NATIONAL INSTITUTE OF ADVANCED INDUSTRIAL SCIENCE AND TECHNOLOGY (AIST), Geochemical map of Japan, AIST, Tsukuba (2004).
https://staff.aist.go.jp/a.ohata/english/GeochemicalMap_en.htm
- [3.4] NATIONAL INSTITUTE OF RADIOLOGICAL SCIENCE, Survey of Environmental Transfer Parameter of Radionuclides in Japan – Summary of 6 years (Uchida, S., Ed.) (2013).
https://www.enecho.meti.go.jp/category/electricity_and_gas/nuclear/rw/library/2012/24-19-2.pdf.

- [3.5] TAGAMI, K., UCHIDA, S., Use of a natural U/Th concentration ratio for estimation of anthropogenic uranium concentration in Japanese agricultural soils due to application of phosphatic fertilizers, *Radioisotopes* **55** 2 (2006) 71 (in Japanese). DOI: [10.3769/radioisotopes.55.71](https://doi.org/10.3769/radioisotopes.55.71)
- [3.6] YOSDHIDA, M., INOUE, K., OGAWA, Y. Influence of Al ion in acidic river water to paddy field soils, *Japanese Society of Soil Science and Plant Nutrition* **48** (1977) 160 (In Japanese).
- [3.7] KOSHIKAWA, M.K., TAKAMATSU, T., Behavior and chemistry of aluminum in soil-river-lake systems, *Chiku Kankyo* 9 (2004) 83 (In Japanese).
- [3.8] ISHIKAWA, N.K., UCHIDA, S., TAGAMI, K., Soil-soil solution distribution coefficients for Se, Sr, Sn, Sb, and Cs in Japanese agricultural soils. *Proceedings of Waste Management*, **8** (2008) 1–7.
<https://archivedproceedings.econference.io/wmsym/2008/pdfs/8093.pdf>
- [3.9] ISHIKAWA, N.K., UCHIDA, S., TAGAMI, K., SATTA, N., Soil Solution Ni Concentrations over which K_d is Constant in Japanese Agricultural Soils, *J. Nucl. Sci. Tech.*, **48**(3) (2011) 337–343.
<https://doi.org/10.1080/18811248.2011.9711708>
- [3.10] INTERNATIONAL ATOMIC ENERGY AGENCY, Sediment Distribution Coefficients and Concentration Factors for Biota in the Marine Environment, Technical Reports Series No. 422, IAEA, Vienna (2004).
- [3.11] CIFFROY, P. DURRIEU, G., GARNIER, J.-M., Probabilistic distribution coefficients (K_{ds}) in freshwater for radioisotopes of Ag, Am, Ba, Be, Ce, Co, Cs, I, Mn, Pu Ra, Ru, Sb, Sr and Th. Implications for uncertainty analysis of models simulating the transport of radionuclides in rivers, *J. Environ. Radioact.* **100** (2009) 785. <https://doi.org/10.1016/j.jenvrad.2008.10.019>
- [3.12] SHEPPARD, S.C., Robust Prediction of K_d from Soil Properties for Environmental Assessment, *Human and Ecological Risk Assessment: An International Journal* **17** (2011) 263. <https://doi.org/10.1080/10807039.2011.538641>
- [3.13] DURRIEU, G., CIFFROY, P., GARNIER, J.M., A weighted bootstrap method for the determination of probability density functions of freshwater distribution coefficients (K_{ds}) of Co, Cs, Sr and I radioisotopes, *Chemosphere* **65** (2006) 1308. <https://doi.org/10.1016/j.chemosphere.2006.04.028>
- [3.14] STANKEVICA, K., VINCEVICA-GAILE, Z., KLAVINS, M., Freshwater sapropel (gyttja): its description, properties and opportunities of use in contemporary agriculture, *Agronomy Research* **14**(3) (2016) 929.
https://www.researchgate.net/publication/303790078_Freshwater_sapropel_gyttja_Its_description_properties_and_opportunities_of_use_in_contemporary_agriculture
- [3.15] DREIMANIS, A., Tills: Their genetic terminology and classification, In: GOLDTHWAIT R.P., MATSCH, C.L., Eds., *Genetic classification of glacial deposits: Final report of the INQUA Commission Genesis & Lithology of Quaternary Deposits*, A. A. Balkema, Rotterdam, CRC Press (1989) 17.
- [3.16] INTERNATIONAL ATOMIC ENERGY AGENCY, Handbook of Parameter Values for the Prediction of Radionuclide Transfer in Terrestrial and Freshwater Environment, Technical Reports Series No. 472, IAEA, Vienna (2010).

- [3.17] INTERNATIONAL ATOMIC ENERGY AGENCY, Quantification of Radionuclide Transfers in Terrestrial and Freshwater Environments for Radiological Assessments, IAEA-TECDOC-1616, IAEA, Vienna (2009).
- [3.18] INTERNATIONAL ATOMIC ENERGY AGENCY, Handbook of Parameter Values for the Prediction of Radionuclide Transfer in Temperate Environments, Technical Report Series No. 364, IAEA, Vienna (1994).
- [3.19] SHEPPARD, M.I., THIBAUT, D.H., Default soil solid/liquid partition coefficients, K_{ds} , for four major soil types: a compendium, Health Phys. **59** (1990) 471.
- [3.20] WAUTERS, J., ELSEN, A., CREMERS, A., KONOPLEV, A.V., BULGAKOV, A.A., COMANS, R.N.J., Prediction of solid liquid distribution coefficients of radiocaesium in soils and sediments. Part 1: A simplified procedure for the solid characterization, Appl. Geochem. **11** (1996) 589.
[https://doi.org/10.1016/0883-2927\(96\)00027-3](https://doi.org/10.1016/0883-2927(96)00027-3)
- [3.21] VIDAL, M., et al., Two approaches to the study of radiocaesium partitioning and mobility in agricultural soils from the Chernobyl area, Analyst **120** (1995) 1785.
<https://doi.org/10.1039/AN9952001785>
- [3.22] GIL-GARCÍA, C.J., RIGOL, A., VIDAL, M., Comparison of mechanistic and PLS-based regression models to predict radiocaesium distribution coefficients in soils, J. Haz. Mat. **197** (2011) 11. DOI: [10.1016/j.jhazmat.2011.09.048](https://doi.org/10.1016/j.jhazmat.2011.09.048)
- [3.23] WAEGENEERS, N., SMOLDERS, E., MERCKX, R., A statistical approach for estimating the radiocaesium interception potential of soils, J. Environ. Qual. **28** (1999) 1005. <https://doi.org/10.2134/jeq1999.00472425002800030034x>
- [3.24] VANDEBROEK, L., VAN HEES, M., DELVAUX, B., SPAARGAREN, O., THIRY, Y., Relevance of Radiocaesium Interception Potential (RIP) on a worldwide scale to assess soil vulnerability to ^{137}Cs contamination, J. Environ. Radioact. **102** (2012) 87. DOI: [10.1016/j.jenvrad.2011.09.002](https://doi.org/10.1016/j.jenvrad.2011.09.002)
- [3.25] NAKAO, A., et al., Relationships between paddy soil radiocaesium interception potentials and physicochemical properties in Fukushima, Japan, J. Environ. Quality **44** (2015) 780. DOI: [10.2134/jeq2014.10.0423](https://doi.org/10.2134/jeq2014.10.0423)
- [3.26] UEMATSU, S., et al., Predicting radiocaesium sorption characteristics with soil chemical properties for Japanese soils, Sci. Total Environ. **524–525** (2015) 148. DOI: [10.1016/j.scitotenv.2015.04.028](https://doi.org/10.1016/j.scitotenv.2015.04.028)
- [3.27] MATUS, F., RUMPEL, C., NECULMAN, R., PANICHINI, M., MORA, M.L., Soil carbon storage and stabilisation in andic soils: a review, Catena **120** (2014) 102. DOI: [10.1016/j.catena.2014.04.008](https://doi.org/10.1016/j.catena.2014.04.008)
- [3.28] SHEPPARD, S., Solid/liquid partition coefficients (K_d) and plant/soil concentration ratios (CR) for selected soils, tills and sediments at Forsmark. R-11-24, Svensk Kämbränslehantering AB-Swedish Nuclear Fuel and Waste Management Co, Sweden (2011).
<https://www.skb.se/publication/2267316/R-11-24.pdf>
- [3.29] LAHDENPERÄ, A.-M., Working Report 2013-66: Geochemical and physical properties, distribution coefficients of soils and sediments at the Olkiluoto Island and in the reference area in 2010-2011, POSIVA Oy, Finland (2014).
https://inis.iaea.org/collection/NCLCollectionStore/_Public/45/107/45107620.pdf

- [3.30] CHOPPIN, G.R., Actinide speciation in the environment, *J. Radioanal. Nucl. Chem.* **273** (2007) 695. <https://doi.org/10.1007/s10967-007-0933-3>
- [3.31] RAMÍREZ-GUINART, O., VIDAL, M., RIGOL, A., Univariate and multivariate analysis to elucidate soil properties governing americium sorption in soils, *Geoderma* **269** (2016) 19. <https://doi.org/10.1016/j.geoderma.2016.01.026>

4. FRESHWATER K_d DATASET

PATRICK BOYER, VIRGINIA TOMCZAK

Institut de Radioprotection et de Sûreté Nucléaire (IRSN), FRANCE

YUICHI ONDA

University of Tsukuba, JAPAN

This chapter describes various properties of sediments in freshwater systems to provide a framework for considering the applicability of the different K_d approaches. A summary of previous compilations of freshwater K_d values is presented, along with the data that have been compiled under the MODARIA programme. An updated dataset is provided for freshwater K_d values, and the log-normal distributions obtained for the various elements, conditions for solid–liquid exchange (sorption, desorption, *in situ*) and sediment type (suspended sediments and deposited sediments) are presented. To reduce the variability of these distributions, conditional log-normal distributions of K_d values are proposed, according to mass/volume ratio, dissolved organic carbon and pH.

4.1. SEDIMENTS IN FRESHWATER SYSTEMS AND K_d APPROACHES

The approach developed for soils in Chapter 3 has demonstrated that the K_d concept is not as simple as it might appear, largely because of the associated assumptions of instantaneity and reversibility. This chapter addresses other sources of misinterpretation linked to the concept of solid and liquid phases for suspended sediments and deposited sediments and their relevance to the different K_d approaches that can be applied to describe their behaviour in rivers.

4.1.1. Suspended sediments in aquatic systems

Suspended sediments (SS) are solid particles maintained in suspension in the water column, which are part of the freshwater system located between the river or lakebed and the water surface. Suspended sediments are more spread out and less dense than deposited sediments and they may be sampled using a variety of methods, such as filtration, sediment traps located in the flow, sedimentation and centrifugation. Each of these methods is characterized by a specific cut-off of particle sizes. For example, for the filtration method, the cut-off size is usually 0.45 μm , which means that all the particles smaller than 0.45 μm are assumed to be part of the liquid phase. By this definition, colloids, which are very fine particles, with more reactive surface properties compared to coarser particles, are part of the defined liquid phase [4.1, 4.2].

For suspended sediments, K_d is defined as the ratio between the radionuclide activity concentration in the suspended sediments and in the filtered water of the water column (FWC):

$$K_{dSS|FWC} = \frac{C_{SS}}{C_{FWC}} \quad (4.1)$$

where C_{SS} is the activity concentration of radionuclides in suspended sediments (Bq/kg DM); and C_{FWC} is the activity concentration of radionuclides in filtered water from the water column (Bq/L).

4.1.2. Deposited sediment in aquatic systems (oxic and anoxic layers)

Deposited sediments (DS) are mixtures of water and various particles accumulated on the bottom of surface waters, such as rivers, lakes and oceans, by bed load transport and sedimentation of suspended sediments. Some confusion arises about the applicability of K_d to deposited sediments because the liquid phases can be either the pore water or the water column. Consequently, the K_d approach is more ambiguous than for suspended sediments and different operational definitions can be encountered, including:

$$K_{dDS|WC} = \frac{C_{DS}}{C_{RWC}} \quad (4.2)$$

where C_{DS} is the activity concentration of radionuclides in deposited sediment (Bq/kg DM) and C_{RWC} is the raw activity concentration in the water column (dissolved + SS) (Bq/L).

$$K_{dDS|FWC} = \frac{C_{DS}}{C_{FWC}} \quad (4.3)$$

where C_{DS} is the activity concentration in deposited sediment (Bq/kg DM) and C_{FWC} is the activity concentration in filtered water of the water column (Bq/L).

$$K_{dDS|PW} = \frac{C_{DS}}{C_{PW}} \quad (4.4)$$

where C_{DS} is the activity concentration in deposited sediments (Bq/kg DM) and C_{PW} is the activity concentration in pore water within the deposited sediment (Bq/L).

The main properties of deposited sediments needs to be considered to determine the applicability of these different operational definitions of K_d values. The accumulation of deposited sediments creates superimposed layers of mixtures of particles and water that are subject to diagenetic processes that occur after their deposition [4.3]. Such diagenetic processes include biochemical (e.g. bioturbation, degradation of OM) and physical processes (e.g. sedimentation, self-consolidation, erosion). Porosity decreases with depth in deposited sediments due to the above processes, which in turn reduces the exchange between the pore water and the water column as a function of depth. Except for the superficial layer, deposited sediments become anoxic because dissolved oxygen is consumed faster by bacteria than it is replaced by diffusion. Deposited sediments can, therefore, be considered as two specific successive layers (Fig. 4.1): (i) an oxygenated fine superficial layer (generally 1 to 2 cm depth) in contact with the water column; and (ii) an anoxic layer, which is much less responsive to changes in the chemical conditions of the overlying water.

For the oxic superficial layer, the estimation of K_d needs to take into account the equilibrium conditions between the superficial layer of deposited sediments and the water column. Since the particles of the superficial layer are progressively buried as a function of the sedimentation rate, the $K_{dDS|FWC}$ approach only needs to be applied if all the particles in this layer have been accumulated over a time period when constant contamination of the water column can be assumed [4.4]. Consequently, this K_d approach is not relevant for accidental or transitory situations, as shown in Fig. 4.2, which illustrates the generic behaviour of the ratio between the radionuclide activity concentration in superficial deposited sediments with that in the water column for a pulse input of a pollutant element.

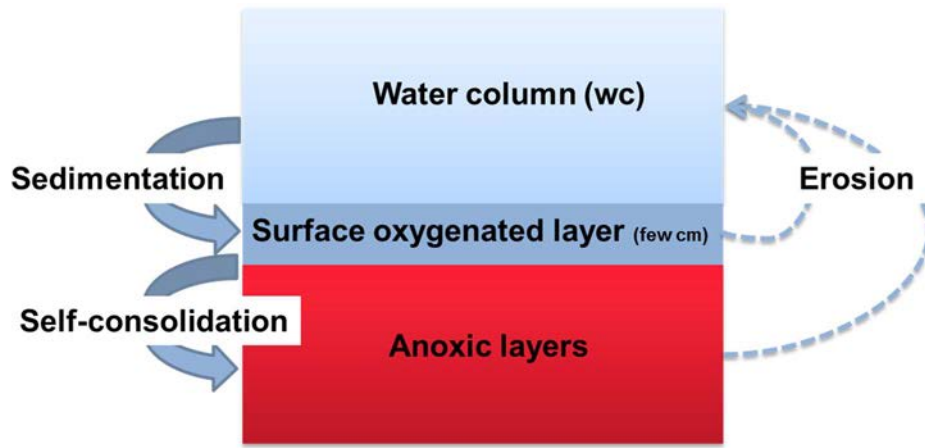


FIG. 4.1. Main layers of deposited sediments.

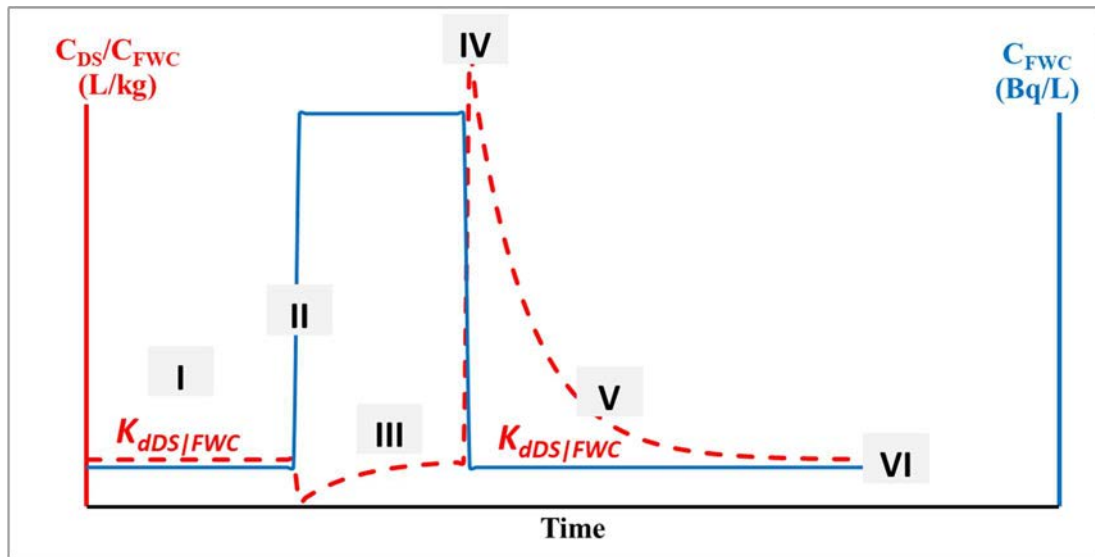


FIG. 4.2. Generic behaviour of the ratio, $K_{dDS|FWC}$, between the radionuclide activity concentration in superficial dried deposited sediments (C_{DS}) with that in the filtered water column (C_{FWC}) for a pulse input of a pollutant element (adapted from Ref. [4.4], with permission).

The water column and the deposited sediments are in equilibrium before the pulse input of the pollutant occurs (I), and the ratio corresponds to $K_{dDS|FWC}$. The ratio decreases strongly after the pulse (II) occurs, because the water column contaminant concentration, C_{FWC} , increases more quickly than the contaminant concentrations in the bottom sediments, C_{DS} , due to kinetic limitations of the sedimentation rate, thereby resulting in the observed decrease in $K_{dDS|FWC}$. During pulse (III), the ratio gradually increases as a function of the sedimentation rate and will only correspond to $K_{dDS|FWC}$ if the passing time of the pulse is long enough to reach equilibrium conditions [4.4]. Because of the decrease in the pollutant element concentration in the water column at the end of pulse (IV) and its retention by the sediment, the ratio increases strongly. Under these conditions the ratio does not corresponds to $K_{dDS|FWC}$. Thereafter (V), the ratio decreases slowly to reach $K_{dDS|FWC}$ (VI).

Figure 4.2 illustrates that in situations when a pulse input of a pollutant occurs, modelling with a constant K_d value representative of the ratio between the element concentration of deposited sediments and the concentration in the water column is not appropriate. For such situations, and consistent with the solid/liquid exchanges, the variation of the activity concentration of deposited sediments involves several processes such as the sedimentation of suspended particles, the interstitial diffusion, the bioturbation, etc.

For the case of a pulse of contamination, the porosity (n_{DS}) and the thickness (h_{DS}) of the oxic layer can be assumed to be constant over time. In this case, variation in the radionuclide activity concentration of deposited sediments in the superficial oxic layer is mainly driven by the sedimentation of contaminated suspended sediments:

$$\frac{dC_{DS}}{dt} = \frac{w_{SS^*} \times SS^*}{\rho_{DS} \times h_{DS} \times (1 - n_{DS})} \times (C_{SS^*} - C_{DS}) - \lambda \times C_{DS} \quad (4.5)$$

where:

SS^* is the mass of the range of suspended particles that contribute to sedimentation according to the hydraulic conditions (kg/m^3);

C_{SS^*} is the radionuclide activity concentration of the particles of the range of suspended particles that contribute to sedimentation according to the hydraulic conditions (Bq/kg);

w_{SS^*} is the sedimentation velocity (m/s);

ρ_{DS} is the volume mass of dried deposited sediments (kg/m^3);

n_{DS} is the porosity of the oxic superficial layer (no units);

h_{DS} is the thickness of the oxic superficial layer (m).

The SS^* parameter captures the condition when not all suspended sediments are equally effective at binding contaminants, that is, the K_d varies with particle size. Under steady state conditions, when neglecting radioactive decay (λ) so $C_{SS^*} = C_{DS}$ and, consequently:

$$K_{dDS|FWC} = K_{dSS^*|FWC} \quad (4.6)$$

However, it is reasonable to expect that $K_{dSS^*|FWC} < K_{dDS|FWC}$ because the sedimentation process results in a sorting of particle sizes. The particles within the deposited sediments are coarser than those comprising the suspended sediments, which is important, as the K_d has been reported to decrease when the particle sizes increases [4.5, 4.6].

For anoxic layers, only $K_{dDS|PW}$ is relevant because these layers are not directly connected to the water column. In practice, such a K_d is only valid if it has been quantified under the same anoxic conditions as in the deposited sediments. The use of $K_{dDS|PW}$ allows the determination of the solid–liquid fractionation of radionuclides between dry particles and pore water, which can be useful in assessing the bioavailability and transfer of radionuclides to benthic organisms.

4.2. INTRODUCTION TO PREVIOUS COMPILATIONS OF K_d

Early reference values of freshwater K_d values were given in TRS 364 [4.7] and Safety Reports Series (SRS) 19 [4.8]. In the framework of the IAEA EMRAS programme, an improved compilation of K_d values for freshwater systems was developed [4.9, 4.10] and reported in TRS 472 [4.11, 4.12]. The main advancement made during the EMRAS programme was to refine the description of K_d in fresh water by providing operational PDFs. The compilation considered 86 bibliographic references (mainly peer reviewed publications) published before 2004. Data for stable elements were not considered. TRS 472 [4.11] contains K_d values of

15 elements in suspended sediments and superficial deposited sediments in rivers and lakes. Among these 15 elements, eight (Ag, Am, Co, Cs, I, Mn, Pu and Sr) had sufficient data (defined as having no less than ten data entries originating from no less than five different references) to allow the calculation of conditional PDFs. These PDFs were conditioned to account for a limited number of parameters, such as pH and contact time, and can be applied when some parametric information is available for the site under consideration. For Ba, Be, Ce, Ra, Ru, Sb and Th, the datasets were only sufficient to allow the determination of non-conditional PDFs⁴, which are useful for initial or screening level assessments when no additional knowledge about the site of interest is available.

The compilation of freshwater K_d data generated during the EMRAS programme was classified according to the chemical element. Each K_d value was associated with several groups of parameters connected with the source reference, location (river or lake name), type of sediment (deposited or suspended), data acquisition protocol (ratio of solid mass to water volume (m/V), contact time, sorption process and number of replicates), chemical conditions (pH, dissolved and particulate carbon (DOC and POC), potassium and ammonium concentrations and ion exchange capacity), and presentation of data (e.g. figure, table) [4.4]. The dataset for each element was analysed assuming a log-normal distribution characterized by a geometric mean (GM) and a geometric standard deviation (GSD). These statistical parameters were determined by applying a two step procedure [4.9]: (1) a weighted bootstrap method to increase the weight given to data that satisfy specific quality criteria; and (2) a fit of a log-normal function to the weighted data using the likelihood method.

The data from TRS 472 [4.11] provide reference values and distributions for freshwater K_d but they do not distinguish between suspended and deposited sediments. For elements for which the most information was available (Ag, Am, Co, Cs, I, Mn, Pu and Sr), TRS 472 [4.11] provides conditional log-normal distributions (GM and GSD) and minimum and maximum K_d values as a function of adsorption and desorption conditions and for *in situ* measurements. For a second group of elements (Ba, Be, Ce, Ra, Ru, Sb and Th), non-conditional log-normal distributions (GM and GSD) and minimum and maximum K_d values are provided. Finally, a third group of ten elements (Cr, Fe, Zn, Zr, Tc, Pm, Eu, U, Np and Cm) is considered, for which only mean, maximum and minimum K_d values are suggested based on a single publication [4.13] or expert judgement.

The concept of *in situ* K_d was introduced in TRS 472 [4.11] because K_d values for sorption or desorption are generally obtained in laboratories where these processes are identified and controlled, whereas the specific prevailing circumstances are less well defined for data acquired *in situ*. Because of this issue, K_d values derived from *in situ* measurements are often termed as ‘apparent’ (see Chapter 2, Section 2.1.2.3).

4.2.1. The need to update K_d compilations

The information provided in TRS 472 [4.11] is the outcome of an international consensus and it is considered as a key source reference by modelers when site specific *in situ* K_d values are not available. Such information is, therefore, an important support for assessment of radionuclide transfer and needs to be regularly updated, especially because, in its present state, it includes only a limited number of elements and there are several important data gaps that need to be filled.

⁴ A conditional probability density function is linked to criteria such as: sorption conditions, components etc. A non-conditional probability density function is not linked to any criteria.

TABLE 4.1. LIST OF THE CHEMICAL ELEMENTS INCLUDED IN THE ERICA TOOL AND THE SYMBIOSE PLATFORM AND ASSOCIATED QUALITY CRITERION FOR THEIR REFERENCE K_d ¹

| Element | Quality criterion | Element | Quality criterion | Element | Quality criterion |
|---------|-------------------|---------|-------------------|---------|-------------------|
| Ac | 0 | Fr | 1 | Pu | 3 |
| Ag | 3 | Gd | 0 | Ra | 3 |
| Am | 3 | H | 1 | Rb | 0 |
| As | 1 | Hg | 1 | Rh | 1 |
| At | 1 | I | 3 | Rn | 0 |
| Au | 0 | In | 1 | Ru | 3 |
| Ba | 3 | Ir | 0 | S | 1 |
| Be | 3 | La | 0 | Sb | 3 |
| Bi | 1 | Mn | 3 | Se | 1 |
| Br | 0 | Mo | 1 | Si | 1 |
| C | 1 | Na | 1 | Sn | 1 |
| Ca | 1 | Nb | 1 | Sr | 3 |
| Cd | 0 | Nd | 0 | Tc | 1 |
| Ce | 3 | Ni | 1 | Te | 1 |
| Cf | 0 | Np | 2 | Th | 3 |
| Cl | 1 | P | 0 | Tl | 1 |
| Cm | 2 | Pa | 0 | U | 2 |
| Co | 3 | Pb | 1 | W | 0 |
| Cr | 1 | Pd | 0 | Y | 1 |
| Cs | 3 | Pm | 2 | Zn | 2 |
| Eu | 2 | Po | 1 | Zr | 2 |
| Fe | 2 | Pr | 1 | | |

¹ Adapted after Ref. [4.4], with permission.

To illustrate these omissions, Table 4.1 provides a list of the chemical elements included and used in two assessment tools (as examples) for which the application of reference K_d values is an integral component. The ERICA (Environmental Risk from Ionising Contaminants: Assessment and Management) Tool [4.14] which is used to estimate internal and external doses to organisms other than humans, and the SYMBIOSE platform [4.15, 4.16] used to assess radionuclide transfers in the environment and corresponding doses to humans. The list in Table 4.1 contains 64 chemical elements for which a quality criterion is indicated that was specified according to the following guidance:

- (1) Set to 3 when the freshwater K_d dataset allowed the determination of conditional distribution (≥ 5 references and ≥ 10 K_d values);
- (2) Set to 2 when the dataset is just large enough to determine unconditional distributions (< 5 references and/or < 10 K_d values);
- (3) Set to 1 when there is a single publication or only expert judgement;
- (4) Set to 0 when there is no information available.

The distribution of the quality criterion for K_d values is summarized in Fig. 4.3.

Conditional distributions are available for only 23% of the listed radionuclides and 13% are associated with unconditional distributions. The evaluation reveals a lack of data, as K_d values for 42% of the elements considered in this publication are based on a single publication or expert judgement, and there are no data for 23% of the elements considered. Therefore, 65% of the K_d values for the elements considered are poorly justified or not supported, which highlights the need to complete and improve K_d compilations. One aim of the MODARIA WG4 was to contribute to filling some of these gaps, especially for those radionuclides for which the dose contribution to humans or other organisms is potentially important.

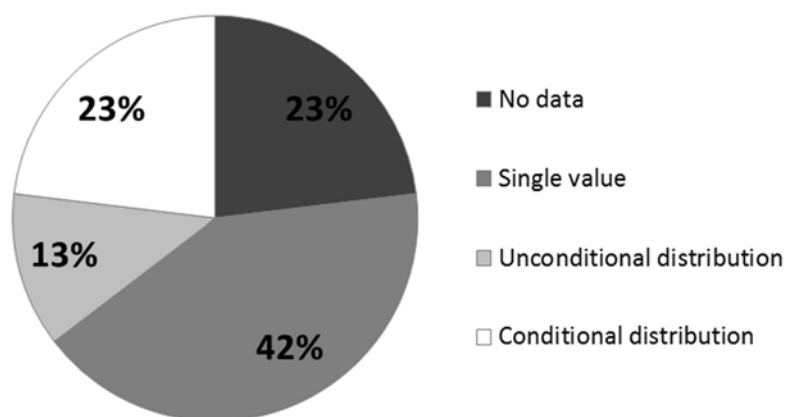


FIG. 4.3. Distribution of the assigned quality criterion for K_d values for the chemical elements included in the ERICA Tool and the SYMBIOSE platform.

4.2.2. Objectives for updating and supplementing the freshwater K_d database

As shown above, there is a considerable need to enhance existing compilations of freshwater K_d values. Therefore, the main objectives of MODARIA WG4 with respect to freshwater K_d were:

- (1) To collate and integrate new data into the previous dataset [4.11] and to revise the dataset structure, where necessary, to create an updated MODARIA dataset;
- (2) To harmonize the approach used to extract conditional and unconditional PDFs from the datasets;
- (3) To provide PDFs for relevant subcategories for modelling freshwater systems, such as for deposited and suspended sediments.

The aim of the resulting enhanced K_d MODARIA datasets was to improve:

- (1) Knowledge of general K_d properties through comparison of the statistical freshwater K_d distributions as functions of radionuclides and environmental components (which is not feasible for individual values, as site specific parameters would need to be considered);
- (2) Analysis of the variability in K_d values due to site specific conditions.

4.3. EXPANSION OF THE FRESHWATER K_d DATASET

In 2014, the dataset used to determine values and distributions of K_d values, and published in TRS 472 [4.11], for freshwater ecosystems was provided to MODARIA WG4. For Ag, Am, Co, Cs, I, Mn, Pu and Sr, this dataset included more than 100 values per element. Subsequently, the dataset was expanded by MODARIA WG4, and priority given to elements with few or no data. The new K_d values were derived from peer reviewed publications for both radionuclides and stable elements [4.4, 4.17]. Major stable element inputs were included from large datasets, such as those published by the United States Geological Survey (USGS) for Colorado River⁵, the Geochemical Atlas of Europe⁶, and water quality data from 26 Ribble and Wyre River basin sites in Northwest England [4.3]. By incorporating these additional data, over 3300 K_d values

⁵ <http://puDS.usgs.gov/ds/614/contents/>

⁶ <http://weppi.gtk.fi/publ/foregsatlas/>

have been compiled for 29 new elements (Al, As, B, Ca, Cd, Cu, Dy, Er, Gd, Hf, Hg, Ho, K, La, Li, Mg, Mo, Na, Ni, Pb, Po, Pr, Rb, S, Se, Si, Sn, Ti, V). Additionally, a total of 1807 new K_d values were added to the dataset for the 25 elements already included in TRS 472 [4.11] (Ag, Am, Ba, Be, Ce, Cm, Co, Cr, Cs, Eu, Fe, I, Mn, Np, Pm, Pu, Ra, Ru, Sb, Sr, Tc, Th, U, Zn, Zr). The final MODARIA II freshwater K_d database contains 8564 K_d values for 54 elements.

In TRS 472 [4.11], there are 10 elements (Cm, Cr, Eu, Fe, Np, Pm, Tc, U, Zn and Zr) for which the derivation of log-normal distributions is not possible due to the limited number of data. The MODARIA dataset has provided adequate set of data to derive log-normal distributions for Cm, Cr, Eu, Fe, U and Zn. For the other four elements (Np, Pm, Tc and Zr) there has been no change to those values reported in TRS 472 [4.11] and TRS 364 [4.7].

In practice, when an REIA is carried out for pathway evaluation, the type of K_d approach needs to be chosen with care. For example, has the considered K_d value been estimated specifically for suspended sediments or deposited sediments? This kind of information is often not available in typical reference publications (however, there are exceptions [4.18]) that tend to present freshwater K_d values without distinguishing between these two components. Within MODARIA, this issue has been addressed by analysing the MODARIA K_d dataset in relation to its applicability to suspended or deposited sediments as well as sorption–desorption processes and field measurements, as used in TRS 472 [4.11].

For each chemical element, the datasets have been subdivided according to the environmental component (suspended sediments and deposited sediments) and the methodology (sorption–desorption laboratory studies or *in situ* measurements). Each dataset (*radionuclides* × *environmental components* × *laboratory or field*) has been analysed according to the number of values available. When the number of values available was less than 10, the information provided is limited to a geometric mean, and minimum and maximum values, and the geometric mean is an indicative value without any associated statistical distribution function. When the number of values exceeded 10, the dataset is described by a log-normal distribution, which is considered as the most appropriate distribution for K_d values [4.19].

Analysis of the 15 elements with log-normal distributions in TRS 472 [4.11] (Ag, Am, Ba, Be, Ce, Co, Cs, I, Mn, Pu, Ra, Ru, Sb, Sr and Th) has been extended to distinguish between data for suspended sediments and deposited sediments.

Table 4.2 presents GM and GSD values of freshwater K_d for 54 chemical elements, which constitutes a considerable enhancement compared with the information given in TRS 472 [4.11]. To identify and explain significant changes from the reference values previously published, Table 4.2 provides, for comparison, the values published in the IAEA publications TRS 364 [4.7], SRS 19 [4.8] and TRS 472 [4.11] and in a report of the United States Environmental Protection Agency [4.18]. Reference [4.18] provides median K_d values for several elements (Ag, As, Ba, Be, Cd, Co, Cr(III), Cr(IV), Cu, Hg, CH, Hg, Mo, Ni, Pb, Sb, Se, Sn, Tl, V, Zn, Cn, N). These K_d values have been allocated to suspended sediments or deposited sediments, but without consideration of the process of liquid–solid exchange.

Table 4.2 specifies the size of the dataset and the number of references available for each chemical element, environmental component (suspended sediments and deposited sediments) and type of solid–liquid exchange.

TABLE 4.2. COMPARISONS OF MODARIA DISTRIBUTIONS FOR K_d (L/kg) OF 53 CHEMICAL ELEMENTS AND PREVIOUS REFERENCE SOURCES

| Element | Component SS, DS ^a | Condition | GM | GSD | Min | Max | 5% | 95% | Nd | Nr | Indicative | Reference |
|---------|----------------------------------|------------|-------------------------|------|------------------------|------------------------|------------------------|------------------------|-----|-----|----------------------|-----------|
| Ag | DS | Field | n.a | n.a | n.a | n.a | n.a | n.a | 1 | 1 | 5.25×10 ² | MODARIA |
| Ag | SS | Adsorption | 8.30 × 10 ⁴ | 2.28 | 1.21 × 10 ⁴ | 1.58 × 10 ⁶ | 2.14 × 10 ⁴ | 3.22 × 10 ⁵ | 81 | 7 | n.r | MODARIA |
| Ag | SS | Desorption | 4.10 × 10 ⁵ | 1.73 | 5.97 × 10 ⁴ | 9.48 × 10 ⁵ | 1.66 × 10 ⁵ | 1.01 × 10 ⁶ | 41 | 2 | n.r | MODARIA |
| Ag | SS | Field | 2.24 × 10 ⁵ | 2.98 | 3.59 × 10 ⁴ | 2.46 × 10 ⁶ | 3.70 × 10 ⁴ | 1.36 × 10 ⁶ | 56 | 3 | n.r | MODARIA |
| Ag | SS+DS | Adsorption | 9.50 × 10 ⁴ | 2.30 | 2.20 × 10 ⁴ | 3.30 × 10 ⁵ | 2.41 × 10 ⁴ | 3.74 × 10 ⁵ | 91 | n.a | n.r | [4.11] |
| Ag | SS+DS | Desorption | 4.40 × 10 ⁵ | 2.70 | 1.90 × 10 ⁵ | 1.00 × 10 ⁶ | 8.59 × 10 ⁴ | 2.25 × 10 ⁶ | 41 | n.a | n.r | [4.11] |
| Ag | DS | n.a | 3.98 × 10 ^{3*} | n.a | 1.26 × 10 ² | 6.31 × 10 ⁵ | n.a | n.a | n.a | n.a | n.r | [4.18] |
| Ag | SS | n.a | 7.94 × 10 ^{4*} | n.a | 2.51 × 10 ⁴ | 2.00 × 10 ⁶ | n.a | n.a | 15 | n.a | n.r | [4.18] |
| Al | SS | Adsorption | 3.21 × 10 ⁵ | 1.78 | 7.86 × 10 ⁴ | 1.46 × 10 ⁶ | 1.24 × 10 ⁵ | 8.33 × 10 ⁵ | 27 | 1 | n.r | MODARIA |
| Al | SS | Field | 4.62 × 10 ⁶ | n.r | 4.62 × 10 ⁶ | 2.75 × 10 ⁸ | n.r | n.r | 2 | 1 | n.r | MODARIA |
| Am | DS | Adsorption | 2.20 × 10 ⁵ | 3.81 | 2.70 × 10 ³ | 2.25 × 10 ⁶ | 2.44 × 10 ⁴ | 1.98 × 10 ⁶ | 88 | 4 | n.r | MODARIA |
| Am | SS | Field | 7.94 × 10 ⁴ | 6.25 | 1.10 × 10 ³ | 1.31 × 10 ⁶ | 3.90 × 10 ³ | 1.62 × 10 ⁶ | 44 | 4 | n.r | MODARIA |
| Am | SS+DS | Adsorption | 2.10 × 10 ⁵ | 3.70 | 2.50 × 10 ⁴ | 1.90 × 10 ⁶ | 2.44 × 10 ⁴ | 1.81 × 10 ⁶ | 91 | n.a | n.r | [4.11] |
| Am | SS+DS | Field | 1.20 × 10 ⁵ | 5.70 | 6.9 × 10 ³ | 2.00 × 10 ⁶ | 6.85 × 10 ³ | 2.10 × 10 ⁶ | 41 | n.a | n.r | [4.11] |
| Am | SS+DS | n.a | n.a | n.a | n.a | n.a | n.a | n.a | n.a | 1 | 5.00×10 ³ | [4.8] |
| Am | SS+DS | n.a | n.a | n.a | 9.00 × 10 ¹ | 4.00 × 10 ⁴ | n.a | n.a | n.a | 1 | 5.00×10 ³ | [4.7] |
| As | DS | Adsorption | 3.79 × 10 ² | 1.47 | 1.76 × 10 ² | 7.18 × 10 ² | 2.00 × 10 ² | 7.18 × 10 ² | 15 | 1 | n.r | MODARIA |
| As | DS | Field | 3.78 × 10 ³ | 3.91 | 6.50 × 10 ¹ | 2.93 × 10 ⁴ | 4.01 × 10 ² | 3.56 × 10 ⁴ | 37 | 8 | n.r | MODARIA |
| As | SS | Field | 5.28 × 10 ⁴ | 3.49 | 1.83 × 10 ³ | 9.59 × 10 ⁶ | 6.75 × 10 ³ | 4.14 × 10 ⁵ | 158 | 9 | n.r | MODARIA |
| B | SS | Field | 1.41 × 10 ³ | 2.56 | 4.42 × 10 ² | 6.20 × 10 ³ | 2.99 × 10 ² | 6.62 × 10 ³ | 21 | 1 | | MODARIA |
| Ba | DS | Field | 8.13 × 10 ³ | n.r | 8.13 × 10 ³ | 1.05 × 10 ⁴ | n.r | n.r | 2 | 2 | n.r | MODARIA |
| Ba | DS | Adsorption | 3.95 × 10 ² | n.r | 4.50 × 10 ¹ | 5.50 × 10 ² | n.r | n.r | 8 | 1 | n.r | MODARIA |
| Ba | SS | Adsorption | 1.75 × 10 ³ | 3.18 | 7.20 × 10 ² | 5.74 × 10 ³ | 2.61 × 10 ² | 1.17 × 10 ⁴ | 11 | 2 | n.r | MODARIA |
| Ba | SS | Field | 1.20 × 10 ³ | 3.17 | 8.48 × 10 ² | 7.84 × 10 ⁴ | 1.80 × 10 ³ | 8.03 × 10 ⁴ | 95 | 7 | n.r | MODARIA |
| Ba | SS+DS | Various | 2.00 × 10 ³ | 3.60 | 2.5 × 10 ² | 1.60 × 10 ⁴ | 2.43 × 10 ² | 1.64 × 10 ⁴ | 48 | 5 | n.r | [4.11] |
| Ba | SS | n.a | 1.00 × 10 ^{4*} | n.a | 1.94 × 10 ² | 3.16 × 10 ⁴ | n.a | n.a | 14 | n.a | n.r | [4.18] |
| Be | DS | Field | 3.54 × 10 ⁴ | 1.95 | 1.02 × 10 ⁴ | 2.25 × 10 ⁵ | 1.18 × 10 ⁴ | 1.06 × 10 ⁵ | 13 | 1 | n.r | MODARIA |
| Be | SS | Adsorption | 1.60 × 10 ⁵ | n.r | 1.60 × 10 ⁵ | 3.60 × 10 ⁵ | n.r | n.r | 2 | 1 | n.r | MODARIA |
| Be | SS | Field | 3.87 × 10 ⁴ | 2.59 | 2.20 × 10 ³ | 2.00 × 10 ⁵ | 8.06 × 10 ³ | 1.85 × 10 ⁵ | 29 | 6 | n.r | MODARIA |
| Be | | Various | 4.20 × 10 ⁴ | 3.60 | 5.10 × 10 ³ | 3.40 × 10 ⁵ | 5.11 × 10 ³ | 3.45 × 10 ⁵ | 28 | n.a | n.r | [4.11] |
| Be | SS | | 1.26 × 10 ^{4*} | n.a | 6.31 × 10 ² | 6.31 × 10 ⁶ | n.a | n.a | 17 | n.a | n.r | [4.18] |
| Ca | DS | Field | 1.38 × 10 ² | n.r | 5.42 × 10 ¹ | 1.47 × 10 ³ | n.r | n.r | 3 | 2 | n.r | MODARIA |

TABLE 4.2. (cont.)

| Element | Component SS, DS ^a | Condition | GM | GSD | Min | Max | 5% | 95% | Nd | Nr | Indicative | Reference |
|---------|----------------------------------|------------|----------------------|------|--------------------|--------------------|--------------------|--------------------|-----|-----|--------------------|-----------|
| Ca | DS | Field | 1.38×10^2 | n.r | 5.42×10^1 | 1.47×10^3 | n.r | n.r | 3 | 2 | n.r | MODARIA |
| Ca | SS | Field | 1.68×10^3 | 2.45 | 4.12×10^2 | 2.32×10^4 | 3.83×10^2 | 7.38×10^3 | 57 | 5 | n.r | MODARIA |
| Cd | DS | Adsorption | 5.24×10^3 | 7.40 | 5.78×10^0 | 3.33×10^5 | 1.95×10^2 | 1.41×10^5 | 52 | 2 | n.r | MODARIA |
| Cd | DS | Field | 4.00×10^3 | 8.63 | 7.69×10^1 | 1.41×10^7 | 1.15×10^2 | 1.38×10^5 | 84 | 12 | n.r | MODARIA |
| Cd | SS | Field | 1.34×10^5 | 7.83 | 1.65×10^3 | 6.91×10^7 | 4.53×10^3 | 3.96×10^6 | 208 | 13 | n.r | MODARIA |
| Cd | DS | n.a | 3.98×10^3 * | n.a | 3.16×10^0 | 2.00×10^7 | n.a | n.a | 21 | n.a | n.r | [4.18] |
| Cd | SS | n.a | 5.01×10^4 * | n.a | 6.31×10^2 | 2.00×10^6 | n.a | n.a | 67 | n.a | n.r | [4.18] |
| Ce | SS | Adsorption | 2.68×10^5 | 2.58 | 5.30×10^4 | 2.10×10^6 | 5.63×10^4 | 1.28×10^6 | 37 | 2 | n.r | MODARIA |
| Ce | SS | Field | 2.58×10^5 | 2.39 | 3.97×10^4 | 3.76×10^6 | 6.16×10^4 | 1.08×10^6 | 80 | 4 | n.r | MODARIA |
| Ce | SS+DS | Various | 2.20×10^5 | 2.90 | 4.2×10^4 | 1.20×10^6 | 3.82×10^4 | 1.27×10^6 | 15 | 3 | n.r | [4.11] |
| Ce | SS+DS | n.a | n.a | n.a | n.a | n.a | n.a | n.a | n.a | n.a | 1.00×10^4 | [4.8] |
| Ce | SS+DS | n.a | n.a | n.a | 8.00×10^3 | 1.00×10^5 | n.a | n.a | n.a | n.a | 1.00×10^4 | [4.7] |
| Cm | DS | Adsorption | 1.64×10^5 | 6.81 | 1.00×10^4 | 2.25×10^6 | 7.00×10^3 | 3.86×10^6 | 29 | 1 | n.r | MODARIA |
| Cm | SS | Field | 1.01×10^5 | n.a | 5.25×10^4 | 2.88×10^5 | n.a | n.a | 4 | 1 | n.r | MODARIA |
| Cm | SS+DS | Various | n.a | n.a | 1.00×10^1 | 7.00×10^4 | n.a | n.a | n.a | n.a | 5.00×10^3 | [4.11] |
| Cm | SS+DS | n.a | n.a | n.a | n.a | n.a | n.a | n.a | n.a | n.a | 5.00×10^3 | [4.8] |
| Cm | SS+DS | n.a | n.a | n.a | 1.00×10^1 | 7.00×10^4 | n.a | n.a | n.a | n.a | 5.00×10^3 | [4.7] |
| Co | DS | Adsorption | 1.59×10^4 | 10.4 | 2.00×10^1 | 5.43×10^5 | 3.40×10^2 | 7.48×10^5 | 300 | 8 | n.r | MODARIA |
| Co | DS | Desorption | 1.57×10^4 | 65.0 | 6.76×10^1 | 2.50×10^6 | 1.63×10^1 | 1.50×10^7 | 34 | 3 | n.r | MODARIA |
| Co | DS | Field | 2.04×10^2 | 34.3 | 2.00×10^1 | 1.40×10^5 | 6.07×10^0 | 6.83×10^4 | 28 | 5 | n.r | MODARIA |
| Co | SS | Adsorption | 7.29×10^4 | 11.7 | 2.79×10^2 | 1.13×10^7 | 1.27×10^3 | 4.19×10^6 | 262 | 17 | n.r | MODARIA |
| Co | SS | Desorption | 1.10×10^6 | 5.05 | 1.20×10^4 | 1.54×10^7 | 7.71×10^4 | 1.58×10^7 | 40 | 2 | n.r | MODARIA |
| Co | SS | Field | 3.93×10^4 | 3.42 | 2.13×10^3 | 1.02×10^6 | 5.19×10^3 | 2.98×10^5 | 104 | 14 | n.r | MODARIA |
| Co | SS+DS | Adsorption | 4.30×10^4 | 9.50 | 1.10×10^3 | 1.70×10^6 | 1.06×10^3 | 1.74×10^6 | 534 | n.a | n.r | [4.11] |
| Co | SS+DS | Desorption | 4.90×10^5 | 4.90 | 3.50×10^4 | 6.60×10^6 | 3.59×10^4 | 6.69×10^6 | 74 | n.a | n.r | [4.11] |
| Co | SS+DS | Field | 4.40×10^4 | 3.90 | 4.90×10^3 | 3.90×10^5 | 4.69×10^3 | 4.13×10^5 | 29 | n.a | n.r | [4.11] |
| Co | SS+DS | n.a | n.a | n.a | n.a | n.a | n.a | n.a | n.a | n.a | 5.00×10^3 | [4.8] |
| Co | SS+DS | n.a | n.a | n.a | 1.00×10^3 | 7.00×10^4 | n.a | n.a | n.a | n.a | 5.00×10^3 | [39] |
| Co | DS | n.a | 2.00×10^3 * | n.a | 7.94×10^2 | 3.98×10^3 | n.a | n.a | 3 | n.a | n.r | [4.18] |
| Co | SS | n.a | 5.01×10^4 * | n.a | 1.58×10^3 | 2.00×10^6 | n.a | n.a | 29 | n.a | n.r | [4.18] |
| Cr | DS | Adsorption | 3.31×10^3 | 88.4 | 4.73×10^1 | 3.43×10^5 | 2.08×10^0 | 5.26×10^6 | 31 | 2 | n.r | MODARIA |
| Cr | DS | Field | 4.41×10^3 | 11.2 | 1.00×10^2 | 1.05×10^6 | 8.26×10^1 | 2.35×10^5 | 73 | 12 | n.r | MODARIA |
| Cr | SS | Field | 1.24×10^5 | 4.00 | 1.23×10^3 | 1.18×10^7 | 1.27×10^4 | 5.30×10^5 | 145 | 12 | n.r | MODARIA |

TABLE 4.2. (cont.)

| Element | Component SS, DS ^a | Condition | GM | GSD | Min | Max | 5% | 95% | Nd | Nr | Indicative | Reference |
|---------|----------------------------------|------------|-----------------------|------|--------------------|--------------------|--------------------|--------------------|-----|-----|--------------------|-----------|
| Cr | | n.a | n.a | n.a | n.a | n.a | n.a | n.a | n.a | n.a | Low | [4.11] |
| Cr | | n.a | n.a | n.a | n.a | n.a | n.a | n.a | n.a | n.a | 1.00×10^4 | [4.8] |
| Cr | | n.a | n.a | n.a | 0.00×10^3 | 1.00×10^3 | n.a | n.a | n.a | n.a | Low | [4.7] |
| Cr(III) | DS | n.a | 3.16×10^4 * | n.a | n.a | n.a | n.a | n.a | n.a | n.a | n.r | [4.18] |
| Cr(III) | SS | n.a | 1.26×10^5 * | n.a | 7.94×10^3 | 1.00×10^6 | n.a | n.a | 25 | n.a | n.r | [4.18] |
| Cs | DS | Adsorption | 4.97×10^3 | 9.74 | 9.92×10^0 | 6.06×10^4 | 1.18×10^2 | 2.10×10^5 | 366 | 10 | n.r | MODARIA |
| Cs | DS | Desorption | 1.35×10^4 | 5.67 | 8.37×10^2 | 2.10×10^5 | 7.76×10^2 | 2.33×10^5 | 55 | 3 | n.r | MODARIA |
| Cs | DS | Field | 6.66×10^3 | 3.91 | 7.25×10^2 | 2.47×10^5 | 7.06×10^2 | 6.28×10^4 | 55 | 7 | n.r | MODARIA |
| Cs | SS | Adsorption | 1.71×10^4 | 2.47 | 1.25×10^3 | 1.37×10^5 | 3.86×10^3 | 7.58×10^4 | 203 | 15 | n.r | MODARIA |
| Cs | SS | Desorption | 3.30×10^4 | 2.50 | 4.36×10^3 | 1.38×10^5 | 7.30×10^3 | 1.49×10^5 | 64 | 4 | n.r | MODARIA |
| Cs | SS | Field | 1.35×10^5 | 2.67 | 2.34×10^3 | 2.70×10^6 | 2.64×10^4 | 6.69×10^5 | 211 | 13 | n.r | MODARIA |
| Cs | SS+DS | Adsorption | 9.50×10^3 | 6.70 | 3.70×10^2 | 1.90×10^5 | 4.16×10^2 | 2.17×10^5 | 569 | n.a | n.r | [4.11] |
| Cs | SS+DS | Desorption | 2.90×10^4 | 2.40 | 6.90×10^3 | 1.20×10^5 | 6.87×10^3 | 1.22×10^5 | 119 | n.a | n.r | [4.11] |
| Cs | SS+DS | Field | 2.90×10^4 | 5.90 | 1.60×10^3 | 5.20×10^5 | 1.56×10^3 | 5.37×10^5 | 219 | n.a | n.r | [4.11] |
| Cs | SS+DS | n.a | n.a | n.a | n.a | n.a | n.a | n.a | n.a | n.a | 1.00×10^3 | [4.8] |
| Cs | SS+DS | n.a | n.a | n.a | 5.00×10^1 | 8.00×10^4 | n.a | n.a | n.a | n.a | 1.00×10^1 | [4.7] |
| Cu | DS | Adsorption | 1.29×10^3 | 7.69 | 1.09×10^2 | 5.40×10^4 | 4.25×10^1 | 3.91×10^4 | 20 | 2 | n.r | MODARIA |
| Cu | DS | Field | 2.23×10^4 | 2.29 | 4.34×10^2 | 3.03×10^5 | 3.68×10^3 | 1.35×10^5 | 166 | 26 | n.r | MODARIA |
| Cu | SS | Adsorption | 1.29×10^4 | 3.89 | 1.76×10^3 | 1.02×10^5 | 1.38×10^3 | 1.20×10^5 | 99 | 2 | n.r | MODARIA |
| Cu | SS | Field | 6.01×10^4 | 4.66 | 1.05×10^2 | 6.92×10^7 | 4.85×10^3 | 7.68×10^5 | 304 | 20 | n.r | MODARIA |
| Cu | DS | n.a | $1.58 \times 10^{4*}$ | n.a | 5.01×10^0 | 1.58×10^6 | n.a | n.a | 12 | n.a | n.r | [4.18] |
| Cu | SS | n.a | $5.01 \times 10^{4*}$ | n.a | 1.26×10^3 | 1.26×10^6 | n.a | n.a | 70 | n.a | n.r | [4.18] |
| Dy | DS | Field | 5.80×10^5 | 2.53 | 4.07×10^4 | 3.66×10^6 | 1.26×10^5 | 2.66×10^6 | 26 | 1 | n.r | MODARIA |
| Er | DS | Field | 4.85×10^5 | 2.24 | 4.28×10^4 | 3.24×10^6 | 1.28×10^5 | 1.83×10^6 | 26 | 1 | n.r | MODARIA |
| Eu | DS | Field | 2.10×10^5 | 2.18 | 2.69×10^4 | 6.52×10^5 | 5.81×10^4 | 7.57×10^5 | 29 | 1 | n.r | MODARIA |
| Eu | SS+DS | n.a | n.a | n.a | 2.00×10^2 | 9.00×10^2 | n.a | n.a | n.a | n.a | 5.00×10^2 | [4.11] |
| Eu | SS+DS | n.a | n.a | n.a | 2.00×10^2 | 9.00×10^2 | n.a | n.a | n.a | n.a | 5.00×10^2 | [4.7] |
| Fe | DS | Field | 1.16×10^4 | 15.2 | 1.05×10^1 | 5.00×10^6 | 1.32×10^2 | 1.03×10^6 | 47 | 11 | n.r | MODARIA |
| Fe | SS | Adsorption | 2.04×10^5 | 1.79 | 5.07×10^4 | 5.34×10^5 | 7.83×10^4 | 5.31×10^5 | 27 | 1 | | MODARIA |
| Fe | SS | Field | 2.46×10^5 | 3.89 | 2.41×10^3 | 7.68×10^6 | 2.64×10^4 | 2.30×10^6 | 322 | 13 | n.r | MODARIA |
| Fe | SS+DS | Field | n.a | n.a | 1.00×10^3 | 1.00×10^4 | n.a | n.a | n.a | n.a | 5.00×10^3 | [4.11] |
| Fe | SS+DS | n.a | n.a | n.a | n.a | n.a | n.a | n.a | n.a | n.a | 5.00×10^3 | [4.8] |
| Fe | SS+DS | n.a | n.a | n.a | 1.00×10^3 | 1.00×10^4 | n.a | n.a | n.a | n.a | 5.00×10^3 | [4.7] |

TABLE 4.2. (cont.)

| Element | Component SS, DS ^a | Condition | GM | GSD | Min | Max | 5% | 95% | Nd | Nr | Indicative | Reference |
|---------|----------------------------------|------------|----------------------|------|-----------------------|--------------------|-----------------------|--------------------|-----|-----|--------------------|-----------|
| Gd | DS | Field | 4.26×10^5 | 3.16 | 3.51×10^4 | 4.35×10^6 | 6.43×10^4 | 2.82×10^6 | 29 | 1 | n.r | MODARIA |
| Hf | DS | Field | 1.93×10^6 | 1.77 | 3.77×10^5 | 6.11×10^6 | 7.56×10^5 | 4.94×10^6 | 26 | 1 | n.r | MODARIA |
| Hg | DS | Field | 2.56×10^1 | 4.44 | 5.85×10^0 | 4.78×10^2 | 2.21×10^0 | 2.97×10^2 | 15 | 1 | n.r | MODARIA |
| Hg | SS | Field | 1.28×10^5 | 3.95 | 1.58×10^3 | 3.33×10^6 | 1.34×10^4 | 1.23×10^6 | 532 | 8 | n.r | MODARIA |
| Ho | DS | Field | 4.25×10^5 | 1.97 | 3.98×10^4 | 1.16×10^6 | 1.39×10^5 | 1.30×10^6 | 26 | 1 | n.r | MODARIA |
| I | DS | Adsorption | 1.93×10^1 | 17.4 | 7.47×10^{-2} | 4.00×10^3 | 1.75×10^{-1} | 2.12×10^3 | 89 | 5 | n.r | MODARIA |
| I | SS | Adsorption | 3.62×10^3 | 4.17 | 1.70×10^2 | 1.05×10^5 | 3.46×10^2 | 3.78×10^4 | 71 | 5 | n.r | MODARIA |
| I | SS | Field | 3.32×10^3 | 1.34 | 7.88×10^2 | 4.64×10^3 | 2.06×10^3 | 5.36×10^3 | 20 | 1 | n.r | MODARIA |
| I | SS+DS | Adsorption | 4.40×10^3 | 14 | 5.90×10^1 | 3.40×10^5 | 5.73×10^1 | 3.38×10^5 | 124 | n.a | n.r | [4.11] |
| I | SS+DS | n.a | n.a | n.a | n.a | n.a | n.a | n.a | n.a | n.a | 1.00×10^1 | [4.8] |
| I | SS+DS | n.a | n.a | n.a | 0.00×10^0 | 8.00×10^1 | n.a | n.a | n.a | n.a | 1.00×10^1 | [4.7] |
| K | SS | Field | 2.53×10^3 | 2.19 | 3.05×10^1 | 2.73×10^4 | 6.95×10^2 | 9.21×10^3 | 106 | 2 | n.r | MODARIA |
| La | DS | Field | 1.03×10^6 | 2.49 | 3.72×10^4 | 1.80×10^7 | 2.31×10^5 | 4.64×10^6 | 32 | 2 | n.r | MODARIA |
| La | SS | Field | 1.36×10^5 | 1.69 | 7.01×10^4 | 4.09×10^5 | 5.73×10^4 | 3.21×10^5 | 21 | 1 | n.r | MODARIA |
| Li | DS | Field | 7.60×10^3 | 2.08 | 9.32×10^1 | 5.01×10^4 | 2.28×10^3 | 2.54×10^4 | 32 | 1 | n.r | MODARIA |
| Mg | DS | Field | 1.33×10^2 | n.r | 6.25×10^1 | 3.04×10^2 | n.r | n.r | 8 | 1 | n.r | MODARIA |
| Mg | SS | Field | 3.16×10^3 | 3.97 | 8.45×10^1 | 1.90×10^7 | 3.27×10^2 | 3.06×10^4 | 85 | 5 | n.r | MODARIA |
| Mn | DS | Adsorption | 5.50×10^3 | 50.3 | 5.33×10^1 | 1.64×10^6 | 8.74×10^0 | 3.46×10^6 | 69 | 2 | n.r | MODARIA |
| Mn | DS | Desorption | 5.94×10^3 | n.r | 1.87×10^3 | 1.64×10^6 | n.r | n.r | 6 | 1 | n.r | MODARIA |
| Mn | DS | Field | 9.74×10^3 | 11.0 | 3.41×10^2 | 3.42×10^6 | 1.90×10^2 | 5.00×10^5 | 57 | 9 | n.r | MODARIA |
| Mn | SS | Adsorption | 1.37×10^5 | 11.7 | 1.88×10^3 | 2.07×10^7 | 2.40×10^3 | 7.80×10^6 | 155 | 15 | n.r | MODARIA |
| Mn | SS | Desorption | 1.33×10^6 | 6.33 | 2.70×10^4 | 1.00×10^7 | 6.38×10^4 | 2.76×10^7 | 40 | 2 | n.r | MODARIA |
| Mn | SS | Field | 1.65×10^5 | 7.12 | 1.62×10^3 | 2.20×10^8 | 6.52×10^3 | 4.16×10^6 | 194 | 18 | n.r | MODARIA |
| Mn | SS+DS | Adsorption | 1.30×10^5 | 12.0 | 2.10×10^3 | 7.40×10^6 | 2.18×10^3 | 7.75×10^6 | 190 | n.a | n.r | [4.11] |
| Mn | SS+DS | Desorption | 6.90×10^5 | 6.60 | 3.20×10^4 | 1.50×10^7 | 3.10×10^4 | 1.54×10^7 | 46 | n.a | n.r | [4.11] |
| Mn | SS+DS | Field | 7.90×10^4 | 1.90 | 3.10×10^4 | 1.90×10^5 | 2.75×10^4 | 2.27×10^5 | 219 | n.a | n.r | [4.11] |
| Mn | SS+DS | n.a | n.a | n.a | n.a | n.a | n.a | n.a | n.a | n.a | 1.00×10^3 | [4.8] |
| Mn | SS+DS | n.a | n.a | n.a | 1.00×10^2 | 1.00×10^4 | n.a | n.a | n.a | n.a | 1.00×10^3 | [4.7] |
| Mo | DS | Field | 7.27×10^1 | n.r | 4.16×10^1 | 2.69×10^2 | n.r | n.r | 3 | 2 | n.r | MODARIA |
| Mo | SS | Field | 6.07×10^3 | 3.09 | 8.08×10^{-1} | 7.11×10^6 | 9.48×10^2 | 3.89×10^4 | 29 | 2 | n.r | MODARIA |
| Mo | DS | n.a | 3.16×10^2 * | n.a | n.a | n.a | n.a | n.a | n.a | n.a | n.r | [4.18] |
| Na | SS | Field | 1.53×10^3 | 1.48 | 4.37×10^2 | 4.29×10^3 | 8.01×10^2 | 2.92×10^3 | 22 | 1 | n.r | MODARIA |
| Ni | DS | Field | 1.03×10^3 | 5.99 | 1.87×10^1 | 5.67×10^4 | 5.41×10^1 | 1.96×10^4 | 39 | 10 | n.r | MODARIA |

TABLE 4.2. (cont.)

| Element | Component SS, DS ^a | Condition | GM | GSD | Min | Max | 5% | 95% | Nd | Nr | Indicative | Reference |
|---------|----------------------------------|------------|-----------------------|------|-----------------------|--------------------|--------------------|--------------------|-----|-----|--------------------|-----------|
| Ni | SS | Field | 3.11×10^4 | 1.27 | 8.69×10^2 | 5.01×10^5 | 3.80×10^3 | 2.55×10^5 | 86 | 10 | n.r | MODARIA |
| Ni | DS | n.a | 1.00×10^4 * | n.a | n.a | n.a | n.a | n.a | n.a | n.a | n.r | [4.18] |
| Ni | SS | n.a | 3.98×10^4 * | n.a | 3.16×10^3 | 5.01×10^5 | n.a | n.a | 30 | n.a | n.r | [4.18] |
| Np | SS+DS | n.a | n.a | n.a | 2.00×10^{-1} | 1.00×10^2 | n.a | n.a | n.a | n.a | 1.00×10^1 | [4.11] |
| Np | SS+DS | n.a | n.a | n.a | 2.00×10^{-1} | 1.00×10^2 | n.a | n.a | n.a | n.a | 1.00×10^1 | [4.7] |
| Pb | DS | Field | 9.01×10^3 | 27.5 | 2.00×10^0 | 2.00×10^7 | 3.86×10^1 | 2.10×10^6 | 129 | 18 | n.r | MODARIA |
| Pb | SS | Adsorption | 2.19×10^5 | 1.87 | 3.05×10^4 | 7.25×10^5 | 7.79×10^4 | 6.16×10^5 | 27 | 1 | n.r | MODARIA |
| Pb | SS | Field | 3.69×10^5 | 2.85 | 1.14×10^4 | 8.87×10^7 | 6.57×10^4 | 2.07×10^6 | 362 | 26 | n.r | MODARIA |
| Pb | DS | n.a | $1.26 \times 10^{5*}$ | n.a | 1.00×10^2 | 1.00×10^7 | n.a | n.a | 24 | n.a | n.r | [4.18] |
| Pb | SS | n.a | 3.98×10^5 * | n.a | 2.51×10^3 | 3.16×10^6 | n.a | n.a | 48 | n.a | n.r | [4.18] |
| Pm | | n.a | n.a | n.a | 1.00×10^3 | 1.00×10^4 | n.a | n.a | n.a | n.a | 5.00×10^3 | [4.11] |
| Pm | | n.a | n.a | n.a | 1.00×10^3 | 1.00×10^4 | n.a | n.a | n.a | n.a | 5.00×10^3 | [4.7] |
| Po | DS | Field | 1.02×10^5 | 5.35 | 2.21×10^4 | 6.10×10^6 | 6.45×10^3 | 1.61×10^6 | 10 | 2 | n.r | MODARIA |
| Po | SS | Field | 1.05×10^5 | 5.68 | 1.79×10^3 | 2.58×10^7 | 5.99×10^3 | 1.83×10^6 | 75 | 4 | n.r | MODARIA |
| Pr | SS | Field | 1.21×10^5 | 1.77 | 5.37×10^4 | 4.21×10^5 | 4.73×10^4 | 3.11×10^5 | 21 | 1 | n.r | MODARIA |
| Pu | DS | Adsorption | 6.49×10^4 | 2.78 | 9.30×10^3 | 4.20×10^5 | 1.21×10^4 | 3.48×10^5 | 33 | 3 | n.r | MODARIA |
| Pu | DS | Desorption | 2.96×10^5 | 2.05 | 3.07×10^4 | 1.25×10^7 | 9.07×10^4 | 9.65×10^5 | 41 | 4 | n.r | MODARIA |
| Pu | SS | Adsorption | 6.04×10^4 | n.r | 6.00×10^3 | 3.00×10^6 | n.r | n.r | 4 | 1 | n.r | MODARIA |
| Pu | SS | Field | 1.47×10^5 | 13.9 | 2.00×10^2 | 1.60×10^7 | 1.94×10^3 | 1.11×10^7 | 79 | 6 | n.r | MODARIA |
| Pu | SS+DS | Adsorption | 7.90×10^4 | 2.20 | 2.10×10^4 | 2.90×10^5 | 2.16×10^4 | 2.89×10^5 | 37 | n.a | n.r | [4.11] |
| Pu | SS+DS | Desorption | 3.00×10^5 | 4.20 | 2.90×10^4 | 3.20×10^6 | 2.83×10^4 | 3.18×10^6 | 41 | n.a | n.r | [4.11] |
| Pu | SS+DS | Field | 2.40×10^5 | 6.60 | 1.10×10^4 | 5.20×10^6 | 1.08×10^4 | 5.35×10^6 | 79 | n.a | n.r | [4.11] |
| Pu | SS+DS | n.a | n.a | n.a | n.a | n.a | n.a | n.a | n.a | n.a | 1.00×10^5 | [4.8] |
| Pu | SS+DS | n.a | n.a | n.a | 1.00×10^2 | 1.00×10^7 | n.a | n.a | n.a | n.a | 1.00×10^5 | [4.7] |
| Ra | DS | Adsorption | 8.18×10^3 | 1.30 | 5.63×10^3 | 2.42×10^4 | 5.33×10^3 | 1.26×10^4 | 10 | 1 | n.r | MODARIA |
| Ra | DS | Field | 1.20×10^3 | 23.9 | 8.24×10^1 | 1.67×10^5 | 6.49×10^0 | 2.22×10^5 | 15 | 4 | n.r | MODARIA |
| Ra | SS | Adsorption | 1.18×10^4 | n.r | 6.30×10^3 | 2.42×10^4 | n.r | n.r | 9 | 1 | n.r | MODARIA |
| Ra | SS | Field | 5.21×10^3 | 2.76 | 1.13×10^2 | 1.73×10^5 | 9.79×10^2 | 2.77×10^4 | 48 | 3 | n.r | MODARIA |
| Ra | SS+DS | Various | 7.40×10^3 | 3.1 | 1.10×10^3 | 5.20×10^4 | 1.15×10^3 | 4.76×10^4 | 75 | n.a | n.r | [4.11] |
| Ra | SS+DS | n.a | n.a | n.a | n.a | n.a | n.a | n.a | n.a | n.a | 5.00×10^2 | [4.8] |
| Ra | SS+DS | n.a | n.a | n.a | 1.00×10^2 | 1.00×10^3 | n.a | n.a | n.a | n.a | 5.00×10^2 | [4.7] |
| Rb | SS | Field | 7.33×10^3 | 1.92 | 2.12×10^3 | 2.38×10^4 | 2.50×10^3 | 2.15×10^4 | 21 | 1 | n.r | MODARIA |
| Ru | DS | Adsorption | 5.28×10^4 | 1.39 | 3.34×10^4 | 7.90×10^4 | 3.09×10^4 | 9.03×10^4 | 36 | 1 | n.r | MODARIA |

TABLE 4.2. (cont.)

| Element | Component SS, DS ^a | Condition | GM | GSD | Min | Max | 5% | 95% | Nd | Nr | Indicative | Reference |
|---------|----------------------------------|------------|-----------------------|------|--------------------|--------------------|--------------------|--------------------|-----|-----|--------------------|-----------|
| Ru | SS | Field | 2.73×10^4 | 1.67 | 4.00×10^2 | 5.39×10^4 | 1.17×10^4 | 6.36×10^4 | 38 | 2 | n.r | MODARIA |
| Ru | SS+DS | Various | 3.20×10^4 | 1.9 | 1.10×10^4 | 9.30×10^4 | 1.11×10^4 | 9.20×10^4 | 74 | n.a | n.r | [4.11] |
| Ru | SS+DS | n.a | n.a | n.a | n.a | n.a | n.a | n.a | n.a | n.a | 5.00×10^2 | [4.8] |
| S | SS | Field | 1.33×10^3 | 1.55 | 7.25×10^2 | 7.06×10^3 | 6.44×10^2 | 2.73×10^3 | 21 | 1 | n.r | MODARIA |
| Sb | DS | Field | 1.20×10^4 | n.r | 1.09×10^4 | 1.94×10^4 | n.r | n.r | 3 | 1 | n.r | MODARIA |
| Sb | SS | Adsorption | 6.75×10^3 | 2.73 | 8.00×10^2 | 4.00×10^4 | 1.29×10^3 | 3.52×10^4 | 16 | 2 | n.r | MODARIA |
| Sb | SS | Field | 8.14×10^3 | 2.64 | 3.40×10^1 | 1.03×10^5 | 1.65×10^3 | 4.01×10^4 | 44 | 8 | n.r | MODARIA |
| Sb | SS+DS | Various | 5.00×10^3 | 3.90 | 5.50×10^2 | 4.60×10^4 | 5.33×10^2 | 4.69×10^4 | 23 | n.a | n.r | [4.11] |
| Sb | SS+DS | n.a | n.a | n.a | n.a | n.a | n.a | n.a | n.a | n.a | 5.00×10^1 | [4.8] |
| Sb | DS | n.a | $1.00 \times 10^{4*}$ | n.a | 3.16×10^2 | 6.31×10^4 | n.a | n.a | 3 | n.a | n.r | [4.18] |
| Se | DS | Field | n.a | n.a | n.a | n.a | n.a | n.a | 1 | 1 | 7.08×10^3 | MODARIA |
| Se | SS | Field | 1.54×10^4 | 2.19 | 5.41×10^3 | 6.65×10^4 | 4.24×10^3 | 5.61×10^4 | 22 | 1 | n.r | MODARIA |
| Se | DS | n.a | $3.98 \times 10^{3*}$ | n.a | n.a | n.a | n.a | n.a | n.a | n.a | n.r | [4.18] |
| Se | SS | n.a | n.a | n.a | 1.26×10^3 | 5.01×10^4 | n.a | n.a | n.a | n.a | n.r | [4.18] |
| Si | SS | Field | 2.72×10^4 | 2.20 | 2.42×10^3 | 4.93×10^5 | 7.41×10^3 | 9.98×10^4 | 187 | 2 | n.r | MODARIA |
| Sn | SS | Field | 1.33×10^5 | 1.59 | 3.72×10^4 | 3.41×10^5 | 6.18×10^4 | 2.86×10^5 | 21 | 1 | n.r | MODARIA |
| Sn | DS | n.a | $5.01 \times 10^{4*}$ | n.a | n.a | n.a | n.a | n.a | n.a | n.a | n.r | [4.18] |
| Sn | SS | n.a | $3.98 \times 10^{5*}$ | n.a | 7.94×10^4 | 2.00×10^6 | n.a | n.a | 3 | n.a | n.r | [4.18] |
| Sr | DS | Adsorption | 5.01×10^1 | 3.21 | 2.84×10^0 | 1.34×10^3 | 7.34×10^0 | 3.42×10^2 | 185 | 7 | n.r | MODARIA |
| Sr | DS | Desorption | 2.71×10^2 | 3.09 | 1.20×10^1 | 2.06×10^3 | 4.25×10^1 | 1.73×10^3 | 50 | 6 | n.r | MODARIA |
| Sr | DS | Field | 8.24×10^2 | 3.21 | 8.00×10^1 | 3.45×10^3 | 1.21×10^2 | 5.62×10^3 | 26 | 5 | n.r | MODARIA |
| Sr | SS | Adsorption | 1.90×10^3 | 2.75 | 1.11×10^2 | 1.99×10^4 | 3.60×10^2 | 1.00×10^4 | 69 | 2 | n.r | MODARIA |
| Sr | SS | Field | 2.96×10^3 | 3.79 | 1.11×10^2 | 1.99×10^4 | 3.31×10^2 | 2.65×10^4 | 39 | 5 | n.r | MODARIA |
| Sr | SS+DS | Adsorption | 1.90×10^2 | 4.60 | 1.40×10^1 | 2.20×10^3 | 1.54×10^1 | 2.34×10^3 | 156 | n.a | n.r | [4.11] |
| Sr | SS+DS | Desorption | 6.20×10^2 | 2.10 | 1.90×10^2 | 2.10×10^3 | 1.83×10^2 | 2.10×10^3 | 34 | n.a | n.r | [4.11] |
| Sr | SS+DS | Field | 1.20×10^3 | 2.70 | 2.30×10^2 | 6.30×10^3 | 2.34×10^2 | 6.15×10^3 | 13 | n.a | n.r | [4.11] |
| Sr | SS+DS | n.a | n.a | n.a | n.a | n.a | n.a | n.a | n.a | n.a | 1.00×10^3 | [4.8] |
| Sr | SS+DS | n.a | n.a | n.a | 8.00×10^0 | 4.00×10^3 | n.a | n.a | n.a | n.a | 1.00×10^3 | [4.7] |
| Tc | SS+DS | n.a | n.a | n.a | 0.00×10^0 | 1.00×10^2 | n.a | n.a | n.a | n.a | 5.00×10^0 | [4.11] |
| Tc | SS+DS | n.a | n.a | n.a | n.a | n.a | n.a | n.a | n.a | n.a | 5.00×10^0 | [4.8] |
| Tc | SS+DS | n.a | n.a | n.a | 0.00×10^0 | 1.00×10^2 | n.a | n.a | n.a | n.a | 5.00×10^0 | [4.7] |
| Th | DS | Adsorption | 1.56×10^5 | 47.8 | 1.15×10^2 | 2.75×10^6 | 2.69×10^2 | 9.04×10^7 | 12 | 2 | n.r | MODARIA |
| Th | DS | Field | 7.40×10^2 | n.a | 3.60×10^2 | 4.72×10^5 | n.a | n.a | 9 | 3 | n.r | MODARIA |

TABLE 4.2. (cont.)

| Element | Component SS, DS ^a | Condition | GM | GSD | Min | Max | 5% | 95% | Nd | Nr | Indicative | Reference |
|---------|----------------------------------|------------|-----------------------|------|--------------------|--------------------|--------------------|--------------------|-----|-----|--------------------|-----------|
| Th | SS | Field | 1.52×10^5 | 2.90 | 1.13×10^4 | 1.60×10^6 | 2.64×10^4 | 8.76×10^5 | 41 | 4 | n.r | MODARIA |
| Th | SS+DS | Various | 1.90×10^5 | 21.0 | 1.20×10^3 | 2.70×10^7 | 1.27×10^3 | 2.84×10^7 | 63 | n.a | n.r | [4.11] |
| Th | SS+DS | n.a | n.a | n.a | n.a | n.a | n.a | n.a | n.a | n.a | 1.00×10^4 | [4.8] |
| Th | SS+DS | n.a | n.a | n.a | 1.00×10^3 | 1.00×10^6 | n.a | n.a | n.a | n.a | 1.00×10^4 | [4.7] |
| Ti | DS | Field | n.a | n.a | n.a | n.a | n.a | n.a | 1 | 1 | 4.07×10^4 | MODARIA |
| Ti | SS | Field | 1.05×10^5 | 1.35 | 2.41×10^4 | 1.58×10^5 | 6.42×10^4 | 1.71×10^5 | 21 | 1 | n.r | MODARIA |
| U | DS | Adsorption | 4.29×10^3 | 30.0 | 1.93×10^1 | 6.26×10^4 | 1.59×10^1 | 2.04×10^6 | 103 | 1 | n.r | MODARIA |
| U | DS | Field | 3.50×10^3 | 40.1 | 9.10×10^1 | 8.04×10^4 | 8.07×10^0 | 1.51×10^6 | 14 | 5 | n.r | MODARIA |
| U | SS | Adsorption | 2.52×10^4 | 2.07 | 3.27×10^3 | 1.03×10^5 | 7.58×10^3 | 8.40×10^4 | 26 | 1 | n.r | MODARIA |
| U | SS | Field | 1.19×10^4 | 5.63 | 3.05×10^2 | 1.27×10^5 | 6.94×10^2 | 2.04×10^5 | 38 | 6 | n.r | MODARIA |
| U | SS+DS | n.a | n.a | n.a | 2.00×10^1 | 1.00×10^3 | n.a | n.a | n.a | n.a | 5.00×10^1 | [4.11] |
| U | SS+DS | n.a | n.a | n.a | n.a | n.a | n.a | n.a | n.a | n.a | 5.00×10^1 | [4.8] |
| U | SS+DS | n.a | n.a | n.a | 2.00×10^1 | 1.00×10^3 | n.a | n.a | n.a | n.a | 5.00×10^1 | [4.7] |
| V | DS | Field | n.a | n.a | n.a | n.a | n.a | n.a | 1 | 1 | 3.71×10^4 | MODARIA |
| V | SS | Field | 4.29×10^4 | 1.40 | 1.19×10^4 | 8.46×10^4 | 2.47×10^4 | 7.44×10^4 | 21 | 1 | n.r | MODARIA |
| Zn | DS | Adsorption | 1.13×10^4 | 10.6 | 5.02×10^1 | 2.63×10^6 | 2.33×10^2 | 5.44×10^5 | 113 | 5 | n.r | MODARIA |
| Zn | DS | Field | 2.09×10^3 | 5.50 | 2.11×10^0 | 2.66×10^5 | 1.27×10^2 | 3.45×10^4 | 127 | 14 | n.r | MODARIA |
| Zn | SS | Adsorption | 1.18×10^4 | 3.69 | 1.68×10^3 | 8.58×10^4 | 1.37×10^3 | 1.01×10^5 | 20 | 1 | n.r | MODARIA |
| Zn | SS | Field | 1.73×10^5 | 4.86 | 3.00×10^3 | 6.77×10^7 | 1.28×10^4 | 2.33×10^6 | 213 | 17 | n.r | MODARIA |
| Zn | SS+DS | n.a | n.a | n.a | 1.00×10^2 | 1.00×10^3 | n.a | n.a | n.a | n.a | 5.00×10^2 | [4.11] |
| Zn | SS+DS | n.a | n.a | n.a | n.a | n.a | n.a | n.a | n.a | n.a | 5.00×10^2 | [4.8] |
| Zn | SS+DS | n.a | n.a | n.a | 1.00×10^2 | 1.00×10^3 | n.a | n.a | n.a | n.a | 5.00×10^2 | [4.7] |
| Zn | DS | n.a | $5.01 \times 10^{3*}$ | n.a | 3.16×10^1 | 1.58×10^6 | n.a | n.a | 18 | n.a | n.r | [4.18] |
| Zn | SS | n.a | $1.26 \times 10^{5*}$ | n.a | 3.16×10^3 | 7.94×10^6 | n.a | n.a | 75 | n.a | n.r | [4.18] |
| Zr | SS+DS | n.a | n.a | n.a | 1.00×10^3 | 1.00×10^4 | n.a | n.a | n.a | n.a | 1.00×10^3 | [4.11] |
| Zr | SS+DS | n.a | n.a | n.a | n.a | n.a | n.a | n.a | n.a | n.a | 1.00×10^3 | [4.8] |
| Zr | SS+DS | n.a | n.a | n.a | 1.00×10^3 | 1.00×10^4 | n.a | n.a | n.a | n.a | 1.00×10^3 | [4.7] |

^a SS: suspended sediments; DS: deposited sediments; (*) indicates median values. No (*) corresponds to GM; Nd = number of data; Nr = number of references; n.a = not available; n.r = not relevant

4.3.1. Analyses of the updated freshwater K_d dataset

For the elements for which there are sufficient data, this section presents four analyses of the updated MODARIA WG4 freshwater K_d database. Initially, the distributions of K_{dSS} and K_{dDS} are compared to highlight the relevance of considering K_d values specifically for suspended and deposited sediments. The subsequent three analyses consider the conditional distributions of *in situ* K_{dSS} as a function of suspended loads (SS), dissolved organic carbon (DOC) and K_{dDS} as a function of pH [4.17].

4.3.1.1. Comparisons between K_{dSS} and K_{dDS}

To assess the relevance of separating K_d for suspended and deposited sediments, this section compares the K_d distributions of these two components. Given the available data, this comparison was possible for As, Be, Cd, Co, Cr, Cs, Cu, Fe, Hg, La, Mn, Ni, Pb, Po, Ra, Sr, U and Zn in field conditions (Fig. 4.4) and for Co, Cs, Cu, I, Mn Sr and Zn in adsorption conditions (Fig. 4.5).

Whatever the condition, $GM(K_{dSS})$ is higher than $GM(K_{dDS})$ as described before, except for Be, La and Po in the case of *in situ* condition and Zn in the case of adsorption condition.

A recurrent difference between the K_d distributions between suspended and deposited sediments was therefore found, which is probably associated with the different properties of the particles rather than with the speciation in the dissolved phase. For example, the mean particle size of deposited sediments is generally higher than those of suspended sediments and, thus, tends to have a lower metal sorption capacity. Deposited sediments are also characterized by lower porosity than suspended sediments, leading to a lower exchange surface and, thus, decreasing metal sorption process. Furthermore, the properties of the organic matter of deposited sediments are different from those of suspended sediments due to the degradation of organic carbon during early diagenesis [4.20, 4.21].

Except for Be in field conditions, the variability of K_{dDS} was higher than that of K_{dSS} whatever the element and the condition. Assuming that the particle size is one of the main parameters that controls K_d in fresh water, this is a logical outcome because the variability and the range of the particle size distribution was much higher for deposited sediments than for suspended sediments.

These data analyses confirmed and highlighted differences between K_{dSS} and K_{dDS} , which reinforces and justifies the need to consider deposited sediments and suspended sediments separately in the freshwater environment when establishing reference K_d values.

4.3.1.2. Conditional log-normal distributions of *in situ* K_{dSS} as a function of suspended sediments

In rivers, the ratio of solid mass to water volume (m/V) corresponds to SS, the load of suspended sediments. This ratio is as important as K_{dSS} in determining solid–liquid fractionation because both contribute to defining the contribution of the particulate activity concentration to the total activity concentration of the water column (C_{WC}), given by the following relationship [4.4]:

$$C_{WC} = C_{FWC} + K_{dSS} \times SS \times C_{FWC} \quad (4.7)$$

where C_{FWC} is the activity concentration in the filtered water of the water column.

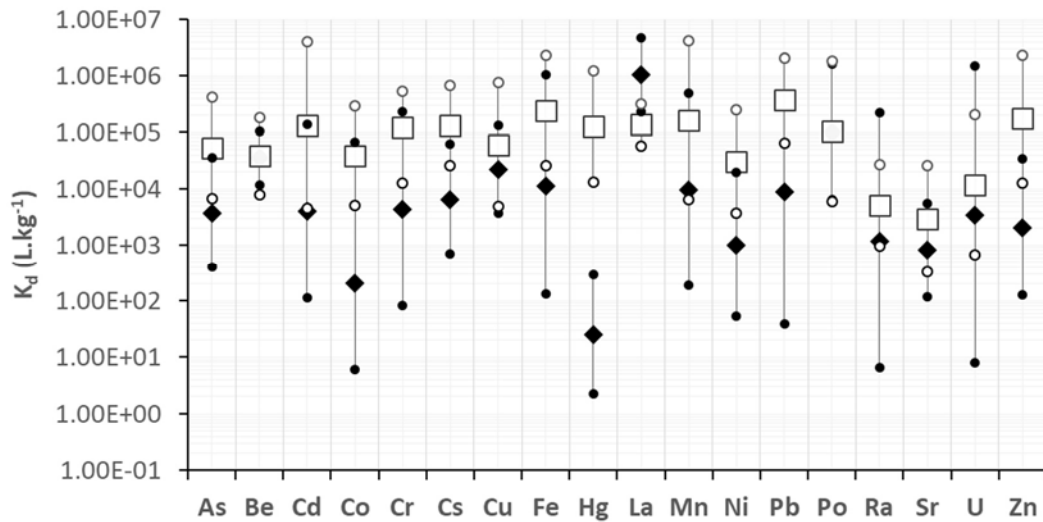


FIG. 4.4. GM and 5th and 95th percentiles of in situ K_{dSS} (white) and K_{dDS} (black).

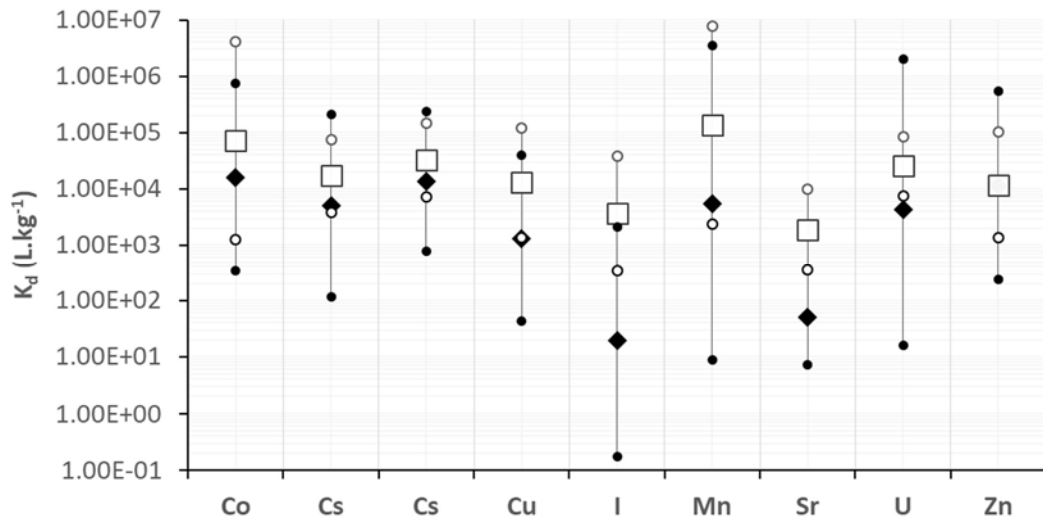


FIG. 4.5. GM and 5th and 95th percentiles of adsorption K_{dSS} (white) and K_{dDS} (black).

For anthropogenic radionuclides, a generic decrease in K_{dSS} is generally observed when the load of suspended sediments increases [4.22–4.24]. This tendency is mainly explained by three phenomena related to the radionuclide activity concentration in superficial dried deposited sediments (C_{DS}) with that in the filtered water column (C_{FWC}).

- (1) Particle size effect: The load and size of suspended sediments are roughly correlated as they both tend to increase at the same time when the water flow increases [4.25, 4.26]. Although this behaviour has not always been observed [4.27], its main effect is to decrease the mean specific surface of suspended matters and, mechanistically, to decrease capacity to adsorb radionuclides and heavy metals.
- (2) Mass/Volume effect: Various geochemical features of elements make up the crystal structure of particles and the relative contribution of their non-exchangeable fractions increases as the size of particles increases. Thereby, these fractions gradually contribute more to the activity concentration of suspended sediments as the size of particles

increases. Conversely, the relative amount of surface binding capacity decreases with particle size. Consequently, an increase in SS leads to a decrease in K_{dSS} if the geochemical contribution is negligible compared with the anthropogenic discharges, and to an increase in K_{dSS} in the opposite situation [4.28].

- (3) Colloidal pumping: The concentration of colloids increases in a similar manner to SS. Very fine particle (<0.45 μm) colloids are highly efficient in adsorbing radionuclides and heavy metals and are poorly retained by filtration [4.29]. Consequently, an increase in their concentration enriches the radionuclide and heavy metal concentrations of the filtered water [4.30] which tends to reduce K_{dSS} .

Thus, SS appears to be an important factor in explaining the variability of K_{dSS} . For this reason, this section presents conditional log-normal distributions of *in situ* K_{dSS} as a function SS. Because it is unlikely that environmental conditions for load and size distributions of suspended sediments can be precisely reproduced in laboratory experiments, this analysis is limited to *in situ* K_{dSS} . The database allows such an analysis for 19 elements: Am, As, Ba, Be, Cd, Co, Cr, Cs, Cu, Fe, Hg, Mg, Mn, Ni, Pb, Pu, Si, Sr, and Zn.

Changes in the conditional geometric means, $GM(K_{dSS|SS})$, and geometric standard deviations, $GSD(K_{dSS|SS})$, as a function of SS are represented by the following power equations:

$$GM(K_{dSS|SS}) = a \times SS^b \quad (4.8)$$

$$GSD(K_{dSS|SS}) = c \times SS^d \quad (4.9)$$

where the parameters a (L/kg)^{b+1} and c (L/kg) are scaling factors with values corresponding to $GM(K_{dSS|SS})$ and $GSD(K_{dSS|SS})$ when $SS = 1$ mg/L. The exponents, b and d , describe the extent of the deviation of the adsorption process from linearity [4.31]. Table 4.3 summarizes these relationships with their p -values and determination coefficient (R^2) which indicates the proportion of the variances that can be explained by these equations.

All the relationships of $GM(K_{dSS|SS})$ are statistically representative (p -value $\ll 0.05$) and negative ($b < 0$). However, they are not significant for Co, Mn, Ni and Si for which R^2 was lower than 0.2. For Am, As, Ba, Be, Cd, Cr, Cs, Cu, Fe, Hg, Mg, Pb, Pu, Sr and Zn, the sensitivity of the K_{dSS} values in the field to SS explains more than 50% of the dataset variability. For example, the total $GSD(K_{dSS})$ of Cd and Cu for *in situ* suspended sediments that initially equal 4.6 and 7.8 respectively (Table 4.2) was reduced to 2–3 and 2–4 by considering SS (Fig. 4.6). As an example, Fig. 4.6 shows the trend for Cd, Cu, Hg and Pb.

Assuming that an element is relatively more impacted by SS the lower the slope b and the higher the coefficient R^2 , Fig. 4.7 indicates that the elements most sensitive to SS are Pu, Cs and Cd, and the least sensitive are Mn, Co, Si and Ni. This is in agreement with Vesely et al. [4.32] who observed small changes in K_{dSS} values for Si, and with Pettine et al. [4.33] who did not find any effect of SS on the K_{dSS} values of Mn and Co in the Po River in Italy.

Therefore, SS appears to be an operational and relevant parameter that can reduce the variability of K_{dSS} distributions by several orders of magnitude. Therefore, it needs to be measured during sampling and evaluated during modelling. Although these results need enhancement and further consideration, especially by improving the datasets, it can be argued that this type of approach could be a promising approach that may reduce uncertainties for K_{dSS} .

TABLE 4.3. PARAMETERS a AND b AND ASSOCIATED R SQUARED (R^2) AND P-VALUE FOR THE *IN SITU* RELATIONSHIPS $GM(K_{dSS|SS}) = a \times SS^b$ and $GSD(K_{dSS|SS}) = c \times SS^d$ *

| Element | $GM(K_{dSS SS})$ | | $GSD(K_{dSS SS})$ | |
|---------|---|----------------------------------|---|-------|
| | Equation | R^2 (p-value) | Equation | R^2 |
| Am | $GM(K_{dSS SS}) = 4.08 \times 10^5 \times SS^{-0.72}$ | 0.89 (2.14×10^{-16}) | $GSD(K_{dSS SS}) = 2.36 \times SS^{0.15}$ | 0.20 |
| As | $GM(K_{dSS SS}) = 1.64 \times 10^5 \times SS^{-0.66}$ | 0.85 (6.34×10^{-15}) | $GSD(K_{dSS SS}) = 3.02 \times SS^{0.08}$ | 0.03 |
| Ba | $GM(K_{dSS SS}) = 2.30 \times 10^4 \times SS^{-0.45}$ | 0.90 (7.65×10^{-34}) | $GSD(K_{dSS SS}) = 1.00 \times SS^{0.18}$ | 0.33 |
| Be | $GM(K_{dSS SS}) = 7.05 \times 10^4 \times SS^{-0.32}$ | 0.65 (2.08×10^{-7}) | $GSD(K_{dSS SS}) = 2.09 \times SS^{0.15}$ | 0.31 |
| Cd | $GM(K_{dSS SS}) = 8.51 \times 10^5 \times SS^{-0.83}$ | 0.91 (3.00×10^{-94}) | $GSD(K_{dSS SS}) = 2.74 \times SS^{0.02}$ | 0.02 |
| Co | $GM(K_{dSS SS}) = 4.74 \times 10^4 \times SS^{-0.16}$ | 0.14 (2.07×10^{-5}) | $GSD(K_{dSS SS}) = 2.24 \times SS^{0.04}$ | 0.01 |
| Cr | $GM(K_{dSS}) = 4.30 \times 10^5 \times SS^{-0.53}$ | 0.68 (1.53×10^{-25}) | $GSD(K_{dSS SS}) = 2.07 \times SS^{0.02}$ | 0.01 |
| Cs | $GM(K_{dSS SS}) = 7.95 \times 10^5 \times SS^{-0.95}$ | 0.94 (5.93×10^{-37}) | $GSD(K_{dSS SS}) = 1.74 \times SS^{0.21}$ | 0.49 |
| Cu | $GM(K_{dSS SS}) = 1.38 \times 10^5 \times SS^{-0.43}$ | 0.79 (1.71×10^{-75}) | $GSD(K_{dSS SS}) = 2.73 \times SS^{-0.02}$ | 0.02 |
| Fe | $GM(K_{dSS SS}) = 8.80 \times 10^5 \times SS^{-0.63}$ | 0.87 (1.00×10^{-57}) | $GSD(K_{dSS SS}) = 2.93 \times SS^{0.06}$ | 0.06 |
| Hg | $GM(K_{dSS SS}) = 4.88 \times 10^5 \times SS^{-0.58}$ | 0.89 (5.70×10^{-160}) | $GSD(K_{dSS SS}) = 2.68 \times SS^{-0.01}$ | 0.001 |
| Mg | $GM(K_{dSS SS}) = 1.25 \times 10^4 \times SS^{-0.67}$ | 0.76 (7.80×10^{-14}) | $GSD(K_{dSS SS}) = 4.07 \times SS^{-0.01}$ | 0.66 |
| Mn | $GM(K_{dSS SS}) = 4.65 \times 10^5 \times SS^{-0.32}$ | 0.25 (3.74×10^{-10}) | $GSD(K_{dSS SS}) = 27.43 \times SS^{-0.52}$ | 0.55 |
| Ni | $GM(K_{dSS SS}) = 3.93 \times 10^4 \times SS^{-0.06}$ | 0.01 (5.13×10^{-3}) | $GSD(K_{dSS SS}) = 0.37 \times SS^{0.74}$ | 0.73 |
| Pb | $GM(K_{dSS SS}) = 8.49 \times 10^5 \times SS^{-0.45}$ | 0.66 (4.51×10^{-47}) | $GSD(K_{dSS SS}) = 2.33 \times SS^{-0.03}$ | 0.03 |
| Pu | $GM(K_{dSS SS}) = 9.82 \times 10^5 \times SS^{-1.25}$ | 0.93 (1.58×10^{-19}) | $GSD(K_{dSS SS}) = 3.67 \times SS^{0.16}$ | 0.15 |
| Si | $GM(K_{dSS SS}) = 2.30 \times 10^4 \times SS^{-0.13}$ | 0.05 (3.37×10^{-4}) | $GSD(K_{dSS SS}) = 1.33 \times SS^{0.38}$ | 0.27 |
| Sr | $GM(K_{dSS SS}) = 3.31 \times 10^4 \times SS^{-0.96}$ | 0.87 (9.86×10^{-13}) | $GSD(K_{dSS SS}) = 1.27 \times SS^{0.15}$ | 0.09 |
| Zn | $GM(K_{dSS SS}) = 4.60 \times 10^5 \times SS^{-0.51}$ | 0.98 (1.65×10^{-66}) | $GSD(K_{dSS SS}) = 4.84 \times SS^{-0.12}$ | 0.5 |

* Adapted after Ref. [4.17], with permission.

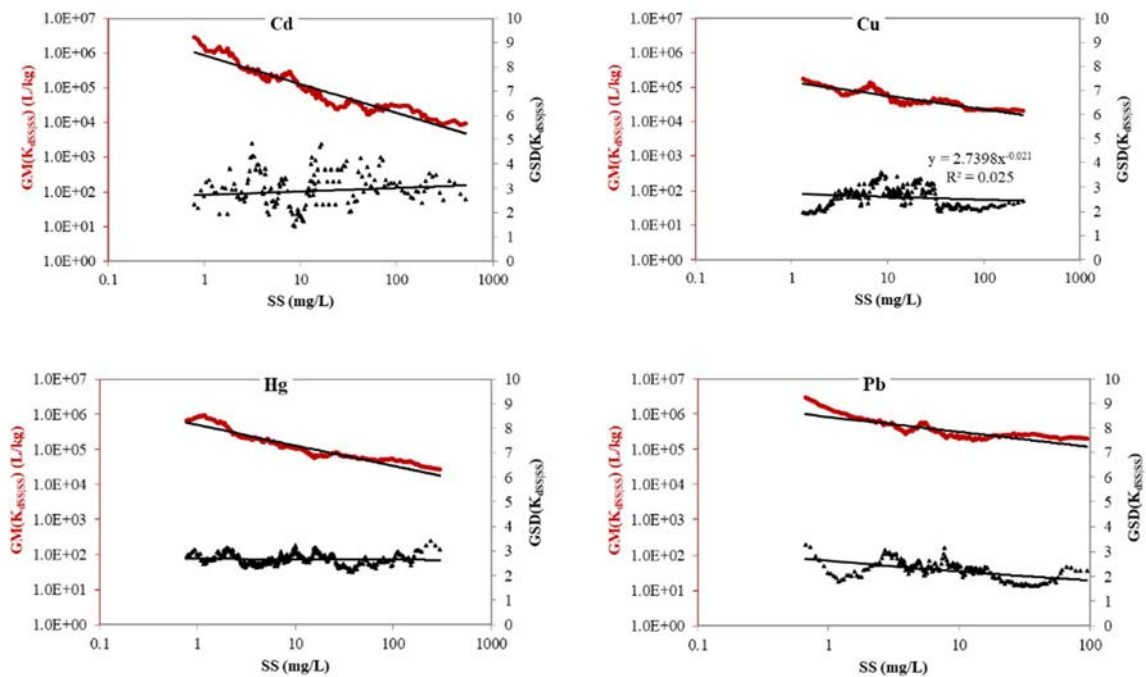


FIG. 4.6. In situ $GM(K_{dSS|SS})$ (Red) and $GSD(K_{dSS|SS})$ (Black) (adapted after [4.17], with permission).

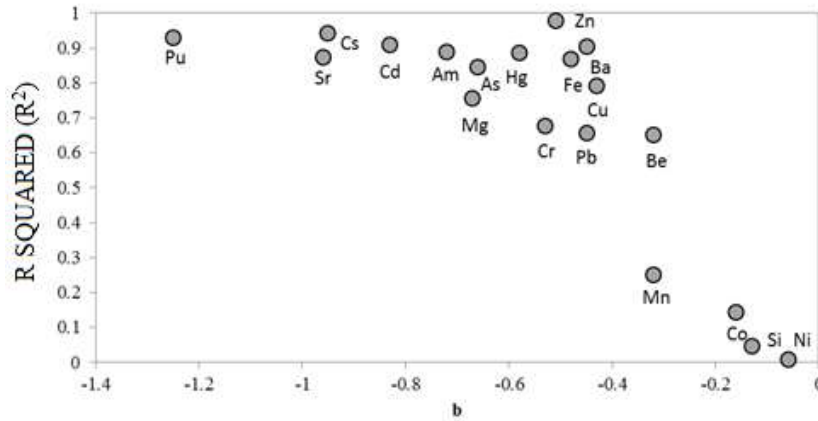


FIG. 4.7. *R squared* (R^2) of the equation $K_{dSS|SS} = a \times SS^b$, as a function of the parameter b (adapted after [4.17], with permission).

4.3.1.3. Conditional log-normal distributions of *in situ* K_{dSS} as a function of dissolved organic carbon

Dissolved and particulate organic carbon has a very high affinity for numerous radionuclides in aquatic systems [4.34]. Dissolved organic carbon (DOC) is a mixture of pedogenic (derived from soil washout) and aquagenic (from material excreted by aquatic biota) compounds [4.35] presenting a high capacity to complex metals and change their speciation, thus impacting their behaviour and their solid–liquid partition. Metals, for example, can be bounded to dissolved organic ligands and maintained for a longer time in these dissolved forms [4.36–4.39]. Thus, inverse correlations between DOC and K_d can be expected for some elements.

The data compiled in the freshwater database allow the determination of conditional log-normal distributions of *in situ* K_{dSS} as a function of DOC concentrations for fourteen elements: As, Cd, Ce, Co, Cr, Cu, Fe, Hg, K, Mg, Mn, Pb, Si and Zn. These distributions are defined by the changes as a function of DOC concentrations of the conditional geometric means, $GM(K_{dSS|DOC})$, and geometric standard deviations, $GSD(K_{dSS|DOC})$, which are represented by the following power equations:

$$GM(K_{dSS|DOC}) = a \times DOC^b \quad (4.10)$$

$$GSD(K_{dSS|DOC}) = c \times DOC^d \quad (4.11)$$

Where the parameters a (L/kg)^{b+1} and c (L/kg) are scaling factors with values corresponding to $GM(K_{dSS|DOC})$ and $GSD(K_{dSS|DOC})$ when $DOC = 1$ mg/L. The exponents, b and d , describe the extent of the deviation of the adsorption process from linearity [4.31]. Table 4.4 summarizes these relationships with their p -values and determination coefficient (R^2) which indicates the proportion of the variances that can be explained by these equations.

All the DOC concentrations range between 2 and 10 mg/L, which is representative of fresh waters but not of pore waters, where DOC can reach 50 mg/L [4.40]. The relationships of $GM(K_{dSS|DOC})$ are all statistically representative (p -value $\ll 0.05$) and negative ($b < 0$) excepted for Co ($b = 1.58$). Thus, the sensitivity of *in situ* K_{dSS} to DOC explains more than 50% of the dataset variability and is inversely related to DOC, as expected. As examples, Fig. 4.8 reports the trend for As, Fe, Hg and Mn.

TABLE 4.4. PARAMETERS a AND b AND ASSOCIATED R SQUARED (R^2) AND p -VALUE FOR THE RELATIONSHIPS $GM(K_{dSS|DOC}) = a \times DOC^b$ and $GSD(K_{dSS|DOC}) = c \times DOC^d$ *

| Element | $GM(K_{dSS DOC})$ | | $GSD(K_{dSS DOC})$ | |
|---------|---|---------------------------------|--|-------|
| | Equation | R^2 (p -value) | Equation | R^2 |
| As | $GM(K_{dSS DOC}) = 4.96 \times 10^5 \times DOC^{-1.59}$ | 0.95 (2.70×10^{-47}) | $GSD(K_{dSS DOC}) = 6.5 \times DOC^{-0.59}$ | 0.77 |
| Cd | $GM(K_{dSS DOC}) = 8.00 \times 10^7 \times DOC^{-3.23}$ | 0.88 (2.27×10^{-5}) | $GSD(K_{dSS DOC}) = 0.2 \times DOC^{0.91}$ | 0.07 |
| Ce | $GM(K_{dSS DOC}) = 1.18 \times 10^6 \times DOC^{-0.92}$ | 0.70 (1.25×10^{-17}) | $GSD(K_{dSS DOC}) = 3.0 \times DOC^{-0.20}$ | 0.15 |
| Co | $GM(K_{dSS DOC}) = 1.00 \times 10^4 \times DOC^{1.58}$ | 0.65 (1.74×10^{-5}) | $GSD(K_{dSS DOC}) = 0.003 \times DOC^{3.01}$ | 0.59 |
| Cr | $GM(K_{dSS DOC}) = 5.04 \times 10^7 \times DOC^{-3.08}$ | 0.84 (2.25×10^{-10}) | $GSD(K_{dSS DOC}) = 7471 \times DOC^{-3.93}$ | 0.77 |
| Cu | $GM(K_{dSS DOC}) = 2.68 \times 10^7 \times DOC^{-3.23}$ | 0.98 (1.50×10^{-16}) | $GSD(K_{dSS DOC}) = 93.0 \times DOC^{-1.75}$ | 0.49 |
| Fe | $GM(K_{dSS DOC}) = 3.69 \times 10^6 \times DOC^{-1.61}$ | 0.94 (9.73×10^{-66}) | $GSD(K_{dSS DOC}) = 3.5 \times DOC^{-0.26}$ | 0.42 |
| Hg | $GM(K_{dSS DOC}) = 1.76 \times 10^6 \times DOC^{-1.49}$ | 0.96 (1.13×10^{-56}) | $GSD(K_{dSS DOC}) = 4.2 \times DOC^{-0.18}$ | 0.26 |
| K | $GM(K_{dSS DOC}) = 1.00 \times 10^4 \times DOC^{-0.73}$ | 0.97 (4.11×10^{-46}) | $GSD(K_{dSS DOC}) = 2.3 \times DOC^{-0.06}$ | 0.07 |
| Mg | $GM(K_{dSS DOC}) = 2.00 \times 10^4 \times DOC^{-1.15}$ | 0.97 (1.50×10^{-16}) | $GSD(K_{dSS DOC}) = 3.8 \times DOC^{-0.32}$ | 0.56 |
| Mn | $GM(K_{dSS DOC}) = 9.27 \times 10^7 \times DOC^{-3.52}$ | 0.94 (9.10×10^{-16}) | $GSD(K_{dSS DOC}) = 2.2 \times DOC^{-0.05}$ | 0.08 |
| Pb | $GM(K_{dSS DOC}) = 8.30 \times 10^5 \times DOC^{-0.58}$ | 0.95 (1.14×10^{-32}) | $GSD(K_{dSS DOC}) = 2.7 \times DOC^{-0.14}$ | 0.43 |
| Si | $GM(K_{dSS DOC}) = 8.00 \times 10^4 \times DOC^{-0.67}$ | 0.73 (2.21×10^{-20}) | $GSD(K_{dSS DOC}) = 0.8 \times DOC^{0.59}$ | 0.861 |
| Zn | $GM(K_{dSS DOC}) = 5.47 \times 10^6 \times DOC^{-1.83}$ | 0.90 (1.70×10^{-21}) | $GSD(K_{dSS DOC}) = 4.5 \times DOC^{-0.25}$ | 0.45 |

* Adapted after Ref. [4.17], with permission.

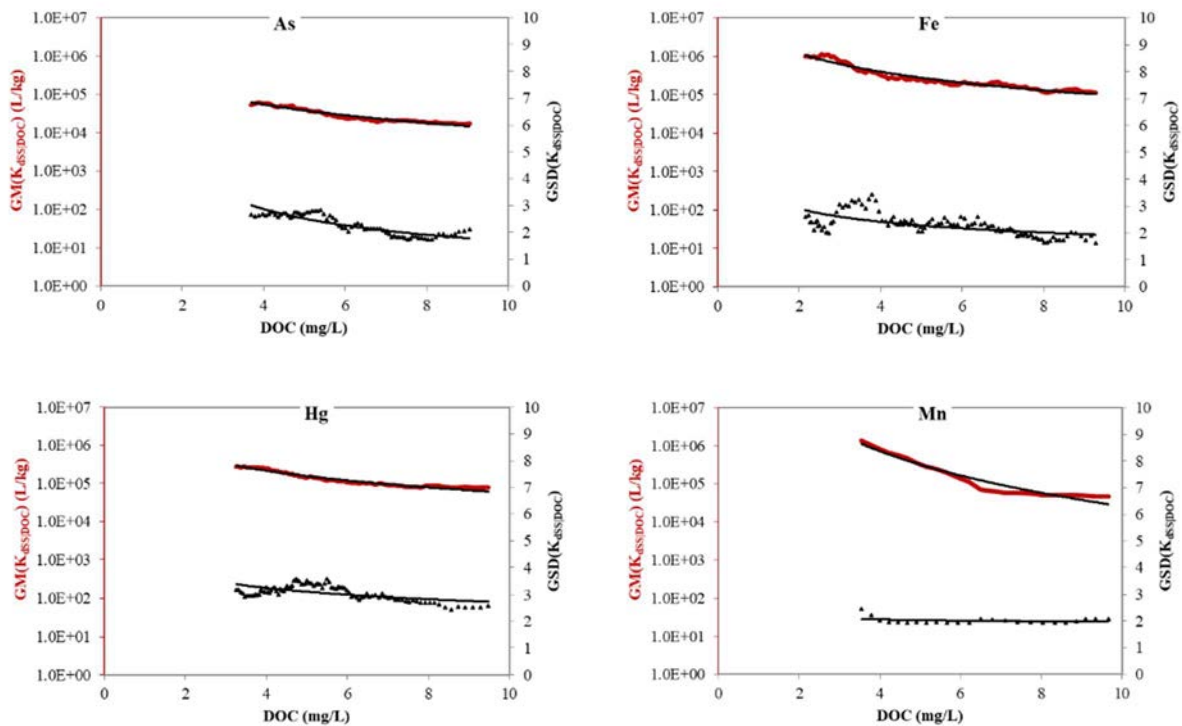


FIG. 4.8. $GM(K_{dSS|DOC})$ (Red) and $GSD(K_{dSS|DOC})$ (Black) in the field (adapted after [4.17], with permission).

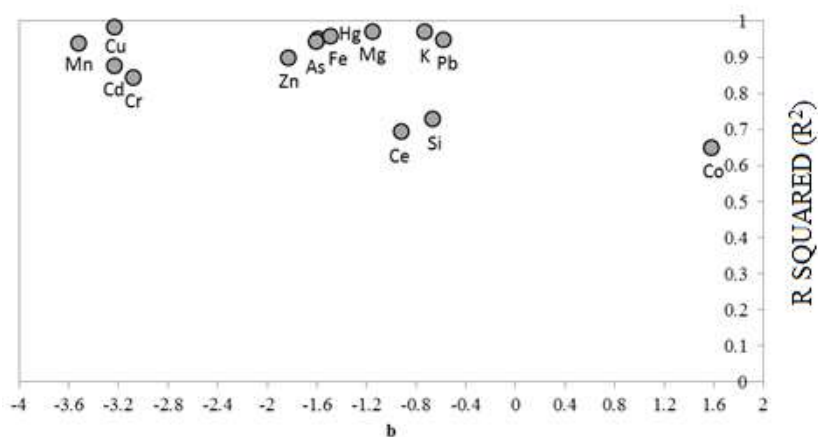


FIG. 4.9. R squared (R^2) of the equation $K_{dSS|DOC} = a \times DOC^b$, as a function of the parameter b (adapted after [4.17], with permission).

For the elements tabulated in Table 4.4, Fig. 4.9 presents the determination coefficient R^2 as a function of the slope b .

By assuming that an element is relatively more impacted by DOC, the more negative the slope b and the higher the coefficient R^2 are, Fig. 4.9 indicates that the most sensitive elements to DOC concentrations are Mn, Cu, Cd and Cr. This point has been previously demonstrated by several studies for Cu (see Refs [4.41–4.43]). Apte et al. [4.44] demonstrated the significance of Cu complexation by DOC by showing that dissolved Cu is predominantly present in the form of organic complexes in the Fly River, and Barreto et al. [4.45] evaluated the formation of DOC and Cd complexes in natural waters. These elements are, thus, easily associated to dissolve organic matter which directly controls their solid–liquid partitioning.

Elements that are less sensitive to the DOC concentrations are Co and Si. In particular, Co is the only element for which the slope b is positive for Si, the low impact of DOC concentrations impact is in accordance with the work of Veselý et al. [4.32]. Furthermore, the *in situ* K_{dSS} distributions of Si and Co are independent of both parameters, SS and DOC.

As for SS , taking into account the DOC concentration leads to a significant reduction of the *in situ* $GSD(K_{dSS})$ values. For example, the total $GSD(K_{dSS})$ for Mn changes from 7.1 (Table 4.4) to 2 by taking DOC concentrations into account, which represents a decrease in variability of more than four orders of magnitude.

4.3.1.4. Relationships between *in situ* K_{dSS} and pH

The *in situ* K_{dSS} values compiled in the database cover a range of pH values between 6.6 and 8.4, which highlights the low variability of pH in the water column of freshwater systems. Moreover, the amount of *in situ* K_{dSS} values which have associated pH values is insufficient to determine conditional log-normal distributions so it was only possible to investigate the mean tendencies without appropriate statistical representativeness. However, these tendencies suggested that the pH does not significantly affect the *in situ* K_{dSS} values, at least for a pH range from 6.4 to 9.3. For example, Fig. 4.10 presents the relevant data trends of $K_{dSS|pH}$ for Cd and Cr.

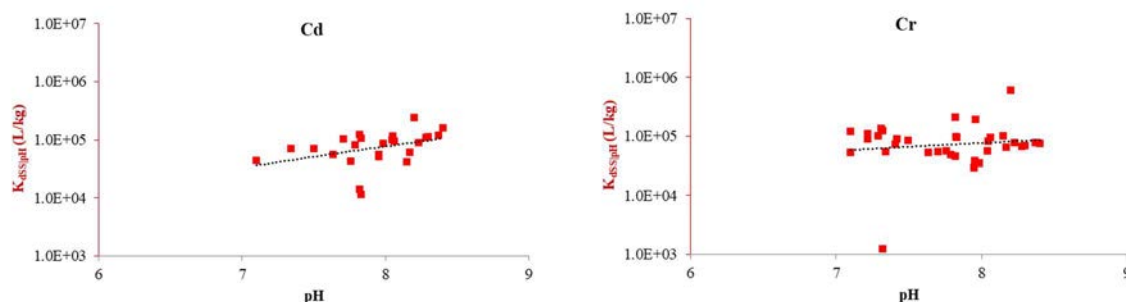


FIG. 4.10. $K_{dSS|pH}$ for Cd and Cr under *in situ* conditions as a function of pH (adapted after [4.17], with permission).

4.3.1.5. Conditional log-normal distributions of K_{dDS} as a function of pH

The compiled K_{dDS} data cover a larger range of pH values than for K_{dSS} (4–8) and they are quite numerous. The data coverage allowed the determination of conditional log-normal distributions of K_{dDS} according to pH for Am, Co, Cs and Zn in case of adsorption conditions and for As, Cr, Cu, Mn, Pb and Zn in case of *in situ* conditions. These distributions are defined by the changes as a function of pH of the conditional geometric means, $GM(K_{dSS|pH})$, and geometric standard deviations, $GSD(K_{dSS|pH})$, which are represented by the following power equations:

$$GM(K_{dSS|pH}) = a \times pH^b \quad (4.12)$$

$$GSD(K_{dSS|pH}) = c \times pH^d \quad (4.13)$$

Where the parameters a (L/kg)^{b+1} and c (L/kg) are scaling factors with values corresponding to $GM(K_{dSS|pH})$ and $GSD(K_{dSS|pH})$ when $pH = 1$. The exponents, b and d , describe the extent of the deviation of the adsorption process from linearity [4.31]. These relationships are summarized in Table 4.5 with their p -values and their determination coefficient R^2 which indicates the proportion of the variance explained by these equations.

These relationships are all statistically representative (p -value < 0.05) and strongly significant with determination coefficients (R^2) between 0.79 and 0.97. All slopes (b) are positive which demonstrates a systematic increase of K_{dDS} when the pH increases. This trend may be related to an effect of the pH on the adsorption capacities of solid surfaces. Under acidic conditions, metals form free ionic species and protons are fixed by the negatively charged surfaces, inducing a reduction of their sorption capacities. Adsorption increases with increasing pH due to the increase of negative surface charges [4.41] that facilitate the sorption of cations [4.32].

As an example, Fig. 4.11 presents the relationship of $K_{dSS|pH}$ for Co and Zn in the case of adsorption conditions.

For the elements tabulated in Table 4.5, Fig. 4.12 presents the coefficient R^2 as a function of the slope b .

TABLE 4.5. PARAMETERS a AND b AND ASSOCIATED R SQUARED (R^2) AND P-VALUE FOR THE RELATIONSHIPS $GM(K_{ads|pH}) = a \times pH^b$ and $GSD(K_{ads|pH}) = c \times pH^d$ *

| Element | Process exchange | $GM(K_{ads pH})$ | | $GSD(K_{ads pH})$ | |
|---------|------------------|--|------------------------------------|---|-------|
| | | Equation | R^2 (p-value) | Equation | R^2 |
| Am | adsorption | $GM(K_{ads pH}) = 8.25 \times 10^{-1} \times pH^{6.76}$ | 0.97 (3.92×10^{-15}) | $GSD(K_{ads pH}) = 10.87 \times pH^{-0.88}$ | 0.54 |
| As | <i>in situ</i> | $GM(K_{ads pH}) = 5.88 \times 10^2 \times pH^{1.41}$ | 0.61 (3.77×10^{-3}) | $GSD(K_{ads pH}) = 1.60 \times pH^{0.09}$ | 0.04 |
| Co | adsorption | $GM(K_{ads pH}) = 2.00 \times 10^{-8} \times pH^{13.14}$ | 0.95 (3.11×10^{-30}) | $GSD(K_{ads pH}) = 4.00 \times pH^{-0.05}$ | 0.02 |
| Cr | <i>in situ</i> | $GM(K_{ads pH}) = 1.00 \times 10^{-3} \times pH^{9.16}$ | 0.95 (1.60×10^{-7}) | $GSD(K_{ads pH}) = 2.52 \times pH^{-0.16}$ | 0.01 |
| Cs | adsorption | $GM(K_{ads pH}) = 2.12 \times 10^3 \times pH^{0.66}$ | 0.85 (2.18×10^{-20}) | $GSD(K_{ads pH}) = 5.39 \times pH^{-0.27}$ | 0.57 |
| Cu | <i>in situ</i> | $GM(K_{ads pH}) = 2.13 \times 10^{-2} \times pH^{7.72}$ | 0.88 (9.67×10^{-20}) | $GSD(K_{ads pH}) = 1.45 \times pH^{0.17}$ | 0.04 |
| Mn | <i>in situ</i> | $GM(K_{ads pH}) = 7.20 \times 10^1 \times pH^{4.55}$ | 0.95 (5.45×10^{-5}) | $GSD(K_{ads pH}) = 6.75 \times pH^{0.05}$ | 0.22 |
| Pb | <i>in situ</i> | $GM(K_{ads pH}) = 1.20 \times 10^{-3} \times pH^{9.39}$ | 0.96 (2.68×10^{-8}) | $GSD(K_{ads pH}) = 0.94 \times pH^{0.31}$ | 0.15 |
| Zn | adsorption | $GM(K_{ads pH}) = 3.00 \times 10^{-4} \times pH^{10.32}$ | 0.79 (1.31×10^{-53}) | $GSD(K_{ads pH}) = 3.41 \times pH^{-0.17}$ | 0.13 |
| | <i>in situ</i> | $GM(K_{ads pH}) = 8.00 \times 10^{-4} \times pH^{9.61}$ | 0.97 (4.54×10^{-12}) | $GSD(K_{ads pH}) = 4.69 \times pH^{-0.45}$ | 0.04 |

* Adapted after [4.17], with permission.

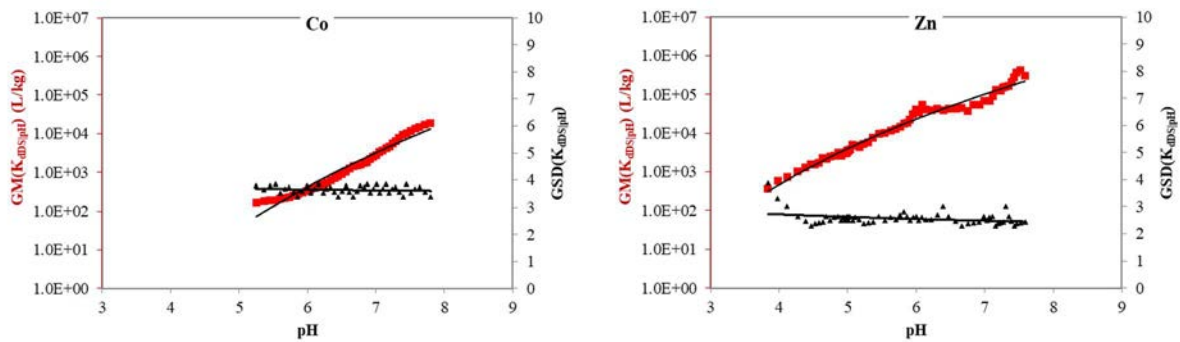


FIG. 4.11. $GM(K_{ads|pH})$ (red) and $GSD(K_{ads|pH})$ (black) in case of adsorption conditions (adapted after [4.17], with permission).

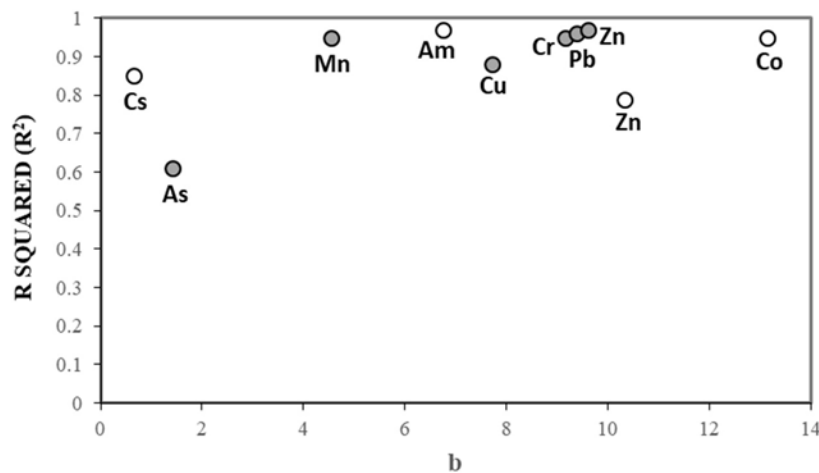


FIG. 4.12. R squared (R^2) of the equation $K_{ads|pH} = a \times pH^b$, as a function of the parameter b (white for adsorption and gray for *in situ*) (adapted after [4.17], with permission).

By assuming that an element is more impacted by pH when the slope b is lower and the coefficient R^2 is higher, Fig. 4.12 indicates that the elements most sensitive to pH are Co, Zn, Pb and Cr whereas K_{dDS} for Cs and As are the least sensitive to pH. This is in agreement with previous publications for Pb, Co and Zn [4.32, 4.46–4.49], but not for Cr [4.50] which highlights that these relationships need to be applied with caution and that the use of local data remains the best choice.

The relationships for $GM(K_{dDS|pH})$ significantly reduced the variability. For example, total $GSD(K_d)$ for Co decreased from 9.4 (Table 4.5) to 3.5 when pH was considered (Fig. 4.11), which reduced the variability of its distribution by over five orders of magnitude.

4.4. CONCLUSIONS FROM ANALYSIS OF THE FRESHWATER K_d DATASET

A brief overview of K_d compilations for freshwater systems showed that 65% of the K_d values for the chemical elements considered in TRS 472 [4.11] were based on a single value or had not been based on measured data (see Fig. 4.3). In this context, the collaborative synthesis of K_d data within MODARIA WG4 has considerably improved the datasets that were previously used to determine freshwater K_d values in TRS 472 [4.11]. Over 3300 K_d values have been compiled for 29 new elements including 1807 new K_d values that were added to the dataset for the 25 elements that were already included in TRS 472 [4.11]. By the end of MODARIA, the freshwater K_d database contained 8564 K_d values for 54 elements.

Inclusion and analysis of the impact of various environmental components provided a new and improved level of information compared with previous IAEA reports. MODARIA WG4 has reported log-normal distributions of K_d values as a function of three conditions of measurement, namely sorption, desorption and *in situ*, and of two environmental components, namely suspended sediments and deposited sediments. For a large majority of elements, derived *in situ* K_d values for suspended sediments were two orders of magnitude higher than for deposited sediments, mainly because particles in deposited sediments tend to be coarser than in suspended sediments.

For the elements sufficiently informed by data, the database enabled determination of conditional log-normal distributions of *in situ* K_d of suspended particles as a function of suspended loads and dissolved organic carbon and of K_d of deposited sediments as a function of pH [4.17]. For most elements these conditional distributions reduced the variability of global K_d distributions by several orders of magnitude. The conditional distributions are useful for decreasing the uncertainties in the prediction of the mobility of elements in freshwater systems when the K_d approach is applied and *in situ* data are not available.

REFERENCES TO CHAPTER 4

- [4.1] LI, Y.-H., BURKHARDT, L., BUCHHOLTZ, M., O'HARA, P., SANTSHI, P.H., Partitioning of radiotracers between suspended particles and sea water, *Geochim. Cosmochim. Acta* **48** (1984) 2011.
[https://doi.org/10.1016/0016-7037\(84\)90382-X](https://doi.org/10.1016/0016-7037(84)90382-X)
- [4.2] HONEYMAN, B.D., SANTSHI, P.H. Critical review: Metals in aquatic systems. Predicting their scavenging residence times from laboratory data remains a challenge, *Environ. Sci. Technol.* **22** (1988) 862.
<https://doi.org/10.1021/es00173a002>

- [4.3] BOUDREAU, P.B., Diagenetic models and their implementation. Modelling transport and reactions in aquatic sediments. Springer (1997) 414.
- [4.4] BOYER, P., WELLS, C., HOWARD, B., Extended K_d distributions for freshwater environment, *J. Environ. Radioact.* **192** (2018) 128.
<https://doi.org/10.1016/j.jenvrad.2018.06.006>
- [4.5] ABRIL, J. M., FRAGA, E., Some physical and chemical features of the variability of K_d distribution coefficients for radionuclides, *J. Environ. Radioact.* **30** (1996) 253. [https://doi.org/10.1016/0265-931X\(95\)00010-8](https://doi.org/10.1016/0265-931X(95)00010-8)
- [4.6] CAZABAT, A.M., VEYSSIE, M., Colloïdes et interfaces, École d'été, Aussois, France, 6-17 septembre 1983. Editions de Physique, Paris (1984) (in French).
- [4.7] INTERNATIONAL ATOMIC ENERGY AGENCY, Handbook of Parameter Values for the Prediction of Radionuclide Transfer in Temperate Environments, Technical Reports Series No. 364, IAEA, Vienna (1994).
- [4.8] INTERNATIONAL ATOMIC ENERGY AGENCY, Generic Models for use in Assessing the impact of discharges of radioactive substances to the environment, Safety Reports Series No. 19, IAEA, Vienna (2001).
- [4.9] DURRIEU, G., CIFFROY, P., GARNIER, J.M., A weighted bootstrap method for the determination of probability density functions of freshwater distribution coefficients (K_d s) of Co, Cs, Sr and I radioisotopes, *Chemosphere* **65** (2006) 1308.
<https://doi.org/10.1016/j.chemosphere.2006.04.028>
- [4.10] CIFFROY, P., DURRIEU, G., GARNIER, J.-M., Probabilistic distribution coefficients (K_d s) in freshwater for radioisotopes of Ag, Am, Ba, Be, Ce, Co, Cs, I, Mn, Pu Ra, Ru, Sb, Sr and Th. – Implications for uncertainty analysis of models simulating the transport of radionuclides in rivers, *J. Environ. Radioact.* **100** (2009) 785. <https://doi.org/10.1016/j.jenvrad.2008.10.019>
- [4.11] INTERNATIONAL ATOMIC ENERGY AGENCY, Handbook of Parameter Values for the Prediction of Radionuclide Transfer in Terrestrial and Freshwater Environment, Technical Reports Series No. 472, IAEA, Vienna (2010).
- [4.12] INTERNATIONAL ATOMIC ENERGY AGENCY, Quantification of Radionuclide Transfers in Terrestrial and Freshwater Environments for Radiological Assessments, IAEA-TECDOC-1616, IAEA, Vienna (2009).
- [4.13] ONISHI, Y., SERNE, R.J., ARNOLD, E.M., COWEN, C.E., THOMPSON, F.L., Critical review: Radionuclide transport, sediment transport, and water quality mathematical modelling and radionuclide adsorption/desorption mechanisms, Rep. NUREG/CR-1322, PNL-2901, Pacific Northwest Lab., Richmond, WA (1981). DOI: [10.2172/10125120](https://doi.org/10.2172/10125120)
- [4.14] BROWN, J.E., et al., The ERICA Tool, *J. Environ. Radioact.* **99** (2008) 1371.
<https://doi.org/10.1016/j.jenvrad.2008.01.008>
- [4.15] GONZE, M.A et al., SYMBIOSE: a simulation platform for conducting radiological risk assessments. International Conference on Radioecology and Environmental Radioactivity (ICRER), 19–24 June 2011, Hamilton, Ontario, Canada (2011).
- [4.16] SIMON-CORNU, M., et al., Evaluating variability and uncertainty in radiological impact assessment using SYMBIOSE, *J. Environ. Radioact.* **139** (2015) 91.
<https://doi.org/10.1016/j.jenvrad.2014.09.014>

- [4.17] TOMCZAK, W., BOYER, P., KRIMISSA, M., RADAKOVITCH, O., K_d distributions in freshwater systems as a function of material type, mass- volume ratio, dissolved organic carbon and pH, *Appl. Geochem.* **105** (2019) 68. <https://doi.org/10.1016/j.apgeochem.2019.04.003>
- [4.18] ALLISON, J.D., ALLISON T.L., Partition coefficient for metals in surface water, soil, and waste, EPA/600/R-05/074 Washington, DC, United States (2005). https://cfpub.epa.gov/si/si_public_record_report.cfm?dirEntryId=135783&Lab=NERL
- [4.19] SHEPPARD, S.C. Robust Prediction of K_d from Soil Properties for Environmental Assessment, *Human and Ecological Risk Assessment: An International Journal* **17** (2011) 263. <https://doi.org/10.1080/10807039.2011.538641>
- [4.20] HENRICHS, S.M., Early diagenesis of organic matter in marine sediments: progress and perplexity, *Mar. Chem.* **39** (1992) 119. [https://doi.org/10.1016/0304-4203\(92\)90098-U](https://doi.org/10.1016/0304-4203(92)90098-U)
- [4.21] ZHANG, Y., KAISER, K., LI, L., ZHANG, D., RAN, Y., BENNER, R., Sources, distributions, and early diagenesis of sedimentary organic matter in the Pearl River region of the South China, Sea. *Mar. Chem.* **158** (2014) 39. <https://doi.org/10.1016/j.marchem.2013.11.003>
- [4.22] HONEYMAN, B.D., SANTOSCHI, P.H., Metals in aquatic systems, *Environ. Sci. Technol.* **22** (1988) 862. <https://doi.org/10.1021/es00173a002>
- [4.23] BENOIT, G., et al., Partitioning of Cu, Pb, Ag, Zn, Fe, Al, and Mn between filter-retained particles, colloids, and solution in six Texas estuaries, *Mar. Chem.* **45** (1994) 307. [https://doi.org/10.1016/0304-4203\(94\)90076-0](https://doi.org/10.1016/0304-4203(94)90076-0)
- [4.24] EYROLLE-BOYER, F., et al., Behaviour of radiocaesium in coastal rivers of the Fukushima Prefecture (Japan) during conditions of low flow and low turbidity - insight on the possible role of small particles and detrital organic compounds, *J. Environ. Radioact.* **151** (2016) 328. <https://doi.org/10.1016/j.jenvrad.2015.10.028>
- [4.25] MÜLLER, G., FÖRSTNER, U., General relationship between suspended sediment concentration and water discharge in the Alpenrhein and other rivers, *Nature* **217** (1968) 244. <https://doi.org/10.1038/217244a0>
- [4.26] MEHTA, A.J., An introduction to hydraulics of fine sediment transport, New Jersey World Scientific. *Adv. Ser. Ocean Eng.* **38** (2014) 1039p. <https://doi.org/10.1142/8708>
- [4.27] WALLING, D.E., OWENS, P.N., WATERFALL, B.D., LEEKS, G.J.L., WASS, P.D., The particle size characteristics of fluvial suspended sediment in the Humber and Tweed catchments, UK, *Sci. Total Environ.* **251/252** (2000) 205. DOI: [10.1016/S0048-9697\(00\)00384-3](https://doi.org/10.1016/S0048-9697(00)00384-3)
- [4.28] ABRIL, J.M., FRAGA, E., Some physical and chemical features of the variability of K_d distribution coefficients for radionuclides, *J. Environ. Radioact.* **30** 3 (1996) 253. [https://doi.org/10.1016/0265-931X\(95\)00010-8](https://doi.org/10.1016/0265-931X(95)00010-8)
- [4.29] LI, Y.-H., BURKHARDT, L., BUCHHOLTZ, M., O'HARA, P., SANTOSCHI, P.H., Partitioning of radiotracers between suspended particles and sea water, *Geochim. Cosmochim. Acta* **48** (1984) 2011. [https://doi.org/10.1016/0016-7037\(84\)90382-X](https://doi.org/10.1016/0016-7037(84)90382-X)

- [4.30] BENOIT, G., ROZAN, T.F., The influence of size distribution on the particle concentration effect and trace metal partitioning in rivers, *Geochem. Cosmochim. Acta* **63** 1 (1999) 113. [https://doi.org/10.1016/S0016-7037\(98\)00276-2](https://doi.org/10.1016/S0016-7037(98)00276-2)
- [4.31] HE, Q., WALLING, D.E., Interpreting particle size effects in the adsorption of unsupported ^{210}Pb by mineral soils and sediments, *J. Environ. Radioact.* **30** 2 (1996) 117. [https://doi.org/10.1016/0265-931X\(96\)89275-7](https://doi.org/10.1016/0265-931X(96)89275-7)
- [4.32] VESELÝ, J., MAJER, V., KUČERA, J., HAVRÁNEK, V., Solid-water partitioning of elements in Czech freshwaters, *Appl. Geochem.* **16** (2001) 437. [https://doi.org/10.1016/S0883-2927\(00\)00041-X](https://doi.org/10.1016/S0883-2927(00)00041-X)
- [4.33] PETTINE, M., et al., Soluble and particulate metals in the Po River: factors affecting concentrations and partitioning, *Sci. Total Environ.* **145** (1994) 243. [https://doi.org/10.1016/0048-9697\(94\)90118-X](https://doi.org/10.1016/0048-9697(94)90118-X)
- [4.34] KÖRDEL, W., DASSENAKIS, M., LINTELMANN, J., PADBERG, S., The importance of natural organic material for environmental processes in waters and soils (Technical Report), *Pure Appl. Chem.* **69** 7 (1992) 1571. <https://doi.org/10.1351/pac199769071571>
- [4.35] TOWN, R.M., FILELLA, M., Size fractionation of trace metal species in freshwaters: implications for understanding their behaviour and fate, *Rev. Environ. Sci. Biotechnol.* **1** 4 (2002) 277. <https://doi.org/10.1023/A:1023229825984>
- [4.36] SAUVE, S., HENDERSHOT, W.H., ALLEN, H.E., Solid-solution partitioning of metals in contaminated soils: dependence on pH, total metal burden, and organic matter, *Environ. Sci. Technol.* **34** 7 (2000) 1125. <https://doi.org/10.1021/es9907764>
- [4.37] SIGG, L., XUE, H., KISTLER, D., SCHÖNENBERGER, R., Size fractionation (dissolved, colloidal and particulate) of trace metals in the Thur River, Switzerland, *Aquat. Geochem.* **6** (2000) 413. <https://doi.org/10.1023/A:1009692919804>
- [4.38] AIKEN, G.R., HSU-KIM, H., RYAN, J.N., Influence of dissolved organic matter on the environmental fate of metals, nanoparticles, and colloids, *Environ. Sci. Technol.* **45** 8 (2011) 3196. <https://doi.org/10.1021/es103992s>
- [4.39] TAKATA, H., AONO, T., TAGAMI, K., UCHIDA, S., Influence of dissolved organic matter on particle-water interactions of Co, Cu and Cd under estuarine conditions, *Estuar. Coast Shelf Sci.* **111** (2012) 75. <https://doi.org/10.1016/j.ecss.2012.06.014>
- [4.40] SIGG, L., BEHRA, P., STUMM, W., *Chimie des milieux aquatiques*, Dunod (2014) 497p. <https://doi.org/10.3917/dunod.sigg.2014.01.0000d>
- [4.41] SHI, B., ALLEN, H.E., GRASSI, M.T., MA, H., Modeling copper partitioning in surface waters, *Water Res.* **32**(12) (1998) 3756. [https://doi.org/10.1016/S0043-1354\(98\)00162-6](https://doi.org/10.1016/S0043-1354(98)00162-6)
- [4.42] SHAFER, M.M., et al., Trace metal levels partitioning in Wisconsin rivers, *Water Air Soil Pollut.* **110** (1999) 273. <https://doi.org/10.1023/A:1005019521097>
- [4.43] LU, Y., ALLEN, H.E., Partitioning of copper onto suspended particulate matter in river waters, *Sci. Total Environ.* **277** (2001) 119. [https://doi.org/10.1016/S0048-9697\(00\)00868-8](https://doi.org/10.1016/S0048-9697(00)00868-8)

- [4.44] APTE, S.C., BENKO, W.I., DAY, G.M., Partitioning and complexation of copper in the Fly River, Papua New Guinea, *J. Geochem. Explor.* **52**(1–2) (1995) 67. [https://doi.org/10.1016/0375-6742\(94\)00031-6](https://doi.org/10.1016/0375-6742(94)00031-6)
- [4.45] BARRETO, S.R.G., BARRETO, W.J., DEDUCH, E.M., Determination of partition coefficients of metals in natural tropical water, *Clean. - Soil, Air, Water* **39**(4) (2011) 362. <https://doi.org/10.1002/clen.201000271>
- [4.46] WHITE, J.R., DRISCOLL, C.T., Zinc cycling in an acidic Adirondack lake, *Environ. Sci. Technol.* **21** (1987) 211. <https://doi.org/10.1021/es00156a014>
- [4.47] TESSIER, A., CARIGNAN, R., DUBREUIL, B., RAPIN, F., Partitioning of zinc between the water column and the oxic sediments in lakes. *Geochem. Cosmochim. Acta* **53** (7) (1989) 1511. [https://doi.org/10.1016/0016-7037\(89\)90234-2](https://doi.org/10.1016/0016-7037(89)90234-2)
- [4.48] ALKHATIB, E.A., CHABOT, T., GRUNZKE, D., Prediction of metal remobilization from sediments under various physical/chemical conditions “Design of experiments Cd, Co and Pb”. *J. Hydrogeol Hydrol. Eng.* **5** (2) (2016). <https://doi.org/10.4172/2325-9647.1000135>
- [4.49] ALKHATIB, E.A., GRUNZKE, D., CHABOT, T., Multi-regression prediction of metal partition coefficients under various physical/chemical conditions design of experiments As, Cr, Cu, Ni and Zn, *Hydrol. Curr. Res.* **7** (2016) 241. DOI: [10.4172/2157-7587.1000241](https://doi.org/10.4172/2157-7587.1000241)
- [4.50] PENG, S.-H., WANG, W.-X., CHEN, J., Partitioning of trace metals in suspended sediments from Huanghe and Changjiang rivers in Eastern China, *Water Air Soil Pollut.* **148** (2003) 243. <https://doi.org/10.1023/A:1025445709276>

5. MARINE K_d DATASET

KEVIN KELLEHER

Environmental Protection Agency, IRELAND

MASASHI KUSAKABE

Marine Ecology Research Institute, JAPAN

HYOE TAKATA

Fukushima University, JAPAN

KEIKO TAGAMI, SHIGEO UCHIDA

National Institutes for Quantum Science and Technology, JAPAN

PAUL MCGINNITY

International Atomic Energy Agency

IAEA TRS 422 [5.1] is a primary source of coastal marine (ocean margin) and open ocean K_d values for use in REIA in the marine environment. TRS 422 does not consider other factors that could influence the variability of K_d in the marine environment and the use of the default values provided is only recommended in the absence of site specific data. Therefore, additional sources of marine datasets were reviewed with the intent of obtaining site specific K_d values in conjunction with ancillary data that could include factors that can influence the behaviour of radionuclides in the environment.

A preliminary investigation of the IAEA's MARIS database⁷ found that it contained sufficient information that could be used to derive site specific *in situ* $K_{d(a)}$ (described in detail in Chapter 2, Section 2.1.2.3). A summary of the Cs $K_{d(a)}$ derived from the dataset in MARIS has provided an important source of new K_d data and is described in this chapter.

Various recent studies on marine K_d values in Japan, before and after the accident at the FDNPP in March 2011, are also summarized in this chapter and also in Annex V. After the accident at the FDNPP, a large proportion of the atmospheric and liquid releases were deposited onto Japanese coastal waters of the Pacific Ocean. The fate of radiocaesium in the marine environment has been, and remains, of interest to the public and to fishing community in the affected regions. The ability of suspended and deposited sediment to bind and retain radiocaesium, thereby reducing radiocaesium activity concentrations in sea water and marine organisms, is a key environmental process that needs to be understood and quantified.

5.1. PREVIOUSLY AVAILABLE INFORMATION ON MARINE K_d DATA

This section describes some key features influencing K_d values in marine systems and gives a summary of information from IAEA TRS 422 [5.1], which focuses on K_d and CR (Concentration Ratio) in the marine environment.

Overall, the physicochemistry of deep marine systems tends to be more uniform than that of freshwater systems [5.2]. The properties of the coastal marine (or ocean margin) systems tend to fall in between those of the open ocean and freshwater systems. Some of the key sediment and water associated factors affecting radionuclide K_d values are salinity, pH, DOC, suspended

⁷ IAEA's MARIS database can be accessed at: <https://maris.iaea.org/>.

load and sediment composition [5.3]. Salinity impacts K_d values because it increases concentrations of cations and anions that can compete with radionuclides for sorption sites on the sediments. Salinity is at its highest in the deep sea and does not vary much between different oceans, with a typical value of 3.6 g/kg [5.4]. In contrast, salinity decreases in coastal areas and is much lower in freshwater systems. Similarly, pH values in the deep ocean generally vary over a small range of 8.0 to 8.5, whereas in continental systems pH values commonly have a much wider range of about 4 to 9. As DOC originates from the decomposition of microorganisms, plants, and animals, measured values of DOC are relatively low in most marine systems, especially the open ocean. There is also less heterogeneity in sediment properties, such as particle size and mineralogical characteristics in open ocean systems compared with freshwater systems, which tend to have much higher DOC levels than those of marine systems. Marine coastal areas have higher DOC values than the open ocean due to inputs from catchments. Various trends that indicate the influence of sedimentary particles and water chemistry on K_d values are evident in coastal areas [5.5]:

- (1) Similar to freshwater ecosystems, K_d values in marine coastal areas increase directly with surface area to volume ratios of particles and inversely with particle size. This is because finer grains have a higher surface area to volume ratios compared with coarser particles, so there are more binding sites per unit mass for elements to bind to;
- (2) K_d values increase with increasing organic content of particles.

Therefore, muddy or fine grained, organic rich sediments have higher K_d values than sandy, organic poor sediments.

For water, the trends are that:

- (1) K_d values are usually higher in fresh water than in sea water (all other things being equal), due to more competing ions in sea water;
- (2) K_d values for radionuclides binding to marine sediments decrease as DOC concentrations increase, due to the dissolved organic matter complexing the dissolved elements, reducing the tendency for the elements to bind to particle surfaces – examples are given for Cu, Cd and Pb in Refs [5.6, 5.7].

The redox status of marine sediments can vary greatly depending on the underlying geological formation, height of overlying water, proximity to the coastline, currents, and inputs from estuarine waters [5.8]. Redox conditions and changes in other characteristics, such as particle size and colloidal complexes, are key factors that control K_d values of sediments. Such redox changes can lead to radionuclide mobilization from sediment, releasing some radionuclides to overlying waters, which may then become bioavailable to organisms in the water column. For example, U and Tc become more mobile under oxidizing conditions, whereas iodine becomes more mobile under reducing conditions [5.9, 5.10].

5.1.1. The derivation of K_d values in TRS 422

IAEA TRS 247 [5.2] originally provided K_d values in the context of the past practices that were carried out at that time, many of which involved the disposal of liquid and solid radioactive waste in marine systems (dumping practices). Such disposal practices have largely ceased, or considerably decreased, after 1983. However, in 1993, the Russian Federation has disclosed information on sea disposal in the Kara Sea, Barents Sea and Sea of Japan [5.11], various seas were contaminated by the accident at the Chornobyl NPP in 1986 and the importance of NORM in the oceans from sources, such as phosphate processing, and offshore oil and gas installations, has been recognized [5.12–5.15]. Subsequently, TRS 422 [5.1] provided sediment K_d values

for the open ocean and ocean margins, taking account of new data and retaining the same generic methodology for K_d estimation as TRS 247 [5.2]. In TRS 422 [5.1], K_d values for 63 elements were reported.

There were three key assumptions underlying the assignment of K_d values in TRS 422 [5.1]:

- (1) Radionuclide equilibrium is established between dissolved and particulate phases;
- (2) Radionuclide exchange is wholly reversible between water and particles;
- (3) Radionuclide exchange is instantaneous between water and particles.

However, these three simplifying assumptions for marine sediment K_d data are rather simplistic compared with the approach currently adopted for soils and fresh water, as outlined in Chapters 3 and 4, respectively. For example, the following observations of radionuclide geochemistry have been reported [5.16]:

- (1) Adsorption is not fully reversible;
- (2) Adsorption can be faster than desorption;
- (3) Adsorption can involve biogenic processes;
- (4) Solid partition involves some irreversible processes;
- (5) Desorption involves dissolution of carrier phases;
- (6) Reaching steady state depends on particle characteristics.

The K_d model assumes that equilibrium and wholly reversible exchange of elements exists between dissolved and particulate phases (see Chapter 2, Section 2.1.1) but this is not the case for most elements. In aquatic systems, part of the matrix of sediment particles is not exchangeable between dissolved and particulate phases and cannot desorb into overlying and or pore waters.

To account for partial desorption, the approach adopted in both TRS 247 [5.2] and TRS 422 [5.1] was that the non-exchangeable fraction of an element, which would not desorb, was not considered in K_d calculations. This was accounted for by adopting correction factors. For each element, the exchangeable fraction $[E]_{\text{exch}}$ was estimated using one of three approaches, all of which tend to overestimate the K_d value:

- (1) The ‘pelagic clay enrichment’ method in relation to source rock was used to subtract the mean concentration in shale from the concentration in the solid phase (e.g. suspended solids or sediment) of the sample. Then the corrected concentrations in the solid phase were divided by dissolved deposited water concentration (mean of Atlantic and Pacific). The difference between shale and sediment concentrations of an element was assumed to represent the exchangeable fraction of an element that was introduced to, and adsorbed onto, sediment.
- (2) Where no pelagic clay enrichment was indicated, the concentration of the exchangeable fractions was assumed to be equal to 10% of the pelagic clay concentration for open water and 20% for ocean margin. For open water K_d values, the elemental concentrations in water (the denominator of the calculated K_d value) were considered relative to marine water chemistry (e.g. DOC), and for ocean margin K_d values, the concentrations per unit mass of sea water were used.
- (3) The exchangeable fraction of the solid phase of a given sample for Ca, Ba, Sr, Ra, and U was assumed to be equal to the concentration in calcareous pelagic sediment.

The K_d values recommended in TRS 422 [5.1] may be underestimated in some cases since they were mainly determined based on the distribution of stable elements between bottom sediments and the adjacent water layer. The approach used in TRS 422 [5.1] does not adequately reflect *in situ* behaviour of radionuclides because it assumes that:

- (1) The basic physical and chemical properties of radionuclides are similar to those of their stable isotopes. However, this is not always the case. Furthermore, for radionuclides discharged into the marine environment, it can take some time for these radionuclides to reach equilibrium between the bottom sediments and adjacent water layer, especially in the early phase after the release (see Section 5.2.2.1 below);
- (2) The proportion of the exchangeable fraction is fixed at the same value for all elements in TRS 422 [5.1], but recent results indicate that this assumption is not always valid (this issue will be discussed in greater detail below in Section 5.2.1 below);
- (3) The extent of radionuclide adsorption to deposited sediments and suspended sediments is similar. The differences in these two sediment types have been discussed in Chapter 4, Section 4.1.1 on freshwater K_d .

5.1.2. Impact of different factors on changes in water–sediment interaction of radionuclides with time

In dose assessment models for humans and other organisms in marine systems, a single fixed K_d value for each radionuclide is usually used to estimate transfer between sediment and water, and subsequent radionuclide transfer to marine organisms. However, this does not accurately reflect the variability of the partitioning of the radionuclide as a result of dynamic inputs into the marine systems [5.17, 5.18].

To evaluate the impact of factors related to K_d and marine sediments, Iosjpe [5.19] conducted kinetic modelling using a compartment model of the transfer of radionuclides between water and sediment. Sensitivity analyses carried out for ^3H , ^{137}Cs , ^{238}Pu , ^{241}Am , and ^{244}Cm were used to identify the parameters controlling water–sediment interactions in a coastal zone.

For all radionuclides except ^3H , particle mixing dominated the transfer of radionuclides between the bottom water and surface sediment compartments under the prevailing conditions in the Norwegian Sea. However, similar calculations under different environmental conditions produced different results. For example, different values for the suspended sediment load and sedimentation rates affected the outcome. Therefore, use of appropriate parameter values for these processes is important to improve future estimation of the fate of radionuclides in marine environments. Complexities were encountered when modelling water–sediment interactions; for instance, the activity concentrations of radionuclides in bottom water and sediment can vary strongly with time.

Thus, provision of site specific parameter values not only for K_d , but also for sedimentation rates and mixing rates, are important to estimate radionuclide activity concentrations in sediments and water. Additional information is necessary to provide more appropriate K_d values, and a revision of K_d information given in TRS 422 [5.1] might be warranted.

5.2. MARINE K_d DATA FROM THE COASTAL AREAS OF JAPAN

5.2.1. Consideration of the impact of the exchangeable phase of elements in sediment on marine K_d

TRS 422 [5.1] assumes that the exchangeable fraction of elements in the marine environment represents 10% of the total fraction for the open ocean and 20% for the ocean margin. Therefore, to calculate the relevant K_d of a radionuclide, the use of Eq. (5.1) is given for the ocean margin in TRS 422 [5.1]:

$$K_d(\text{L/kg}) = \frac{\text{Concentration per unit mass of sediment } \left(\frac{\text{g}}{\text{kg}}\right) \times 0.2}{\text{Concentration per unit mass of seawater } \left(\frac{\text{g}}{\text{L}}\right)} \quad (5.1)$$

In Eq. (5.1), it was assumed that “for all elements except carbon, 20% of the total concentration of the elements in pelitic coastal sediments (clays and silts) represents the exchangeable phase components of the elements.” [5.1]

To evaluate the validity of the equation, the ratios of the exchangeable fractions of global fallout ^{137}Cs and ^{90}Sr in the sediment were estimated using $K_{d(a)}$ values calculated using both global fallout data and stable Cs and Sr data from Japanese coastal areas [5.20].

Concentration data for global fallout of ^{137}Cs and ^{90}Sr in coastal sediment and sea water were collected between 1984 and 2010 (see details in Section 5.2.2). In this analysis, the factor of 0.2 (i.e. 20%) was not applied, as these are not stable elements. Instead, $K_{d(a)}$ values were simply calculated as the concentration ratios between sediment (Bq/kg DM) and sea water (Bq/L).

Stable Cs and Sr data for sediment and sea water samples in Japanese coastal regions collected in 2007–2012 were used to generate sediment–sea water $K_{d(a)}$ values (full results are reported in Section 5.2.2). The calculated stable marine $K_{d(a)}$ values in Japanese coastal regions agreed well with the recommended ocean margin $K_{d(a)}$ values given in TRS 422 [5.1], but this was not the case for the radioisotopes (Fig. 5.1).

Ref [5.21] reported mean $K_{d(a)}$ values for ^{85}Sr (35 and 135 L/kg) and ^{134}Cs (145 and 195 L/kg) for bottom sediments at two different sites. In another study, $K_{d(a)}$ values of 1.8 L/kg for ^{85}Sr and 140–400 L/kg for ^{134}Cs were reported [5.22]. Other $K_{d(a)}$ values for ^{90}Sr and ^{137}Cs for bottom sediments reported in Japan were similar to these values. The $K_{d(a)}$ value of ^{90}Sr in global fallout was one order of magnitude higher than that for stable Sr. Conversely, the ^{137}Cs value in global fallout was one order of magnitude lower than that for stable Cs (Fig. 5.1).

The variability of the $K_{d(a)}$ values for Sr and Cs in sandy and muddy sediments have been compared over the range of exchangeable phase values between 1.0 (wholly exchangeable) and 0.1 (10% exchangeable) (Fig. 5.1). $K_{d(a)}$ values for sandy and muddy sediments have been plotted together with those calculated using all the data combined to determine whether there were differences in $K_{d(a)}$ values of Sr and Cs for different sediment types. The sediment portion that was finer than 63 μm was classified as silt + clay, and the remaining portion that was larger than 63 μm was classified as sand. A ratio of (silt + clay)/(sand + silt + clay) was used to categorize sediments into muddy (>0.5) and sandy (<0.5).

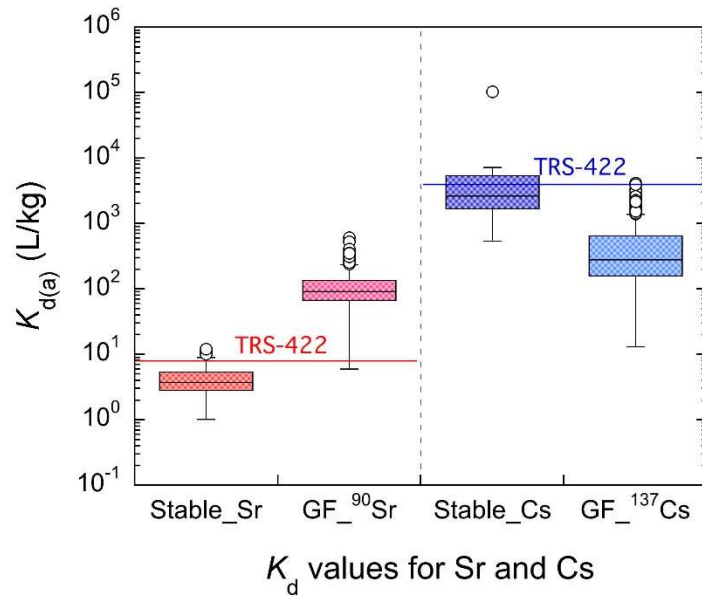


FIG. 5.1. Comparison of $K_{d(a)}$ values obtained by field observations of stable element and global fallout (GF) in Japanese coastal areas (derived using a partial dataset from [5.20]). The K_d values in IAEA TRS422 [5.1] are also shown.

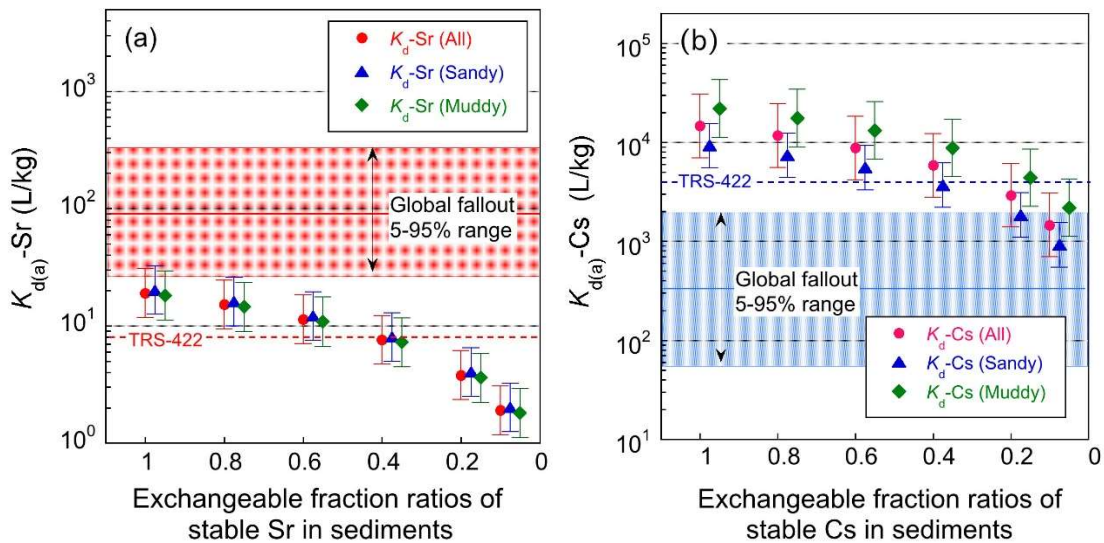


FIG. 5.2. Exchangeable fraction ratio effects on $K_{d(a)}$ values for: (a) stable Sr; and (b) stable Cs, and comparison with $K_{d(a)}$ values obtained using global fallout radioisotope data (5–95% confidence range, see Section 5.2.2.2).

Figure 5.2 (a) shows the impact for stable Sr $K_{d(a)}$ of changing the exchangeable fraction factor, compared with the recommended value for Sr from TRS 422 [5.1] and the 5–95% confidence range of K_d for ^{90}Sr in global fallout. If all stable Sr in sediment is considered wholly exchangeable (i.e. using 1.0 as the factor), then $K_{d(a)}$ values for stable Sr fell within the 5–95% confidence range of ^{90}Sr in global fallout for all types of sediment (i.e. there were no statistical differences between the sediment types). Thus, applying a factor of 0.2 for Sr would not be appropriate, as the exchangeable fraction of Sr is expected to be higher, and probably close to 1.0, for this Japanese coastal area. In the marine environment, the exchangeable stable Sr

fraction in sediment may vary by region. For example, it was reported that 9–18% of stable Sr was exchangeable within the Mississippi River mixing zone, USA [5.23] and 43–89% was exchangeable in Daya Bay, China [5.24]. However, a direct comparison may not be appropriate as the methods used to determine the exchangeable fractions in these studies were different from that used in Japan.

Figure 5.2 (b) shows the impact for stable Cs $K_{d(a)}$ values of applying the exchangeable fraction factor. The outcome was different from that for Sr. When an exchangeable fraction factor of 1.0 was applied, the $K_{d(a)}$ value for stable Cs was about two orders of magnitude higher than the GM of the $K_{d(a)}$ for ^{137}Cs in global fallout. When an exchangeable fraction factor of 0.2 was applied, it was still higher than ^{137}Cs in global fallout; only values for sandy soil fell within the 5–95% confidence range of ^{137}Cs in global fallout. Thus, the exchangeable fraction for Cs could have been overestimated when 0.2 was applied. All the data fell within the range of ^{137}Cs in global fallout when 0.1 or less was used as an exchangeable fraction factor.

To explore this issue, ^{137}Cs was added to a soil collected in Japan, which was then left in contact with sea water for 10 days [5.25]. Within one day, 11% of ^{137}Cs leached from the soil, and thereafter, the extractability did not change for 10 days. The exchangeable ^{137}Cs fraction in two types of Japanese soils, contaminated after the accident at the FDNPP, in contact with sea water was reported to be less than 1% after a few days [5.26]. These data suggested that ^{137}Cs in soil from the terrestrial environment could be extracted with sea water rapidly; however, after a longer contact time, the ^{137}Cs became less exchangeable. Although these results were for soil, they suggest that an exchangeable fraction factor of less than 0.1 for Cs may be appropriate in marine sediments.

These analyses showed that the exchangeable phase differed between elements in Japan. Similar data have been reported elsewhere [5.23, 5.24]. These data suggest that applying a fixed exchangeable fraction factor to all elements could be inaccurate. However, for the Japanese study, the $K_{d(a)}$ values estimated in this manner fell within an order of magnitude of observations for Japanese coastal areas, which likely falls within natural variability. Further work is needed to provide information on the element dependent exchangeable phase for different radioisotopes in marine sediments to provide more appropriate $K_{d(a)}$ values for use in dose assessment models.

5.2.2. Studies on K_d in marine areas of Japan before and after the accident at the Fukushima Daiichi Nuclear Power Plant (FDNPP)

Before the accident at the FDNPP, radionuclide monitoring had been carried out since 1984 in the coastal waters adjacent to NPPs all over Japan, including the FDNPP. The monitoring data are available in Japanese in the annual report of the Nuclear Regulation Authority (NRA). The data can be also freely downloaded from the environmental radiation database; some of these data have also been published [5.27–5.29].

The average $K_{d(a)}$ value for ^{137}Cs , based on all the records since 1984 in the coastal waters near Fukushima, was 620 ± 150 L/kg. However, a reliable $K_{d(a)}$ value was not available because systematic monitoring of marine water was not conducted before 1984. The most recent pre-accident 5 year average ^{137}Cs activity concentration (2006–2010) was 1.6 ± 0.2 mBq/L in sea water [5.30] and 0.87 ± 0.41 Bq/kg DM in sediment [5.31], resulting in a $K_{d(a)}$ of 544 L/kg DM. The larger variability of the ^{137}Cs data in sediment reflects the wide range of grain size distribution in the sediments.

5.2.2.1. $K_{d(a)}$ dataset for stable elements in coastal areas of Japan

Coastal areas with considerable spatial and temporal variation in the salinity of water (e.g. estuaries) were not explicitly considered in TRS 422 [5.1]. There is a need for specific consideration of K_d values in the waters of coastal regions, as they may differ from those in other aquatic areas due to the influence of salinity and potential influx of fresh water from catchments.

This subsection presents $K_{d(a)}$ values for areas with relatively lower salinity levels (21–34 units) compared with that in the ocean margin (of around 34–35 units).

In a dataset compiled by Takata et al. [5.32], data derived using inductively coupled plasma mass spectrometry have been included for 86 sediment (0–5 cm) and sea water samples (1–10 m above the seafloor) collected from the same point at the same time from 19 coastal sites in Japan from 2007 to 2012. Associated data are available for: the near bottom sea water – including properties such as pH and salinity, and for sediments, with associated data available on the silt and organic carbon contents [5.32]. Sediments were subdivided into muddy and sandy sediments, as described in Section 5.2.1 above.

The $K_{d(a)}$ was calculated for all the elements considered, assuming an exchangeable fraction of 0.2 (as specified in TRS 422 [5.1]), so the effect of chemical form for different elements was not considered. The dataset includes $K_{d(a)}$ values for 36 stable elements, summarized in Table 5.1. There were no significant differences (t-test, $p < 0.05$) between the GM of the $K_{d(a)}$ values determined for coastal areas, and TRS 422 [5.1] recommended values for the ocean margin; the current GM values for coastal areas were typically within an order of magnitude of the K_d values in TRS 422 [5.1]. Not all elements listed in Table 5.1 have recommended values in TRS 422 [5.1]; the additional elements measured were Mg, Al, K, V, Cu, Rb, Mo, La, Nd, Ho, Er, and Lu.

Most elements had a maximum/minimum $K_{d(a)}$ ratio of less than 100 (Table 5.1), with the exceptions of Al, Mn, Fe, Se, Cs and Th which had a maximum/minimum $K_{d(a)}$ ratio of >100 . Such variability in $K_{d(a)}$ values occurs because these coastal sites are influenced by various influxes from rivers which leads to considerable spatial and dynamic variation in both physical and chemical factors that can influence $K_{d(a)}$. There may also be effects of the chemical form for some elements (e.g. Al, which may be incorporated into aluminosilicates), and differing exchangeability than the assumed value of 20% (e.g. Fe). Box-plots (first and third quartiles) for $K_{d(a)}$ for coastal areas of Japan are given in Fig. 5.3.

TABLE 5.1. SUMMARIZED $K_{d(a)}$ DATA FOR COASTAL AREAS OF JAPAN (L/kg) [5.5]

| Element | N | GM | GSD | Minimum | Maximum | 5% | 95% |
|-----------|----|----------------------|-----|----------------------|-------------------|----------------------|----------------------|
| Na | 86 | 4.4×10^{-1} | 1.1 | 2.2×10^{-1} | 1.1×10^0 | 2.8×10^{-1} | 8.5×10^{-1} |
| Mg | 86 | 1.9×10^0 | 1.2 | 5.3×10^{-1} | 4.3×10^0 | 9.0×10^{-1} | 3.6×10^0 |
| Al | 86 | 2.5×10^7 | 1.5 | 9.5×10^5 | 1.6×10^8 | 6.9×10^6 | 8.4×10^7 |
| K | 86 | 8.1×10^0 | 1.1 | 3.9×10^0 | 2.2×10^1 | 4.8×10^0 | 1.3×10^1 |
| Ca | 86 | 8.5×10^0 | 1.3 | 1.6×10^0 | 2.3×10^1 | 2.6×10^0 | 2.0×10^1 |
| V | 86 | 1.6×10^4 | 1.2 | 4.4×10^3 | 4.1×10^4 | 8.6×10^3 | 2.9×10^4 |
| Mn | 86 | 6.6×10^4 | 1.8 | 2.4×10^3 | 1.5×10^6 | 5.5×10^3 | 4.0×10^5 |
| Fe | 86 | 1.9×10^7 | 1.5 | 1.6×10^6 | 1.6×10^8 | 4.1×10^6 | 9.1×10^7 |
| Co | 86 | 1.6×10^5 | 1.4 | 1.5×10^4 | 1.1×10^6 | 4.0×10^4 | 5.0×10^5 |
| Ni | 86 | 2.1×10^4 | 1.4 | 3.8×10^3 | 1.0×10^5 | 6.1×10^3 | 7.1×10^4 |
| Cu | 86 | 1.9×10^4 | 1.4 | 1.8×10^3 | 1.3×10^5 | 5.9×10^3 | 6.3×10^4 |
| Se | 46 | 2.3×10^3 | 1.7 | 8.8×10^1 | 1.1×10^4 | 3.3×10^2 | 9.3×10^3 |

TABLE 5.1 (cont.)

| Element | N | GM | GSD | Minimum | Maximum | 5% | 95% |
|-----------|----|-------------------|-----|-------------------|-------------------|-------------------|-------------------|
| Rb | 86 | 8.4×10^1 | 1.3 | 1.4×10^1 | 2.5×10^2 | 3.0×10^1 | 1.9×10^2 |
| Sr | 86 | 3.8×10^0 | 1.2 | 1.0×10^0 | 1.2×10^1 | 1.7×10^0 | 8.6×10^0 |
| Y | 86 | 1.3×10^5 | 1.2 | 3.2×10^4 | 3.1×10^5 | 7.1×10^4 | 2.5×10^5 |
| Mo | 86 | 3.0×10^1 | 1.3 | 7.9×10^0 | 2.0×10^2 | 1.1×10^1 | 1.1×10^2 |
| Cd | 73 | 1.6×10^3 | 1.4 | 2.0×10^2 | 9.3×10^3 | 3.7×10^2 | 6.3×10^3 |
| I | 62 | 2.1×10^1 | 1.5 | 3.9×10^0 | 2.8×10^2 | 5.9×10^0 | 8.9×10^1 |
| Cs | 83 | 2.9×10^3 | 1.4 | 5.4×10^2 | 1.0×10^5 | 1.2×10^3 | 6.3×10^3 |
| La | 86 | 5.1×10^5 | 1.3 | 1.5×10^5 | 2.6×10^6 | 2.0×10^5 | 1.4×10^6 |
| Ce | 86 | 1.8×10^6 | 1.3 | 3.5×10^5 | 5.9×10^6 | 6.5×10^5 | 4.9×10^6 |
| Pr | 86 | 6.4×10^5 | 1.2 | 1.9×10^5 | 2.0×10^6 | 2.6×10^5 | 1.4×10^6 |
| Nd | 86 | 5.6×10^5 | 1.2 | 1.5×10^5 | 1.8×10^6 | 2.3×10^5 | 1.2×10^6 |
| Sm | 86 | 5.0×10^5 | 1.2 | 1.3×10^5 | 1.6×10^6 | 2.3×10^5 | 1.0×10^6 |
| Eu | 86 | 5.2×10^5 | 1.2 | 1.3×10^5 | 1.5×10^6 | 2.2×10^5 | 1.1×10^6 |
| Gd | 86 | 3.3×10^5 | 1.2 | 8.0×10^4 | 1.0×10^6 | 1.6×10^5 | 7.0×10^5 |
| Tb | 86 | 3.6×10^5 | 1.3 | 6.9×10^4 | 1.2×10^6 | 1.6×10^5 | 8.8×10^5 |
| Dy | 86 | 2.7×10^5 | 1.2 | 6.3×10^4 | 6.6×10^5 | 1.5×10^5 | 5.1×10^5 |
| Ho | 86 | 2.3×10^5 | 1.2 | 5.3×10^4 | 6.7×10^5 | 1.3×10^5 | 3.9×10^5 |
| Er | 86 | 2.2×10^5 | 1.2 | 5.7×10^4 | 4.7×10^5 | 1.3×10^5 | 3.7×10^5 |
| Tm | 86 | 2.2×10^5 | 1.2 | 5.3×10^4 | 8.9×10^5 | 1.2×10^5 | 4.2×10^5 |
| Yb | 86 | 2.3×10^5 | 1.2 | 7.6×10^4 | 5.3×10^5 | 1.1×10^5 | 4.5×10^5 |
| Lu | 86 | 1.9×10^5 | 1.2 | 4.2×10^4 | 5.4×10^5 | 8.9×10^4 | 4.0×10^5 |
| Pb | 86 | 1.8×10^5 | 1.5 | 1.8×10^4 | 1.2×10^6 | 3.4×10^4 | 8.4×10^5 |
| Th | 51 | 4.3×10^6 | 1.6 | 6.8×10^4 | 6.7×10^7 | 8.0×10^5 | 2.4×10^7 |
| U | 73 | 1.0×10^2 | 1.2 | 3.9×10^1 | 2.8×10^2 | 4.4×10^1 | 1.9×10^2 |

Bold elements denote that the maximum/minimum ratios are larger than 100.

N: Sample size; GM: Geometric Mean; GSD: Geometric Standard Deviation; Min: Minimum; Max: Maximum; 5th: 5th percentile; 95th percentile.

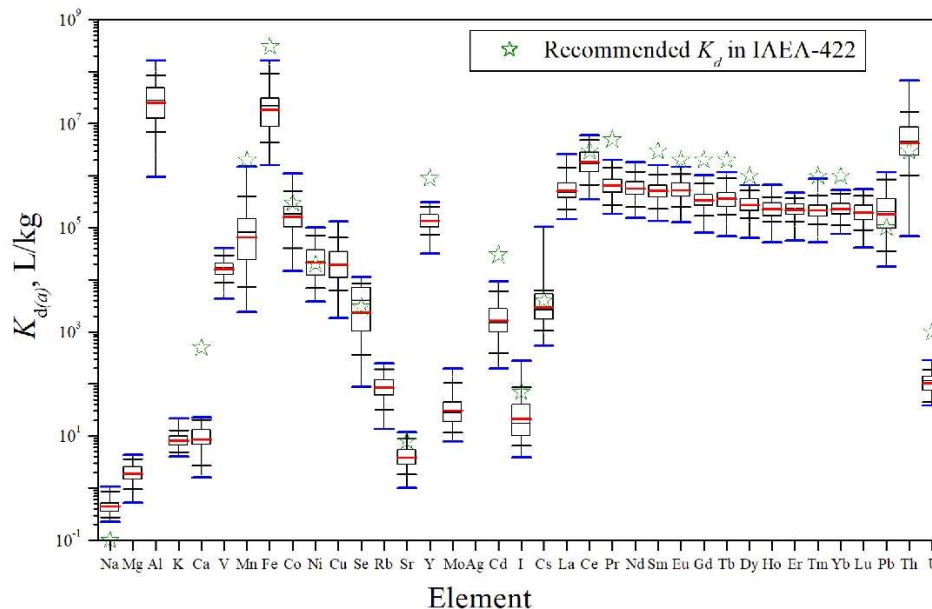


FIG. 5.3. Box plots (first and third quartiles) for $K_{d(a)}$ for coastal areas of Japan represent the median, the interquartile range, and whiskers (black lines: 5th–95th percentiles; red lines: the minimum and maximum values; blue line: GM for each element).

5.2.2.2. $K_{d(a)}$ values for radionuclides in Japanese coastal areas

To generate additional $K_{d(a)}$ values to compare with TRS 422 [5.1], the NRA's Environmental Radiation Database [5.33] was mined to create a dataset compiling radionuclide concentrations in sediment and sea water samples that had been collected at the same sampling site, and within 1 day of each other. The sampling sites in Japan were coastal and marginal seas that were similar to those considered to derive the data for ocean margins in TRS 422 [5.1]. Therefore, the selected data from Japan were comparable to K_d values that had been derived from stable element data for ocean margin in TRS 422 [5.1].

Analysis of the NRA data [5.33] allowed the derivation of radionuclide-specific *in situ* $K_{d(a)}$ values for ^{60}Co , ^{90}Sr , ^{106}Ru , ^{137}Cs , ^{144}Ce , natural U ($^{\text{nat}}\text{U}$) and $^{239+240}\text{Pu}$ (Table 5.2). All datasets had a log-normal distribution (Fig. 5.4). The GM of $K_{d(a)}$ values for $^{239+240}\text{Pu}$ in Japanese coastal areas were similar to the recommended value in TRS 422 [5.1], and to those reported elsewhere [5.21, 5.34], as were those for $^{\text{nat}}\text{U}$. In contrast, the $K_{d(a)}$ GM values for ^{60}Co , ^{106}Ru , ^{137}Cs and ^{144}Ce were one to three orders of magnitude lower in Japan compared with those reported in TRS 422 [5.1]. The $K_{d(a)}$ GM for ^{90}Sr was an order of magnitude higher than the TRS 422 value.

Differences between K_d values in TRS 422 [5.1] (based on stable element data) and values for radionuclides may be due to differences in the proportion of the stable element or radionuclide that is in the exchangeable fraction. In the absence of information on the physicochemical attributes corresponding to the K_d values, it is difficult to comment further on the difference between the Japanese data described here and the values reported in TRS 422 [5.1].

5.2.2.3. Measurements in marine systems in Japan associated with the accident at the Fukushima Daiichi Nuclear Power Plant

After the accident at the FDNPP, the total amount of ^{137}Cs released directly into the ocean (direct liquid release and atmospheric deposition) was estimated to be $(16\text{--}19) \times 10^{15}$ Bq [5.35, 5.36]. As the accidental releases dispersed, there were rapid changes in $K_{d(a)}$ values in the marine coastal environment [5.37]. According to the data from Ref. [5.38], the initial $K_{d(a)}$ values, based on ^{137}Cs activity concentrations in surface sediments and bottom water, varied from ~ 1000 to $200\,000$ L/kg DM. Honda et al [5.39] reported values of $200\text{--}4400$ L/kg DM, with an average value of 2100 L/kg DM. Since early 2013, the $K_{d(a)}$ data indicate a slowly decreasing trend over time for the observation stations used by the Marine Ecology Research Institute (MERI) [5.38]. The slow decline may be because ^{137}Cs activity concentrations in sediment remain significantly higher than those that occurred before the accident [5.31, 5.40], whereas the ^{137}Cs activity concentration in sea water had been approaching the pre-accident level [5.30, 5.32]. Similar data have also been reported after the accident at the Chernobyl Nuclear Power Plant (Chernobyl NPP) [5.34].

Further details regarding changes in radiocaesium in sediment and water before and after the accident at the FDNPP are provided in Annex V and IAEA-TECDOC-1927 [5.41].

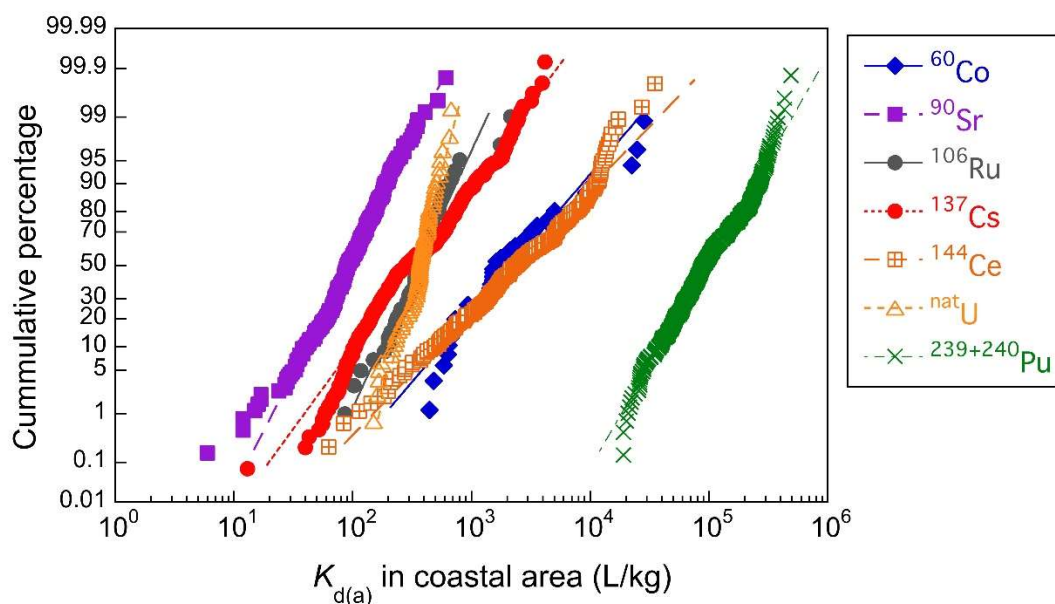


FIG. 5.4. Distributions of $K_{d(a)}$ values for seven radionuclides generated from field measurements in Japanese coastal areas (calculated using data from NRA's Environmental Radiation Database [5.33]).

TABLE 5.2. SUMMARY OF COASTAL $K_{d(a)}$ VALUES FOR SEVEN RADIONUCLIDES IN THE JAPANESE COASTAL ENVIRONMENT ($K_{d(a)}$ L/kg DM)¹

| Nuclide | N ² | GM | GSD | Min | Max | 5% | 95% | Recommended value in TRS 422 [5.1] (ocean margin) |
|------------------|----------------|-------------------|-----|-------------------|-------------------|-------------------|-------------------|---|
| Co-60 | 43 | 2.2×10^3 | 3.0 | 4.4×10^2 | 2.8×10^4 | 2.5×10^2 | 2.0×10^4 | 3×10^5 |
| Sr-90 | 309 | 9.1×10^1 | 1.9 | 6.0×10^0 | 6.1×10^2 | 2.6×10^1 | 3.3×10^2 | 8×10^0 |
| Ru-106 | 51 | 3.6×10^2 | 1.8 | 8.6×10^1 | 2.2×10^3 | 1.1×10^2 | 1.2×10^3 | 4×10^4 |
| Cs-137 | 709 | 3.2×10^2 | 2.5 | 1.3×10^1 | 2.2×10^3 | 5.2×10^1 | 2.0×10^3 | 4×10^3 |
| Ce-144 | 228 | 2.4×10^3 | 3.3 | 6.3×10^1 | 3.5×10^4 | 2.2×10^2 | 2.6×10^4 | 3×10^6 |
| ^{nat} U | 69 | 3.5×10^2 | 1.4 | 1.5×10^2 | 6.8×10^2 | 1.8×10^2 | 6.8×10^2 | 1×10^3 |
| Pu-239+240 | 345 | 9.6×10^4 | 2.0 | 1.9×10^4 | 49×10^5 | 2.3×10^4 | 4.0×10^5 | 1×10^5 |

¹ Calculated using selected data from NRA's environmental radiation database [5.33].

² N: Sample size; GM: Geometric Mean; GSD: Geometric Standard Deviation; Min: Minimum; Max: Maximum; 5th: 5th percentile; 95th percentile.

5.2.2.4. Time trends of $K_{d(a)}$ for ¹³⁷Cs under non-equilibrium conditions after the accident at the Fukushima Daiichi Nuclear Power Plant

Part of the radiocaesium released to the sea after the accident at the FDNPP has accumulated in marine organisms. The radiocaesium in sea water and sediment will lead to both internal and external doses to marine organisms, and potential exposure to seafood consumers [5.42]. After the accident at the FDNPP, radiocaesium activity concentrations in sea water changed rapidly over the first few months. Therefore, the ratio between radiocaesium activity concentrations in sediment versus those in water also changed with time, as contaminated sea water was transported over the deposited sediments and was then replaced with less contaminated sea water. In such a dynamic situation, there was no steady state between the radiocaesium activity

concentrations in sea water and sediments in the 2–3 years after the release. Because K_d assumes steady state conditions for radionuclide partitioning between sediment and sea water, the term $K_{d(a)}$ is more appropriate to describe differences with time in the ratios of radiocaesium activity concentrations in sediments versus sea water after the accident at the FDNPP.

The $K_{d(a)}$ values observed adjacent to the Fukushima Prefecture were generally higher than values that had been previously observed for global fallout [5.37]. Radiocaesium was rapidly sorbed by sediment from sea water [5.43]. Thereafter, radiocaesium in sediment that had originated from contaminated sea water after the accident at the FDNPP was not readily leached by the sea water. Consequently, radionuclide activity concentrations in sediments were much higher than in sea water even during the first few months after the accident, so $K_{d(a)}$ values were also relatively high. Figure 5.5 depicts the ^{137}Cs release to sea water and ^{137}Cs activity concentration data for sea water and sediment at station T-4, ca. 20 km south from the FDNPP (TEPCO's monitoring data [5.38] were used to derive this figure). Other sampling areas showed a similar tendency.

Improved models are needed to explain why the $K_{d(a)}$ values for radiocaesium were higher than those of ^{137}Cs in global fallout for future estimations of radiocaesium fate in the marine environment after an accidental release. In response, a new model using sorption and desorption rates between sea water and sediment, considering two compartments in sea water with short and long sorption–desorption half-lives in marine systems, has been developed [5.37]. Figure 5.6 shows the model structure, with short and long half-life fractions in sea water. Figure 5.7 shows performance analysis data for the T-1 station, located ca. 1 km north from the FDNPP. The estimated data derived using the dynamic compartment model for ^{137}Cs were in good agreement with measured data.

Using measured parameter values from T-1 station, the model simulated activity concentrations of ^{137}Cs in sea water and sediment at other sites. The estimated values for five stations near the FDNPP sites (not shown) were compared with the measured data collected at all stations [5.37]. Most parameter values in the model were determined by fitting; however, more data are needed to derive representative sorption and desorption rates. Further improvement of marine models is needed to understand and quantify the fate of radiocaesium in the marine environment for complex situations, such as in areas adjacent to the FDNPP following the accident. The model results show that the use of $K_{d(a)}$ is appropriate in the early stages after a large release of radionuclides into a water body for a simple estimation of radiocaesium activity concentrations in sediment or sea water over a short time period.

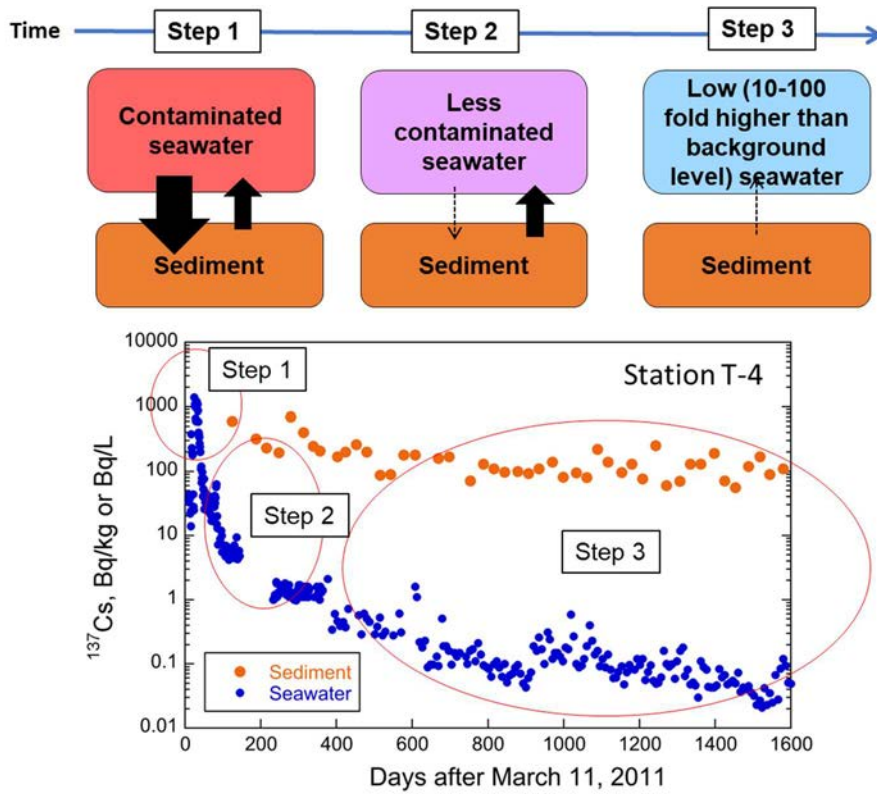


FIG. 5.5. Time dependence of ^{137}Cs behaviour in marine sediment and water following the accident at the FDNPP.

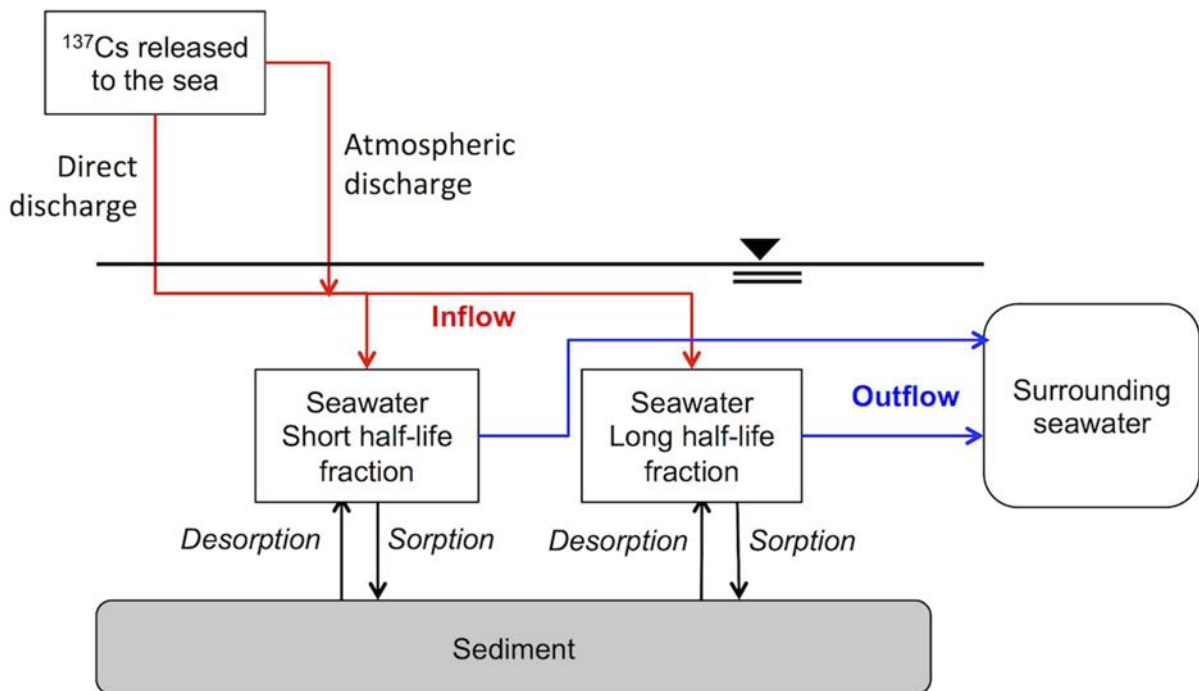


FIG. 5.6. Model structure to estimate ^{137}Cs in sea water and sediment.

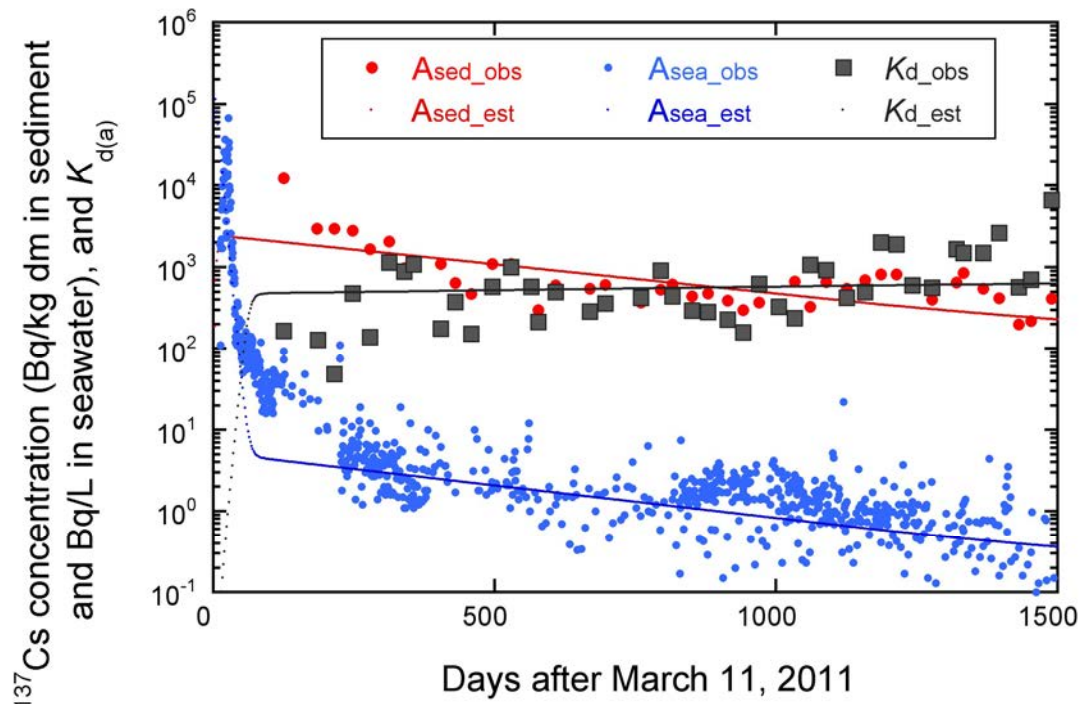


FIG. 5.7. Modelling of ^{137}Cs activity concentrations in sea water (A_{sea}) and sediment (A_{sed}) and the calculated $K_{d(a)}$ value at station T-1. Measured (or observed) and estimated results are described as 'obs' and 'est', respectively.

5.3. DETERMINATION OF $K_{d(a)}$ USING THE IAEA'S MARIS DATABASE – A BALTIC SEA CASE STUDY

TRS 422 [5.1] established the importance of using site specific K_d values for radiological impact assessment models. In addition, one of the outcomes of the IAEA's MODARIA I programme (2012–2015) was identification of the need for more marine K_d data for use in radiological impact assessments. The IAEA's MODARIA II programme (2016–2019) has sought to address this gap through the compilation of existing marine K_d data from scientific publications and other K_d data sources of site specific K_d values for inclusion in an updated K_d dataset for the marine environment. As part of this review, online and offline data repositories were reviewed to determine whether they could be used to derive $K_{d(a)}$ values for the marine environment; these included the PANGAEA data publisher [5.44], US Data.gov [5.45], EDMED [5.46], ICES [5.47], REMOTRANS [5.48], and the IAEA's MARine Information System (MARIS)⁸ [5.49]. After reviewing the datasets within these repositories, only data from the IAEA's MARIS dataset were identified as having the potential to derive $K_{d(a)}$ values.

The IAEA's MARIS database contains over 500 000 radioactivity measurements from the marine environment worldwide. A case study was conducted on data from MARIS to determine whether it could be utilized to derive apparent $K_{d(a)}$ values. The measurement data chosen for the case study were for ^{137}Cs in the Baltic Sea and covered the period 1984–2010. The results are presented below and compared with the recommended Cs K_d value from TRS 422 [5.1].

⁸ IAEA's MARIS database can be accessed at: <https://maris.iaea.org/>.

5.3.1. The MARIS Database

The IAEA's MARIS database is an online, open access database containing radioactivity measurements in sea water, biota, deposited sediments and suspended sediments. The data in MARIS have been extracted from the IAEA's in-house GLObal Marine Radioactivity Database (GLOMARD) [5.50] that collates data from various data providers, including HELCOM (Baltic Sea Area), OSPAR (North-East Atlantic), MEXT (Japan), and NRA (Japan). As of March 2023, the MARIS database contains more than 800 000 radioactivity measurements, representing 60 different radionuclides in the marine environment.

5.3.1.1. Data selected for the case study

To test whether the data available in MARIS could be used to derive $K_{d(a)}$ values for use in radiological impact assessments, a subset of the data from MARIS was selected that:

- (1) Had sufficient data to derive a large number of $K_{d(a)}$ values to allow for appropriate statistical analysis;
- (2) Is of interest to users performing radiological data assessments in the future;
- (3) Had to contain sufficient ancillary data to ensure the $K_{d(a)}$ values could be derived and used into the future for further data analysis.

Based on these criteria, ^{137}Cs data in sea water, bed sediment and suspended sediment measurements from the Baltic Sea between 1984–2010 were selected for further analysis (Fig 5.8).

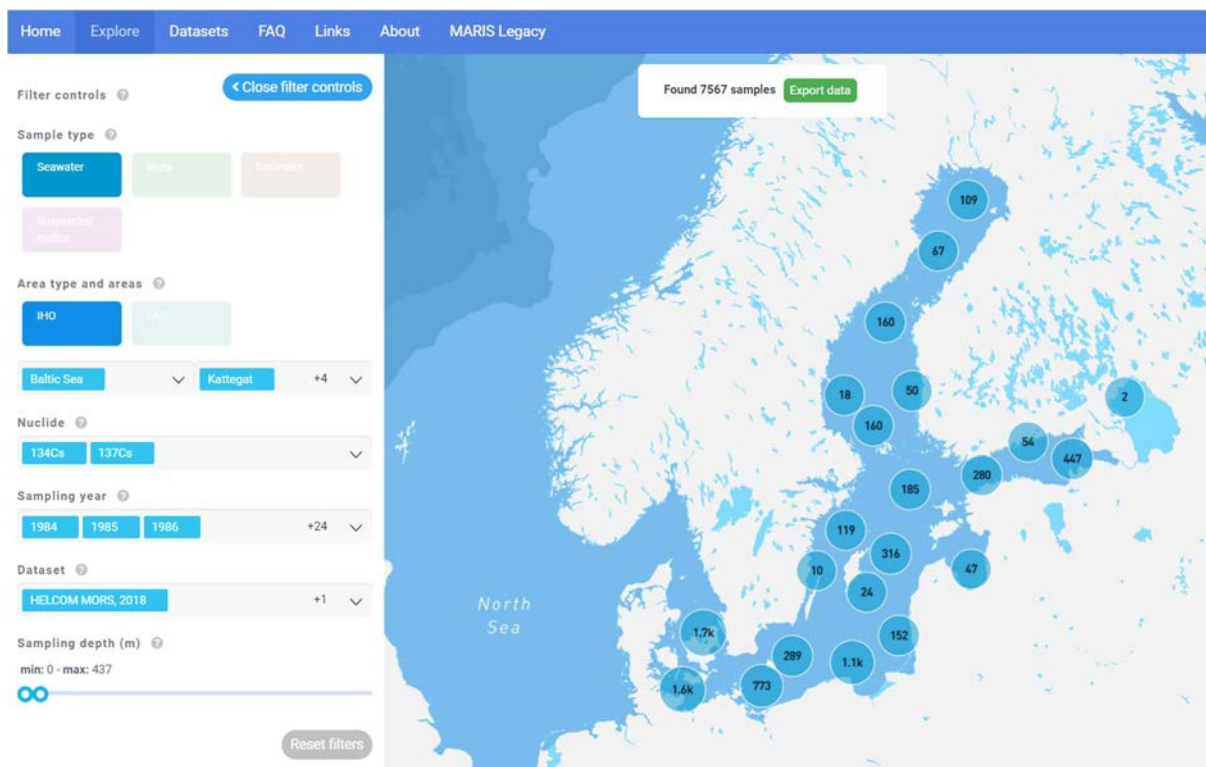


FIG. 5.8. Baltic Sea Region in MARIS highlighting location of measurements used in this case study (<https://maris.iaea.org/>).

TABLE 5.3. DATA EXTRACTED FROM MARIS FOR THIS CASE STUDY

| Common Information | Additional Seawater Data | Additional Sediment Data |
|----------------------------|--------------------------|--------------------------|
| Sampling Date | Salinity | Sediment Type |
| Location (GPS coordinates) | Temperature | Organic Content |
| Total Depth | | Oxic/Anoxic |
| Sampling Depth | | |
| Radionuclide | | |
| Activity | | |
| Uncertainty | | |

This dataset was provided to MARIS repository by the Baltic Marine Environment Protection Commission (HELCOM) from the HELCOM Monitoring Of Radioactive Substances (MORS) database [5.51] and contains a large volume of data on radioactivity measurements in sea water, deposited sediments and suspended sediments. The Baltic Sea region is of significant interest for radiological impact assessments due to the enhanced radiocaesium activity concentrations in the Baltic Sea and surrounding regions arising from radioactive fallout from the accident at the Chernobyl NPP in 1986. The dataset also contains location data to allow the derivation of $K_{d(a)}$ values.

The specific data information extracted from the MARIS repository to derive the $K_{d(a)}$ values are outlined in Table 5.3 and grouped into common information and additional data. The ^{137}Cs dataset from the Baltic Sea case study, covering the period 1984–2010, contains 7500 sea water sediment, 6600 deposited sediment and 66 suspended sediment data entries.

5.3.1.2. Derivation of $K_{d(a)}$ values from MARIS dataset for the Baltic Sea

Site specific $K_{d(a)}$ values are those derived from empirical measurements in the field and differ from those obtained in laboratories that use sorption and desorption experiments. These site specific values are also time dependent and, as such, show large variability in the environment. The site specific field derived $K_{d(a)}$ values are also referred to as apparent $K_{d(a)}$ values (see also Chapter 2, Section 2.1.2.3). The site specific $K_{d(a)}$ values were derived from the MARIS dataset using the following formula:

$$K_{d(a)} = \frac{C_{sed} \text{ (Bq/kg DM)}}{C_{seawater} \text{ (Bq/L)}} \quad (5.2)$$

where:

- $K_{d(a)}$ is the apparent site specific K_d (L/kg DM);
- C_{sed} is the sediment activity concentration (Bq/kg DM);
- $C_{seawater}$ is the sea water activity concentration (Bq/L).

$K_{d(a)}$ values were derived for specific sampling locations using the following criteria:

- (1) The sediment and sea water samples were sampled at the same monitoring location. The sea water and sediment activity concentration measurements were matched based on the GPS coordinates of the measurements;
- (2) The sediment and sea water samples were measured at the same time; a tolerance of plus or minus one day was given to take into account the challenges of marine sampling;

- (3) Sea water activity measurements for samples closest to the deposited were chosen for deriving the $K_{d(a)}$, for locations where a depth profile of the sea water activity concentrations was available;
- (4) Sample locations that had a sea water or sediment activity concentrations reported as below limits of detection were excluded.

Taking the above criteria into consideration, over 6000 $K_{d(a)}$ values for ^{137}Cs in the Baltic Sea were derived, covering the period from 1984 to 2010. The majority of the sediment measurements made in the Baltic Sea were on deposited sediments allowing derivation of a total of 6589 $K_{d(a)}$ values. Only 46 $K_{d(a)}$ values were derived for suspended sediments.

5.3.1.3. Deposited sediments

The median value of the $K_{d(a)}$ for ^{137}Cs is 1000 (L/kg), with most of the results falling within one order of magnitude ranging from 500 to 5000 (L/kg) (Fig. 5.9).

The variability of the site specific $K_{d(a)}$ values is shown in a box and whisker plot (Fig. 5.10). After the removal of statistical outliers, the $K_{d(a)}$ values vary from 2 to 7318 (L/kg), with a range of 194 to 3046 between the first and third quartile.

These values are broadly in agreement with the recommended Cs K_d value in TRS 422 of 4000 L/kg, with a maximum and minimum K_d value in TRS 422 assumed to be within one order of magnitude of the recommended value.

The influence of the accident at the Chernobyl NPP on the $K_{d(a)}$ values is clearly observed from the yearly temporal variation from 1984 to 2010 (Fig. 5.11).

The $K_{d(a)}$ values decreased by an order of magnitude in the year following the accident at the Chernobyl NPP in 1986. The median Cs $K_{d(a)}$ value in 1985 is 2200 L/kg and this decreased to 250 L/kg in 1986, with a gradual increase in $K_{d(a)}$ over the following ten to fifteen years. The $K_{d(a)}$ values only returned to pre-Chernobyl levels approximately 15 years later. The large decrease in $K_{d(a)}$ values is due to an increase in ^{137}Cs sea water activity concentrations due to fallout from the accident at the Chernobyl NPP.

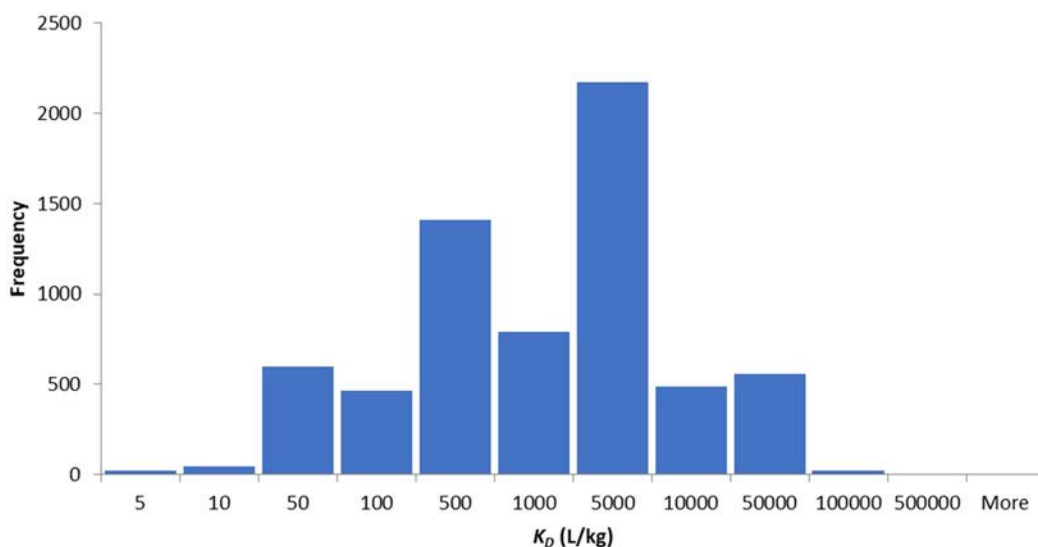


FIG. 5.9. Histogram of Cs $K_{d(a)}$ values in the Baltic Sea.

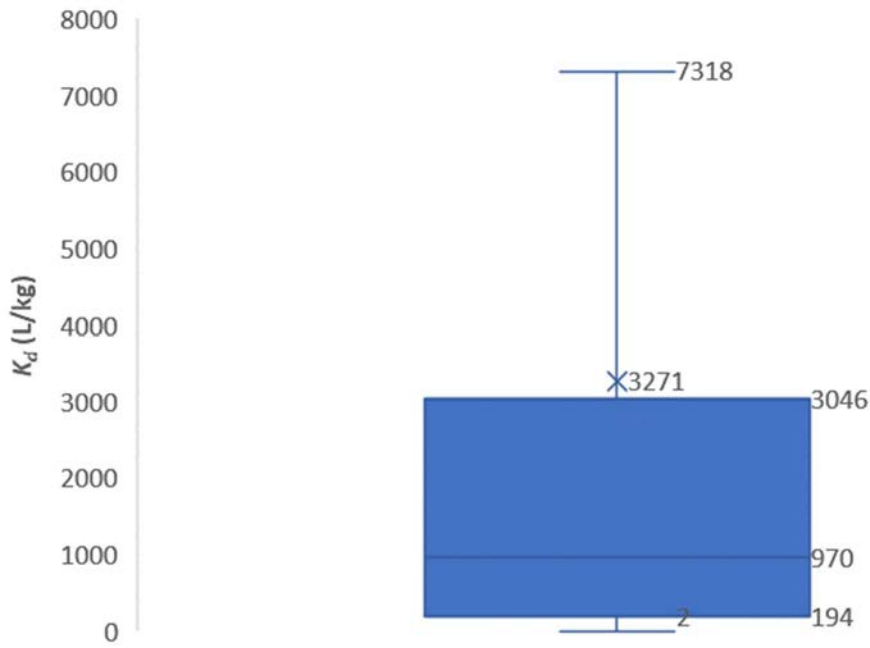


FIG. 5.10. Box and whisker plot of Cs $K_{d(a)}$ values in the Baltic Sea.

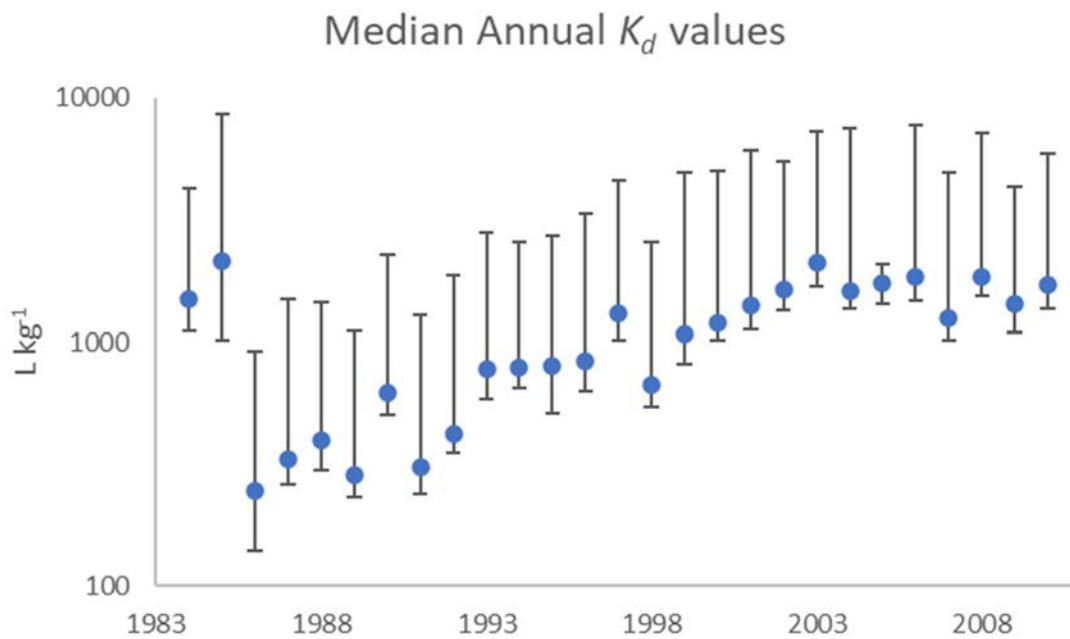


FIG. 5.11. Temporal variation of Cs median $K_{d(a)}$ values in the Baltic Sea from 1984–2010. The error bars denote the 1st and 3rd quartiles of the Cs $K_{d(a)}$ values.

5.3.1.4. *Suspended sediments*

The Cs $K_{d(a)}$ values derived from the suspended sediment data for the Baltic Sea has a median value of 10 000 L/kg. This median value is based on a reduced dataset ($N = 46$), reported over the period 1984–1990 (Fig. 5.12).

The suspended sediment data used to derive the Cs $K_{d(a)}$ values for the Baltic Sea include the period of the accident at the Chornobyl NPP. However, the accident at the Chornobyl NPP had only a short time impact on the $K_{d(a)}$ values. The $K_{d(a)}$ increased to a value greater than 100 000 L/kg on the 8 May 1986, but in just over one month it returned to the same order of magnitude reported prior to the accident. This observation can be attributed to rapid adsorption of Cs onto suspended sediments following the accident whereas for deposited sediment the uptake of Cs was much slower as the time taken for partitioning between the water layer and bottom sediments was much greater (Fig. 5.13).

5.3.2. **Conclusions from the MARIS case study for the Baltic Sea**

The work from the MARIS case study indicated that the Cs $K_{d(a)}$ for deposited sediments were broadly in agreement with the recommended value from TRS 422. Moreover, it was also possible to derive $K_{d(a)}$ values from other data in the MARIS database, if the selection criteria were met (see Section 5.3.1.2 above). The accident at the Chornobyl NPP decreased the Cs $K_{d(a)}$ values by an order of magnitude in the Baltic Sea due to a short term increase in ^{137}Cs in sea water activity concentrations. As a result of the increase in ^{137}Cs activity concentrations in sea water, it took approximately 15 years for the Cs $K_{d(a)}$ to return to values reported prior to the accident at the Chornobyl NPP.

The Cs $K_{d(a)}$ values derived from suspended sediment data are an order of magnitude higher than that derived for the deposited sediments and the TRS 422 recommended value for Cs. Furthermore, the impact of the accident at the Chornobyl NPP on the Cs $K_{d(a)}$ derived from suspended sediments was short lived.

This analysis also demonstrates that MARIS data can be used to derive Cs $K_{d(a)}$ for the marine environment. However, in analysing MARIS data, some issues were identified that would need to be addressed before additional data extraction and analysis could be conducted. In reviewing and analysing data from MARIS many duplicate entries were identified in the time period of interest for this case study. These duplicate entries need to be removed to ensure that any $K_{d(a)}$ distributions derived from the data are not skewed by duplicate data. Closer analysis of deposited sediment data in MARIS for a specific sampling location and time showed that multiple ^{137}Cs activity concentrations can be associated with it. For this study, the average activity concentration of all these measurements were used to determine the Cs $K_{d(a)}$ value. These multiple activity concentration values are most likely to arise from soil core profile measurements being conducted at these specific locations, however, there is a lack of sufficient data in MARIS to distinguish between these soil core depth profiles. To assist end users in the derivation of Cs $K_{d(a)}$ values from these locations, it would be useful if the depth of the soil core measurement was available in MARIS.

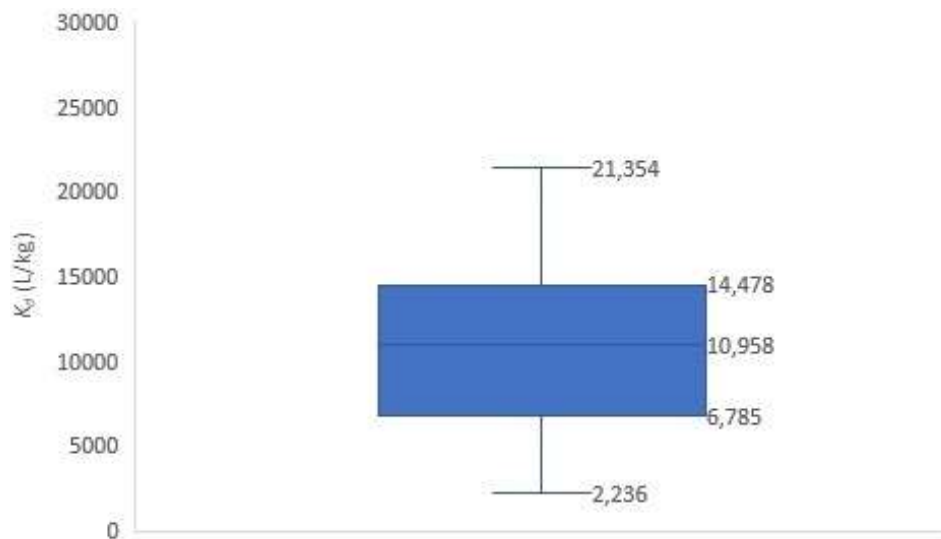


FIG. 5.12. Box and whisker plot of Cs $K_{d(a)}$ values derived from suspended sediment in the Baltic Sea.

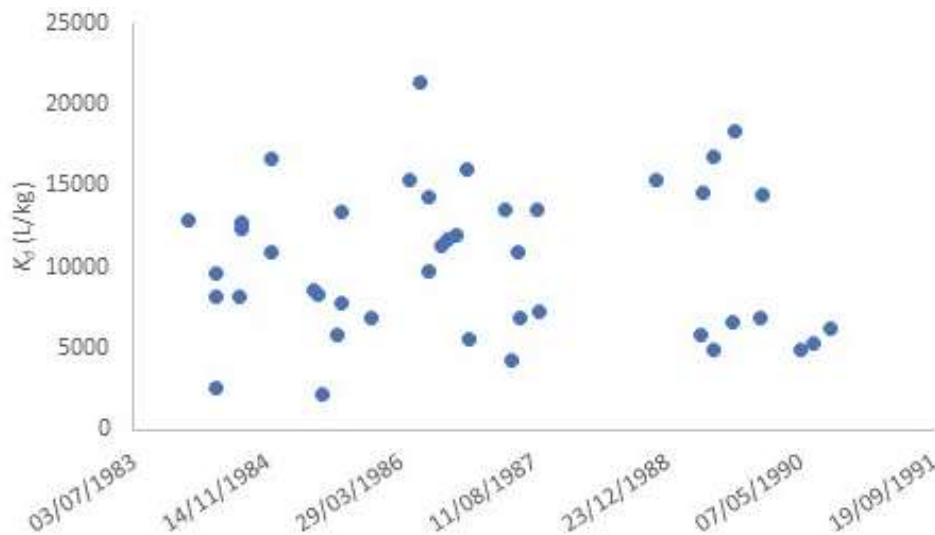


FIG. 5.13. Cs $K_{d(a)}$ values of suspended sediment in the Baltic Sea (1984–1990) (The $K_{d(a)}$ value of > 100 000 L/kg from the 8th May 1986 is omitted from the figure).

5.4. PRELIMINARY CONCLUSIONS FROM MARINE STUDIES ON K_d

Important sediment and water related properties affecting marine radionuclide $K_{d(a)}$ values include salinity, pH, DOC, suspended load, and sediment composition. However, marine $K_{d(a)}$ values are generally considered to be less variable than those for freshwater environments [5.2]. This assumption has been tested using data for stable element $K_{d(a)}$ values in Japanese coastal sediment calculated by assuming that 20% of the total element is exchangeable (as assumed in TRS 422 [5.1] for the ocean margin). By using this approach, new $K_{d(a)}$ values for Mg, Al, K, V, Cu, Rb, Mo, La, Nd, Ho, Er, and Lu were generated, which had not previously been reported in TRS 422 [5.1]. The GM values derived for the elements were similar to those that were compiled in TRS 422 [5.1] where a comparison could be made, and maximum / minimum $K_{d(a)}$ ratios for most elements were less than 100.

Recent studies in Japan [5.20], have shown that the proportion of the exchangeable phase differed between ^{137}Cs and stable Cs, as well as between ^{90}Sr and stable Sr, although the differences in the values were small. This observation, together with other data on soils and fresh water, suggests that, for some elements, the application of a fixed (single) exchangeable fraction to all elements is not an optimal approach. Collection of further data is needed to determine how relevant factors affect the variation for different elements in marine $K_{d(a)}$.

A preliminary investigation of the data contained in the IAEA MARIS database demonstrated that these data are suitable for the derivation of $K_{d(a)}$ values. The MARIS dataset not only contains sediment and sea water activity concentration data that are used to derive $K_{d(a)}$ values, but also other ancillary data such as salinity, specific surface area of sediments and pH that and therefore has the potential to be used to refine K_d values in the marine environment. Furthermore, the MARIS database includes location coordinates for the measurements used to derive the $K_{d(a)}$ values which could be used to further generate $K_{d(a)}$ values for use in REIA [5.52]. Other marine datasets were investigated for their possible use in deriving K_d values, but these were not found to be appropriate.

REFERENCES TO CHAPTER 5

- [5.1] INTERNATIONAL ATOMIC ENERGY AGENCY, Sediment Distribution Coefficients and Concentration Factors for Biota in the Marine Environment, Technical Reports Series No. 422, IAEA, Vienna (2004).
- [5.2] INTERNATIONAL ATOMIC ENERGY AGENCY, Sediment K_{ds} and Concentration Factors for Radionuclides in the Marine Environment, Technical Report Series No. 247, IAEA, Vienna (1985).
- [5.3] ATWOOD, D.A., Radionuclides in the Environment, Wiley, John Wiley & Sons Ltd., New York (2010).
- [5.4] BOYER, T. P., S. LEVITUS, J. I. ANTONOV, R. A. LOCARNINI, AND H. E. GARCIA, 2005: Linear trends in salinity for the world 50 ocean, 1955–1998. Geophysical Research Letters NZ, 32. doi:10.1029/2004gl021791
- [5.5] TAKATA, H., AONO, T., TAGAMI, K., UCHIDA, S., A new approach to evaluate factors controlling elemental sediment-seawater distribution coefficients (K_d) in coastal regions, Japan. Sci. Total Environ. **543** (2016) 315–325. <https://doi.org/10.1016/j.scitotenv.2015.11.034>
- [5.6] BASKARAN, M., RAVICHANDRAN, M., BIANCHI, T.S., Cycling of ^7Be and ^{210}Pb in a high DOC, shallow, turbid estuary of south-east Texas, Estuar. Coastal Shelf Sci. **45** (1997) 165. <https://doi.org/10.1006/ecss.1996.0181>
- [5.7] HAMILTON-TAYLOR, J., KELLY, M., MUDGE, S., BRADSHAW, K., Rapid remobilisation of plutonium from estuarine sediments, J. Environ. Radioact. **5** (1987) 409. [https://doi.org/10.1016/0265-931X\(87\)90017-8](https://doi.org/10.1016/0265-931X(87)90017-8)
- [5.8] HAMILTON, E.I., Radionuclides and large particles in estuarine sediments, Mar. Pollut. Bull. **20** (1989) 603. [https://doi.org/10.1016/0025-326X\(89\)90396-2](https://doi.org/10.1016/0025-326X(89)90396-2)
- [5.9] FUKUI, M., Desorption kinetics and mobility of some radionuclides in sediments, Health Phys. **59** (1990) 879. DOI: [10.1097/00004032-199012000-00011](https://doi.org/10.1097/00004032-199012000-00011)

- [5.10] KERSHAW, P.J., PENTREATH, R.J., WOODHEAD, D.S., HUNT, G.J., A review of radioactivity in the Irish Sea. A report prepared for the Marine Pollution Monitoring Management Group (1992).
<https://www.cefas.co.uk/publications/aquatic/aemr32.pdf>
- [5.11] YABLOKOV, A.V., et al., Facts and Problems Related to Radioactive Waste Disposal in Seas Adjacent to the Territory of the Russian Federation, Office of the President of the Russian Federation, Moscow (1993).
- [5.12] VAN WEERS, A.W., et al., Current Practice of Dealing with Natural Radioactivity from Oil and Gas Production in EU Member States, Rep. EUR-17621-EN, European Commission, Luxembourg (1997).
<https://op.europa.eu/en/publication-detail/-/publication/ae0d4076-0b10-4e4f-b945-7ba4c8e97822>
- [5.13] LYSEBO, I., TUFTO, P., Handling of Natural Occurring Radioactive Deposits in the Oil and Gas Industry in Norway, United Kingdom and the Netherlands, Rep. NRPA-1999:2, Norwegian Radiation Protection Authority, Østerås (1999).
- [5.14] OSPAR CONVENTION FOR THE PROTECTION OF THE ENVIRONMENT OF THE NORTH EAST ATLANTIC, Report on Discharges of Radioactive Substances by Non-nuclear Industries, Oslo and Paris Commissions, Paris (1997).
- [5.15] RUTHERFORD, P.M., DUDAS, M.J., SAMEK, R.A., Environmental impact of phosphogypsum, *Sci. Total Environ.* **149** (1994) 1.
[https://doi.org/10.1016/0048-9697\(94\)90002-7](https://doi.org/10.1016/0048-9697(94)90002-7)
- [5.16] SIEGEL, M.D., BRYAN, C.R., Environmental Geochemistry of Radioactive Contamination, Sandia National Laboratories, NM (2003).
https://www.researchgate.net/publication/236402427_Environmental_Geochemistry_of_Radioactive_Contamination
- [5.17] LEPICARD, S., HELING, R., MADERICH, V., POSEIDON/RODOS models for radiological assessment of marine environment after accidental releases: application to coastal areas for the Baltic, Black and North Seas. *J. Environ. Radioactiv.* **72** (2004) 153. [https://doi.org/10.1016/S0265-931X\(03\)00197-8](https://doi.org/10.1016/S0265-931X(03)00197-8)
- [5.18] VIVES i BATLLE, J., et al., Dynamic model for the assessment of radiological exposure to marine biota. *J. Environ. Radioact.* **99** (2008) 1711.
<https://doi.org/10.1016/j.jenvrad.2007.11.002>
- [5.19] IOSJPE, M., A sensitivity analysis of the parameters controlling water-sediment interactions in the coastal zone: Consequences to man and environment, *J. Marine Systems* **88** (2011) 82. <https://doi.org/10.1016/j.jmarsys.2011.02.013>
- [5.20] UCHIDA, S., TAGAMI, K., Comparison of coastal area sediment-seawater distribution coefficients (K_d) of stable and radioactive Sr and Cs, *Appl. Geochem.* **85** (2017) 148. <https://doi.org/10.1016/j.apgeochem.2016.12.023>
- [5.21] CARROLL, J. et al., Distribution coefficients (K_d 's) for use in risk assessment models of the Kara Sea, *Appl. Radiat. Isot.* **51** (1999) 121.
[https://doi.org/10.1016/S0969-8043\(98\)00165-1](https://doi.org/10.1016/S0969-8043(98)00165-1)
- [5.22] NYFFELER, U.P., Li, Y.-H., SANTSCHI, P. H., A kinetic approach to describe trace-element distribution between particle and solution in natural aquatic systems, *Geochim. Cosmochim. Acta* **48** (1984) 1513.
[https://doi.org/10.1016/0016-7037\(84\)90407-1](https://doi.org/10.1016/0016-7037(84)90407-1)

- [5.23] XU, Y.-F., MARCANTONIO, F., Speciation of strontium in particulates and sediments from the Mississippi River mixing zone, *Geochim. Cosmochim. Acta* **68** (2004) 2649. [10.1016/j.gca.2003.12.016](https://doi.org/10.1016/j.gca.2003.12.016)
- [5.24] GAO, X., et al., Environmental status of Daya Bay surface sediments inferred from a sequential extraction technique, *Estuarine Coastal Shelf Sci.* **86** (2010) 369. <https://doi.org/10.1016/j.ecss.2009.10.012>
- [5.25] TAGAMI, K., UCHIDA, S., Sediment-seawater distribution coefficient for radionuclides and estimation of radionuclide desorption ratio from soil in seawater, *Bunseki Kagaku* **62** (2013) 527 (In Japanese). DOI: [10.2116/bunsekikagaku.62.527](https://doi.org/10.2116/bunsekikagaku.62.527)
- [5.26] TAGAMI, K., UCHIDA, S., Aging effect on technetium behavior in soil under aerobic and anaerobic conditions, *Toxicol. Environm.Chem.* **56** (1996) 235. <https://doi.org/10.1080/02772249609358366>
- [5.27] KASAMATSU F. AND INATOMI, N., Effective environmental half-lives of Sr and Cs in the coastal seawater of Japan, *J. Geophys. Res.* **103** (1998) 1209. <https://doi.org/10.1029/97JC02807>
- [5.28] OIKAWA, S., et al., Plutonium isotopes concentration in seawater and bottom sediment off the pacific coast of Aomori sea area during 1991–2005, *J. Environ. Radioact.* **102** (2011) 302. <https://doi.org/10.1016/j.jenvrad.2010.12.007>
- [5.29] WATABE, T., et al., Spatiotemporal distribution of ¹³⁷Cs in the sea surrounding Japanese islands in the decades before the disaster at the Fukushima Daiichi nuclear power plant in 2011, *Sci. Total Environ.* **463-464** (2013) 913. <https://doi.org/10.1016/j.scitotenv.2013.06.031>
- [5.30] OIKAWA, S., TAKATA, H., WATABE, T., MISONOO, J., KUSAKABE, M., Distribution of the Fukushima-derived radionuclides in seawater in the pacific off the coast of Miyagi, Fukushima, and Ibaraki prefectures, Japan, *Biogeosciences* **10** (2013) 5031. <https://doi.org/10.5194/bg-10-5031-2013>
- [5.31] KUSAKABE, M., OIKAWA, S., TAKATA, H., MISONOO, J., Spatiotemporal distributions of Fukushima-derived radionuclides in nearby marine surface sediments, *Biogeosciences* **10** (2013) 5019. <https://doi.org/10.5194/bg-10-5019-2013>
- [5.32] TAKATA, H., KUSAKABE, M., INATOMI, N., IKENOUE, T., and HASEGAWA, K., The Contribution of Sources to the Sustained Elevated Inventory of ¹³⁷Cs in Offshore Waters East of Japan after the Fukushima Daiichi Nuclear Power Station Accident, *Environ. Sci. Technol.* **50** (2016) 6957. <https://doi.org/10.1021/acs.est.6b00613>
- [5.33] NUCLEAR REGULATION AUTHORITY (NRA), Environmental Radiation Database, Japan (2015) (In Japanese). <https://www.kankyo-hoshano.go.jp/data/database/>
- [5.34] RUDJORD, A.L., OUGHTON, D., BERGAN, T.D., CHRISTENSEN, G., Radionuclides in marine sediments – Distribution and processes, In: *Marine radioecology. Final reports from sub-projects within the Nordic nuclear safety research project EKO-1* (Ed. Plasson, S.E.), Nordisk Kernesikkerhedsforskning, Roskilde, ISBN 87-7893-056-1 (2001) 81. https://inis.iaea.org/search/search.aspx?orig_q=RN:33004743

- [5.35] TSUMUNE, D., et al., One-year, regional-scale simulation of ^{137}Cs radioactivity in the ocean following the Fukushima Daiichi nuclear power plant accident, *Biogeosciences* **10** (2013) 5601. DOI: [10.5194/bg-10-5601-2013](https://doi.org/10.5194/bg-10-5601-2013)
- [5.36] AOYAMA, M., et al., ^{134}Cs and ^{137}Cs in the North Pacific Ocean derived from the March 2011 TEPCO Fukushima Daiichi Nuclear Power Plant accident, Japan. Part two: Estimation of ^{134}Cs and ^{137}Cs inventories in the North Pacific Ocean, *J. Oceanogr.* **72** (2016) 67. <https://doi.org/10.1007/s10872-015-0332-2>
- [5.37] YAMAMOTO, K., TAGAMI, K., UCHIDA, S., ISHII, N., Model estimation of ^{137}Cs concentration change with time in seawater and sediment around the Fukushima Daiichi Nuclear Power Plant site considering fast and slow reactions in the seawater-sediment systems, *J. Radioanal. Nucl. Chem.* **304** (2015) 867. <https://doi.org/10.1007/s10967-014-3897-0>
- [5.38] TEPCO, Daily analysis results on radioactive material at Fukushima Daiichi Nuclear Power Station, (2016) (In Japanese). <http://www.tepco.co.jp/decommission/planaction/monitoring/index-j.html>
- [5.39] HONDA, M.C., et al., Dispersion of artificial caesium-134 and -137 in the western North Pacific one month after the Fukushima accident, *Geochemical J.* **46** (2012) 1. <https://doi.org/10.2343/geochemj.1.0152>
- [5.40] KUSAKABE, M., INATOMI, N., TAKATA, H., IKENOUE T., Decline in radiocesium in seafloor sediments off Fukushima and nearby prefectures, *J. Oceanogr.* **73** (2017) 529. <https://doi.org/10.1007/s10872-017-0440-2>
- [5.41] INTERNATIONAL ATOMIC ENERGY AGENCY, Environmental Transfer of Radionuclides in Japan following the Accident at the Fukushima Daiichi Nuclear Power Plant, IAEA-TECDOC-1927, IAEA, Vienna (2020).
- [5.42] FISHER, N.S., et al., Evaluation of radiation doses and associated risk from the Fukushima nuclear accident to marine biota and human consumers of seafood, *PNAS* **110** (2013) 10670. <https://doi.org/10.1073/pnas.1221834110>
- [5.43] FUHRMANN, M., PIETRZAK, R., NEIHEISEL, J.R., DYER, R.S., Partitioning between sediment and pore water of radiocesium from Chernobyl fallout, BNL-46348, New York (1991). <https://digital.library.unt.edu/ark:/67531/metadc1084944/>
- [5.44] DIEPENBROEK, M., GROBE, H., REINKE, M., SCHINDLER, U., SCHLITZER, R., SIGER, R., WEFER, G., PANGAEA - an information system for environmental sciences, *Computers & Geosciences* **28** 10 (2002) 1201. [https://doi.org/10.1016/S0098-3004\(02\)00039-0](https://doi.org/10.1016/S0098-3004(02)00039-0)
- [5.45] US GENERAL SERVICES ADMINISTRATION, DATA.GOV, Datasets www.data.gov
- [5.46] PAN-EUROPEAN INFRASTRUCTURE FOR OCEAN & MARINE DATA MANAGEMENT, EUROPEAN DIRECTORY OF MARINE ENVIRONMENTAL DATA SETS (EDMED), <https://www.seadatanet.org/Metadata/EDMED-Datasets>
- [5.47] INTERNATIONAL COUNCIL FOR EXPLORATION OF THE SEA, ICES Datasets, <https://www.ices.dk/marine-data/dataset-collections/Pages/default.aspx>
- [5.48] REMOTRANS, REMOTRANS 5FP Final Report, European Commission (2003).

- [5.49] INTERNATIONAL ATOMIC ENERGY AGENCY, MARIS Database, <https://maris.iaea.org/>
- [5.50] INTERNATIONAL ATOMIC ENERGY AGENCY, Global Marine Radioactivity Database (GLOMARD), IAEA, Vienna (2000).
<https://www.iaea.org/publications/5948/global-marine-radioactivity-database-glomard>
- [5.51] HELCOM, Thematic assessment of long-term changes in radioactivity in the Baltic Sea, 2007-2010, Baltic Sea Environmental Proceedings No. 135, Helsinki (2013).
<https://helcom.fi/wp-content/uploads/2019/08/BSEP135.pdf>
- [5.52] KELLEHER, K., MCGINNITY, P., HOWARD, B.J., BOYER, P., VIDAL, M., BILDSTEIN, O., The use of the IAEA MARIS database in determining the variability of sediment distribution coefficients in the marine environment and potential implications for marine dispersion modelling, J. Radiol. Prot. **42** 3 (2022) 501.
<https://iopscience.iop.org/article/10.1088/1361-6498/ac8a53>

6. CONCEPT FOR A K_d DATABASE AND SOFTWARE TOOL FOR DERIVING K_d DATA

KEVIN KELLEHER

Environmental Protection Agency, IRELAND

PATRICK BOYER

Institut de Radioprotection et de Sûreté Nucléaire (IRSN), FRANCE

MIQUEL VIDAL, ORIOL TOLL

Universitat de Barcelona, SPAIN

PAUL MCGINNITY

International Atomic Energy Agency

6.1. DEVELOPMENT OF A PROPOSED DATABASE STRUCTURE

As outlined in the preceding sections, a significant amount of K_d values has been collated prior to, and during MODARIA programmes (see Chapters 3–5). Extensive research has highlighted that K_d values are dependent upon a significant number of factors, which are radionuclide dependent and that can affect the K_d values in the soil, freshwater and marine environment compartments. The factors include, for example, pH, organic matter and texture for soils, suspended load and dissolved organic carbon for freshwater systems, and organic content and specific surface area for the marine environment. The K_d values and their supplementary data are typically stored in multiple locations such as scientific publications, personal spreadsheets or paper based records. For many of these sources it is difficult to access the component data used to derive the K_d values which hampers interpretation of these K_d datasets. The end users of the K_d data, such as those conducting REIA, may need to carry out their assessments over one or more environmental compartments and, therefore, K_d data may need to be refined based on the environmental conditions in these compartments.

The structure and content of a prototype database has been developed during the MODARIA programme that would constitute a single repository for collating and preserving all K_d data in a standard format with standardized functionality for accessing and refining K_d values based on the end user needs. The database could be used to store K_d values for soil, freshwater and marine environmental compartments. It could also include supplementary data that could be used to refine the K_d values, according to various environmental characteristics, for use in radiological impact assessments. The database is not yet currently available for public use. However, the structures and concepts outlined in this chapter provide an initial overview of such a database.

This chapter outlines the proposed structure of the data and the K_d parameters to be stored within a database for soil, freshwater and marine environments and provides an example of how such a database could be used in conjunction with the commercially available Tableau software⁹ to refine soil Cs K_d values based on soil characteristics and site specific *in situ* $K_{d(a)}$ values in the marine environment for use in REIA.

⁹ <https://www.tableau.com/products>

6.1.1. End user needs

To develop any database it is important to consult with potential end users to ensure that the database developed is fit for purpose. To determine the end user needs of a K_d database, a questionnaire was circulated to all MODARIA II programme participants to gauge the level of interest in the development of a database and to get an overview of the perspectives and current challenges of potential end users.

The following questions were presented to MODARIA II participants:

- (1) What do you use K_d data for, and how – what type of assessment?
- (2) What sources of information do you use for deciding on K_d values?
- (3) How useful would you find the development of a K_d database with an interactive front end, given your use of K_d ?
- (4) Please give a short example on how/when would you use a K_d interactive database.

There were 25 responses to the questionnaire from MODARIA II participants, including a group response from the WG7 on the Assessment of the Fate and Transport of Radionuclides Released in the Marine Environment.

The majority of respondents indicated that they used K_d values as part of safety assessments for storage or geological disposal of spent nuclear fuel. K_d values are also used for modelling the routine and accidental discharges from licensed sites of nuclear facilities, biosphere modelling, environmental impact assessments, remediation activities, and managing NORM waste.

The K_d values typically used in their assessments are mainly from IAEA publications such as IAEA TRS 422 [6.1] and TRS 472 [6.2], and other technical publications such as IAEA TECDOC 1375 [6.3] and TECDOC 1380 [6.4]. Other sources of information include scientific literature, site specific measurements, data from laboratory studies, or the use of other chemical analogues if data for specific elements or radionuclides are not available.

Most of the respondents stated that the development of a K_d database would be very useful for them, as it would provide a single source of data. However, such a dataset would only be effective if:

- (1) It included information on other factors that can influence K_d values, to allow for refinement of these values.
- (2) References for K_d values were included for verification purposes and to enable end users to further investigate the K_d values if needed.
- (3) The K_d values could be expressed in terms of both arithmetic mean and/or geometric mean with a distribution function.

These factors were considered and included in the development of the structure of the proposed database, to ensure the database could be used effectively by the end users in their assessments. Sufficient K_d values and data were identified to be included to enable refinement of the values based on the relevant factors influencing the behaviour of K_d for different radionuclides in the environmental compartments of interest.

6.1.2. The proposed K_d database structure

The proposed K_d database structure was primarily based on the existing dataset structures developed for both soil and freshwater compartments. At the time of development, a standard

structure did not exist for the K_d values in the marine environment. However, the IAEA’s MARIS database (see Chapter 5, Section 5.3.1) was identified as a possible repository of marine K_d values. The structure of the MARIS database provides a useful framework for determining the fields and tables that could be needed for the compilation of marine data. A standard data structure for all compartments was developed in Microsoft Access consisting of nine tables used to store both the K_d values and the ancillary data. The tables, fields, structure of the proposed database, their relationships, and a brief description of the key fields are outlined in Appendix I. A wide range of variables are included within the dataset for the three types of environment. Only some of the fields outlined in each table will be relevant for each of the environmental compartments. Therefore, only certain key fields in each table would be set to mandatory fields, which the user would need to provide. The majority of fields are optional for the user.

6.2. CURRENT STATUS OF THE PROTOTYPE K_d DATABASE

The K_d database structure outlined in Section 6.1.2 was tested using caesium K_d data for soil, freshwater and marine compartments. The data was imported using Microsoft Access after reconfiguration and harmonization of the existing caesium Microsoft Excel datasets for soil, freshwater and marine environments. A summary of the imported data sets is outlined in Table 6.1.

6.3. EXTRACTION AND REFINEMENT OF K_d DATA FROM THE PROTOTYPE DATABASE

End users of a K_d database need a simple, intuitive approach for the extraction and refinement of data for use in assessments. An effective tool was sought to fulfil this in conjunction with the end user needs outlined in Section 6.1.1. The commercially available Tableau data visualization software¹⁰ was chosen as a suitable tool as it is also capable of data analysis that can be utilized to refine datasets relatively easily from the prototype K_d database.

Two examples of the application of Tableau are provided below. One example describes of the refinement of the Cs K_d dataset and the estimation of the radiocaesium interception potential (RIP) for soil. The other example considers marine Cs K_d values based on site specific *in situ* $K_{d(a)}$ data.

TABLE 6.1. SUMMARY OF Cs K_d ENTRIES AND ANCILLARY DATA IMPORTED TO THE K_d DATABASE

| Cs K_d entries to the data table | Soil (S) | Fresh water (FW) | Marine (M) |
|------------------------------------|----------|------------------|------------|
| Cs K_d (S+FW+M) | 769 | 981 | 282 |
| Solid data (FW+M) | n.a. | 981 | 282 |
| Liquid data (FW+M) | n.a. | 981 | 282 |
| Location data | n.a. | 82 | 138 |
| References | 31 | 46 | 10 |

n.a.: not applicable.

¹⁰ Tableau, Oriol Toll Public Profile, (2020).
<https://public.tableau.com/profile/oriol.toll6623#!/vizhome/SoilDatabase/Compartment>

6.3.1. Example of refinement of soil Cs K_d and estimation of the radiocaesium interception potential using the Tableau application

The visualization and analytical capabilities of the Tableau application can be readily demonstrated using the soil K_d dataset. Tableau can be used to derive a best estimate of Cs K_d and to display its variability through the refinement of several soil properties that influence K_d .

For example, within Tableau, the end user can be prompted to select an element. Upon selecting the Cs K_d option, the end user is presented with a dashboard. The dashboard can be used to estimate the Cs K_d and its related uncertainty through the refinement of four different filters covering time and soil properties:

- (1) Short term or long term: This filter distinguishes between short term and long term experimental approaches for the determination of K_d . Short term conditions would correspond to a short term radionuclide release, whereas long term conditions would be applicable to long term discharges such as those evaluated in safety assessments of deep geological disposal facilities.
- (2) Organic matter: The end user can refine the K_d values for a particular range of organic matter content (%) of the soil being considered.
- (3) Mineral or Organic: If the organic matter content of the soil is >50% for short term data or >90% for long term data the soil is classified as 'Organic', otherwise it is 'Mineral'.
- (4) Texture: Mineral soils only can be refined by selecting either sand (sand >65% and clay <18% with respect to the mineral matter) or clay + loam.

Through the refinement of the above soil properties, the Tableau software generates and plots a cumulative distribution function (CDF) based on the approach outlined in Chapter 3, Section 3.2.3 and as described in a recent study [6.5]. The following data can also be generated and reported:

- (1) The geometric mean (GM) of the refined dataset, which is calculated from the 50th percentile of the CDF;
- (2) The geometric standard deviation (GSD) calculated from the CDF;
- (3) The minimum and maximum K_d values in the refined dataset;
- (4) 5th and 95th percentile values of the CDF in the refined dataset;
- (5) The number of K_d values in the refined dataset.

The K_d soil data for Cs in the dataset can also be used to predict RIP based on the clay and silt contents in a soil sample. The end user is given two options to predict RIP, either through the cumulative distribution function outlined in Chapter 3, Section 3.2.3 or through the multivariate linear regression equation outlined in Section 3.3.5 (Eq. (3.5) [6.5]).

To determine the RIP through the cumulative distribution function, the end user can vary the clay (%) and soil (%) using sliding toolbars, which subsequently regenerates the cumulative distribution function. Tableau then calculates RIP parameters such as GM, GSD, minimum and maximum values based on the regenerated cumulative distribution function. Alternatively, the end user can calculate RIP by inputting specific values for clay (%) and soil (%) and generating the RIP using the linear model.

6.3.2. Example of refinement of marine K_d values using the prototype database

Site specific K_d data are also important for end users in REIA, especially for environmental compartments that are not in a state of equilibrium. A lack of equilibrium may occur in both marine and coastal environments after short term inputs; for example, the Baltic Sea, as a result of fallout from the accident at the Chernobyl NPP, and the coastline of Japan after the accident at the FDNPP. It can also occur because marine environments are not closed systems and K_d can vary as a result of different inputs and losses to the system over time. The marine K_d dataset within the prototype K_d database could be utilized in conjunction with the Tableau software to derive Cs $K_{d(a)}$ values for the Baltic Sea and around the coast of Japan using the data visualization functionality of the software¹¹.

All 282 marine $K_{d(a)}$ values in the prototype K_d database have location data, including GPS coordinates and location codes, associated with the $K_{d(a)}$ values that can be used to refine the data based on the *in situ* sampling locations. If the prototype K_d database is linked to the Tableau application, the marine $K_{d(a)}$ is visualized on satellite image as shown in Fig. 6.1.

The user can select the location(s) of interest using the selection tools on the dashboard, and the $K_{d(a)}$ dataset is then refined based on the user selection. For example, a user can select the measurement locations on the Japanese coastline and compare these data to the $K_{d(a)}$ derived from measurements made in the Baltic Sea as seen in Table 6.2.



FIG. 6.1. A visualization of site specific $K_{d(a)}$ values mapped in the Baltic Sea and around Japan using Tableau mapping functionality.

¹¹ Tableau, Paul McGinnity Public Profile, (2020).
<https://public.tableau.com/s/profile/paul.mcginnity6639#!/vizhome/MarineKddatasatellite/Maplocations>

TABLE 6.2. REFINEMENT OF Cs $K_{d(a)}$ BASED ON MEASUREMENT LOCATION

| Location | N | GM | GSD | Min | Max |
|------------|-----|-------------------|------|-----|-------------------|
| Baltic Sea | 207 | 2.5×10^3 | 4.37 | 28 | 62×10^3 |
| Japan | 70 | 2.8×10^3 | 2.14 | 540 | 102×10^3 |

6.3.3. Preliminary outcomes of using the Tableau application with the prototype K_d database

The Tableau application can be utilized to visualize, refine and analyse K_d data to better estimate K_d for the different environmental compartments. By coupling the prototype K_d database to the Tableau software, end users could interact relatively easily with the K_d database to generate the K_d values needed for assessments. As demonstrated in the example above, the outcome would be an estimation of K_d values through the refinement of soil properties and the use of maps to obtain $K_{d(a)}$ values for the marine environment [6.6].

Although the K_d database contains K_d data for soil, freshwater and marine environmental compartments, the refinement of the K_d values will differ for the three environments. Therefore, the dashboards in a tool such as Tableau used to refine K_d data for each of the compartments will need to be different, based on the factors influencing the behaviour of elements in the different compartments and specific end user needs for use in assessments.

6.4. THE WAY FORWARD

The structure and content of a prototype database has been developed to store K_d values and all other relevant data for soil, freshwater and marine environments. A prototype database has been created using Microsoft Access and successfully tested using Cs datasets from the soil, freshwater and marine environmental compartments. The analysis suggests that the K_d datasets for the three environments can be stored in a single repository in a standard format.

The commercially available Tableau software could be configured so that end users of the data can obtain the K_d values they need for all environmental compartments based on their own specific needs for REIA. However, additional work would be needed to ensure the prototype K_d database is further developed into an integrated system.

The database structure has been tested using Cs datasets, but data for all elements in all three compartments are not yet available to populate an entire database. A significant amount of work was conducted to harmonize the data structure across the three compartments and an import template was developed for adding K_d data to the database. The K_d data for all elements would need to be compiled in the import template and be critically reviewed before importing them into the database, to ensure the quality of the dataset. Import functionality would need to be configured to ensure the data can be easily uploaded once new data become available.

Further development of end user functionality in Tableau would be needed. The feedback received from potential end users has indicated that the development of the K_d database would be applicable and useful for REIA. High level requests from these potential users have been compiled. Development of specific end user functionality is needed based on specific end user needs and the characteristics that can influence K_d in the soil, freshwater and marine compartments. The use of the K_d database in conjunction with transport and assessment models, such as CROM, SYMBIOSE and RESRAD (Annex I), also needs to be considered.

Finally, future development and configuration of the database can only occur if a suitable database host is available and sufficient maintenance and development can be supported.

REFERENCES TO CHAPTER 6

- [6.1] INTERNATIONAL ATOMIC ENERGY AGENCY, Sediment Distribution Coefficients and Concentration Factors for Biota in the Marine Environment, Technical Reports Series No. 422, IAEA, Vienna (2004).
- [6.2] INTERNATIONAL ATOMIC ENERGY AGENCY, Handbook of Parameter Values for the Prediction of Radionuclide Transfer in Terrestrial and Freshwater Environment, Technical Reports Series No. 472, IAEA, Vienna (2010).
- [6.3] INTERNATIONAL ATOMIC ENERGY AGENCY, Determining the suitability of materials for disposal at sea under the London Convention 1972: A radiological assessment procedure, IAEA-TECDOC-1375, IAEA, Vienna (2003).
- [6.4] INTERNATIONAL ATOMIC ENERGY AGENCY, Derivation of activity limits for the disposal of radioactive waste in near surface disposal facilities, IAEA-TECDOC-1380, IAEA, Vienna (2003).
- [6.5] RAMÍREZ-GUINART, O., et al., Deriving probabilistic soil distribution coefficients (K_d). Part 2: Reducing caesium K_d uncertainty by accounting for experimental approach and soil type, J. Environ. Radioactiv. **222-223** (2020) 106407. <https://doi.org/10.1016/j.jenvrad.2020.106407>
- [6.6] KELLEHER, K., MCGINNITY, P., HOWARD, B.J., BOYER, P., VIDAL, M., BILDSTEIN, O., The use of the IAEA MARIS database in determining the variability of sediment distribution coefficients in the marine environment and potential implications for marine dispersion modelling, J. Radiol. Prot. **42** 3 (2022) 501. <https://iopscience.iop.org/article/10.1088/1361-6498/ac8a53>

7. SUMMARY AND CONCLUSIONS

DANIEL KAPLAN

Savannah River Ecology Laboratory, University of Georgia, USA

MIQUEL VIDAL

Universitat de Barcelona, SPAIN

PATRICK BOYER

Institut de Radioprotection et de Sûreté Nucléaire (IRSN), FRANCE

KEVIN KELLEHER

Environmental Protection Agency, IRELAND

BRENDA HOWARD

UK Centre for Ecology and Hydrology, UNITED KINGDOM

University of Nottingham, Nottingham, UNITED KINGDOM

ANDRA HARBOTTLE

International Atomic Energy Agency

K_d is used within radiological impact assessment models, since it is the simplest parameterization that can be practically used to describe how dissolved radionuclides interact with solids in terrestrial, freshwater and marine systems. The most common uses of K_d are to predict how radionuclides move through porous and fractured media and radionuclide partitioning between water and suspended particles in freshwater and marine systems. K_d values are also used to predict the desorption of radionuclides from various materials (i.e. to predict the amount and rate that radionuclides desorb from contaminated materials). Another use of K_d values is to predict the tendency of radionuclides to be taken up by plants.

K_d is an important parameter for all aquatic and some terrestrial models, although it represents a simplification of the underlying processes occurring under field conditions. It is necessary, therefore, to understand how these simplifications may influence model outcomes. For example, if a radionuclide is not reversibly bound to a soil (e.g. for high- K_d radionuclides), the reversibility assumption commonly made by hydrologists may not be valid and may influence interpretation of the resultant calculations. However, for screening purposes, it may be pragmatic to apply K_d values in a conservative manner to identify whether transfer pathways are important or not.

An improved K_d dataset for soils and freshwater sediments have been compiled that includes chemical, physical, mineralogical and other ancillary properties associated with the K_d values, as well as information on the methodology used to determine the K_d values, to assist the end user in selecting appropriate K_d values, particularly in cases where complex modelling approaches are needed. The freshwater dataset has been updated from that reported in TRS 472 [7.1] and has been critically reviewed. An improved dataset for K_d values in soils has been compiled, using Am and Cs as examples. This soil K_d dataset (for Am and Cs) illustrates the improvement of the selection and derivation of soil K_d values for given situations using a new approach based on secondary soil properties and an improved statistical treatment of the data.

A systematic approach for selecting high quality data for inclusion in K_d datasets has been developed. Data that did not include sufficient information about the methodology or conditions of the aqueous and solid phase were generally rejected. Furthermore, measurements made under

extreme environmental conditions that are not common in natural systems (e.g. extreme pH, salinity, or highly elevated radionuclide activity concentrations) were also rejected. This process has greatly improved the quality and value of the datasets for use by the international community.

There are several radionuclides for which there are few, or no, reliable K_d values. In cases where such radionuclides could be relevant in a radiological impact assessment, missing data needs to be estimated, typically using chemical analogues (elements that are not identical but may geochemically behave like other elements for which data are available), or data from other similar environmental solid materials analogous to soils and sediments. To facilitate this, datasets have been constructed that include and generate analogous data.

K_d values often vary greatly, creating uncertainty in estimations of radionuclide activity concentrations in particles versus water and corresponding radiological exposure. However, such variability can be greatly reduced by grouping K_d data based on identified key characteristics of the solid and liquid phases that influence radionuclide sorption. For soils K_d , (see Chapter 3) these key factors were identified in two case studies (radio-caesium and americium) through statistical analysis of available datasets and knowledge of the mechanisms governing interactions. The developed approach now supports the generation of distribution functions for K_d for some radionuclide solid matrix combinations, thereby allowing sensitivity analyses, as not only best estimate K_d values (such as GM) are provided, but also quantitative estimations of their variability.

While site specific K_d values are generally the preferred choice of modelers, such values are often not available and make it difficult to extrapolate data between different sets of conditions. Therefore, an informed selection of the most relevant values is needed, as well as a better understanding of the processes affecting variability in K_d values. For the marine system, first steps have been taken using the same approach that has been applied in freshwater systems.

For the marine system, further work is needed to update and critically review the $K_{d(a)}$ dataset. For example, a critical review of the existing marine $K_{d(a)}$ data is needed to ensure that the way they were measured is appropriate for modelling of transport and radiological impact assessment, and that it accounts for 'reversible' sorption. Many of these data comprise radionuclide concentration measurements comparing filtered and unfiltered aqueous marine samples. An issue is that a fraction of the radionuclide assumed to be in the 'exchangeable' form would be held within the structure of the particles, and therefore, would not be 'exchangeable' with the aqueous phase. Furthermore, some marine $K_{d(a)}$ values were converted to 'exchangeable K_d ' through the use of a constant factor (0.2) in TRS 422 [7.2]. Recent data have shown that the application of this constant factor is not consistent with measured values for specific radionuclides. Anthropogenic isotopes may also provide useful $K_{d(a)}$ values.

K_d values vary greatly, and so it is important to understand the variability associated with ancillary data. Variability in K_d can be greatly reduced by identifying key factors relating to the solid and liquid phases that influence radionuclide sorption. Enhanced identification is needed of such key factors through statistical analysis of the dataset for more radionuclides than those used in the present publication to be able to apply such an approach in REIA. The methodology of K_d determination (e.g. desorption, sorption, *in situ*) has also been identified as a key factor that needs to be known to decrease K_d variability. This factor was not considered for all datasets in TRS 472 [7.1] and its consideration has been a major step forward in the work of MODARIA WG4.

Given the large variation in K_d data, it is important to not only provide estimates of its variability and uncertainty, but also distribution functions of K_d for a given radionuclide solid matrix combination (if sufficient data are available). Such distributions, as well as sensitivity analyses, would help to determine the influence of various parameters on K_d . Density functions are a useful tool not only to describe K_d distributions, but also to reduce variability through the exclusion of data that fall beyond appropriate percentile thresholds.

The next step could be to progress from independent datasets to an integrated, smart database. Suitable systems of accessing and interrogating the datasets could then be devised to derive K_d values, along with appropriate information on variability.

The use of the Tableau data visualization software has demonstrated that it can, in principle, be used to refine K_d values and distributions, based on appropriate solid and liquid parameters. Tableau has also been used to derive $K_{d(a)}$ in the marine environment based on empirical measurements of radionuclide concentrations in sea water and sediments. Therefore, the use of Tableau merits future consideration when developing suitable K_d database systems.

Future plans and remaining challenges have been identified and involve the following key tasks:

- (1) Identify key gaps in K_d data, and continue building the integrated K_d database for the soil and freshwater environments, especially for radionuclides relevant for consideration in radiological impact assessment. Also explore the use of analogue data to fill identified gaps;
- (2) Extend the Tableau approach to other radionuclides, such as Am, Cs or Ra, to help end users derive their own K_d best estimates values according to the scenarios to be assessed;
- (3) Identify other potential key factors to decrease variability in K_d and to facilitate K_d selection for a larger number of radionuclides, through statistical analyses and improved knowledge of the mechanisms governing radionuclide interactions;
- (4) Investigate the possibility of extracting appropriate data from the IAEA MARIS database to derive $K_{d(a)}$ for the marine environment;
- (5) Interact directly with K_d data end users to expand the use and improve the applicability of the newly developed datasets;
- (6) Compile datasets into a global K_d database appropriate for soils, freshwater, and marine systems for REIA, including the modelling of the impact of large accidental releases, such as the accident at the FDNPS).

REFERENCES TO CHAPTER 7

- [7.1] INTERNATIONAL ATOMIC ENERGY AGENCY, Handbook of Parameter Values for the Prediction of Radionuclide Transfer in Terrestrial and Freshwater Environment, Technical Reports Series No. 472, IAEA, Vienna (2010).
- [7.2] INTERNATIONAL ATOMIC ENERGY AGENCY, Sediment Distribution Coefficients and Concentration Factors for Biota in the Marine Environment, Technical Reports Series No. 422, IAEA, Vienna (2004).

APPENDIX I. PROTOTYPE K_d DATABASE TABLES AND FIELDS

This Appendix provides information on the database tables and fields in the prototype K_d database. The database has been developed in Microsoft Access and the proposed database structure is outlined in Fig. I.1.

I.1. THE K_d TABLE

The K_d Table (Table I.1) contains the K_d values in the 'RAW_VALUE' field (L/kg DM). The key information needed for all K_d values stored is the 'COMPARTMENT', 'ELEMENT', the type of 'KD_VALUE' and the 'DATA_TYPE' and these are all mandatory fields in the K_d table.

The 'COMPARTMENT' defines the environmental compartment of interest and is either the soil, freshwater or marine environment. The database currently has the capacity to store data for 84 elements and these are listed in the 'ELEMENT' table. The K_d types are defined in the 'KD_DEFINITION' Table in the database and are described in Table I.2.

The K_d data type describes the source of the K_d value, this can be data from a table with or without replicate values or data from a figure with or without an indication of the dispersion of the K_d value. These are defined in the KD_DATA_TYPE (Table I.2).

The remaining fields in the K_d table are:

- SOLID_ID – This links to the 'SOLID Table' (Table I.3);
- LIQUID_ID – This links to the 'LIQUID Table' (Table I.4);
- RADIONUCLIDE – The radionuclide used to determine the K_d value (if available) and this is linked to the 'ISOTOPE Table' (Table I.5), that currently contains 21 isotopes;
- REFERENCE – This is linked to the 'REFERENCE Table' (Table I.6) that outlines the source of the K_d value inputted to the database;
- METHODOLOGY – This outlines the methodology used to derive the K_d value. The various methodologies that could be included are sorption, desorption, adsorption and *in situ*;
- DEVICE – this field can be used to specify the device used to determine the K_d value if it is known;
- EXPERIMENTAL_APPROACH – outlines whether the experimental approach taken is long term or short term sorption or desorption, which is particularly important for soil K_d values;
- LOCATION – This links to the 'Location table' (Table I.7).

These fields are optional, and some are linked to other tables in the database but may not be needed for certain environmental compartments. A more detailed description of the database tables and their fields are outlined below.

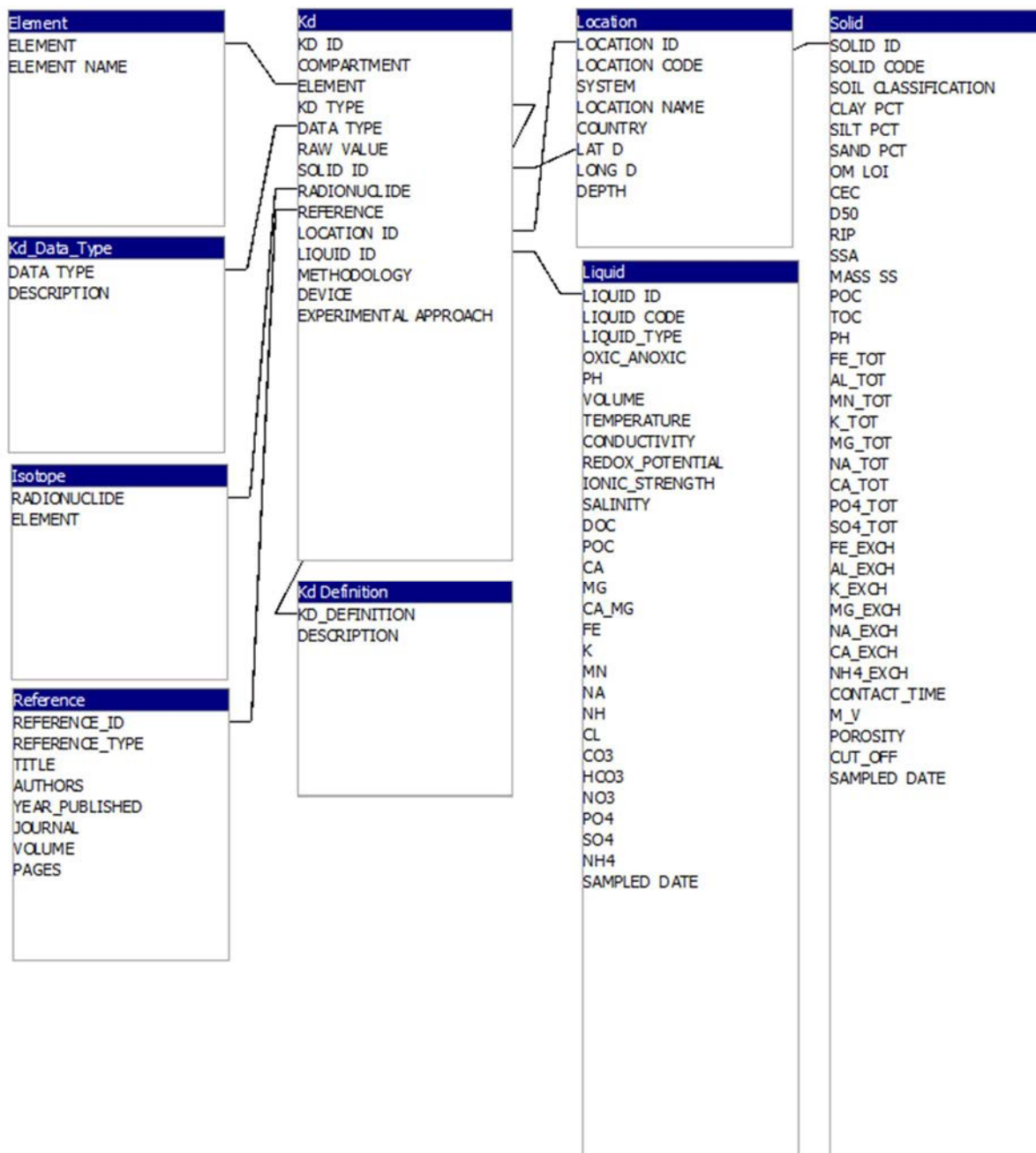


FIG. I.1. Prototype K_d database tables, fields, structure and relationships.

I.2. THE ‘SOLID TABLE’

The ‘SOLID table’ (Table I.3) in the K_d database contains information on the soils, geological materials analogue to soils, river and marine sediments (both bottom and suspended) used to determine the K_d values in the database. The table contains 36 fields, the majority of which are optional, to capture all the important factors in the solid matrices that could influence the variability of K_d in the soil, freshwater and marine environmental compartments.

These fields take into consideration various properties of solids and liquids that include:

- (1) Soil properties;
- (2) Physicochemical properties;
- (3) Total contents of chemical species;
- (4) The exchangeable fraction of these chemical species.

The soil property fields define the soil texture and the composition of the soil as percentages of clay, silt, sand and organic matter content (OM% or LOI%). The physicochemical properties of interest include, among others, the pH, the cation exchange capacity, exchangeable cations and the RIP.

I.3. THE ‘LIQUID TABLE’

The ‘LIQUID table’ (Table I.4) contains information on the river water and sea water used to determine the K_d values in all environmental compartments. These fields are optional and include:

- The liquid type: This defines whether the liquid is river water, estuarine water or sea water and can either be filtered or unfiltered.
- Physicochemical properties: The properties of interest are the oxic conditions (oxic, anoxic or unknown), pH, volume, temperature, electrical conductivity, redox potential, ionic strength, and salinity.
- Chemical composition: This includes dissolved organic carbon and the concentration of soluble cations and anions, among others.

I.4. THE ‘LOCATION TABLE’

The ‘LOCATION table’ (Table I.7) contains information on the location of the samples taken to derive the K_d values in the database. The location can be for the solid or liquid sample taken in the field and used in laboratory based experiments or could be related to a site specific *in situ* $K_{d(a)}$ values derived from measurements conducted in the field. The information recorded is entirely optional and can be as broad as the country from which the sample was taken but additional fields are also available to provide information on the system it was taken from e.g. a river system or sea, the depth at which the sample was taken and the specific GPS coordinates of the sampling if they are available. This information could be used by end users of the database if site specific data is needed for assessments.

TABLE I.1. TABLE STRUCTURE

| Field names | Description | Field Properties | Unit |
|-----------------------|---|---|------|
| KD_ID | The unique K_d ID for the database | Primary Key Field, Long Integer, Necessary, No Duplicates | n.a. |
| COMPARTMENT | Defines the Environmental Compartment | Short Text, Necessary | n.a. |
| ELEMENT | The K_d Element (linked to 'ELEMENT Table' (Table I.8)) | Short Text, Necessary | n.a. |
| KD_TYPE | The type of K_d (linked to ' K_d DEFINITION Table' (Table I.9)) | Short Text, Necessary | n.a. |
| DATA TYPE | The data type of the K_d (linked to ' K_d DATA TYPE Table' (Table I.10)) | Short Text, Necessary | n.a. |
| RAW VALUE | The K_d Value | Number, Scientific, Necessary | L/kg |
| METHODOLOGY | The method used to determine the K_d | Long Text, Optional | n.a. |
| SOLID_ID | The soil, sediment, suspended sediment associated with the K_d (links to 'SOLID Table' (Table I.3)) | Short Text, Optional | n.a. |
| RADIONUCLIDE | The radionuclide associated with the K_d (links to 'ISOTOPE Table' (Table I.5)) | Short Text, Optional | n.a. |
| REFERENCE | The source of the K_d value (links to the 'REFERENCE Table' (Table I.7)) | Short Text, Optional | n.a. |
| LOCATION_ID | The location associated with the K_d (links to 'LOCATION Table' (Table I.6)) | Short Text, Optional | n.a. |
| LIQUID_ID | The water or sea water associated with the K_d (links to the 'LIQUID Table' (Table I.4)) | Short Text, Optional | n.a. |
| DEVICE | The device used to determine the K_d | Short Text, Optional | n.a. |
| EXPERIMENTAL_APPROACH | The experimental approach used to determine the K_d | Long Text, Optional | n.a. |

n.a.: not applicable.

TABLE I.2. DEFINITION OF K_d VALUES IN THE PROTOTYPE K_d DATABASE

| K_d definition | Description |
|------------------|--|
| KdBS_PW | The ratio between the radionuclide concentration sorbed on a solid phase and the radionuclide concentration in the pore water between the solid phase. |
| KdBS_W | The ratio between radionuclide concentration sorbed on a solid phase and the radionuclide concentration in the filtered water of the water column. |
| KdBS_WC | The ratio between radionuclide concentration sorbed on a solid phase and the radionuclide concentration in the raw water (not filtered) of the water column. |
| kdNS | The ratio between radionuclide concentration sorbed on a solid phase and the radionuclide concentration in a liquid phase (not specified). |
| KdSS_W | The ratio between radionuclides concentration sorbed on solid matter suspended in the water column and the radionuclide concentration in the filtered water of the water column. |

TABLE I.3. SOLID TABLE

| Field names | Description | Field Properties | Unit |
|---------------------|--|---|-----------------------|
| SOLID_ID | The unique Solid ID for the database | Primary Key Field, Long Integer, Necessary, No Duplicates | n.a. |
| SOLID_CODE | Identifier of solid from original source | Short Text, Optional | n.a. |
| SOIL_CLASSIFICATION | Soil Texture (Sand, Silt, Clay) | Short Text, Optional | n.a. |
| CLAY_PCT | Percentage Clay | Short Text, Optional | % |
| SILT_PCT | Percentage Silt | Short Text, Optional | % |
| SAND_PCT | Percentage Sand | Short Text, Optional | % |
| OM_LOI | Percentage Organic Matter | Short Text, Optional | % |
| CEC | Cation Exchange Capacity | Short Text, Optional | mmol/kg |
| D50 | Median Diameter | Short Text, Optional | μm |
| RIP | Radiocaesium Interception Potential | Short Text, Optional | mmol/kg |
| SSA | Specific Surface Area | Short Text, Optional | m^2/g |
| POC | Percent Organic Carbon | Short Text, Optional | % |
| TOC | Total Organic Carbon | Short Text, Optional | mg/kg |
| PH | pH | Short Text, Optional | n.a. |
| FE_TOT | Iron content | Short Text, Optional | mg/kg |
| AL_TOT | Aluminium content | Short Text, Optional | mg/kg |

TABLE I.3. (cont.)

| Field names | Description | Field Properties | Unit |
|--------------|--------------------------------|----------------------|-------------------|
| PH | pH | Short Text, Optional | n.a. |
| FE_TOT | Iron content | Short Text, Optional | mg/kg |
| AL_TOT | Aluminium content | Short Text, Optional | mg/kg |
| MN_TOT | Manganese content | Short Text, Optional | mg/kg |
| K_TOT | Potassium content | Short Text, Optional | mg/kg |
| MG_TOT | Magnesium content | Short Text, Optional | mg/kg |
| NA_TOT | Sodium content | Short Text, Optional | mg/kg |
| CA_TOT | Calcium content | Short Text, Optional | mg/kg |
| PO4_TOT | Phosphate content | Short Text, Optional | mg/kg |
| SO4_TOT | Sulphate content | Short Text, Optional | mg/kg |
| FE_EXCH | Exchangeable Iron | Short Text, Optional | mmol/kg |
| AL_EXCH | Exchangeable Aluminium | Short Text, Optional | mmol/kg |
| MG_EXCH | Exchangeable Manganese | Short Text, Optional | mmol/kg |
| NA_EXCH | Exchangeable Sodium | Short Text, Optional | mmol/kg |
| CA_EXCH | Exchangeable Calcium | Short Text, Optional | mmol/kg |
| NH4_EXCH | Exchangeable Ammonium | Short Text, Optional | mmol/kg |
| CONTACT_TIME | Time spent exposed to liquid | Short Text, Optional | Days |
| M_V | Solid to liquid ratio | Short Text, Optional | Kg/m ³ |
| POROSITY | Porosity of solid | Short Text, Optional | % |
| CUT-OFF | | Short Text, Optional | n.a. |
| SAMPLED_DATE | Date of sampling of the liquid | Short Text, Optional | n.a. |

n.a.: not applicable.

TABLE I.4. LIQUID TABLE

| Field names | Description | Field Properties | Unit |
|-----------------|--|---|--------|
| LIQUID_ID | The unique Liquid ID for the database | Primary Key Field, Long Integer, Necessary, No Duplicates | n.a. |
| LIQUID_CODE | Identifier of liquid from original source | Short Text, Optional | n.a. |
| LIQUID_TYPE | Type of Liquid (sea water, river water estuary, etc.) | Short Text, Optional | n.a. |
| OXIC_ANOXIC | Oxic condition | Short Text, Optional | n.a. |
| PH | pH of liquid | Short Text, Optional | n.a. |
| VOLUME | Volume of liquid used for K_d determination | Short Text, Optional | L |
| TEMPERATURE | Temperature of liquid | Short Text, Optional | C |
| CONDUCTIVITY | Electrical conductivity of the liquid | Short Text, Optional | µS/cm |
| REDOX_POTENTIAL | The redox potential of the liquid | Short Text, Optional | mV |
| IONIC_STRENGTH | The ionic strength | Short Text, Optional | mol/kg |
| SALINITY | The salinity of the liquid | Short Text, Optional | g/kg |
| DOC | Dissolved Organic Carbon | Short Text, Optional | mg/L |
| POC | Percent Organic Carbon | Short Text, Optional | % |
| CA | Calcium content | Short Text, Optional | mg/L |
| MG | Magnesium Content | Short Text, Optional | mg/L |
| CA_MG | Calcium and Magnesium dissolved in the liquid (Hardness) | Short Text, Optional | mg/L |
| FE | Iron content | Short Text, Optional | mg/L |
| K | Potassium content | Short Text, Optional | mg/L |
| MN | Manganese content | Short Text, Optional | mg/L |
| NA | Total Sodium content | Short Text, Optional | mg/L |
| NH | Total Calcium content | Short Text, Optional | mg/L |
| CL | Total Calcium content | Short Text, Optional | mg/L |
| CO3 | Carbonate content | Short Text, Optional | mg/L |
| HCO3 | Bicarbonate content | Short Text, Optional | mg/L |
| NO3 | Nitrate content | Short Text, Optional | mg/L |
| PO4 | Phosphate content | Short Text, Optional | mg/L |
| SO4 | Sulphate content | Short Text, Optional | mg/L |
| NH4 | Ammonium content | Short Text, Optional | mg/L |
| SAMPLED_DATE | Date of sampling of the liquid | Short Text, Optional | mg/L |

n.a.: not applicable.

TABLE I.5. ISOTOPE TABLE

| Field names | Description | Field Properties | Unit |
|--------------|-------------|---|------|
| RADIONUCLIDE | Isotope | Primary Key Field, Short Text, Necessary, No Duplicates | n.a. |
| ELEMENT | Element | Short Text, Necessary | n.a. |

n.a.: not applicable.

TABLE I.6. REFERENCE ID

| Field names | Description | Field Properties | Unit |
|----------------|---|---|------|
| REFERENCE_ID | The unique Reference ID for the database | Primary Key Field, Short Text, Necessary, No Duplicates | n.a. |
| REFERENCE_TYPE | Source of Reference (Journal, Thesis, Paper etc.) | Short Text, Optional | n.a. |
| TITLE | Reference Title | Short Text, Optional | n.a. |
| AUTHORS | Authors | Short Text, Optional | n.a. |
| YEAR PUBLISHED | Year of Publication | Number, Optional | n.a. |
| JOURNAL | Journal Name | Short Text, Optional | n.a. |
| VOLUME | Volume Number | Short Text, Optional | n.a. |
| PAGES | Page Numbers | Short Text, Optional | n.a. |

n.a.: not applicable.

TABLE I.7. LOCATION TABLE

| Field names | Description | Field Properties | Unit |
|---------------|---|---|------|
| LOCATION_ID | The unique Location ID for the database | Primary Key Field, Short Text, Necessary, No Duplicates | n.a. |
| LOCATION_CODE | Identifier of Location from original source | Short Text, Optional | n.a. |
| SYSTEM | Environmental System (River, Estuary, Sea, Ocean) | Short Text, Optional | n.a. |
| LOCATION_NAME | Location Name | Short Text, Optional | n.a. |
| COUNTRY | Country | Short Text, Optional | n.a. |
| LAT_D | Decimal Latitude | Short Text, Optional | n.a. |
| LONG_D | Decimal Longitude | Short Text, Optional | n.a. |
| DEPTH | Depth of sampling location | Short Text, Optional | M |

n.a.: not applicable.

TABLE I.8. ELEMENT TABLE

| Field names | Description | Field Properties | Unit |
|--------------|----------------|---|------|
| ELEMENT | Element Symbol | Primary Key Field, Short Text, Necessary, No Duplicates | n.a. |
| ELEMENT_NAME | Element Name | Short Text, Necessary | n.a. |

n.a.: not applicable.

TABLE I.9. K_d DEFINITION TABLE

| Field names | Description | Field Properties | Unit |
|---------------|--|---|------|
| KD_DEFINITION | The unique Reference ID K_d Definition | Primary Key Field, Short Text, Necessary, No Duplicates | n.a. |
| DESCRIPTION | Description of K_d | Short Text, Necessary | n.a. |

n.a.: not applicable.

TABLE I.10. K_d DATA TYPE TABLE

| Field names | Description | Field Properties | Unit |
|-------------|--------------------------------|---|------|
| DATA_TYPE | The K_d Data Type | Primary Key Field, Short Text, Necessary, No Duplicates | n.a. |
| DESCRIPTION | Description of K_d Data Type | Short Text, Necessary | n.a. |

n.a.: not applicable.

ANNEX I. EXAMPLES OF THE USE OF K_d VALUES IN MODELS AND CODES

DANIEL KAPLAN

Savannah River Ecology Laboratory, University of Georgia, USA

MIQUEL VIDAL

Universitat de Barcelona, SPAIN

PATRICK BOYER

Institut de Radioprotection et de Sûreté Nucléaire (IRSN), FRANCE

CHRISTOPHE MOURLON

Institut de Radioprotection et de Sûreté Nucléaire (IRSN), FRANCE

VALERIE NICOULAUD-GOUIN

Institut de Radioprotection et de Sûreté Nucléaire (IRSN), FRANCE

BRENDA HOWARD

UK Centre for Ecology and Hydrology, UNITED KINGDOM

University of Nottingham, Nottingham, UNITED KINGDOM

JUAN CARLOS MORA

CIEMAT, SPAIN

CHARLEY YU

Argonne National Laboratory, USA

There are several ways in which models use K_d values to estimate radionuclide partitioning. Some examples for transport and assessment models and codes are given in this Annex.

I-1. INTEGRATION OF THE K_d PARAMETER INTO TRANSPORT MODELS

The retardation factor, R_f (unitless), is defined as:

$$R_f = \frac{v_p}{v_c} \quad (\text{I-1})$$

where:

v_p is the velocity of the water through a control volume (m/s);

v_c = velocity of the radionuclide through the controlled volume (m/s).

The retardation factor does not equal unity when the radionuclide interacts with a solid phase, almost always the retardation factor is greater than 1 due to solute sorption. In rare cases, the retardation factor is less than 1, due to anion exclusion or colloid facilitated transport. To predict the effects of retardation, sorption processes need to be described in quantitative terms, and the K_d provides such a quantitative estimate. To incorporate the K_d value into the R_f term, data are needed for the bulk density (ρ_b) and effective porosity (n_e) of the medium. For porous flow with saturated moisture conditions, the relationship between K_d and R_f is as follows:

$$R_f = 1 + \frac{\rho_b}{n_e} K_d \quad (\text{I-2})$$

When the K_d term is incorporated into the R_f term, the latter implicitly assumes that the reactions go to equilibrium and are reversible and that the chemical environment along the solute flow path does not vary in either space or time [I-1].

I-2. EXAMPLES OF HOW K_D VALUES ARE USED IN SPECIFIC CODES

I-2.1. CROM

CROM¹² [I-2–I-4] is a code designed to calculate: (1) radionuclide transfer between various environmental compartments; (2) radionuclide transfer to the human food chain; (3) effective dose to humans; and (4) absorbed dose to biota. The code is distributed by the IAEA and can be downloaded from <ftp://ftp.ciemat.es/pub/CROM>.

CROM includes generic models for dilution and diffusion, based on SRS 19 [I-5], and allows the use of site specific values. To estimate the radionuclide activity concentrations in environmental media, CROM needs input of the quantities of each radionuclide in the source, the mode and characteristics of the discharge, and the receptor points.

The atmospheric dispersion model is a Gaussian plume model that estimates the annual averaged radionuclide concentrations in air [I-6]. Input needed for each individual air concentration calculation are wind direction and the geometric mean (GM) of the wind speed at the release point. Different diffusion factors for different atmospheric stability categories other than D (neutral), and effective heights can be included in the CROM calculation.

The surface water models are analytical solutions of advection–diffusion equations describing radionuclide transport in surface water with steady state uniform flow conditions. They estimate radionuclide dispersion in rivers, small lakes, large lakes, estuaries, and along the coast. Transfer of radionuclides from atmospheric deposition to surface water can also be calculated.

The terrestrial food chain models estimate the buildup of radionuclides on surface soil and vegetation from the atmosphere and the hydrosphere. These models account for radioactive decay. Calculations of radionuclide uptake and retention by aquatic biota is based on bioaccumulation factors (radionuclide concentration ratio of biota to water).

CROM calculates the effective dose or biota absorbed dose for combined external and internal sources based on estimated radionuclide concentrations in air, soil, sediment, food and water discharged, as well as the annual rates of intake, occupancy factors, and dose conversion coefficients. The dose conversion coefficients are taken from GRS Part 3 [I-7] for internal exposure for humans and from Federal Guidance Report No 12 [I-8] for external exposure for humans.

Several parameters for absorbed dose assessments for biota were taken from the ERICA Tool and are included in the code database, comprising 163 radionuclides for humans and 63 radionuclides for biota in total. Furthermore, CROM can propagate uncertainties using Monte Carlo methods. The code allows the use of probability density functions for almost all the parameters and variables used in the code. Radionuclide activity concentrations in plants are calculated using transfer factors from the concentration in the water source, and the radionuclide activity concentration in soils can be estimated from that in the irrigation water by using default K_d values.

In the IAEA publication SRS 19 [I-5], K_d values are used to calculate the fraction of the radionuclides sorbed by the sediments in all aquatic systems due to contamination of the unfiltered water. In the most conservative, simple, approach of SRS 19, the effect of sediment sorption is neglected, but for a more detailed assessment K_d values are used for the calculation

¹² CROM. Intellectual Property Registry No M-000481/2006. Registration Entry 16/2011/3841, 12 May 2011.

of radionuclide activity concentrations in sediments and filtered water. This approach is also used in CROM. Radionuclide activity concentrations in plants and aquatic biota are calculated using transfer and bioaccumulation factors from the concentration in unfiltered water, so that the radionuclide activity concentration in soil can be estimated from that in irrigation water.

I-2.2. SYMBIOSE

In SYMBIOSE, K_d values are used in the river abiotic module, the sea abiotic module and in soil modules.

I-2.2.1. Abiotic sea module

The abiotic sea module of SYMBIOSE uses an equilibrium approach, whereby K_d values are used via Eq. I-3 to derive radionuclide activity concentrations (A_i) in the sand and/or sediment from those in sea water (C_i):

$$K_d = \frac{A_i}{C_i} \quad (\text{I-3})$$

I-2.2.2. Abiotic river module

The abiotic river module of SYMBIOSE is the CASTEAUR model [I-9–I-11]. In CASTEAUR, the river is described through its water column and three sediments layers: interface, active, and passive. To calculate the radionuclide fluxes between these layers, the radioecological model is coupled to a sedimentary dynamic model involving several classes of suspended particles described by their specific K_d and sedimentary parameters. In the water column, K_d values are used to determine radionuclide fractionation between the dissolved and particulate phases as a function of these particle classes (using Eq. I-3) weighting K_d values as a function of particle size [I-12]. Applying the assumption that the interface and active layers are geochemically similar (i.e. they are both oxygenated), the same K_d values are assigned to both layers to determine radionuclide fractionation between particles and interstitial water.

For soils, SYMBIOSE allows the user to select either a ‘simple’ soil model or a vadose soil model.

I-2.2.3. Simple soil model

For the simple soil model, SYMBIOSE offers two sub models: a single layer model or a two layer model.

- In the single layer model, radionuclide activity concentrations are instantly diluted in the rooting layer depth of the soil. In this model, K_d values are used to evaluate a migration activity flux that transfers the radionuclide from the bioavailable pool of radionuclides in the root layer to the less mobile underlying layer. These calculations need to estimate the proportion of radionuclide that exists in the interstitial solution and can be carried away by infiltrating water.
- The two layer model includes a surface layer which lies above the root layer. Contamination is assumed to be homogeneous in each layer. K_d values are used to calculate the surface migration flux that transfers the radionuclide from the surface layer to the root layer. A migration flux is used from the root layer to the underlying layer which is considered to be external to the parts of the environment (spatial, temporal, compartments and components) that are represented by the model.

I-2.2.4. Vadose soil model

In this soil model, the soil can be vertically divided into successive layers in which liquid/solid exchanges are governed by an equilibrium kinetic approach distinguishing between two types of solid site: one with a rapid equilibrium between solid and liquid phase (using K_d values) and one governed by kinetically limited exchanges. The spatial migration of the dissolved radionuclide by convection and dispersion is also modeled.

The Vadose soil model is more precise in time and space than the Simple Soil Model, but it needs more memory and more calculation time. In practice, the choice between these two models depends on operational criteria related to calculation times and/or memory capacities.

I-2.3. RWM biosphere model

The Radioactive Waste Management Limited (RWM) biosphere model is published in Refs [I-13, I-14] and forms the basis of the following text. The terrestrial soil-plant model is based on principles given in Ref. [I-15].

The terrestrial component of the RWM biosphere model relates to agricultural ecosystems and includes a point scale model employing two soil compartments (topsoil and subsoil). Water flows into, out of, and between these compartments are specified, but the degree of saturation of the compartments is not computed. The K_d values for the soils are based on information given in Ref. [I-16], but in defining distributions for use in the assessment, the following additional considerations are applied:

- (1) Similar K_d values are expected for lanthanide and higher actinide elements;
- (2) Soil sorption coefficients are typically taken to be log-normally distributed. However, in cases where there are relatively few data or very wide distributions, then a log-normal distribution is not appropriate, and a log-uniform distribution is used.

The primary use of the K_d values is to represent the retardation of radionuclides in their transport between and out of the two soil compartments. In the freshwater system, the distribution coefficient is used only to derive the fraction of radionuclide in solution, e.g. to define the concentration assumed to be present in drinking water.

The soil K_d values are also used to estimate the plant/soil concentration ratio (CR). Based on the assumption that plants primarily take up radionuclides from the porewater solution phase, CR values can be calculated using the K_d value as follows:

$$CR = \frac{\delta}{(\theta + \rho_b K_d)} \quad (I-4)$$

where:

δ is the affinity for plants to take up an element from the soil solution to the edible component of the plant;

θ is the water filled porosity;

ρ_b is the bulk density (kg/m^3).

A similar approach to that used in the RWM model for soils and plants is adopted in the PRISM model developed for the UK Food Standards Agency, but in that case in the context of a multilayer soil model in which the degree of saturation of the individual soil layers varies on a monthly basis [I-13, I-14, I-17].

The estuarine and marine model developed for RWM uses a compartmental approach implemented in GoldSim. Water and solid flows between the compartments are computed. Each region in the model comprises a vertical column that consists of a water compartment, including both bulk water and suspended sediments, and several underlying sediment compartments, comprising solids and included pore water. Water and solid transport occur between adjacent pairs of compartments throughout the vertical column (i.e. both water flow and sediment erosion and/or deposition are represented). Also, horizontal movement of water and suspended sediment occurs between the water compartments, and sediment exchanges occur between the marine environment and the beach. Distribution coefficients are used to partition radionuclides between bulk water and suspended sediments and between pore waters and deposited sediments.

I-2.4. CIEMAT soil–plant model

The CIEMAT soil–plant model has been described in Refs [I-17, I-18–I-20]. The model uses a water balance approach to calculate the monthly hydrological characteristics of a multilayered soil column, as in the PRISM model. Thus, for each month, each layer of the soil column is characterized by an upward or downward water flow across its boundaries and by a fractional water content, which is equal to the total porosity below the water table and then decreases across a user specified depth of capillary fringe to a lower value in the upper part of the soil. The position of the water table is altered at the end of each month based on the net water balance over the previous month. Drainage of the soil column and discharge of groundwater through its base can both be represented in terms of a water flux across the base of the column. Rates of radionuclide migration up and down the column are determined by rate constants defined by the ratio of the water flow outward across a layer boundary to the effective volume of the layer from which the flow originates:

$$\lambda = \frac{F}{d(\theta + \rho_b K_d)} \quad (\text{I-5})$$

where:

- λ (1/s) is the rate constant;
- F (m/s) is the flow per unit area;
- d (m) is the thickness of the layer;
- θ is the water filled porosity;
- ρ_b (kg m^{-3}) is the dry bulk density;
- K_d ($\text{m}^3 \text{ kg}^{-1}$) is the distribution coefficient.

The key feature in this model is that the water content, θ , is regarded as a surrogate for redox potential and, therefore, the K_d values of redox sensitive elements are defined as functions of θ . In practice, a simple distinction is made using linear interpolation between values defined to be applicable in dry soil above the capillary fringe and at saturation. Thus, the K_d value used varies linearly across the capillary fringe and changes with time as the water table moves up and down on a seasonal basis.

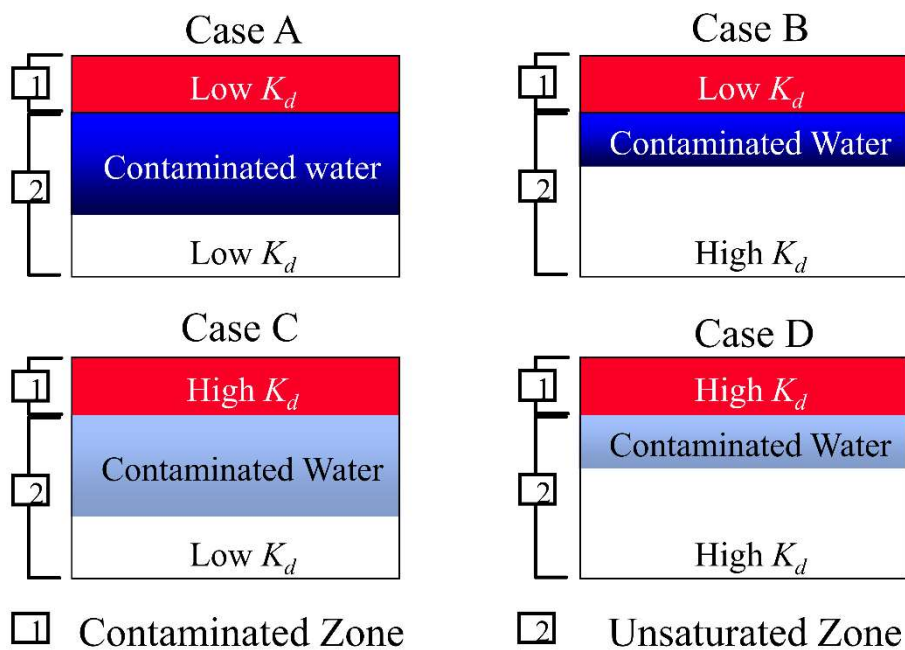


FIG. I-1. Changes in the transport of radionuclides according to the K_d values of surface contaminated and unsaturated uncontaminated soil layers (adapted from RESRAD training course, with permission).

I-2.5. RESRAD code: description of K_d in leaching and transport of radionuclides in soil column

For radioactively contaminated soil, the K_d is used in estimating the leaching of radionuclide from surface soil and transport in the unsaturated zone (vadose zone) and saturated zone (groundwater). The transport of radionuclides in the soil–water system is described by the advection–dispersion equation, which uses the retardation factor (Eq. (I-2)) to characterize the delay of radionuclide transport in the soil water system compared with the transport of water.

The effect of K_d on transport of radionuclides is illustrated in Fig. I-1. The top (surface soil) layer (Layer 1) is contaminated with radionuclides, whereas layer 2 is the unsaturated (and initially uncontaminated) zone. Cases A and B assume that the top contaminated zone has a low K_d compared with Cases C and D, which top layers have a high K_d . For Cases A and B, radionuclides would leach out more quickly due to the low K_d in the surface soil (Zone 1), and hence the concentration in the unsaturated zone (Zone 2) is higher (shown with darker blue colour) when compared with Cases C and D (with lighter blue colour). In Cases A and C the unsaturated regions (Zone 2) have a low K_d compared to Cases B and D. Hence, the radionuclides would travel faster and move downward farther compared with Cases B and D, respectively.

I-2.6. THE ERICA Tool

The ERICA Tool was developed as an assessment tool to characterize radiological impacts on wildlife [I-21]. The software is freely available for download (<http://www.ERICA-tool.com>). The ERICA Tool was designed with particular emphasis upon planned, routine discharges of radionuclides. It allows assessments for a comprehensive list of radionuclides and organism types.

In the ERICA Tool, $CR_{wo-water}$ (wo = whole organism) values are used to estimate the whole body radionuclide activity concentration from that in the water. Sediment radionuclide activity concentrations are used to estimate external doses to organisms. Users can input either only sediment or water radionuclide activity concentrations and the tool will estimate that of the missing associated sediment or water using K_d values.

The impact of the K_d values varies, depending on whether the radionuclide is introduced via the water or the sediment. If the radionuclide enters the sediment, a high K_d will lead to relatively high external doses to benthic organisms, whereas a low K_d will lead to a relatively low external dose to benthic organisms. Conversely, when the radionuclide is discharged into the water, a low K_d would lead to a higher radionuclide activity concentration in water and, therefore, a relatively higher internal dose to aquatic organisms. A high K_d for this case will mean there is a low radionuclide activity concentration in water and, therefore, a relatively low internal dose to aquatic organisms (but a higher external dose to benthic organisms).

The development of the revised ERICA Tool databases relied heavily upon the $CR_{wo-media}$ values reported in Refs [I-16, I-22], while less focus was placed on K_d values. The majority of the distribution coefficients in the original version of the ERICA Tool for freshwater ecosystems have been derived from compilations of data by the IAEA in SRS 19 [I-5] and TRS 472 [I-16], with some values from Ref. [I-23]. However, when no data were available from these sources, there was widespread use of marine K_d values for freshwater ecosystems.

The ERICA Tool was revised in 2015 [I-24]. An important difference in this updated version is that default K_d values for freshwater ecosystems no longer originate from measurements primarily originating from marine systems. Only one freshwater K_d value, that for iridium, relies on measurements made in marine systems. For marine systems, all the K_d values were taken from TRS 422 [I-22] that provides recommended values, along with minimum and maximum values assumed to be within one order of magnitude of the recommended values. The ERICA Tool redefined these minimum and maximum values as 5th and 95th percentiles. The following Eqs (I-6) and (I-7) were used to estimate the 5th percentile and 95th percentile, respectively:

$$Min = \frac{recommended\ value}{10} = 5^{th} percentile \quad (I-6)$$

$$Max = recommended\ value \times 10 = 95^{th} percentile \quad (I-7)$$

Mean deviation (μ) and standard deviation (σ) were then derived assuming a log-normal distribution such that:

$$\mu = \frac{[\ln(Max) + \ln(Min)]}{2} \quad (I-8)$$

$$\sigma = \frac{[\ln(Max) - \ln(Min)]}{2 \times 1.6449} \quad (I-9)$$

and, for a log-normal distribution, the arithmetic mean (expected value) and its standard deviation were derived by the following equations:

$$Mean = e^{\mu + 0.5\sigma^2} \quad (I-10)$$

$$Standard\ deviation = \sqrt{(e^{\sigma^2} - 1) \cdot e^{2\mu + \sigma^2}} \quad (I-11)$$

REFERENCES

- [I-1] KRUPKA, K.M., KAPLAN, D.I., WHELAN, G., SERNE, R. J., MATTIGOD, S.V., Understanding Variation in Partition Coefficient, K_d , Values, Volume I: The K_d Model Measurement and Application of Chemical Reaction Codes, EPA402-R-99-004A, EPA, Washington, DC (1999).
<https://www.epa.gov/sites/default/files/2015-05/documents/402-r-99-004a.pdf>
- [I-2] ROBLES, B., SUAÑEZ, A., CANCIO, J.C.M.Y.D., Modelos implementados en el código CROM (Código de cRiba para evaluación de iMpacto). In: Colección Documentos Ciemat; CIEMAT, Madrid (2007).
- [I-3] MORA, J.C., et al., Generic Model for Combined Tier-1 Assessments for Humans and Wildlife; STAR (Contract Number: Fission-2010-3.5.1-269672) Deliverable (D-Nº3.1) (2015). DOI: [10.13140/RG.2.1.1020.5289](https://doi.org/10.13140/RG.2.1.1020.5289)
- [I-4] MORA, J.C., et al., CROM 8 – Integrated Dose Assessments for Humans and Non-Human Biota. (2016) doi:10.13140/RG.2.2.13782.45123. Available online: <ftp://ftp.ciemat.es>
- [I-5] INTERNATIONAL ATOMIC ENERGY AGENCY, Generic Models for Use in Assessing the Impact of Discharges of Radioactive Substances to the Environment, Safety Reports Series No. 19, IAEA, Vienna (2001).
- [I-6] MILLER, C.W., HIVELY, L.M., A review of validation studies for the Gaussian plume atmospheric dispersion model, Nucl. Saf. **28** (1987) 522.
https://www.researchgate.net/publication/236436685_A_Review_of_Validation_Studies_for_the_Gaussian_Plume_Atmospheric_Dispersion_Model#fullTextFileContent
- [I-7] EUROPEAN COMMISSION, FOOD AND AGRICULTURE ORGANIZATION OF THE UNITED NATIONS, INTERNATIONAL ATOMIC ENERGY AGENCY, INTERNATIONAL LABOUR ORGANIZATION, OECD NUCLEAR ENERGY AGENCY, PAN AMERICAN HEALTH ORGANIZATION, UNITED NATIONS ENVIRONMENT PROGRAMME, WORLD HEALTH ORGANIZATION, Radiation Protection and Safety of Radiation Sources: International Basic Safety Standards, IAEA Safety Standards Series No. GSR Part 3, IAEA, Vienna (2014), <https://doi.org/10.61092/iaea.u2pu-60vm>
- [I-8] ECKERMAN, K.F., RYMAN, J.C., Federal Guidance Report No. 12, External Exposure to Radionuclides in Air, Water, and Soil (EPA-402-R-93-081), U.S. Environmental Protection Agency, Washington, DC (1993).
<https://www.epa.gov/sites/default/files/2015-05/documents/402-r-93-081.pdf>
- [I-9] BEAUGELIN-SEILLER, K., BOYER, P., GARNIER-LAPLACE, J., ADAM, C., CASTEAUR, a simple tool to assess the transfer of radionuclides in waterways, Health Phys. **84** (2002) 539. DOI: [10.1097/00004032-200210000-00013](https://doi.org/10.1097/00004032-200210000-00013)
- [I-10] BOYER, P., BEAUGELIN-SEILLER, K., CASTEAUR, a tool for operational assessments of radioactive nuclides transfers in river ecosystems, Radioprotection – Colloques **37**(C1), (2002) 1127. <https://doi.org/10.1051/radiopro/2002136>
- [I-11] KRYSHEV, I.I., et al., Model testing of radioactive contamination by ^{90}Sr , ^{137}Cs and $^{239,240}\text{Pu}$ of water and bottom sediments in the Techa River (Southern Urals, Russia), Sci. Total Environ. **407** (2009) 2349.
<https://doi.org/10.1016/j.scitotenv.2008.12.012>

- [I-12] ABRIL, J.M., FRAGA, E., Some physical and chemical features of the variability of Kd distributions coefficients for radionuclides, *J. Environ. Radioact.* **30** (1996) 253. [https://doi.org/10.1016/0265-931X\(95\)00010-8](https://doi.org/10.1016/0265-931X(95)00010-8)
- [I-13] WALKE, R., THORNE, M., WATSON, C., LIMER, L., The PRISM Foodchain Modelling Software: Version 3.3 Technical Report, Quintessa Limited report to the Food Standards Agency QRS-3004G-1, Version 1.0 (2012).
- [I-14] WALKE, R.C., THORNE, M.C., LIMER, L.M.C., The PRISM food chain modelling software: version 3.3 data report, Quintessa report to the Food Standards Agency (FSA) QRS-3004G-2, Version 1.0 (2012).
- [I-15] STANSBY, S.J., THORNE, M.C., Generic Biosphere Modelling: Final Report. AEA Technology Report AEAT/R/ENV/0296 produced for United Kingdom Nirex Limited, Curie Avenue, Didcot, Harwell, Oxfordshire, OX11 0RH, UK, December 2000.
- [I-16] INTERNATIONAL ATOMIC ENERGY AGENCY, Handbook of Parameter Values for the Prediction of Radionuclide Transfer in Terrestrial and Freshwater Environment, Technical Reports Series No. 472, IAEA, Vienna (2010).
- [I-17] THORNE, M.C., Kinetic Models for Representing the Uptake of Radionuclides in Plants. In: Gupta D., Walther C. (eds) Radionuclide Contamination and Remediation Through Plants. Springer, Cham. (2014).
https://doi.org/10.1007/978-3-319-07665-2_11
- [I-18] PEREZ-SANCHEZ, D., THORNE, M.C., LIMER, L.M.C., A mathematical model for the behaviour of Se-79 in soils and plants that takes account of seasonal variations in soil hydrology, *J. Radiol. Prot.* **32** (2012) 11.
<https://doi.org/10.1088/0952-4746/32/1/11>
- [I-19] PÉREZ-SÁNCHEZ, D., THORNE, M.C., Modelling the behaviour of uranium-series radionuclides in soils and plants taking into account seasonal variations in soil hydrology, *J. Environ. Radioact.* **131** (2014) 19.
<https://doi.org/10.1016/j.jenvrad.2013.09.008>
- [I-20] KLOS, R.A., LIMER, L., SHAW, G., PEREZ-SANCHEZ, D., XU, S., Advanced spatio-temporal modelling in long-term radiological assessment models-radionuclides in the soil column, *J. Radio. Protection* **34** (2014) 31.
<https://doi.org/10.1088/0952-4746/34/1/31>
- [I-21] BROWN, J.E., et al., The ERICA Tool, *J. Environ. Radioact.* **99** (2008) 1371.
<https://doi.org/10.1016/j.jenvrad.2008.01.008>
- [I-22] INTERNATIONAL ATOMIC ENERGY AGENCY, Sediment distribution coefficients and Concentration Factors for biota in the Marine Environment, Technical Reports Series No. 422, IAEA, Vienna (2004).
- [I-23] COPPLESTONE, D., BIELBY, S., JONES, S.R., PATTON, D., DANIEL, P., GIZE, I., Impact Assessment of Ionising Radiation on Wildlife, R & D Publication 128, Environment Agency, Bristol, UK (2001).
<https://assets.publishing.service.gov.uk/media/642aa0717de82b000c313476/sr-dpub-128-e-e.pdf>
- [I-24] BROWN, J.E., et al., A new version of the ERICA Tool to facilitate impact assessments of radioactivity on wild plants and animals, *J. Environ. Radioact.* **153** (2016) 141. <https://doi.org/10.1016/j.jenvrad.2015.12.011>

ANNEX II. EFFECT OF MICROBIAL ACTIVITY ON THE K_d OF RADIOCARBON AND RADIOIODINE

SHIGEO UCHIDA, NOBUYOSHI ISHII and KEIKO TAGAMI

National Institutes for Quantum and Radiological Science and Technology (QST), JAPAN

NAO K. ISHIKAWA

Iwate University, JAPAN

Some elements (e.g. C, Se and I) are re-emitted from soil to the air in gaseous forms. Soil microorganisms play an important role in this phenomenon as some long lived radionuclides may also be discharged to the air through microbial activity changing their distributions between air-soil solution-soil particles [II-1–II-5]. Examples of the mechanism are given below for the effect of microbial activity on the K_d values of radiocarbon and radioiodine and of the releases as a gas.

II-1. CARBON-14 PARTITIONING IN THREE PHASES (SOLID, LIQUID, AND GAS) AND DISTRIBUTION COEFFICIENTS

Reference [II-6] mentions that ^{14}C transport from underground waste disposal needs to consider volatilization as a loss process from soil. Reference [II-7] investigated the partitioning percentages of ^{14}C in solid, liquid, and gas phases by a batch sorption technique using 97 paddy soil samples. Figure II-1 shows the solid, liquid and gas partitioning percentages of ^{14}C added as sodium acetate for 97 soil–solution batch cultures after 7 days incubation. About 30% of the total ^{14}C added was partitioned to the solid phase and that remaining in the liquid phase was small. The GM K_d at the end of incubation was 81 L/kg (range: 6.8–284 L/kg, log-normal distribution).

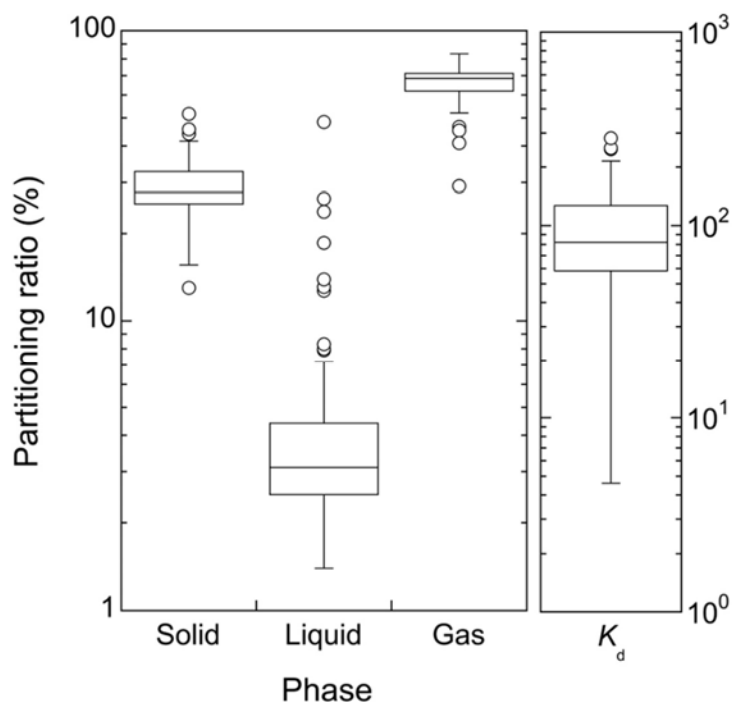


FIG. II-1. Boxplots illustrating the range of the partitioning percentages of ^{14}C for 97 paddy soils.

When soil microorganisms in the soil were sterilized by adding glutaraldehyde (1,5-Pentandial, sum formula $C_5H_8O_2$) with a final concentration of 2%, $(96.8 \pm 1.2)\%$ of the spiked ^{14}C remained in the liquid phase, while the rest of the ^{14}C was released into the air and no ^{14}C remained associated with the solid phase. For samples without glutaraldehyde, the partitioning ratios were like those discussed above.

The data showed that microorganisms play an important role in controlling the partitioning of ^{14}C in the liquid phase to the solid and gas phases [II-7, II-8]. Generally, for the determination of K_d , a specified amount of radionuclide is added and only the concentration in the liquid phase is measured. However, for C such a technique provides an overestimation of K_d because C releases into the gas phase are assumed to be fixed in the solid phase.

II-2. THE CHEMICAL FORM AND SORPTION OF IODINE IN SOIL SOLUTION

References [II-9, II-10] investigated the effect of biological activity on iodide (I^-) partitioning in solid, liquid, and gas phases in agricultural soils in Japan by changing the temperature and sterilizing soil samples.

A batch sorption experiment was conducted at $4^\circ C$ to minimize microbial activity and $23^\circ C$ to enhance microbial activity. For the $23^\circ C$ treatment two further variables were included of (i) chemical sterilization by addition of 0.05% (weight per volume) of streptomycin, tetracycline and cycloheximide, or (ii) glucose amendment. The variation of K_d in time under different experimental conditions is presented in Fig. II-2. The K_d values increased in the following order: sterilized \approx cool $<$ standard $<$ glucose added, which is consistent with the hypothesis that iodine partitioning to soil is microbially mediated. For the glucose added treatment, K_d slightly increased with contact time probably due to stimulation of biological activity. Together, these results suggest that biological activity had a significant effect on the sorption kinetics of I^- in soil.

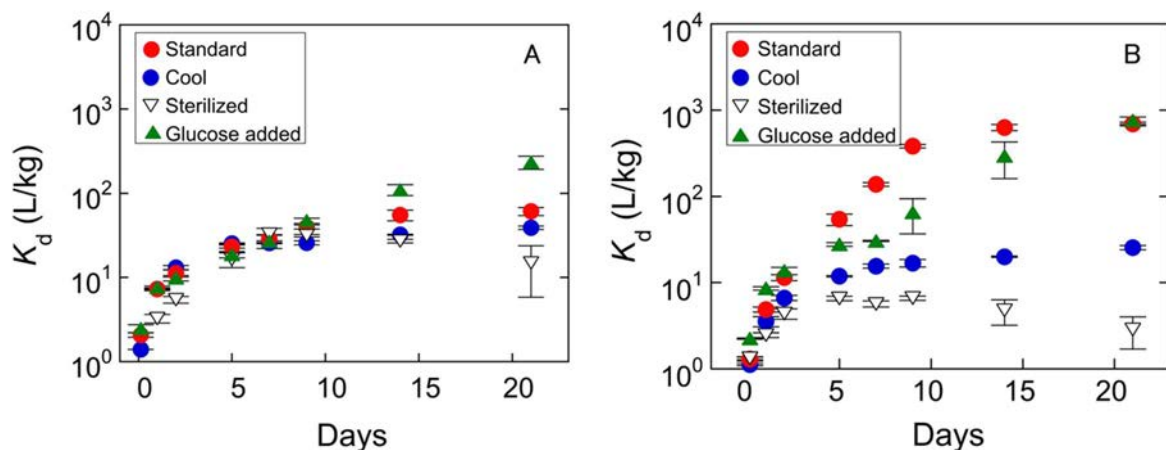


FIG. II-2. Time variation of iodine (added as iodide) K_d values for two soils for 4 different experimental condition sets: standard ($23^\circ C$), cool ($4^\circ C$), sterilized and glucose added. Error bars show standard deviation (1σ) of 3 replicates.

TABLE II-1. GM OF PARTITIONING PERCENTAGES (%) OF IODINE (ADDED AS IODIDE (I⁻) INTO SOLID, LIQUID AND GAS PHASES IN THE BATCH SORPTION TEST FOR 63 PADDY AND 79 UPLAND SOILS (RANGES ARE SHOWN IN PARENTHESES)

| Land use | Phase ^a | Partitioning (%) | |
|---------------|--------------------|------------------|-------------|
| | | 4 °C | 23 °C |
| All | Solid | 50 (13–84) | 63 (26–100) |
| | Liquid | 36 (11–87) | 17 (2–64) |
| | Gas | 6 (0–27) | 11 (0–42) |
| Paddy fields | Solid | 61 (16–84) | 73 (29–100) |
| | Liquid | 28 (11–82) | 10 (2–64) |
| | Gas | 7 (0–27) | 13 (0–42) |
| Upland fields | Solid | 42 (13–75) | 57 (26–92) |
| | Liquid | 46 (16–87) | 27 (5–64) |
| | Gas | 6 (0–15) | 9 (20–26) |

^a Partitioning ratio in solid (P_S), liquid (P_L) and gas (P_G) phases, are defined by Eqs (II-1), (II-2), and (II-3), respectively.

Table II-1 shows the ranges of solid, liquid, and gas phases partitioning ratios (P_S , P_L and P_G) at each temperature for 63 paddy and 79 upland soil samples. The equations below were applied for the calculation of partitioning ratios in solid, liquid and gas phases, as well as K_d values:

$$P_S = \left\{ \frac{(C_S \times W_S)}{(C_i \times W_L)} \right\} \times 100 (\%) \quad (\text{II-1})$$

$$P_L = \left(\frac{C_L}{C_i} \right) \times 100 (\%) \quad (\text{II-2})$$

$$P_G = 100 - (P_S + P_L) (\%) \quad (\text{II-3})$$

$$K_d = \frac{C_S}{C_L} \quad (\text{L/kg}) \quad (\text{II-4})$$

where:

C_i (Bq/L) is the initial radionuclide activity concentration in the liquid phase;

C_L (Bq/L) and C_S (Bq/kg DM) are the radionuclide activity concentrations in the liquid phase and solid phase, respectively;

W_L (L) is the solution volume;

W_S (kg) is the soil DM.

When antibiotics were added to the samples to inhibit microbial activity the sorption of I⁻ in soil at 4°C was similar to that at 23°C. Thus, the limited amount of I⁻ partitioning to the gas and solid phases at 4°C was attributed to diminished microbial activity at this lower temperature. There was no correlation between the partitioning ratios for solid, liquid and gas at 4°C and 23°C and soil properties such as pH, redox potential (Eh), and electrical conductivity.

The calculated K_d values for I⁻ are shown in Fig. II-3. For paddy soils, K_d at 4°C ranged from 2.0–80 L/kg (GM = 22 L/kg) and K_d at 23°C ranged from 4.5–567 L/kg (GM = 67 L/kg). For upland soils, K_d at 4°C ranged from 1.6–46 L/kg (GM = 9.3 L/kg) and K_d at 23°C ranged from 4.4–183 L/kg (GM = 21 L/kg) which was similar to the results obtained for paddy soils. In both cases the K_d values at 4°C and 23°C were statistically different (t -test, $p < 0.001$). According to K_d data compiled by Ref. [II-11] and used as the revised IAEA reference values in TRS 472 [II-12], the K_d values of iodine ranged from 0.01–580 L/kg ($n = 250$) with a GM of 6.9 L/kg. The K_d values reported by Refs [II-9, II-10] at 4°C and 23°C were within this range.

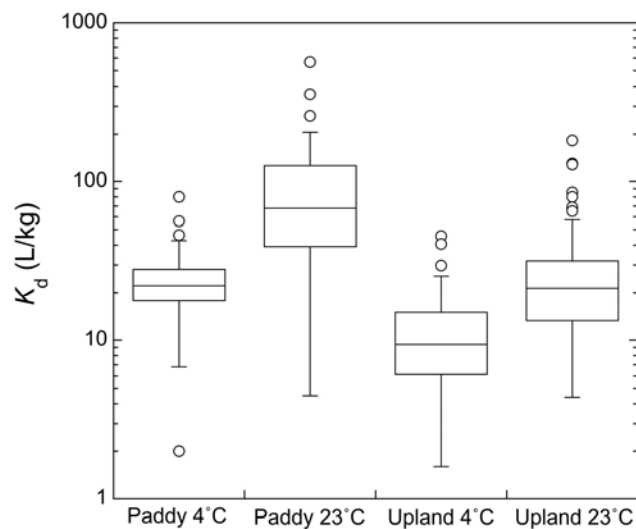


FIG. II-3. Box-whisker plot of K_d values for iodine (added as iodide) collected at 4°C and 23°C in paddy and upland field soil samples.

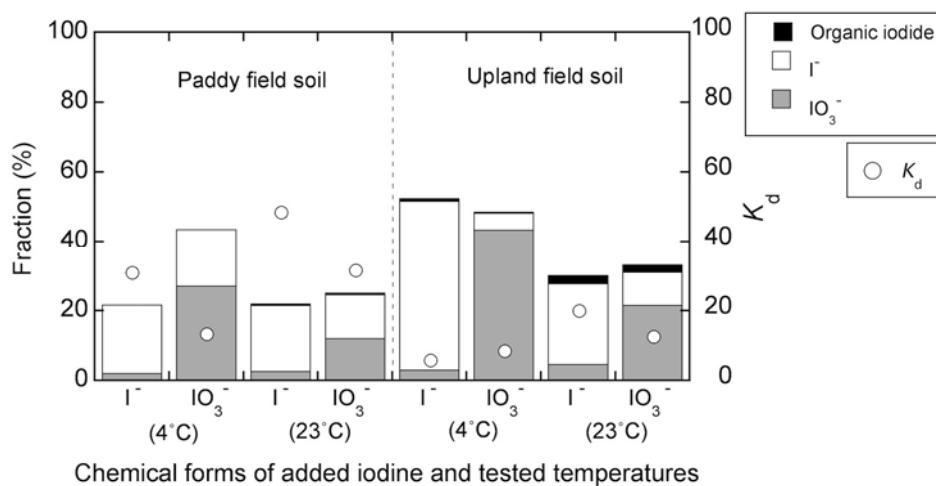


FIG. II-4. Percentage (left Y-axis) of elemental iodine and organic iodine, I^- , and IO_3^- in the soil solution after 7 days relative to the initially added I (added as either I^- or IO_3^- , and the corresponding K_d values (right Y-axis). The temperatures for these experiments were set to either 4°C or 23°C.

There was a good correlation between $\lg(K_d)$ at 4°C and 23°C by t-test ($R = 0.817$, $p < 0.001$) expressed as $\lg(K_{d-23^\circ\text{C}}) = 0.334 + 1.077 * \lg(K_{d-4^\circ\text{C}})$ (data not shown). From this equation, $\lg(K_d)$ measured at 23°C could be about three times as high as that at 4°C.

Reference [II-13] also reported a change in chemical form of iodine in the soil–solution system. For iodide (I^-) addition, the chemical forms of I in soil solution were unchanged, while some iodate (IO_3^-) added to the soil solution became I^- (Fig. II-4) suggesting that the difference in sorption kinetics of IO_3^- depended on whether IO_3^- forms I^- in the soil solution. The data show that to determine the difference in sorption kinetics between I^- and IO_3^- , it is important to check the chemical forms of I in soil solution when IO_3^- is added to the sample.

REFERENCES

- [II-1] AMACHI, S., et al., Microbial participation in iodine volatilization from soils, *Environ. Sci. Technol.* **37** (2003) 3885. DOI: [10.1021/es0210751](https://doi.org/10.1021/es0210751)
- [II-2] DORAN, J.M., ALEXANDER, M., Microbial formation of volatile selenium compounds in soil, *Soil Sci. Soc. Am. J.* **40** (1976) 687.
<https://doi.org/10.2136/sssaj1976.03615995004000050052x>
- [II-3] ISHII, N., TAGAMI, K., UCHIDA, S., The ¹⁴C partitioning of [^{1,2-¹⁴C}] sodium acetate in three phases (solid, liquid, and gas) in Japanese agricultural soils, *J. Radioanal. Nucl. Chem.* **303** (2015) 1389.
<https://doi.org/10.1007/s10967-014-3536-9>
- [II-4] REDEKER, K.R., et al., Emissions of methyl halides and methane from rice paddies, *Science* **290** (2000) 966. DOI: [10.1126/science.290.5493.966](https://doi.org/10.1126/science.290.5493.966)
- [II-5] WHITEHEAD, D. C., The volatilisation, from soils and mixtures of soil components, of iodine added as potassium iodide, *European J. Soil Sci.* **32** (1981) 97–102. <https://doi.org/10.1111/j.1365-2389.1981.tb01689.x>
- [II-6] SHEPPARD, M.I., SHEPPARD, S.C., AMIRO, B.D., Mobility and plant uptake of inorganic ¹⁴C and ¹⁴C-labelled PCB in soils of high and low retention, *Health Phys.* **61** (1991) 481. DOI: [10.1097/00004032-199110000-00003](https://doi.org/10.1097/00004032-199110000-00003)
- [II-7] ISHII, N., KOISO, H., TAKEDA, H., UCHIDA, S., Partitioning of ¹⁴C into solid, liquid, and gas phases in various paddy soils in Japan, *J. Nucl. Sci. Technol.* **47** (2010) 238. DOI: [10.1080/18811248.2010.9711950](https://doi.org/10.1080/18811248.2010.9711950)
- [II-8] HARA, A., KOZAKI, T., SATO, S., NAKAZAWA, T., KATO, H., The effect of microbial activities on sorption behaviour of organic ¹⁴C, *Geochim. Cosmochim. Acta* **72** Suppl. (2008) A352. <https://doi.org/10.1016/j.gca.2008.05.011>
- [II-9] ISHIKAWA, N., UCHIDA, S., TAGAMI, K., Iodide sorption and partitioning in solid, liquid and gas phases in soil samples collected from Japanese paddy fields, *Radiat. Prot. Dosim.* **146** (2011) 155. <https://doi.org/10.1093/rpd/ncr126>
- [II-10] ISHIKAWA, N. K., TAGAMI, K., UCHIDA, S., Effect of biological activity due to different temperatures on iodide partitioning in solid, liquid, and gas phases in Japanese agricultural soils, *J. Radioanal. Nucl. Chem.* **295** (2013) 1763.
<https://doi.org/10.1007/s10967-012-2096-0>
- [II-11] GIL-GARCÍA, C., TAGAMI, K., UCHIDA, S., RIGOL, A., VIDAL, M., New best estimates for radionuclide solid-liquid distribution coefficients in soils. Part 3: miscellany of radionuclides (Cd, Co, Ni, Zn, I, Se, Sb, Pu, Am, and others), *J. Environ. Radioactiv.* **100** (2009) 704. <https://doi.org/10.1016/j.jenvrad.2008.12.001>
- [II-12] INTERNATIONAL ATOMIC ENERGY AGENCY, Handbook of Parameter Values for the Prediction of Radionuclide Transfer in Terrestrial and Freshwater Environment, Technical Reports Series No. 472, IAEA, Vienna (2010).
[https://doi.org/10.1016/0265-931X\(95\)00010-8](https://doi.org/10.1016/0265-931X(95)00010-8)
- [II-13] ISHIKAWA, N. K., UCHIDA, S., TAGAMI, K., Iodine sorption and its chemical form in the soil–soil solution system in Japanese agricultural fields, *Proceedings of the 19th World Congress of Soil Science* (ISBN: 978-0-646-53783-2) (2010) 125.
<https://www.old.iuss.org/19th%20WCSS/Symposium/pdf/1709.pdf>

ANNEX III. EXAMPLE OF COUPLING BETWEEN K_d AND KINETIC APPROACHES

PATRICK BOYER, LAURENT GARCIA-SANCHEZ and
VALERIE NICOULAUD-GOUIN
Institut de Radioprotection et de Sûreté Nucléaire (IRSN), FRANCE

The E-K sorption model is an example of a kinetic model (see also Chapter 4) [III-1] that considers two types of solid sites of sorption:

- (1) The first sorption sites consider a pool of exchangeable fractions (termed ex) sorbed by a solid phase (termed s1) that reacts rapidly and reversibly with the soluble phase (termed w). Exchanges between these two phases are modelled using the K_d approach:

$$C_{s1} = K_{d_{s1}} \times C_w \quad \text{(III-1)}$$

- (2) The second type (termed s2), incorporates solid sites characterized by slower and poorly reversible exchanges with the dissolved phase. Variations of the concentration arising from radionuclide interactions with these sites, C_{s2} , are modelled using a kinetic description of both sorption and desorption:

$$\frac{dC_{ex}}{dt} = -\frac{M}{V} \times \frac{dC_{s2}}{dt} \quad \text{(III-2)}$$

$$\frac{dC_{s2}}{dt} = k^+ \times C_w - k^- \times C_{s2} \quad \text{(III-3)}$$

where:

C_{ex} is the activity concentration of radionuclide in the exchangeable fraction ($C_{ex} = C_w + \frac{M}{V} \times C_{s1}$);

V (L) is the volume of water;

M (kg) is the dry mass of solid;

k^+ (m³/kg/s) and k^- (s) are the kinetics of sorption and desorption, respectively.

The conceptual diagram of this model is shown in Fig. III-1. The total concentration in the solid phase C_s is then given by:

$$C_s = K_{d_{s1}} \times C_w + C_{s2} \quad \text{(III-4)}$$

The E-K sorption model using only three parameters, k^+ , k^- and $K_{d_{s1}}$ can describe, in a relatively simple manner, complex systems that cannot be described with K_d approaches. The model can be further improved to take into account the effects of site saturation by adding maximal concentrations for sites s1 and s2 (C_{s1}^{max} and C_{s2}^{max} , Bq/kg):

$$C_{s1} = \frac{K_d}{1 + \frac{C_w}{C_{s1}^{max}} \times K_d} \times C_w \quad \text{and} \quad \frac{dC_{s2}}{dt} = k^+ \times \left(1 - \frac{C_{s2}}{C_{s2}^{max}}\right) \times C_w - k^- \times C_{s2} \quad \text{(III-5)}$$

The added value of this approach is illustrated in Fig. III-2 which compares the E-K and K_d approaches [III-2] using experimental data on Cs sorption in a soil system simulated with a stirred flow reactor [III-3]. The E-K sorption model reproduces the change with time in the sorption process, which cannot be adequately simulated with the K_d approach.

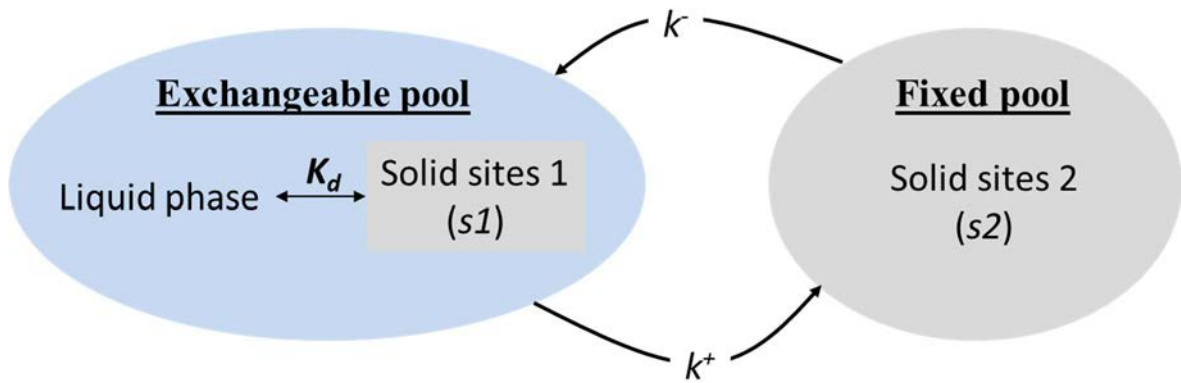


FIG. III-1. Conceptual diagram of the E-K sorption model.

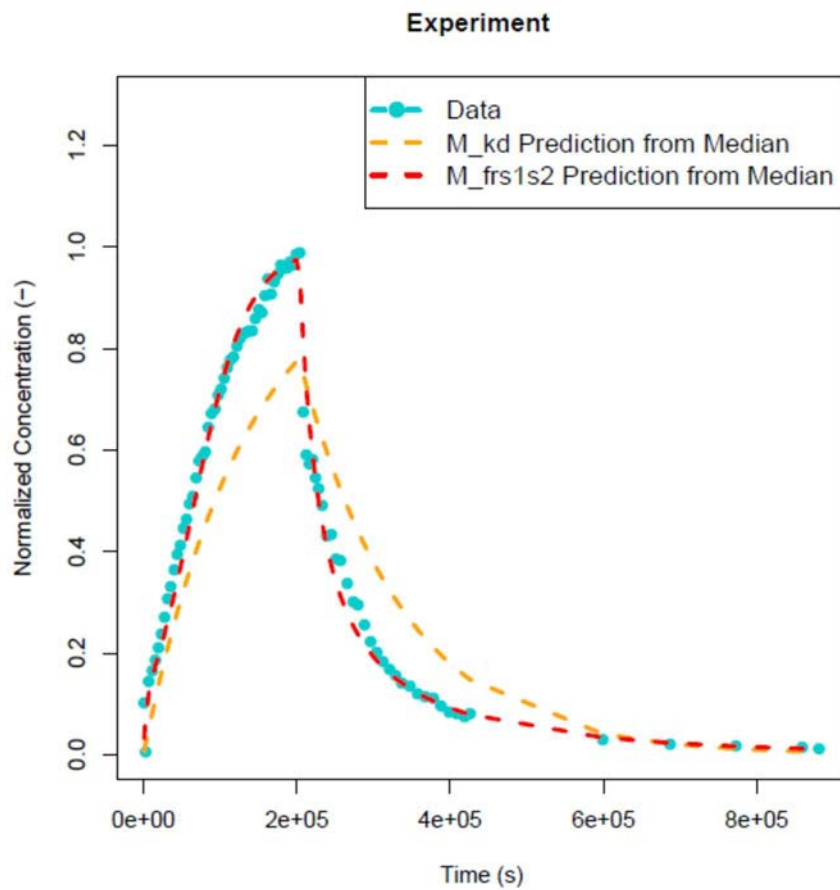


FIG. III-2. predictions from the E-K sorption model and a K_d model compared with experimental data of C_s sorption in a soil system simulated by a stirred flow reactor [III-3]. The y-axis is the normalized aqueous C_s concentration (C_w/C_0), where C_w is the aqueous C_s concentration in the effluent and C_0 is the initial C_s concentration introduced in the influent; x-axis is time since the introduction of C_s into the soil).

REFERENCES

- [III-1] GARCIA-SANCHEZ, L., LOFFREDO, N., MOUNIER, S., MARTIN-GARIN, A., COPPIN, F., Kinetics of selenate sorption in soil as influenced by biotic and abiotic conditions: a stirred flow-through reactor study, *J. Environ. Radioact.* **138** (2014) 38. <https://doi.org/10.1016/j.jenvrad.2014.07.009>
- [III-2] NICOULAUD-GOUIN, V., GIACALONE, M., GONZE, M.A., MARTIN-GARIN, A., GARCIA-SANCHEZ, L., Calibration of radionuclides transfer models in the environment using a Bayesian approach with Markov chain Monte Carlo simulation and comparison of models. ICRER 2014, Session 02 Risk characterization and assessment ICRER Conference Barcelona, Spain (2014).
- [III-3] VAN GENUCHTEN, M.Th., DAVIDSON, J.M., WIERENGA, P.J., An evaluation of kinetic and equilibrium equations for the prediction of pesticide movement in porous media, *Soil Sci. Soc. Am. J.* **38** (1974) 29. <https://doi.org/10.2136/sssaj1974.03615995003800010016x>

ANNEX IV. RELATIONSHIP BETWEEN K_d AND ADSORPTION AND DESORPTION KINETICS

PATRICK BOYER

Institut de Radioprotection et de Sûreté Nucléaire (IRSN), FRANCE

One of the main assumptions underlying the K_d approach is the instantaneous equilibrium (or steady state) between liquid and solid concentrations. Steady state conditions are normally reached after a length of time (often between a few seconds to several days) and the K_d assumption of equilibrium is incorrect during these transitory periods.

Starting from a pure solid phase and a contaminated solution, the distribution coefficient changes with time (Fig. IV-1). The K_d value is strictly valid only once equilibrium has been reached. *In situ* data are less likely to be at true equilibrium (see also Chapter 4) so are termed apparent $K_{d(a)}$ in this publication.

In the case of complete reversibility between adsorption and desorption conditions (another assumption of the K_d approach leading to the same K_d value for both), the following equations give the temporal evolution of liquid (w) and solid (s) concentrations as a function of sorption (k^- , s^{-1}) and desorption (k^+ , s^{-1}) kinetics, where $[s]$ is the solid concentration (kg/m^3).

$$\frac{\partial C_w}{\partial t} = -k^- C_w + k^+ [s] C_s \quad (IV-1)$$

$$\frac{\partial C_s}{\partial t} = \frac{k^-}{[s]} C_w - k^+ C_s \quad (IV-2)$$

These equations make possible to model the temporal variations of liquid and solid element concentrations and to consider the time needed to reach equilibrated conditions where the K_d term becomes valid.

$$\frac{\partial C_w}{\partial t} = \frac{\partial C_s}{\partial t} = 0 \Rightarrow K_d = \frac{C_s}{C_w} = \frac{k^-}{k^+ [s]} \quad (IV-3)$$

Currently, information about kinetics is sparse, so kinetic approaches are currently not often used in most operational models.

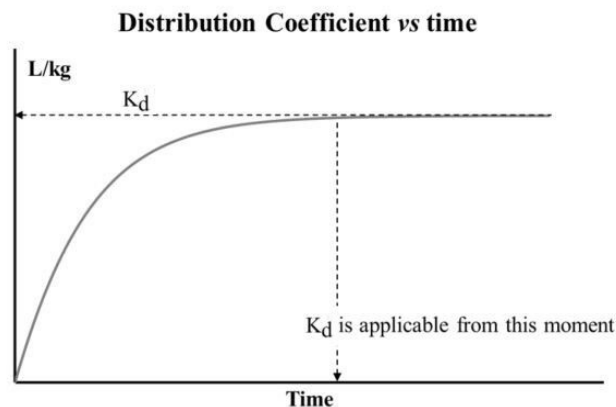


FIG. IV-1. Temporal evolution of distribution coefficient and representativeness of K_d .

ANNEX V. IMPACT OF THE ACCIDENT AT THE FUKUSHIMA DAIICHI NUCLEAR POWER STATION ON THE DISTRIBUTION OF RADIOCAESIUM IN COASTAL WATERS

MASASHI KUSAKABE

Marine Ecology Research Institute (MERI), JAPAN

HYOE TAKATA

Institute of Environmental Radioactivity, Fukushima University, JAPAN

V-1. PRE-ACCIDENT SITUATION IN THE WATERS OFF FUKUSHIMA DAIICHI NUCLEAR POWER STATION

Monitoring has been routinely conducted of the waters and sediments near the FDNPS since 1972. The data can be freely downloaded from the Environmental Radiation Database collated by Japan Nuclear Regulation Authority (NRA) [V-1].

Radionuclide monitoring has also been carried out since 1984 in the coastal waters near NPP sites in Japan, including near the FDNPS, by the Marine Ecology Research Institute (MERI). The data are also available from Ref. [V-1]. The main source of radiocaesium in the North Pacific Ocean in these years was global fallout from atomic weapons testing and, to a lesser extent, authorized discharges from NPPs.

The data obtained in the waters off the Fukushima Prefecture by the MERI are shown in Fig. V-1 with calculated $K_{d(a)}$ values. The ^{137}Cs activity concentrations in surface and bottom water decreased with time with an effective environmental half-life estimated to be 15–18 years before the accident at the FDNPS [V-2–V-4]. The decrease was ascribed to dilution of surface water with unpolluted deep water. The ^{137}Cs activity concentration in the sediment also decreased with time with a similar pattern to that of sea water. These trends implied that a possible equilibrium was established between Cs in sea water and sediment in the area. However, a mathematical model consisting of three boxes (surface water, bottom water and sediment) applied to the monitoring data to estimate transfer rates between the compartments, gave a much shorter half life (2.2 years) in sediment than in water [V-4]. ^{137}Cs derived from the accident at the Chernobyl NPP raised the activity concentration to ca. 7 mBq/L in surface water for only 1 year but did not increase that in bottom water and sediment.

In Fig. V-1, $K_{d(a)}$ values calculated using the ^{137}Cs data in sediment and bottom water collected off Fukushima by MERI are also plotted to show the time trend. The average of $K_{d(a)}$ was ca. 620 L/kg for the period from 1983 to 2010.

V-2. POST-ACCIDENT SITUATION IN THE WATERS OFF FUKUSHIMA AND NEARBY PREFECTURES

On 11 March 2011, the Great East Japan Earthquake occurred, and a series of tsunami damaged the electrical systems of the FDNPS, resulting in a large radionuclide release to the surrounding environment. The total amount of ^{137}Cs released directly into the ocean was estimated to be $(3.5 \pm 0.7) \times 10^{15}$ Bq [V-5]. Soon after the accident at the FDNPS, associated monitoring schemes, such as that described above, were considerably enhanced [V-6–V-12].

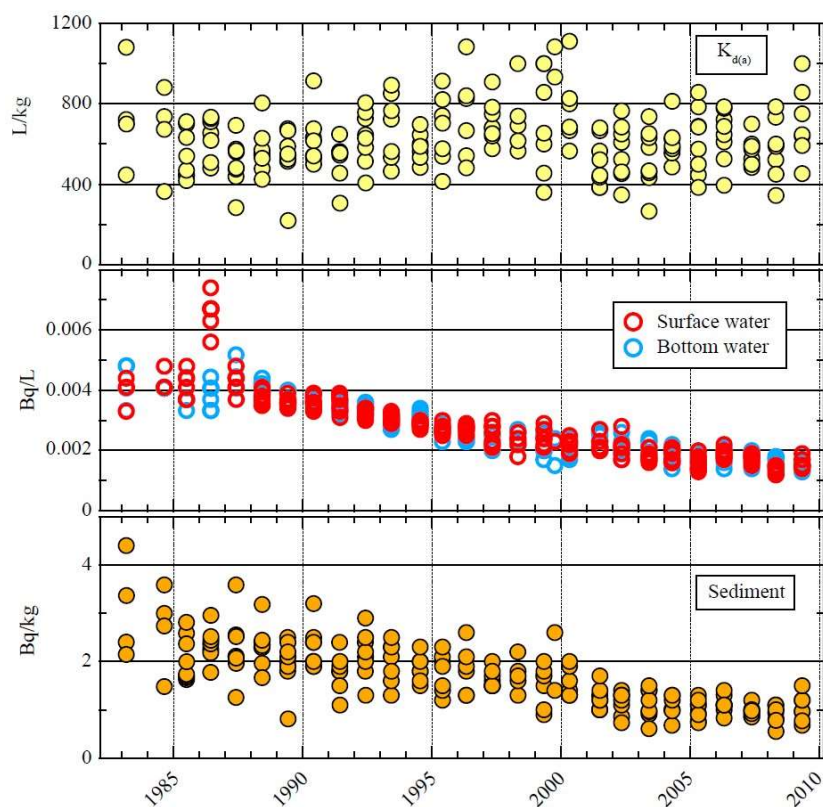


FIG. V-1. Time dependence of ^{137}Cs activity concentrations in sediment and sea water collected at eight sites off Fukushima Prefecture with calculated $K_{d(a)}$.

From 2011 to 2015, the activity concentration of radionuclides, especially ^{137}Cs , in sea water and surface sediments showed unprecedented variation [V-7, V-10, V-12] (Fig. V-2). The ^{137}Cs activity concentration in surface waters at stations located beyond the 30 km zone from the FDNPS after the accident reached a maximum of 190 Bq/L on 15 April 2011, which was about five orders of magnitude higher than the pre-accident value; it then decreased exponentially with time (Fig. V-2(a)).

In early May 2011, ^{137}Cs -polluted water was advected towards north, but partly detached and was transported to the south, suggesting that dispersion patterns of ^{137}Cs in surface waters are dependent on the currents. In addition, elevated ^{137}Cs activity concentrations derived from the accident at the FDNPS were observed in subsurface waters only 1–2 months after the accident, probably due to vertical mixing processes during the winter.

From 2012 to January–February 2015, the ^{137}Cs activity concentrations ranged between ~ 1 and 100 mBq/L depending on the sampling location. The main environmental factors controlling ^{137}Cs activity concentrations in the waters are dilution and subduction with less contaminated deep sea waters [V-7, V-13, V-14] as well as the outflow to open ocean via the Kuroshio Current [V-5]. Data obtained in May 2015 [V-6] showed that the ^{137}Cs activity concentration ranged from 1 mBq/L (\approx pre-accident value) to 10 mBq/L. Despite the vigorous mixing of sea water in the monitoring area, some sites still had consistently higher ^{137}Cs activity concentrations in January 2016 [V-6] than that prior to the accident. The elevated values were probably due to the continuous direct release from the FDNPS [V-12, V-15], riverine inputs [V-16–V-19], redissolution and/or resuspension of sedimentary ^{137}Cs [V-10, V-20], and desorption of ^{137}Cs from beach sands contaminated at the time of the accident through wave and tide driven exchange [V-21].

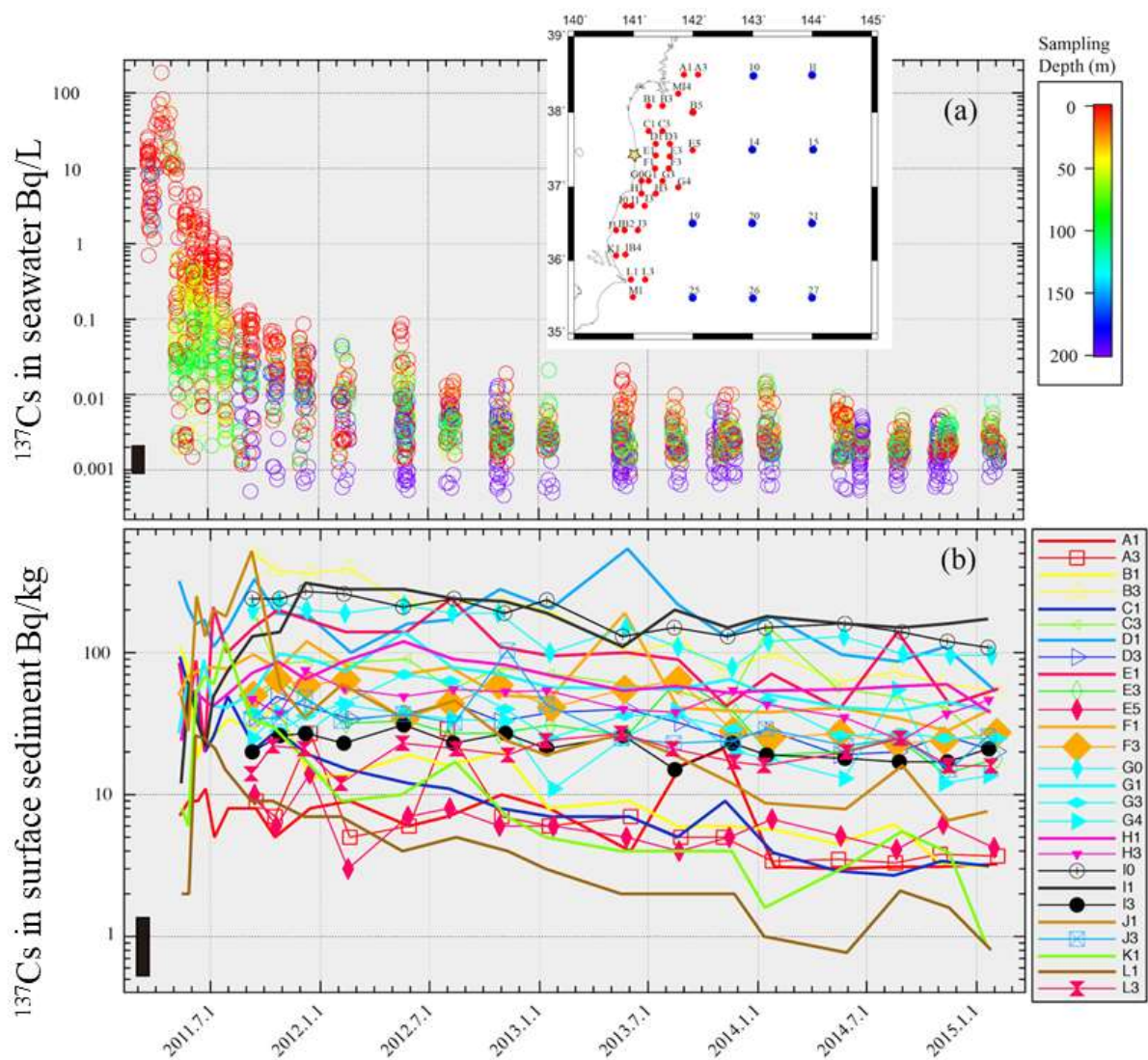


FIG. V-2. Spatio-temporal variation of ^{137}Cs activity concentration in (a) sea water and (b) surface sediment after the accident at the FDNPS. Black squares in the left side of the figures show the 5 year average before the accident. The inset figure indicates sites for sampling; red circles: sea water and sediment; blue circles: sea water. The key in part (b) indicates sampling locations shown in the inset map.

The distribution of ^{137}Cs in the surface sediments initially reflected the pathway of the polluted water, with some of the higher values of ^{137}Cs activity concentrations north of the FDNPS and thereafter south of the FDNPS. The ^{137}Cs activity concentrations in most sediments reached a maximum in September 2011 and varied from ~ 10 to 580 Bq/kg dry mass (DM) (Fig. V-2(b)). The amount of ^{137}Cs in the 3 cm top layer of the sediments in the monitoring area was estimated to be 4.0×10^{13} Bq as of September 2011 [V-10]. Since then, the GM of the ^{137}Cs activity concentration of surface sediments has been decreasing with an effective half-life of ca. 2 years in the monitored areas. The decrease may be due to desorption and/or dissolution from the sediment, bioturbation into deeper layer, and resuspension and its subsequent lateral transport of the sediment. Inspection of vertical profiles of ^{137}Cs in the sediments revealed no temporal increase in the intermediate layer of the sediment (i.e. below the concentration maximum layer), suggesting that bioturbation has not had a strong effect. Resuspension is probably also playing a role, to some extent, in redistribution of ^{137}Cs in the surface sediment [V-11, V-20]. Data

obtained from monitoring has indicated that the ^{137}Cs activity concentration in the sediment associated with large grain sizes is decreasing to a greater degree than that associated with small particles. The data also shows that the ^{137}Cs activity concentration in shallow water has a higher rate of decrease than that at greater depth, suggesting that resuspension and lateral transportation are contributory mechanisms [V-11].

It is not suitable to use the concept of K_d for the coastal and marine waters off the FDNPS, as this system is still not in a state of equilibrium. Nevertheless, it is worthwhile to calculate a temporal change of $K_{d(a)}$ values based on ^{137}Cs activity concentrations in surface sediments and bottom water in the environment in the process of recovery.

The accident at the FDNPS has provided an opportunity to quantify parameters relevant to the fate of radionuclides in the marine environment which have yet to be stabilized. They seem to be highly complex, involving kinetics and dynamics of sea water and sediment. They provide, however, the possibility to ensure that long term recovery processes in the marine environment can be predicted. Close examination of the spatiotemporal variation of $K_{d(a)}$ will help understand quantitatively the fate of radionuclides released accidentally to the marine environment.

REFERENCES

- [V-1] NUCLEAR REGULATION AUTHORITY (NRA), Environmental Radiation Database (2016). <http://search.kankyo-hoshano.go.jp/servlet/search.top>
- [V-2] KASAMATSU, F., INATOMI, N., Effective environmental half-lives of ^{90}Sr and ^{137}Cs in the coastal seawater of Japan, J. Geophys. Res. **103** (1998) 1209. <https://doi.org/10.1029/97JC02807>
- [V-3] OIKAWA, S., et al., Plutonium isotopes concentration in seawater and bottom sediment off the Pacific coast of Aomori sea area during 1991–2005, J. Environ. Radioact. **102** (2011) 302. <https://doi.org/10.1016/j.jenvrad.2010.12.007>
- [V-4] WATABE, T., et al., Spatiotemporal distribution of ^{137}Cs in the sea surrounding Japanese Islands in the decades before the disaster at the Fukushima Daiichi Nuclear Power Plant in 2011, Sci. Total Environ. **463–464** (2013) 913. <https://doi.org/10.1016/j.scitotenv.2013.06.031>
- [V-5] TSUMUNE, D., et al., One-year, regional-scale simulation of ^{137}Cs radioactivity in the ocean following the Fukushima Daiichi Nuclear Power Plant accident, Biogeosciences **10** (2013) 5601. DOI: [10.5194/bg-10-5601-2013](https://doi.org/10.5194/bg-10-5601-2013)
- [V-6] JAPAN NUCLEAR REGULATION AUTHORITY (NRA), Monitoring information of environmental radioactivity level (2016). <http://radioactivity.nsr.go.jp/en/list/292/list-1.html>
- [V-7] OIKAWA, S., TAKATA, H., WATABE, T., MISONOO, J., KUSAKABE, M., Distribution of the Fukushima-derived radionuclides in seawater in the Pacific off the coast of Miyagi, Fukushima, and Ibaraki Prefectures, Japan, Biogeosciences **10** (2013) 5031. <https://doi.org/10.5194/bg-10-5031-2013>

- [V-8] OIKAWA S., WATABE, T., TAKATA, H., MISONOO, J., KUSAKABE, M., Plutonium isotopes and ^{241}Am in surface sediments off the coast of the Japanese islands before and soon after the Fukushima Dai-ichi nuclear power plant accident, *J Radioanal. Nucl. Chem.* **303** (2014) 1513.
<https://doi.org/10.1007/s10967-014-3530-2>
- [V-9] OIKAWA, S., WATABE, T., TAKATA, H., Distributions of Pu isotopes in seawater and bottom sediments in the coast of the Japanese archipelago before and soon after the Fukushima Dai-ichi Nuclear Power Station accident, *J. Environ. Radioact.* **142** (2015) 113. <https://doi.org/10.1016/j.jenvrad.2015.01.003>
- [V-10] KUSAKABE, M., OIKAWA, S., TAKATA, H., MISONOO, J., Spatiotemporal distributions of Fukushima-derived radionuclides in nearby marine surface sediments, *Biogeosciences* **10** (2013) 5019.
<https://doi.org/10.5194/bg-10-5019-2013>
- [V-11] KUSAKABE, M., INTOMI, N., TAKATA, H., IKENOUE, T., Decline in radiocesium in seafloor sediments off Fukushima and nearby prefectures, *J. Oceanogr.* **73** (2017) 529. <https://doi.org/10.1007/s10872-017-0440-2>
- [V-12] TATATA H., KUSAKABE, M, INATOMI, N., IKENOUE, T., HASEGAWA, K., The contribution of sources to the sustained elevated inventory of ^{137}Cs in offshore waters east of Japan after the Fukushima Dai-ichi Nuclear Power Station accident, *Environ. Sci. Tech.* **50** (2016) 6957. <https://doi.org/10.1021/acs.est.6b00613>
- [V-13] KAERIYAMA, H., et al., Southwest Intrusion of ^{134}Cs and ^{137}Cs Derived from the Fukushima Dai-ichi Nuclear Power Plant Accident in the Western North Pacific, *Environ. Tech. Sci.* **48** (2014) 3120. <https://doi.org/10.1021/es403686v>
- [V-14] KUMAMOTO, Y., et al., Southward spreading of the Fukushima-derived radiocesium across the Kuroshio Extension in the North Pacific, *Sci. Rep.* **4** (2014) 4276. <https://doi.org/10.1038/srep04276>
- [V-15] KANDA, J., Continuing ^{137}Cs release to the sea from the Fukushima Dai-ichi Nuclear Power Plant through 2012, *Biogeosciences* **10** (2013) 6107.
<https://doi.org/10.5194/bg-10-6107-2013>
- [V-16] NAGAO, S., et al., Export of ^{134}Cs and ^{137}Cs in the Fukushima river systems at heavy rains by Typhoon Roke in September 2011, *Biogeosciences* **10** (2013) 6215.
<https://doi.org/10.5194/bg-10-6215-2013>
- [V-17] SAKAGUCHI, A., et al., Size distribution studies of ^{137}Cs in river water in the Abukuma riverine system following the Fukushima Dai-ichi Nuclear Power Plant accident, *J. Environ. Radioact.* **139** (2015) 379.
<https://doi.org/10.1016/j.jenvrad.2014.05.011>
- [V-18] TAKATA, H., et al., Remobilization of radiocesium on riverine particles in seawater: The contribution of desorption to the export flux to the marine environment, *Mar. Chem.* **176** (2015) 51.
<https://doi.org/10.1016/j.marchem.2015.07.004>
- [V-19] TSUJI, H., YASUTAKA, T., KAWABE, Y., ONISHI, T., KOMAI, T., Distribution of dissolved and particulate radiocesium concentrations along rivers and the relations between radiocesium concentration and deposition after the nuclear power plant accident in Fukushima, *Water Res.* **60** (2014) 15.
<https://doi.org/10.1016/j.watres.2014.04.024>

- [V-20] OTOSAKA S., KOBAYASHI, T., Sedimentation and remobilization of radiocesium in the coastal area of Ibaraki, 70 km south of the Fukushima Dai-ichi Nuclear Power Plant, *Environ. Monit. Assess.* **185** (2013) 5419. <https://doi.org/10.1007/s10661-012-2956-7>
- [V-21] SANIAL V., BUESSELER K.O., CHARETTE M.A., NAGAO S., Unexpected source of Fukushima-derived radiocaesium to the coastal ocean of Japan, *Proc. Natl Acad Sci USA* **114** (2017) 11092. <https://doi.org/10.1073/pnas.1708659114>

LIST OF ABBREVIATIONS

| | |
|---------|---|
| CDF | cumulative distribution function |
| CEA | Commissariat à l'Énergie Atomique et aux Énergies Alternatives, France |
| CIEMAT | Centro de Investigaciones Energéticas, Medioambientales y Tecnológicas, Spain |
| EMRAS | Environmental Modelling for Radiation Safety |
| ERICA | Environmental Risk from Ionising Contaminants: Assessment and Management |
| FDNPP | Fukushima Daiichi Nuclear Power Plant |
| FLSD | Fisher's least significant differences |
| GM | geometric mean |
| GMC | group mean centering |
| GSD | geometric standard deviation |
| HELCOM | Baltic Marine Environment Protection Commission |
| IAEA | International Atomic Energy Agency |
| ICRP | International Commission on Radiological Protection |
| IRSN | Institut of Radioprotection and Nuclear Safety, France |
| MARIS | IAEA's Marine Information System |
| MERI | Marine Ecology Research Institute, Japan |
| MEXT | Ministry of Education, Culture, Sports, Science and Technology, Japan |
| MODARIA | Modelling and Data for Radiological Impact Assessments |
| NORM | naturally occurring radioactive material |
| NRA | Nuclear Regulation Authority, Japan |
| OM | organic matter |
| OSPAR | Protection of the Marine Environment of the North-East Atlantic |
| PDF | probability density function |
| REIA | radiological environmental impact assessment |

| | |
|--------|--|
| RIP | radiocaesium interception potential |
| RWM | Radioactive Waste Management Limited, United Kingdom |
| SCM | surface complexation model |
| SRS | Safety Reports Series |
| TECDOC | (IAEA) Technical Document |
| TRS | (IAEA) Technical Reports Series |
| USGS | United States Geological Survey |

CONTRIBUTORS TO DRAFTING AND REVIEW

| | |
|---------------------|--|
| Bildstein, O. | Commissariat à l'Energie Atomique et aux Énergies Alternatives, France |
| Boyer, P. | Institut de Radioprotection et de Sûreté Nucléaire, France |
| Brown, J | International Atomic Energy Agency |
| Garcia-Sanchez, L. | Institut de Radioprotection et de Sûreté Nucléaire, France |
| Halsall, C. | International Atomic Energy Agency |
| Harbottle, A.-R. | International Atomic Energy Agency |
| Howard, B.J. | University of Nottingham and UK Centre for Ecology and Hydrology, United Kingdom |
| Howard, D. | UK Centre for Ecology and Hydrology, United Kingdom |
| Ishida, K. | Nuclear Waste Management Organization, Japan |
| Ishii, N. | National Institutes for Quantum Science and Technology, Japan |
| Ishikawa, N. | Iwate University, Japan |
| Kaplan, D.I. | Savannah River Ecology Laboratory, University of Georgia, United States of America |
| Kelleher, K. | Environmental Protection Agency, Ireland |
| Kusakabe, M. | Marine Ecology Research Institute, Japan |
| Lahdenpera, A.-M. | Saanio & Riekkola Oy, Finland |
| McGinnity, P. | International Atomic Energy Agency |
| Mora, J.C. | Centro de Investigaciones Energéticas, Medioambientales y Tecnológicas, Spain |
| Mourlon, C. | Institut de Radioprotection et de Sûreté Nucléaire, France |
| Nicoulaud-Gouin, V. | Institut de Radioprotection et de Sûreté Nucléaire, France |
| Onda, Y. | University of Tsukuba, Japan |
| Phaneuf, M. | Canadian Nuclear Safety Commission (CNSC) |
| Ramirez-Guinart, O. | Universitat de Barcelona, Spain |
| Rigol, A. | Universitat de Barcelona, Spain |
| Sheppard, S. | ECOMATTERS, Canada |
| Shibutani, S. | Nuclear Waste Management Organization, Japan |
| Tagami, K. | National Institutes for Quantum Science and Technology, Japan |
| Takata, H. | Fukushima University, Japan |
| Thorne, M. | Mike Thorne and Associates Limited, United Kingdom |
| Toll, O. | Universitat de Barcelona, Spain |
| Tomczak, W. | Institut de Radioprotection et de Sûreté Nucléaire, France |
| Turtiainen, T. | Radiation and Nuclear Safety Authority, Finland |

| | |
|---------------|---|
| Vidal, M. | Universitat de Barcelona, Spain |
| Uchida, S. | National Institutes for Quantum Science and Technology, Japan |
| Wells, C. | Centre for Ecology and Hydrology, United Kingdom |
| Yankovich, T. | International Atomic Energy Agency |
| Yu, C. | Argonne National Laboratory, United States of America |

LIST OF PARTICIPANTS OF WORKING GROUP 4, SUBGROUP 1

| | |
|-----------------------|--|
| Al Neaimi, A. | Emirates Nuclear Energy Corporation, United Arab Emirates |
| Andersson, P. | Swedish Radiation Safety Authority, Sweden |
| Aravin, A. | Atomic Energy Regulatory Board, India |
| Attarilar, A. | Atomic Energy Organization of Iran, Islamic Republic of Iran |
| Barnett C. | Centre for Ecology and Hydrology, United Kingdom |
| Bartusková, M. | National Radiation Protection Institute, Czech Republic |
| Beaugelin-Seiller, K. | Institut de Radioprotection et de Sûreté Nucléaire, France |
| Beleznai, P. | Centre for Energy Research, Hungary |
| Benkrid, M. | Commissariat à l'Energie Atomique, Algeria |
| Beresford, N. | Centre for Ecology and Hydrology, United Kingdom |
| Bollhöfer, A. | Environmental Research Institute of the Supervising Scientist, Australia |
| Boust, D. | Institut de Radioprotection et de Sûreté Nucléaire, France |
| Boyer, C. | Electricité de France, France |
| Boyer, P. | Institut de Radioprotection et de Sûreté Nucléaire, France |
| Bradshaw, C. | Stockholm University, Sweden |
| Brittain, J. | University of Oslo, Norway |
| Brown, J. | Environmental Radioactivity Consultancy, United Kingdom |
| Bucher, B. | Swiss Federal Nuclear Safety Inspectorate, Switzerland |
| Bugai, D. | National Academy of Sciences of the Ukraine, Ukraine |
| Caffrey, E. | Oregon State University, United States of America |
| Calmon, P. | Institut de Radioprotection et de Sûreté Nucléaire, France |
| Carini, F. | Retired, Italy |
| Charrasse, B. | Commissariat à l'Energie Atomique et aux Énergies Alternatives, France |
| Chen, J. | Health Canada, Canada |
| Choi, Y. | Korea Atomic Energy Research Institute, Republic of Korea |
| Chouhan, S. | Atomic Energy of Canada Limited, Canada |
| Cook, M. | Department of Health, Australia |
| Copplestone, D. | University of Stirling, United Kingdom |
| Cujic, M. | University of Belgrade, Serbia |
| Czerniczyniec, M. | Autoridad Regulatoria Nuclear, Argentina |
| da Costa Lauria, D. | Instituto de Radioproteção e Dosimetria, Brazil |
| De Sanctis, J. | SOGIN S.p.A, Italy |

| | |
|--------------------|--|
| Doering, C. | Environmental Research Institute of the Supervising Scientist, Australia |
| Fesenko, E. | International Atomic Energy Agency |
| Fesenko, S. | International Atomic Energy Agency |
| Florou, H. | National Center for Scientific Research “Demokritos”, Greece |
| Garcia-Sanchez, L. | Institut de Radioprotection et de Sûreté Nucléaire, France |
| Grzechnik, M. | Australian Radiation Protection and Nuclear Safety Agency, Australia |
| Gudkov, D. | National Academy of Sciences of the Ukraine, Ukraine |
| Higley, K. | Oregon State University, United States of America |
| Hinton, T. | Institut de Radioprotection et de Sûreté Nucléaire, France |
| Hirth, G. | Australian Radiation Protection and Nuclear Safety Agency, Australia |
| Howard, B. | University of Nottingham and UK Centre for Ecology and Hydrology, United Kingdom |
| Howard, D. | UK Centre for Ecology and Hydrology, United Kingdom |
| Iosjpe, M. | Norwegian Radiation Protection Authority, Norway |
| Ishii, N. | National Institutes for Quantum Science and Technology, Japan |
| Ishikawa, N. | Iwate University, Japan |
| Johansen, M. | Australian Nuclear Science and Technology Organization, Australia |
| Harbottle, A.R. | International Atomic Energy Agency |
| Kangasniemi, V. | EnviroCase Limited, Finland |
| Kaplan, D.I. | Savannah River Ecology Laboratory, University of Georgia, United States of America |
| Kashparov, V. | Nation University of Life & Environmental Sciences, Ukraine |
| Kausky, M. | United States Department of Energy, United States of America |
| Kautsky, U. | Swedish Nuclear Fuel and Waste Management Company, Sweden |
| Kawaguchi, I. | National Institutes for Quantum Science and Technology, Japan |
| Kelleher, K. | Environmental Protection Agency, Ireland |
| Kennedy, P. | Food Standards Agency, United Kingdom |
| Keum, D. | Korea Atomic Energy Research Institute, Republic of Korea |
| Kim, S. | Khalifa University of Science, Technology and Research, United Arab Emirates |
| KimKhalifa, S. | University of Science, Technology and Research, United Arab Emirates |
| Konoplev, A. | University of Fukushima, Japan |

| | |
|-------------------------|--|
| Krajewska, G. | Central Laboratory for Radiological Protection, Poland |
| Kryshev, A. | Research and Production Association “Typhoon”, Russian Federation |
| Kusakabe, M. | Marine Ecological Research Institute, Japan |
| Lahdenperä, A. | Saanio & Riekkola Oy, Finland |
| Lamego Simões Filho, F. | Instituto de Engenharia Nuclear, Brazil |
| Le Druillenec, T. | Electricité de France, France |
| Li, W. | Ministry of Environmental Protection of the People’s Republic of China, China |
| Libert, M. | Commissariat à l’Energie Atomique et aux Énergies Alternatives, France |
| Lourino Cabana, B. | Electricité de France, France |
| Lukashenko, S. | National Nuclear Center of the Republic of Kazakhstan, Kazakhstan |
| Mao, Y. | Ministry of Environmental Protection of the People’s Republic of China, China |
| Marang, L. | Electricité de France, France |
| Maskalchuk, L. | International Sakharov Environmental Institute of the Belarusian State University, Belarus |
| McGuire, C. | Scottish Environment Protection Agency, United Kingdom |
| Melintescu, A. | “Horia Hulubei” National Institute of Physics and Nuclear Engineering, Romania |
| Mihalik, J. | National Radiation Protection Institute, Czech Republic |
| Miyamoto, K. | Marine Ecology Research Institute, Japan |
| Mothersill, C. | McMaster University, Canada |
| Muikku, M. | Radiation and Nuclear Safety Authority, Finland |
| Mustonen, J. | EnviroCase Limited, Finland |
| Nordén, S. | Swedish Nuclear Fuel and Waste Management Company, Sweden |
| Osvath, I. | International Atomic Energy Agency |
| Outola, I. | Radiation and Nuclear Safety Authority, Finland |
| Parami, V. | Philippine Nuclear Research Institute, Philippines |
| Parviainen, L. | Posiva Oy, Finland |
| Pérez-Sánchez, D. | Centro de Investigaciones Energéticas, Medioambientales y Tecnológicas, Spain |
| Phaneuf, M. | International Atomic Energy Agency |
| Picel, M. | Argonne National Laboratory, United States of America |
| Psaltaki, M. | National Technical University of Athens, Greece |

| | |
|---------------------|---|
| Punt, K. | RadEcol Consulting Limited, United Kingdom |
| Putyatin, Y. | Belorussian for Soil Science and Agrochemistry, Belarus |
| Radenkovic, M. | University of Belgrade, Serbia |
| Ramadan, A. | Atomic Energy Authority, Egypt |
| Ramirez-Guinart, O. | University of Barcelona, Spain |
| Real, A. | Centro de Investigaciones Energéticas, Medioambientales y Tecnológicas, Spain |
| Rigol, A. | University of Barcelona, Spain |
| Ruedig, E. | Oregon State University, United States of America |
| Saito, M. | Kyoto University, Japan |
| Sazykina, T. | Research and Production Association “Typhoon”, Russian Federation |
| Sekongo, M. | Ministère de la Santé Publique et de la Population, France |
| Seymour, C. | McMaster University, Canada |
| Shang, Z. | Ministry of Environmental Protection of the People’s Republic of China, China |
| Sheppard, S. | ECOMATTERS, Canada |
| Sika-Boafo, D. | Ghana Atomic Energy Commission, Ghana |
| Sim, S. | Defence Science Organisation National Laboratories, Singapore |
| Skuterud, L. | Norwegian Radiation Protection Authority, Norway |
| Smodis, B. | Jožef Stefan Institute, Slovenia |
| Sotiropoulou, M. | CERN, Switzerland |
| Stark, K. | Stockholm University, Sweden |
| Strok, M. | Jožef Stefan Institute, Slovenia |
| Sundell-Bergman, S. | Swedish University of Agricultural Science, Sweden |
| Tagami, K. | National Institutes for Quantum Science and Technology, Japan |
| Takata, H. | Fukushima University, Japan |
| Tanaka, T. | Electricité de France, France |
| Turtiainen, T. | Radiation and Nuclear Safety Authority, Finland |
| Twining, J. | Austral Radioecology, Australia |
| Uchida, S. | National Institutes for Quantum Science and Technology, Japan |
| Vandenhove, H. | Belgian Nuclear Research Centre, Belgium |
| Varga, B. | National Foodchain Safety Office, Food and Feed Safety Directorate, Hungary |
| Vermorel, F. | Electricité de France, France |
| Vetrov, V. | Institute of Global Climate and Ecology, Russian Federation |
| Vidal, M. | Universidad de Barcelona, Spain |

| | |
|---------------|---|
| Wells, C. | Centre for Ecology and Hydrology, United Kingdom |
| Willemsen, S. | Nuclear Research and Consultancy Group, Netherlands |
| Willrodt, C. | Bundesamt für Strahlenschutz, Germany |
| Wood, M. | University of Salford, United Kingdom |
| Wu, Q. | Tsinghua University, China |
| Yankovich, T. | International Atomic Energy Agency |
| Yu, C. | Argonne National Laboratory, United States of America |
| Zhang, A. | Ministry of Environmental Protection of the People's Republic of China, China |
| Zhaorong, S. | Ministry of Environmental Protection of the People's Republic of China, China |

MODARIA Technical Meetings, IAEA Headquarters, Vienna

19–22 November 2012, 11–15 November 2013, 10–14 November 2014,
9–13 November 2015

MODARIA II Technical Meetings, IAEA Headquarters, Vienna

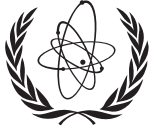
31 October – 4 November 2016, 30 October – 3 November 2017, 22–25 October 2018,
21–24 October 2019

Interim Working Group Meetings, MODARIA Working Group 4, Subgroup 1: K_d

Vienna, Austria: 29–30 May 2013, Oslo, Norway: 20–22 May 2014,
Monaco: 27–28 March 2014, Vienna, Austria: 20–23 April 2015, Monaco: 14–17 April 2015

Interim Working Group Meetings, MODARIA II Working Group 4, Subgroup 1: K_d

Monaco: 31 May–2 June 2017, Monaco: 15–16 May 2018, Vienna, Austria: 27–31 May 2019



IAEA

International Atomic Energy Agency

CONTACT IAEA PUBLISHING

Feedback on IAEA publications may be given via the on-line form available at:
www.iaea.org/publications/feedback

This form may also be used to report safety issues or environmental queries concerning IAEA publications.

Alternatively, contact IAEA Publishing:

Publishing Section
International Atomic Energy Agency
Vienna International Centre, PO Box 100, 1400 Vienna, Austria
Telephone: +43 1 2600 22529 or 22530
Email: sales.publications@iaea.org
www.iaea.org/publications

Priced and unpriced IAEA publications may be ordered directly from the IAEA.

ORDERING LOCALLY

Priced IAEA publications may be purchased from regional distributors and from major local booksellers.